MODELING ADSORPTION: INVESTIGATING ADSORBATE AND ADSORBENT PROPERTIES

By

CHARLES EDWIN WEBSTER

A DISSERTATION PRESENTED TO THE GRADUATE SCHOOL
OF THE UNIVERSITY OF FLORIDA IN PARTIAL FULFILLMENT
OF THE REQUIREMENTS FOR THE DEGREE OF
DOCTOR OF PHILOSOPHY

UNIVERSITY OF FLORIDA

1999

ACKNOWLEDGMENTS

In my scientific career, I must first and foremost thank my family, especially my parents, Charlie and Eileen, my brother, Alex, and my soon-to-be wife, Candace. My brother and my parents have done so much for me over the years--I could never thank them enough. Candace is always there for me when I need help and support. Next, I must thank Dr. Russell S. Drago. He inspired me throughout the time I spent under his direction. Dr. Drago always gave us as much rope as we wanted!

I must also thank some of my undergraduate professors at the University of West Florida, Dr. Jerry Gurst, Dr. Peter Tanner, Dr. Grace Chiu, Dr. Clifford Chang, Dr. and Mrs. John Riehm, and of course, the late Dr. Ralph Birdwhistell.

At the University of Florida, I have had many positive contacts with a variety of people. I must thank my committee members Dr. Michael J. Scott, Dr. Michael C. Zerner, Dr. R. Carl Stoufer, Dr. Willis B. Person, Dr. David E. Richardson, and Dr. David A. Denslow. They have all helped me cope with a difficult situation, Dr. Drago's death. Even before Doc died, I had worked quite a bit with Dr. Zerner. He has been an incredible help. I taught for Dr. Stoufer for three semesters, CHM 2046 twice and CHM 2041 once. I learned a lot about teaching those first two semesters, and with Dr. Drago's permission, I chose to teach for Dr. Stoufer for a third semester. Dr. Person has been a tremendous resource of knowledge about molecular complexes and a great person with which to discuss my research. I must also thank Dr. C. Russell Bowers, who has been a great source of detailed knowledge about Nuclear Magnetic Resonance (NMR) theory and experiment.

Many students here have been good friends and scientific colleagues, especially Ben Gordon, John Osegovic, Ted "A" O'Brien, Steve Jeorg, and Mike McGilvray. Ben is a great person, and I have really enjoyed working with him over the years. I have known John for quite a long time, maybe too long! (Just kidding John.) John always knows something, and he is definitely willing to share it (as am I). Ted has also been a great resource, and we all know that he will go far. Before he graduated, Steve was my "lab mate" for the past few years. He is a great guy and a real "straight arrow!" Mike was smart enough to go to dental school and get out of chemistry, for now! I must send out a general thanks to all of the present and former Drago group members, the Scott group, the Zerner group, and the Bowers group.

I must also thank April Rose for her help with the simplex code of 421.exe, the program for fitting the adsorption isotherm data. I learned a great deal more about programming with her help.

For their assistance with some of the material in Chapter 5, I should acknowledge Dr. Clarence D. Chang (Mobil Corporation) and Dr. Paul B. Weisz (Distinguished Professor of Bio-Chemical Engineering Emeritus, University of Pennsylvania) both of which were pioneers in the research of shape and size-selective catalysis in zeolites.

TABLE OF CONTENTS

page

ACKNOWLEDGMENTS ii

TABLE OF CONTENTS iv

LIST OF TABLES vi

LIST OF FIGURES viii

ABSTRACT ix

CHAPTERS

1 INTRODUCTION 1

2 MOLECULAR DIMENSIONS FOR ADSORPTIVES 6

Introduction 6
Calculations 9
Results and Discussion 9
Conclusions 27

3 A MULTIPLE-PROCESS EQUILIBRIUM ANALYSIS OF SILICA GEL AND HZSM-5 28

Introduction 28
Experimental 31
Results and Discussion 33
Conclusions 55

4 THE MULTIPLE EQUILIBRIUM ANALYSIS DESCRIPTION OF ADSORPTION ON Na-MORDENITE AND H-MORDENITE 57

Introduction 57
Experimental 61
Results and Discussion 65
Conclusions 89

5 A METHOD FOR CHARACTERIZING EFFECTIVE PORE SIZES OF CATALYSTS 92

Introduction 92
Calculations 97
Results and Discussion 97
Conclusions 112

6 THE MULTIPLE EQUILIBRIUM ANALYSIS QUANTITATIVE PREDICTION OF SINGLE AND MULTI-COMPONENT ADSORPTION ISOTHERMS ON CARBONACEOUS AND ZEOLITIC SOLIDS 115

Introduction 115
Prediction of Isotherms by MEA 119
Results and Discussion 121
Conclusions 125

APPENDICES

A FORTRAN 77 CODE FOR 421.EXE AND COMMENTS ON INPUT AND OUTPUT FILES 134

B FORTRAN 77 CODE FOR AREA.EXE AND COMMENTS ON INPUT AND OUTPUT FILES 156

REFERENCES 173

BIOGRAPHICAL SKETCH 182

LIST OF TABLES

Table		page
2-1	Molecular and Molar Volumes	11
2-2	Excluded Areas for Different Molecular Orientations	17
2-3	Molecular *x*, *y*, *z*, MIN-1, and MIN-2 Dimensions	22
3-1	Physical Properties of Adsorbents	34
3-2	Summary of Gases and Physical Properties	36
3-3	Equilibrium Constants and Total Amount Adsorbed for HZSM-5	37
3-4	MEA Accessible Surface Areas and Volumes for HZSM-5	38
3-5	Enthalpies and Entropies of Adsorption for HZSM-5	39
4-1	Summary of Physical and Molecular Properties of Adsorbates	62
4-2	Physical Properties of Na-Mordenite and H-Mordenite	63
4-3	Equilibrium Constants and Total Volume Adsorbed for Na-Mordenite	68
4-4	MEA Accessible Surface Areas and Volumes of Na-Mordenite	69
4-5	Equilibrium Constants and Total Volume Adsorbed for Na-Mordenite	75
4-6	MEA Accessible Surface Areas and Volumes of H-Mordenite	76
4-7	Enthalpies and Entropies of Adsorption with Na-Mordenite	77
4-8	Enthalpies and Entropies of Adsorption with H-Mordenite	77
5-1	Molecular *x*, *y*, *z*, MIN-1, and MIN-2 Dimensions	98
5-2	Distribution of Aromatics in the Product Stream and in the Adsorbed Phase	101
5-3	Comparison of Space Velocity Effects on Distribution of Xylenes	108
5-4	Distribution of Aromatics in the Product Stream	109

Table		page
6-1	Prediction of N_2 Adsorption Capacity for Solids at Various Temperatures	125
6-2	Prediction of CO Adsorption Capacity for Solids at Various Temperatures	126
6-3	Prediction of CH_4 Adsorption Capacity for Solids at Various Temperatures	127
6-4	Prediction of C_2H_6 Adsorption Capacity for Solids at Various Temperatures	128
6-5	Prediction of SF_6 Adsorption Capacity for Solids at Various Temperatures	129
6-6	Average Error of Predicted Adsorption Capacity for All Solids for All Methods	130
6-7	Average Error of Predicted Adsorption Capacity for All Solids for the Two n_i Methods	130
6-8	Average Error of Predicted Adsorption Capacity for All Solids for the Two K_i Methods	131

LIST OF FIGURES

Figure		page
1-1	Diagrammatic representation of adsorption from the gas phase	1
1-2	Crystalline and amorphous solids	2
2-1	Correlation of the experimental molar volume to calculated molar volumes	14
2-2	Illustration of the excluded molecular area	18
2-3	Illustration of surface adsorbed SF_6	19
2-4	Application of the MIN-1 and MIN-2	24
3-1	Adsorption isotherms for the small molecules	35
3-2	Adsorption isotherms for the larger molecules	35
3-3	van't Hoff plots ($\ln K_{1,ads}$ vs 1/T(K)) for various adsorptives with HZSM-5	40
3-4	$-\Delta S_{small\ pore}$ vs $-\Delta H_{small\ pore}$ for HZSM-5	43
3-5	Plot of the entropy of adsorption vs the entropy of vaporization	45
3-6	Enthalpy of adsorption vs van der Waals $(a)^{½}$	46
3-7	Process resolved isotherms for CH_4 adsorption	48
4-1	Schematic for the Mordenite aluminosilicate framework	60
4-2	Adsorption isotherms for the small adsorbates on Na-mordenite	66
4-3	Adsorption isotherms for the larger adsorbates Na-mordenite	66
4-4	Resolved adsorption isotherm for N_2	70
4-5	Adsorption isotherms for the adsorbates on H-mordenite	71
4-6	Example of van't Hoff plots ($\ln K_i$ vs 1/T (K)) on Na-mordenite	76
4-7a	CO entropy-enthalpy plots	80
4-7b	C_2H_6 entropy-enthalpy plots	81

Figure		page
4-8	Enthalpy of adsorption vs $a^{1/3}$	83
4-9	Linear free energy relationship	86
5-1	Selectivity in zeolites	93
5-2	Selectivity in zeolites	94
5-3	Crystallographic pore size vs center-to-center distance	95
5-4	Application of the MIN-1 and MIN-2	100
5-5	Determination of the activation energy of diffusion	105
5-6	Illustration of the isomerization of 1,2,4,5-tetramethylbenzene	110
5-7	Illustration of the isomerization of 1,2,4-trimethylbenzene	111
6-1	Experimental and predicted adsorption isotherms for CO on three solids	122
6-2	Experimental and predicted adsorption isotherms for CH_4 and N_2	123
6-3	Experimental and predicted adsorption isotherms for C_2H_6 and SF_6	124
6-4	Experimental and predicted CH_4 isotherm	125

Abstract of Dissertation Presented to the Graduate School
of the University of Florida in Partial Fulfillment of the
Requirements for the Degree of Doctor of Philosophy

MODELING ADSORPTION:
INVESTIGATING ADSORBATE
AND
ADSORBENT PROPERTIES

By

Charles Edwin Webster

May 1999

Chair: Dr. Michael J. Scott
Major Department: Chemistry

Surface catalyzed reactions play a major role in current chemical production technology. Currently, 90% of all chemicals are produced by heterogeneously catalyzed reactions. Most of these catalyzed reactions involve adsorption, concentrating the substrate(s) (the adsorbate) on the surface of the solid (the adsorbent). Pore volumes, accessible surface areas, and the thermodynamics of adsorption are essential in the understanding of solid surface characteristics fundamental to catalyst and adsorbent screening and selection. Molecular properties such as molecular volumes and projected molecular areas are needed in order to convert moles adsorbed to surface volumes and areas. Generally, these molecular properties have been estimated from bulk properties, but many assumptions are required. As a result, different literature values are employed for these essential molecular properties. Calculated molar volumes and excluded molecular areas are determined and tabulated for a variety of molecules. Molecular dimensions of molecules are important in the understanding of molecular exclusion as well as size and shape selectivity, diffusion, and adsorbent selection. Molecular dimensions can also be used in the

determination of the effective catalytic pore size of a catalyst. Adsorption isotherms, on zeolites, (crystalline mineral oxides) and amorphous solids, can be analyzed with the Multiple Equilibrium Analysis (MEA) description of adsorption. The MEA produces equilibrium constants (K_i), capacities (n_i), and thermodynamic parameters (enthalpies, ΔH_i, and entropies, ΔS_i) of adsorption for each process. Pore volumes and accessible surface areas are calculated from the process capacities. Adsorption isotherms can also be predicted for existing and new adsorbate-adsorbent systems with the MEA. The results show that MEA has the potential of becoming a standard characterization method for microporous solids that will lead to an increased understanding of their behavior in gas adsorption and catalysis. These studies are also applicable to environmental cleanup applications, such as waste stream purification and separation procedures as well as decontamination of chemical warfare agents.

CHAPTER 1
INTRODUCTION

Work presented in this dissertation involves several projects aimed at an improved fundamental understanding of molecular interactions and solid surface properties, particularly adsorption--the concentration of a molecule from either the gas phase or from solution onto a surface (see Figure 1-1). The work presented in this dissertation is divided into five chapters. The second chapter deals with the assignment of molecular dimensions for molecules, adsorptives, which may undergo physisorption/chemisorption interactions with a solid. This chapter sets the theme for the remainder of the dissertation--describing adsorption through theoretical and empirical modeling. The third and fourth chapters deal with the Multiple Equilibrium Analysis (MEA) description of adsorption with zeolitic (crystalline oxides, Figure 1-2a) and carbonaceous (amorphous, Figure 1-2b) solids. The fifth chapter demonstrates the

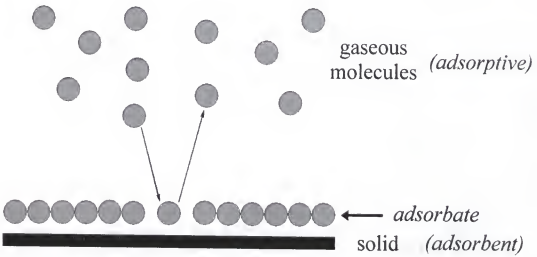

Figure 1-1: Diagrammatic representation of adsorption from the gas phase.

utilization of the MEA for a quantitative prediction of adsorption isotherms on a variety of solids at multiple temperatures with a series of adsorbate molecules. The sixth and final chapter describes the effective catalytic pore size (ECPS) as well as the exterior shape selectivity (nest effect) of the zeolite HZSM-5. The determination of the ECPS is made by an analysis of the products observed from the heterogeneously catalyzed conversion of methanol to gasoline (MTG) over HZSM-5 at elevated temperatures. With knowledge of the molecular dimensions of the potential MTG products, the ECPS may be determined by observing the product stream by gas chromatography (GC) and reaction products by magic angle spinning nuclear magnetic resonance (MAS NMR). The nest effect may be observed by a comparison of the products from the MTG process at several different reactant flow rates.

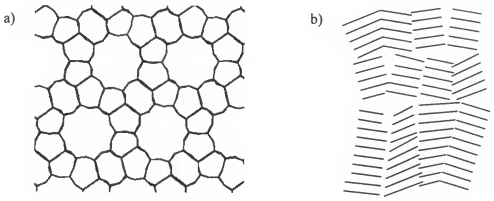

Figure 1-2: Crystalline and amorphous solids. (a) View of the large channel of HZSM-5 (*b* symmetry axis). (b) Diagrammatic representation of an amorphous carbonaceous solid which contains parallel sheets or planes with localized graphitic domains.

Data Analysis

Computer programming plays a major role in many facets of chemical research, from simulation and calculation to instrument control and data processing. Historically, the Fortran programming language has been the standard language used in scientific applications. The work in this dissertation (and other projects in our research group) has involved several different

computer programs written in Fortran 77. Without the modification and implementation of these programs, this project and others could have never been completed. The Fortran 77 programming will not be discussed outside of this chapter. The Appendices include the commented code as well as instructions and sample input decks.

In the determination of an excluded molecular area, one must use the projection of the molecule onto a plane. The position of the points which describe the molecule are calculated by the GEPOL subroutine implemented in ZINDO, a series of molecular electronic structure programs from the Quantum Theory Project at the University of Florida. For a given conformer, this subroutine computes the surface for the molecule as a distribution of points and calculates its area and the volume enclosed. Each point represents a piece of the surface named a tessera. For our purposes, the van der Waals molecular surface was the envelope surface computed, which is a set of intersecting spheres with given atomic radii centered on the nuclei of the atoms of the molecule. It is necessary to have a computer program (Appendix B, written in Fortran 77) that finds the outermost points of the projection and calculates an area by summing the areas of small-inscribed rectangles, similar to the application of the Trapezoidal Rule. (See Chapter 2 for more details on the results of this program.)

In the application of the Multiple Equilibrium Analysis (MEA) to an array of adsorption isotherm data from several temperatures, the optimization of n_i (the capacity of the solid for adsorption) and K_i (the thermodynamic equilibrium constant for adsorption) is required. A computer program that takes the initial seed values of the parameters, n_i and K_i estimated by the user and optimizes the parameter values to reproduce the experimental data and describe the adsorption process was designed (Appendix A, written in Fortran 77). The implementation of the program employs a constrained, downhill simplex minimization algorithm. Since a valid mathematical solution for the solved MEA equation can contain negative values for the n_i and K_i parameters (which have no physical significance), the parameter optimization is constrained. This program calculates the iterative errors in the n_i and K_i parameters and performs a weighted

(or unweighted) least-squares linear regression of the natural logarithm of K_i ($\ln K_i$) vs the reciprocal of the temperature in Kelvin (1/T(K)) for the temperature-dependent adsorption experiments. A graph of the $\ln K_i$ vs (1/T(K)) is a van't Hoff plot from which the enthalpies and entropies of adsorption for the interaction of a gaseous molecule with a solid surface can be determined. Other optional output includes the individual and total process surface areas and pore volumes (calculated with the input of a excluded molecular area and calculated molar volume of the probe) as well as the ability to have the program write a new input file with the new calculated parameters. (See Chapters 3 and 4 for more details on the application of the MEA.)

In the Cal-Ad method developed by Drago and coworkers, optimization of the parameters (n_i, K_i, and ΔH_i) is also achieved with a simplex algorithm. Here again, since the mathematical solution to the solved equation requires positive parameters for a meaningful interpretation, the Fortran 77 code was modified to make this a constrained simplex algorithm to ensure positive calculated parameters (which have physical significance). The program was modified to automatically rerun the algorithm with the newly calculated parameters. This restart of the algorithm is a requirement of simplex to test the soundness of the achieved minimum. Additional features were also added to the program, including the capability to write both the sum of the squares of the errors of the calorimetric and adsorption data and the best residual to the output file. The value of the minimizing function is the best residual, which is the square root of the total sum of the squares of the errors divided by the total number of data points minus one. An error in the calculation of the estimated standard deviation of the n_i and K_i parameters was corrected. To aid the monitoring of the refinement of the parameters, a graphical indicator was added--the current best residual and a count of the current internal loop and external loop is written to the computer screen while the program is operating.

In the determination of the parameters of the Unified Solvation Model developed by Drago and coworkers, a program is required to solve multiple simultaneous equations of various

related chemical systems. In order to enhance the ability to accurately model chemical systems, the program was modified to allow for the determination of more parameters.

CHAPTER 2
MOLECULAR DIMENSIONS FOR ADSORPTIVES

Introduction

Surface composition, area, and porosity are fundamental properties of solids that determine their suitability as adsorbents and catalyst supports. Porosity leads to shape selectivity in reactions as well as in separations and microporosity leads to large surface areas. Surface composition influences the acidity, basicity, hydrophobicity, and hydrophilicity of the solid. Acidity, surface area, pore volume, and pore dimensions of solids are routinely described with quantitative scales, but a fundamental basis for the scales is lacking, and therefore, the meaning often is uncertain. Pore volumes, surface areas, and pore size distributions of solids are calculated from experimental adsorption isotherms using a variety of empirical models.[1] Pore volumes and surface areas are often quoted based on measurements with nitrogen but are adsorbate-dependent quantities that depend on the pore sizes in the distribution that are accessed. For example, adsorptives larger than nitrogen may be excluded from small pores included in the nitrogen measurements. Adsorptives that give rise to specific donor-acceptor interactions result in dissimilar surface coverage when compared to those that do not.[2] Localized adsorption accompanying specific interactions (*i.e.*, one site-one adsorbate) leads to molecular orientations of the adsorptive on specific parts of the solid surface that prevent complete coverage by influencing lateral interactions between adjacent adsorbates.[3] An underestimate of the adsorbent surface area results. Even larger errors result in estimating areas when multilayer coverage occurs, and the assumption is made that there was a monolayer. Mobile adsorption gives an overestimate of the adsorbent surface area since the mean molecular occupancy is more than one molecule per surface

site. The assumption is made that the adsorbed layer is liquidlike even below the saturation pressure. Criticism of this assumption arises from the application of the Clausius-Clapeyron equation to adsorption and to vapor pressure data and comparing the integration constants which do not show the correspondence of the two required by the Brunauer, Emmett, and Teller (BET) theory.[4] Finally, the BET theory assumes indefinite uptake of a saturated liquid (adsorption) over porous and planar solids. Careful measurements have shown that this adsorption is a strictly limited quantity.[5] Adamson[1] discusses the problems encountered in the calculation and empirical determination of adsorbent surface areas in detail.

For high surface area, microporous solids, traditional methods give inadequate measures of pore volumes and surface area. This insufficiency is unfortunate because microporous solids are important for efficient adsorption and for high surface area supports. Recently, a multiple equilibrium model has been proposed to interpret gas adsorption isotherms.[6,7] A series of *i*-equilibrium constants and *i*-capacities are used to characterize the minimal *i*-processes required to fit the isotherm. Each process corresponds to adsorption in a different size pore regime. The isotherms measured at several temperatures produce equilibrium constants, enthalpies, and capacities in moles per gram for each process.

With all models, knowledge of molecular dimensions is needed to convert moles of adsorbate to volumes and surface areas. Pore volume determination, mL g^{-1}, requires knowledge of molecular volumes to convert the experimental measure of moles adsorbed in units of moles g^{-1} to volume per gram. When known, the molar volume at the normal boiling point is used to make this conversion. However, reported measures of molar volumes show considerable variation. When not measured, boiling point molar volumes may be estimated both by additive methods and from critical volumes.[8] The shortcomings of these estimates have been discussed.[8]

The determination of occupied areas, $m^2 g^{-1}$, from the experimental measure of moles adsorbed in units of moles g^{-1} requires knowledge of the molecular area. Areas occupied by a

molecule in a monomolecular coating have been estimated using simple drop shadow model calculations.[9] Hill[10] has derived Equation 2-1 to calculate areas of molecules in $Å^2$ from the two dimensional van der Waals constant, b'.

$$\text{area}_{VDW} = b' = 6.354 \left(T_c / P_c \right)^{2/3} \tag{2-1}$$

T_c and P_c are the critical temperature (K) and pressure (atm).[10] Brunauer, Emmett, and Teller (BET) surface areas ($m^2\ g^{-1}$) are commonly determined using a molecular area calculated from the liquid density, assuming spherical symmetry and a hexagonal close packing of the adsorbed layer. These approximations lead to the liquid density surface area, area_{LD} of Equation 2-2 in cm^2 per molecule, where MW is the molecular mass in Daltons, N_A is Avogadro's number, and ρ is the density ($g\ cm^{-3}$) at a given temperature.

$$\text{area}_{LD}\ (cm^2) = 1.091\ (MW / N_A \rho)^{2/3} \tag{2-2}$$

Although hexagonal close packing has been the standard in the literature, other packing factors have been proposed.[11] The areas that result from Equation 2-2 are similar to the values obtained from Equation 2-1.

Calculation of molecular volumes and areas with quantum mechanics is feasible and would have several advantages over existing compilations. The variable literature reports and different experimental estimates would be replaced by an internally consistent set of dimensions which could be calculated for new systems without recourse to time-intensive experiments. In this chapter, ZINDO molecular orbital calculations are carried out on a variety of molecules to produce structures from which molecular volumes, molecular areas, and critical molecular dimensions are

calculated. These quantities are essential for the determination of surface areas and pore volumes as well as many other applications of porous solids including shape and size selectivity.

Calculations

ZINDO, a series of molecular electronic structure programs from the Quantum Theory Project at the University of Florida, was used to calculate molecular dimensions for both the lowest energy molecular structure and other relevant molecular conformations.[12] Implementation of the subroutine GEPOL (GEometria POLihedro,1993) calculates the molecular surface area and the molecular volume of a molecule from the calculated structure.[13] The excluded molecular areas are calculated by projecting the shadow of the three-dimensional molecule onto a plane and connecting the outermost points. From these outermost points, an area is calculated from summing the areas of small-inscribed rectangles, similar to the application of the Trapezoidal Rule. A FORTRAN 77 program was written to calculate the excluded molecular areas in Table 2-2.

Results and Discussion

Pore Volumes

The porosity of a solid can be expressed in terms of a pore volume, which usually is calculated from the molar volume of an adsorbate needed to fill the pores. This measure of porosity will vary with the adsorbate, for some may be too large to fit in the smaller pores. Pore volumes from adsorbates will also differ from structural volumes, because voids are created by adsorption of a molecule on one wall of a channel when the space between it and the opposite wall is too small for a second molecule. These voids lead to a lower pore volume than the structural pore volume of the solid. Our use of the term *pore volume* will refer to the volume capacity of the adsorbate, the term *structural pore volume* will be used to describe the solid's structural porosity, and *surface areas* will refer to the area of the pore or channel covered by the adsorbate.

To obtain a consistent set of adsorbate volumes for use in the conversion of moles per gram adsorbed to volume per gram, we propose to use molecular volumes determined using the GEPOL package from structures calculated with ZINDO. The calculated molecular volumes, in $Å^3$ molecule^{-1}, for a series of molecules are presented in Table 2-1 under the column labeled mVG. Converting these mVG values in $Å^3$ molecule^{-1} to mL mole^{-1} produces calculated molar volumes, *M*VG, which are also presented in Table 2-1.

In order to determine the relation of these calculated values for *M*VG to experimental measurements, a correlation to experimental molar volumes, MV_{EXP} is attempted. For adsorbates that are liquid at room temperature, the molar volumes are determined from the liquid density at 25 °C and the molecular weight, *e.g.*, pentane has a density of 0.6262 g mL^{-1} that leads to a molar volume of 115.2 mL mole^{-1}. For adsorbates that are gases at room temperature, the liquid density at the normal boiling point is used in the calculation of the value used in the correlation. Over 100 polar, nonpolar, saturated, unsaturated, aromatic, and other molecules with experimental molar volumes ranging from approximately 18 (water) to 274 (tributylphosphate) mL mole^{-1} give an excellent linear correlation to the calculated values of *M*VG shown by Equation 2-3. It is significant that the slope of the line in Equation 2-3 is equal to the cube of the reaction field correction factor (RFCF) of 1.2 employed by ZINDO.* Thus, the volume calculated from the ZINDO geometry, with the reaction field correction applied, gives the molar volume when converted to mL mole^{-1}.

$$MV_{EXP} = 1.7328\, MVG \qquad (R^2 = 0.9797) \qquad (2\text{-}3)$$

*A common scaling of all van der Waal radii by 1.2 is used in most reaction field models to give good energies of solvation as well as excitation energies. The cube of this, 1.728, might be compared with the empirically determined slope of 1.733 of Equation 2-3.

The liquid molar volumes, MVL, calculated from *M*VG with Equation 2-3, compared to the experimental values, MV_{EXP}, in Table 2-1 are plotted in Figure 2-1. The quantity Δs (Table 2-1) is the percent error in the calculated relative to the experimental molar volumes.

Table 2-1. Molecular and Molar Volumes

compound (source[a])	density ($g\ mL^{-1}$)	MW ($g\ mol^{-1}$)	MV_{EXP} ($mL\ mol^{-1}$)	mVG ($Å^3\ molc^{-1}$)	*M*VG ($mL\ mol^{-1}$)	MVL ($mL\ mol^{-1}$)	Δs[b] (%)
acetone (L)	0.7908	58.08	73.45	64.447	38.81	67.25	-8.4
acetonitrile (L)	0.7868	41.05	52.17	45.943	27.67	47.94	-8.1
acetophenone (L)	1.026	120.15	117.11	120.490	72.56	125.73	7.4
ammonia (L)	0.6818	17.04	24.99	23.392	14.09	24.41	-2.3
aniline (L)	1.0217	93.13	91.15	96.448	58.08	100.64	10
anisole (L)	0.9942	108.14	108.77	108.960	65.62	113.70	4.5
benzene (L)	0.8787	78.11	88.89	85.319	51.38	89.03	0.2
benzonitrile (CRC)	1.010	103.12	102.10	102.640	61.81	107.11	4.9
benzylbromide (L)	1.438	171.04	118.94	119.300	71.84	124.48	4.7
benzylchloride (L)	1.100	126.59	115.08	115.140	69.34	120.15	4.4
bromobenzene (CRC)	1.4950	157.02	105.03	102.120	61.50	106.56	1.5
butane (L)	0.6011	58.12	96.69	78.609	47.34	82.03	-15
2-butanone (CRC)	0.8054	72.11	89.53	81.232	48.92	84.76	-5.3
1-butene (L)	0.6255	56.10	89.69	73.288	44.13	76.48	-15
butylacetate (CRC)	0.8825	116.16	131.63	121.950	73.44	127.25	-3.3
4-butyrolactone (L)	1.124	86.09	76.59	79.555	47.91	83.02	8.4
carbon dioxide (CRC)	1.101	44.01	39.97	34.048	20.50	35.53	-11
carbon disulfide (L)	1.2632	76.14	60.28	53.612	32.29	55.94	-7.2
carbon monoxide (L)	0.814	28.01	34.41	27.104	16.32	28.28	-18
carbon tetrachloride (CRC)	1.594	153.82	96.50	83.667	50.38	87.31	-9.5
carbon tetrafluoride (L)	1.96	88.00	44.90	48.073	28.95	50.16	12
chlorine (L)	1.5649	70.91	45.31	39.928	24.04	41.66	-8.0
chlorine monofluoride (L)	1.67	54.56	32.67	30.376	18.29	31.70	-3.0
chlorine trifluoride (L)	1.825	92.45	50.66	47.432	28.56	49.49	-2.3
chlorobenzene (CRC)	1.1058	112.56	101.79	98.478	59.30	102.76	1.0
chloroform (L)	1.484	119.39	80.45	69.944	42.12	72.99	-9.3
chloromethane (L)	0.92	50.49	54.88	42.534	25.61	44.38	-19
cyclobutane (CRC)	0.720	56.10	77.92	69.614	41.92	72.64	-6.8
cyclodecane (L)	0.871	140.27	161.04	164.340	98.97	171.49	6.5
cycloheptane (L)	0.811	98.18	121.06	116.820	70.35	121.90	0.7
cyclohexane (CRC)	0.7785	82.15	105.52	101.060	60.86	105.45	-0.1
cyclohexanone (L)	0.9478	98.15	103.56	103.630	62.41	108.14	4.4
cyclooctane (L)	0.834	112.22	134.56	133.970	80.67	139.79	3.9
cyclopentane (CRC)	0.7457	70.13	94.05	84.550	50.92	88.23	-6.2
cyclopropane (L)	0.720	42.08	58.44	54.718	32.95	57.10	-2.3

Table 2-1--continued

compound (source[a])	density ($g\ mL^{-1}$)	MW ($g\ mol^{-1}$)	MV_{EXP} ($mL\ mol^{-1}$)	mVG ($Å^3\ molc^{-1}$)	*M*VG ($mL\ mol^{-1}$)	MVL ($mL\ mol^{-1}$)	Δs^b (%)
decane (L)	0.7301	142.28	194.88	179.310	107.98	187.10	-4.0
dibutylether (CRC)	0.7689	130.22	169.36	153.120	92.21	159.78	-5.7
2,6-di-t-butylpyridine (A)	0.852	191.31	224.54	210.310	126.65	219.46	-2.3
1,2-dichlorobenzene (CRC)	1.3048	147.01	112.67	111.510	67.15	116.36	3.3
dichloromethane (CRC)	1.3266	84.93	64.02	56.301	33.90	58.75	-8.2
diethylether (CRC)	0.7138	74.12	103.84	87.121	52.46	90.91	-12
N,N-diethylformate (L)	0.908	101.15	111.40	109.420	65.89	114.18	2.5
diisoproether (L)	0.7258	102.17	140.77	120.220	72.40	125.45	-11
N,N-dimethylacetate (L)	0.9366	87.12	93.02	92.813	55.89	96.85	4.1
N,N-dimethylaniline (L)	0.9559	121.18	126.77	128.930	77.64	134.53	6.1
N,N-dimethylcyanamide (L)	0.867	70.09	80.84	72.154	43.45	75.29	-6.9
dimethylether (L)	0.661	46.07	69.70	54.012	32.53	56.36	-19
N,N-dimethylformate (L)	0.9445	73.10	77.40	76.822	46.26	80.16	3.6
1,4-dioxane (L)	1.0329	88.10	85.29	84.342	50.79	88.01	3.2
diphenylether (L)	1.0661	170.21	159.66	163.480	98.45	170.59	6.9
dodecane (L)	0.7490	170.41	227.52	211.590	127.42	220.79	-3.0
ethane (CRC)	0.5720	30.07	52.57	45.241	27.24	47.21	-10
ethylacetate (L)	0.9006	88.11	97.83	89.700	54.02	93.60	-4.3
ethylbenzene (L)	0.8670	106.17	122.46	118.140	71.14	123.28	0.7
ethylformate (L)	0.917	74.08	80.79	73.026	43.98	76.20	-5.7
fluorine (L)	1.513	38.00	25.11	20.737	12.49	21.64	-14
fluorine monooxide (CRC)	1.90	54.00	28.42	28.775	17.33	30.03	5.6
heptane (L)	0.6838	100.20	146.54	128.510	77.39	134.10	-8.5
hexamethylphosphoramide (CRC)	1.024	179.20	175.00	176.090	106.04	183.75	5.0
hexane (CRC)	0.6603	86.18	130.52	112.320	67.64	117.20	-10
hexylacetate (L)	0.8779	144.21	164.27	156.450	94.21	163.25	-0.6
2,6-lutidine (L)	0.9200	107.15	116.47	113.070	68.09	117.99	1.3
methane (CRC)	0.4660	16.04	34.42	28.498	17.16	29.74	-14
methylacetate (L)	0.9342	74.08	79.30	72.762	43.82	75.93	-4.3
N-methylimidazole (L)	1.03	82.11	79.72	82.123	49.45	85.69	7.5
4-methylpyridine (CRC)	0.9548	93.13	97.54	96.381	58.04	100.57	3.1
N-methyl-2-pyrolidinone (CRC)	1.026	99.13	96.62	100.380	60.45	104.74	8.4
N-methylpyrrolidine (L)	0.819	85.15	103.97	96.795	58.29	101.00	-2.9
3-methylsulfonane (L)	1.191	134.20	112.68	121.610	73.23	126.89	13
naphthalene (CRC)	0.9625	128.17	133.16	128.260	77.24	133.84	0.5
nitrobenzene (CRC)	1.2037	123.11	102.28	106.860	64.35	111.51	9.0
nitroethane (L)	1.0528	75.07	71.31	67.885	40.88	70.84	-0.7
1-nitropropane (CRC)	1.0081	89.09	88.37	84.634	50.97	88.31	-0.1
nitrogen (CRC)	0.8081	28.03	34.69	23.981	14.44	25.02	-28
nitrogen dioxide (CRC)	1.4494	46.01	31.74	31.416	18.92	32.78	3.3
nitromethane (CRC)	1.1371	61.04	53.68	51.378	30.94	53.61	-0.1
nitrosyl chloride (L)	1.592	65.47	41.12	40.285	24.26	42.04	2.2

Table 2-1--continued

compound (source[a])	density ($g\ mL^{-1}$)	MW ($g\ mol^{-1}$)	MV_{EXP} ($mL\ mol^{-1}$)	mVG ($Å^3 molc^{-1}$)	*M*VG ($mL\ mol^{-1}$)	MVL ($mL\ mol^{-1}$)	Δs^b (%)
nonane (L)	0.7176	128.26	178.73	161.800	97.44	168.84	-5.5
octane (L)	0.7025	114.23	162.61	145.270	87.48	151.59	-6.8
oxygen (CRC)	1.149	32.00	27.85	22.573	13.59	23.55	-15
p-xylene (CRC)	0.8611	106.16	123.28	117.570	70.80	122.69	-0.5
pentamethylbenzene (L)	0.917	148.25	161.67	165.250	99.51	172.43	6.7
pentane (L)	0.6262	72.15	115.22	95.537	57.53	99.69	-13
3-pentanone (L)	0.8143	86.13	105.77	97.744	58.86	102.00	-3.6
propane (CRC)	0.5853	44.10	75.35	61.839	37.24	64.53	-14
propionitrile (CRC)	0.7818	55.08	70.45	62.586	37.69	65.31	-7.3
propylacetate (CRC)	0.8878	102.13	115.04	106.190	63.95	110.81	-3.7
propylbenzene (L)	0.8621	120.20	139.43	134.260	80.85	140.10	0.5
propylene carbonate (L)	1.204	102.09	84.79	87.825	52.89	91.64	8.1
pyridine (A)	0.978	79.10	80.88	79.479	47.86	82.94	2.5
quinoline (CRC)	1.0929	129.16	118.18	123.270	74.23	128.63	8.8
sulfur dioxide (CRC)	1.434	64.06	44.67	41.227	24.83	43.02	-3.7
sulfur hexafluoride (L)	1.88	146.07	77.70	73.825	44.46	77.04	-0.9
sulfur tetrafluoride (L)	1.919	108.07	56.32	56.697	34.14	59.16	5.1
sulfur trioxide (L)	1.9225	80.07	41.65	50.243	30.26	52.43	26
tetrahydrofuran (L)	0.8892	72.11	81.10	76.790	46.24	80.13	-1.2
tetrahydropuran (L)	0.8814	86.14	97.73	92.937	55.97	96.98	-0.8
tetrahydrothiophene (L)	0.9987	88.17	88.28	86.102	51.85	89.85	1.8
tetramethylene sulfone (L)	1.2614	120.17	95.27	104.670	63.03	109.22	15
1,1,3,3-tetramethylurea (L)	0.9687	116.16	119.91	121.040	72.89	126.30	5.3
thiophene (CRC)	1.0649	84.14	79.01	75.391	45.40	78.67	-0.4
toluene (CRC)	0.8669	92.14	106.29	101.320	61.01	105.73	-0.5
tributylphosphate (L)	0.972	266.32	273.99	269.330	162.19	281.04	2.6
1,1,1-trichloroethane (CRC)	1.3390	133.42	99.64	86.526	52.11	90.29	-9.4
1,1,2-trichloroethane (L)	1.4416	133.42	92.55	86.316	51.98	90.07	-2.7
triethylphosphate (CRC)	1.0725	182.16	169.85	170.150	102.47	177.55	4.5
1,2,4-trimethylbenzene (L)	0.8756	120.20	137.28	134.310	80.88	140.15	2.1
1,3,5-trimethylbenzene (L)	0.8637	120.20	139.17	134.140	80.78	139.98	0.6
tripropylphosphate (A)	1.012	224.24	221.58	220.590	132.84	230.18	3.9
undecane (L)	0.7402	156.31	211.17	195.400	117.67	203.89	-3.4
water (CRC)	0.9970	18.02	18.07	19.714	11.87	20.57	14

a. Source of data:
L: *Lange's Handbook of Chemistry*, 13th Edition; McGraw-Hill: NY, 1985.
CRC: *Handbook of Chemistry and Physics*, 71st Edition; CRC Press: Florida, 1991.
A: *Aldrich Catalog 1994-1995*, Aldrich Chemical Company: Milwaukee, WI, 1994.

b. $\Delta s = (100 \times (MVL - MV_{EXP})) \div MV_{EXP}$

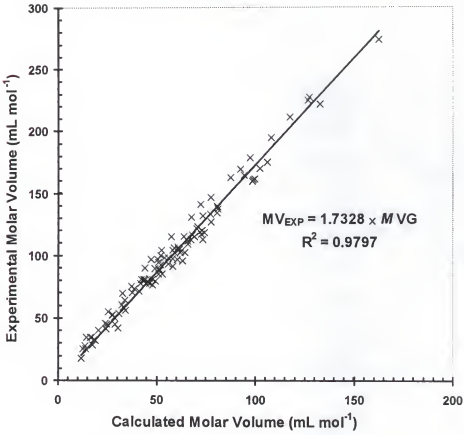

Figure 2-1: Correlation of the experimental molar volume, MV_{EXP}, to calculated molar volumes, *M*VG. The slope of the line is the cube of the reaction field correction factor employed by ZINDO.

The excellent correlation of the calculated and experimental values indicates that molecular packing in the liquid phase has a minor effect on the bulk density. This is an important result, for it indicates that the molecular volumes are directly proportional to the molar volumes. Thus, molecular volumes can be calculated with GEPOL using a reaction field correction factor (RFCF) and converted mL $mole^{-1}$ to give the molar volume in the liquid state, without any of the conventional assumptions involving packing or molecular symmetry. With molar volumes given by density divided by molar mass, the correlation of molar volumes also implies a prediction of liquid densities.

In porosity analyses, MVL can be used to calculate the pore volume occupied by the adsorbate by converting the total moles adsorbed to a volume. For most adsorbates, the occupied

pore volume calculated from the moles adsorbed will be an underestimate of the structural porosity because packing of molecules smaller than the pore dimensions will result in voids. The adsorptive-dependent occupied pore volumes are relevant quantities, for they represent the volume available for the adsorptive in the solid. For a solid with fixed pore dimensions, *e.g.*, a zeolite, the most reliable estimates of the structural pore volume will come from the study of adsorbates whose dimensions are close to those of the pores, so packing will be most efficient.

Multiple equilibrium analyses, MEA, of adsorption isotherms have produced adsorption equilibrium constants (K_i) and capacities (n_i) in moles per gram for adsorption into the *i*-different groups of pore size distributions in a given solid. The smallest group of pores, with the largest equilibrium constant for binding, give rise to process 1. Smaller equilibrium constants, corresponding to groupings of larger pores, are numbered consecutively. The minimum number of processes required to fit isotherms measured at three or more temperatures are used to define the system. The pore volumes for the adsorption of six different molecules by HZSM-5 (Si/Al = 53) are obtained by summing the mmoles g^{-1} for all the processes[6] and converting to volume with MVL for N_2, CO, CH_4, C_2H_6, C_3H_8, and SF_6 to yield total pore volumes of 0.071, 0.082, 0.080, 0.091, 0.099, and 0.138 mL g^{-1}, respectively, show that the capacities depend on the adsorbate. SF_6, the probe closest to the dimensions of the HZSM-5 pore, produces the highest calculated pore volume. These calculations are in accordance with the view that probe molecules smaller than the pore dimensions give rise to voids in filling the HZSM-5 channels. The calculated micropore volume from Harkins-Jura *t*-plots is 0.14 mL g^{-1}, which is in excellent agreement with the result from SF_6 adsorption.

Surface Areas

Conversion of moles g^{-1} adsorbed in a monolayer to area g^{-1} produces the accessible solid surface areas for the different adsorbates. For adsorbates undergoing non-specific interactions, the

calculated *molecular* surface area is determined by the projection of the molecule onto a plane. This calculated area is termed the excluded surface area. The geometry of the adsorbate on the surface will influence the amount covering the surface and needs to be predicted to calculate the area occupied by an adsorbate molecule. The conformation of the molecule may not necessarily be the same as the minimum energy structure in the gas state, or even in solution. For a non-polar adsorptive, the predicted conformation is the one that maximizes surface contact, with ambiguities resolved by selecting the conformation expected to maximize dispersion interactions. However, the energy change to the predicted conformation from the minimum energy structure must only be a few kcal $mole^{-1}$, so that the net interaction is more exothermic than that of simply binding the minimum energy structure. For example, an ethane molecule, with the carbon-carbon bond parallel to the surface, can interact with the surface with four hydrogens of an eclipsed conformation or with three hydrogens of the minimum energy staggered conformer. The energy cost of 2.8 kcal $mole^{-1}$ to give the eclipsed conformation would have to be provided by an increase in the surface interaction for the eclipsed compared to the staggered form. In view of the ambiguity in the selection of geometries, excluded molecular areas with the RFCF applied are presented in Table 2-2 for the minimum energy conformation and other orientations of the adsorbate molecule on the surface. The calculation of excluded molecular area is illustrated for the SF_6 molecule in Figure 2-2.

For monolayer adsorption, the process capacities in mmol g^{-1} can be converted to surface areas by knowing the molecular area of an adsorbate for the molecular configuration involved in the adsorbate-adsorbent interaction. The process capacities from the MEA of HZSM-5 are summed and converted to surface areas for N_2, CO, CH_4, C_2H_6, C_3H_8, and SF_6. The resulting values are 260, 260, 262, 261, 273, and 335 $m^2 g^{-1}$, respectively.

The value for SF_6 is calculated assuming an open structure in which the molecules adsorb as shown in Figure 2-3a with no overlap of the excluded area. Tighter packing is possible in which

the top triangle of fluorines of one molecule overlaps the bottom triangle of another, *e.g.*, a second SF_6 molecule approaches the first molecule along the *y* axis or similarly the diagonal of Figure 2-3b. Tighter packing is expected because of increased intermolecular dispersion interactions with no loss in adsorbate-surface interactions and leads to an area of 319 $m^2 g^{-1}$.

Ethane in the staggered conformation with three hydrogens interacting or in the eclipsed conformation with four hydrogens interacting have the same area when the C-C bond is parallel to the surface. An ethane molecule could interact in a staggered conformation with the C-C bond perpendicular to the surface. Three hydrogens would interact with one wall of the channel and, to lesser extent, three with the distant wall. This orientation is ruled out in HZSM-5 because the

Table 2-2. Excluded Areas for Different Molecular Orientations

Molecule	Orientation	Area (Å^2)	Molecule	Orientation	Area (Å^2)
acetone	4 CH_3 H's	28.783	methane(2)	2 CH_4 H's	15.350[a]
benzene	6 C's	48.205	methane(3)	3 CH_4 H's	16.261
butane	2 CH_3 H's; 2 CH_2 H's	35.268	N_2	NN	15.272
chloroform	3 Cl's	34.165	NH_3	N	14.785
CO	CO	15.773	nonane	4 CH_3 H's; 6 CH_2 H's	67.588
CO (acid)	C	11.312	O_2	OO	14.655
CCl_4(2)	2 Cl's	34.314	octane	2 CH_3 H's; 6 CH_2 H's	61.477
CCl_4(3)	3 Cl's	34.017	pentane	4 CH_3 H's; 2 CH_2 H's	42.026
CO_2	OCO	19.163	propane(4a)	4 CH_3 H's	28.268
CS_2	SCS	27.293	propane(4b)	2 CH_3 H's; 2 CH_2 H's	26.812
cyclohexane	3 axial H's	47.460	propane(5)	4 CH_3 H's; 1 CH_2 H	29.596
decane	2 CH_3 H's; 8 CH_2 H's	72.944	propylbenzene	9 C's	69.525
diethylether	4 CH_3 H's; O	40.161	pyridine	5 C's; N	45.795
dme	O	26.163	SF_6	3 F's	31.179[b]
ethane(3)	3 CH_3 H's	19.317	SO_2	S	20.908
ethane(4)	4 CH_3 H's	24.009	toluene	7 C's	55.346
ethylbenzene	8 C's	61.615	1,3,5-trimethyl-benzene	9 C's	70.276
H_2O	O	11.130	*m*-xylene	8 C's	64.306
heptane	4 CH_3 H's; 4 CH_2 H's	55.322	*o*-xylene	8 C's	62.382
hexane	2 CH_3 H's; 4 CH_2 H's	48.623	*p*-xylene	8 C's	64.319

a. For a tight-packed methane in this orientation, the excluded molecular area will be 13.441 Å^2.
b. For a tight-packed SF_6 in this orientation, the excluded molecular area will be 29.660 Å^2.

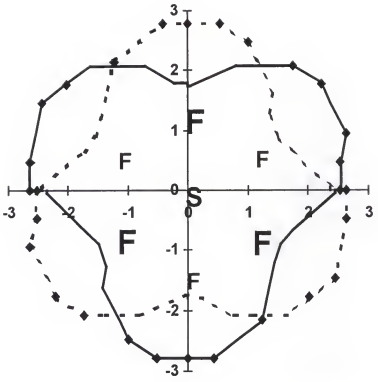

Figure 2-2: Illustration of the excluded molecular area. The SF_6 molecule is chosen to illustrate the projection of a surface bound molecule onto a planar surface. The molecule is arranged to maximize surface interaction. The dashed line outlines the surface bound fluorines illustrated with a large F, and the solid line those on the opposite face of the octahedron illustrated with a small F. The solid diamonds outline the projected area.

resulting surface area would only be 223 $m^2 g^{-1}$. More ethane would be adsorbed in the experiment if this were the orientation of the adsorptive. Thus, the free energy gained by adsorbing more molecules and packing more ethane into the pores does not compensate for the free energy lost in rearranging fewer ethane molecules interacting with the C-C bond parallel to the surface.

Methane was calculated in a conformation with the three hydrogens of the face of the tetrahedron flat on the surface. In HZSM-5, methane could pack with two hydrogens interacting with the surface. Since this orientation leads to a weaker surface interaction and a tight-packed area of 235 $m^2 g^{-1}$, the calculated surface areas distinguish the two possibilities.

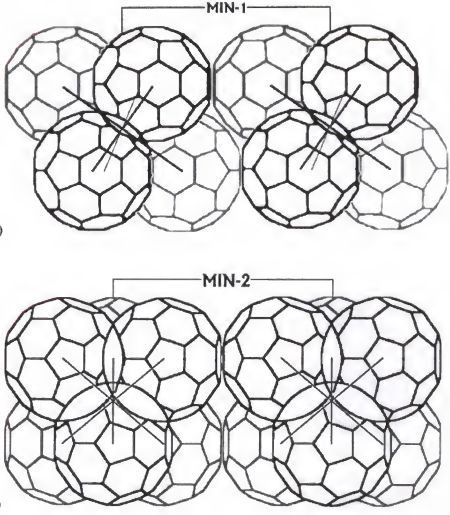

Figure 2-3: Illustration of Surface Adsorbed SF_6 (a) loose packed and (b) tight packed. In (a), the straight lines define the orientation of the octahedron and point to all six fluorines of which all six are visible in this orientation. The two molecules shown are separated by MIN-2. In (b), the straight lines define the orientation of the octahedron and point to all six fluorines of which only four are visible in this orientation. The two molecules shown are separated by MIN-1.

Propane could interact with the surface through five hydrogens (two from each CH_3 and one from CH_2), four hydrogens (from the two CH_3 groups), or four hydrogens (two from methyl and two from CH_2). Areas of 273 $m^2 g^{-1}$, 261 $m^2 g^{-1}$, and 248 $m^2 g^{-1}$, respectively, result. The conformation involving four hydrogens from methyl and methylene groups can be ruled out because of the low surface area calculated. These examples illustrate the added insight into the adsorption process that results from determining adsorbate dependent areas.

These adsorbent surface areas are probe dependent quantities because the accessibility of the solid's porosity will depend on the minimum dimensions of the adsorptive (*vide infra*). Even if a given adsorbate molecule experiences interactions with opposite pore walls (in pores with molecular dimensions), the calculated adsorbent surface area has an inherent accessibility dependence. In a study of the MEA of Na-mordenite,[14] the calculated surface areas demonstrate this probe accessibility dependence quite clearly. Since the side channel of the mordenite structure is only accessed by the smaller adsorptives (N_2 and CO), there is a three-process description of adsorption, while larger adsorptives only have a two-process description of adsorption (for adsorption in the main channel). The calculated surface areas for N_2 and CO are approximately 350 $m^2 g^{-1}$, while the larger adsorptives (CH_4, C_2H_6, SF_6, etc.) have calculated surface areas progressively less than 265 $m^2 g^{-1}$. Therefore, while a given solid could have pores that are of molecular dimensions, the calculated surface area will show this accessibility dependence for adsorptives of similar minimum dimensions (*vide infra*). At this point, it should be noted that the calculated surface area alone can not discriminate pores of molecular dimension from those greater than molecular dimensions. The excluded area of a given probe only describes the area taken by its projection onto a plane. However, since the probe dependent, occupied pore volume represents a three-dimensional occupancy, the calculated pore volume will not be conditional on the ratio of the pore dimension to the adsorptive dimension.

The calculated accessible surface area is by necessity and definition the area excluded by the adsorptive molecules in a plane. An increase in the calculated pore volumes will represent a decrease in the ratio of pore diameter to effective molecular diameter, but only when the pore diameter is less than two molecular diameters. In the case where the pore diameter becomes less than two molecular diameters, by definition, the calculated accessible surface area does not change.

In the case where two or more populations of pores are present for which the diameters are near that of the adsorptive molecule, these pore regimes would be resolvable with an MEA study.

For example, in the HZSM-5 study, the two pores of the structure that are very close in dimensions are resolved by the description of the adsorption process, which MEA provides. If not resolvable, these pores would calculate a given capacity, n_i (more than likely, with a larger error), and therefore one surface area.

The areas from liquid density and the McClellan's average areas[9] (from probe molecules which were measured more than five times, independently) correlate well to each other, R^2 of 0.974. These areas differ significantly from those in Table 2-2, especially for long chain and cyclic hydrocarbons. Our concern, the area of the solid occupied, is for a molecular configuration that maximizes the dispersion contribution and not necessarily the configuration the molecule has in the liquid state. For example, it has been reported that long chain hydrocarbons adsorbed to a surface are elongated to maximize dispersion interactions.[15]

The data in Table 2-2 should find wide application in surface area determination. Different cross sections for complex molecular structures can be calculated and information gained about adsorbate binding configuration. Furthermore, in a solid whose area is known, the number of mmoles of a new adsorbate taken up by the solid can be estimated from the adsorbates surface area. This estimate requires that the molecular dimensions of the new adsorbate and the adsorbate used to determine the solids area permit access to the same pores.

Critical Dimensions

Knowledge of the dimensions of molecules is essential to understanding molecular exclusions as well as shape and size selectivity in zeolites.[16] Table 2-3 contains the dimensions of the molecule along the *x*, *y*, and *z* symmetry axes of the molecule calculated for each atom surrounded by a van der Waal sphere, without the reaction field correction factor of 1.2. The dimension of the adsorbate that is critical for entry into a pore will depend upon the shape of the pore. For example, in slit-shaped pores the size of the adsorptive in the minimum dimension,

MIN-1, will determine if the molecule can enter the pore (see Figure 2-4a). This direction can be determined by rotating the molecule to find an axis which represents the minimum distance through the molecule. In cylindrical pores, the size of the molecule in two directions must be considered. The relevant dimensions are MIN-1 and the next to the smallest perpendicular distance for low energy conformations or molecular orientations that enable a molecule to enter a cylinder, MIN-2 (see Figure 2-4b). Table 2-3 contains the MIN-1 and MIN-2 dimensions of molecules that are relevant to size and shape selectivity considerations. The MIN-1 and MIN-2 distances are specified for each molecule with each atom surrounded by a van der Waal sphere, without the reaction field correction. For example, pentane and hexane are elongated cylinders with approximately the same minimum critical dimensions since they have the same cross sectional diameter.

Table 2-3. Molecular *x*, *y*, *z*, MIN-1, and MIN-2 Dimensions

Molecule	*x*	*y*	*z*	MIN-1	MIN-2
acetone	6.600	4.129	5.233	4.129	5.233
benzene	6.628	7.337	3.277	3.277	6.628
butane	7.855	4.519	4.014	4.014	4.519
chloroform	6.181	5.713	4.613	4.613	5.713
CCl_4	6.207	5.723	5.748	5.723	5.748
CO	3.280	3.339	4.182	3.280	3.339
CO_2	3.339	3.189	5.361	3.189	3.339
CS_2	3.535	3.376	6.655	3.376	3.535
cyclohexane	7.168	6.580	4.982	4.982	6.580
decane	15.319	4.538	4.014	4.014	4.538
diethylether	4.027	8.822	4.556	4.027	4.556
2,6-di-*tert*-butylpyridine	11.344	6.454	8.294	6.454	8.294
dimethyl ether	4.083	6.319	4.127	4.083	4.127
ethane	3.809	4.079	4.821	3.809	4.079

Table 2-3--continued

Molecule	*x*	*y*	*z*	MIN-1	MIN-2
ethylbenzene	6.625	5.285	9.361	5.285	6.625
H_2O	3.226	2.917	3.888	2.917	3.226
heptane	11.589	4.523	4.014	4.014	4.523
hexane	10.344	4.536	4.014	4.014	4.536
2,6-lutidine	8.927	4.127	6.957	4.127	6.957
methane	3.829	4.101	3.942	3.829	3.942
N_2	3.054	2.991	4.046	2.991	3.054
NH_3	3.697	3.989	3.111	3.111	3.697
nonane	14.076	4.524	4.014	4.014	4.524
octane	12.833	4.537	4.014	4.014	4.537
O_2	2.985	2.930	4.052	2.930	2.985
pentane	9.101	4.522	4.014	4.014	4.522
propane	6.606	4.516	4.020	4.020	4.516
propylbenzene	6.625	5.277	10.274	5.277	6.625
pyridine	6.648	3.339	6.475	3.339	6.475
SF_6	6.270	6.182	6.321	4.871	5.266
SO_2	4.227	3.365	5.462	3.365	4.227
toluene	6.625	4.012	8.252	4.012	6.625
1,2,3-trimethybenzene	9.058	4.116	8.227	4.116	7.881
1,2,4-trimethybenzene	7.576	4.024	9.145	4.024	7.251
1,3,5-trimethybenzene	8.276	8.553	4.062	4.062	8.178
m-xylene	9.079	4.012	7.314	4.012	7.258
o-xylene	7.269	3.834	7.826	3.834	7.269
p-xylene	6.618	3.810	9.146	3.810	6.618
HD[a]	9.923	5.098	6.076	5.098	6.076
VX[b]	12.719	9.192	7.804	7.804	9.192
Sarin (GB)[c]	8.299	6.763	6.690	5.622	5.794
Soman (GD)[d]	9.731	8.152	7.247	6.991	7.247

a. 2,2'-dichlorodiethyl sulfide
b. *O*-ethyl S-2-(diisopropylamino)ethylmethylphosphonothiolate
c. 2-propyl methylphosponofluoridate
d. 3,3-dimethyl-2-butylmethylphosphonofluoridate

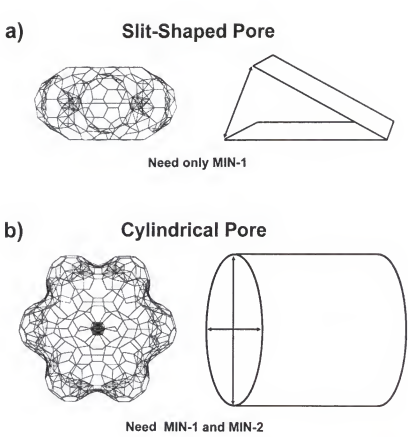

Figure 2-4: Application of the MIN-1 and MIN-2 of a benzene adsorptive molecule to pore access. The minimum dimensions of the adsorptive dictate pore access. In (a), MIN-1 less than the dimension of a slit-shaped pore is required for access. In (b), MIN-1 and MIN-2 less than the two dimensions of a cylindrical pore is required for access.

The critical dimensions reported in Table 2-3 are in accord with experimental observations attributed to shape selectivity.[17] Shape selectivity in HZSM-5 by MAS NMR showed that when 1,2,3,-, 1,3,5- and 1,2,4-trimethylbenzene (MIN-2 of 7.64, 8.18, and 7.25 Å, respectively) were all produced inside in the 9 Å channel intersections of HZSM-5, only 1,2,4-trimethylbenzene is obtained as a product.[17] Only this isomer is small enough to exit through the channels,[18] and the others rearrange to reestablish equilibrium between those remaining in the pores. Additionally, a previous report from our laboratory concluded that the strongest Brønsted acid sites reside in the smaller straight channels of HZSM-5.[19] Pyridine interacted with the strongest sites in the solid to produce an enthalpy of -42.1 kcal $mole^{-1}$. 2,6-Lutidine could not access these strongest sites, and

the largest enthalpy was -19.0 kcal mole^{-1}. Pyridine has a smaller critical dimension of 6.43 Å, compared to 2,6-lutidine with 6.95 Å. With a critical dimension of 8.29 Å, 2,6-di-*tert*-butylpyridine can not access either channel. This denied access was manifested in the calorimetric measurements with 2,6-di-*tert*-butylpyridine by a small negative enthalpy from a small number of hydrogen bonding sites residing on the exterior of HZSM-5. For more discussion on the determination of effective catalytic pore sizes see reference 18.

Kinetic diameters or Lennard-Jones potentials constants, σ_k, have been employed to determine the accessibility of molecules to zeolite channels and are related to the minimum equilibrium diameter of a molecule, r_{min}, given by a Leonard-Jones 12-6 potential, *i.e.*, $r_{min} = 2^{1/6}\sigma_k$,[20] and assume the molecule is effectively spherical. Kinetic diameters do not take into account molecular orientation, and this orientation is crucial in determining whether a molecule will fit into a small pore of fixed size.* For large, non-spherically symmetrical molecules, kinetic diameters will not be useful in determining whether or not the molecule can enter a pore. Thus, the critical diameters reported here should be considered as a better criterion of molecular exclusion.

It is of interest to determine the relation of Breck's kinetic diameters[21] as well as Svehla's kinetic diameters[22] to our calculated values of MIN-1 and MIN-2. The correlation coefficients (R^2) for MIN-1 are 0.656 and 0.744 and for MIN-2 are 0.623 and 0.837, respectively. From these results, one can conclude that reported kinetic diameters at best provide estimates of the critical molecular dimensions that determine access to a pore.

---

*Breck attempted to include molecular orientation in some of the molecules listed, *e.g.*, *n*-butane has a smaller σ_k than propane as determined from both viscosity data or second virial coefficients. Therefore, Breck quoted the σ_k of butane as the same as propane.[22] The minimum dimension (MIN-1) for propane and butane are the same, the difference is in MIN-2. MIN-2 in this chapter is quoted for an elongated butane. Although an elongated butane has less steric strain than a "cis"-butane, the elongated conformer has a larger apparent diameter.

The next concern is to determine if the reported kinetic diameters have any physical significance. This was evaluated by calculating a molecular volume for the assumed spherically symmetric molecule from the reported kinetic diameter and comparing the volume to mVG. The correlation coefficient (R^2) is 0.882 for Svehla's diameters and is 0.781 for Breck's diameters. Thus, one can conclude that MIN-1 and MIN-2 provide a more realistic measure of molecular access.

In the absence of specific interactions, molecular dimensions are relevant to diffusion. Diffusivities (D) of a series of n-alkanes are reported[23a] in HZSM-5. With comparable values of MIN-1 and MIN-2 for long chain alkanes in the elongated conformer expected on solids, MIN-3 will be the controlling factor. The correlation produced the equation: $\ln D = -0.525$ (MIN-3) - 12.9 with an R^2 of 0.986 (MIN-3 is the z-axis for ethane and x for longer chain hydrocarbons). Methane is left out of the correlation and deviates in the direction of diffusing too rapidly. This is expected behavior for the Knudsen diffusion found for methane compared to configurational diffusion[23b] of higher alkanes.

General Applications

To illustrate the utility of the methods presented above in adsorbent design and selection, the adsorption of chemical warfare agents (CWA)[24] are discussed. A ZINDO calculation was carried out on Mustard, VX, Sarin, and Soman molecules. The conversion of these results to MVL gave 130.5, 274.4, 127.7, and 181.0 mL mole^{-1} respectively. The excellent agreement of these calculated values with experimental values of 124.9, 265.2, 127.1, and 178.2 mL mole^{-1} provides confirmation of Equation 2-3. The critical dimensions of these molecules indicate that microporosity 7 Å or less will not be utilized for adsorption. Furthermore, for mustard and VX adsorptives, adsorbents with slit shaped pores will be more effective than those with cylindrical pores because MIN-2 is much larger than MIN-1 for these molecules. In evaluating adsorbents for

CWA's, simulant molecules are more convenient to work with than the agents. In selecting compounds to model non-specific adsorption of agents, molecules with similar critical dimensions should be employed. Molar volumes of the simulants and agents can be compared to estimate adsorbent capacities.

Conclusions

The comparison of experimental molar volumes (MV_{EXP}) to molar volumes calculated with ZINDO (*M*VG) yields an excellent correlation (see Equation 2-3 and Figure 2-1) confirming the feasibility of the quantum mechanical calculation of molar volumes and densities. Since the calculated molar volumes correlate to experimental molar volumes without regard to molecular packing, the MVL values in Table 2-1 are the best quantities for the conversion of mmoles adsorbed per gram to volume adsorbed per gram.

Physical surface characteristics can be explored with the application of the molecular volumes and the projected molecular surface areas (Table 2-2 and Table 2-3) derived from the molecular dimensions. Pore volumes and areas can be calculated for a given adsorbent from the moles adsorbed. Adsorbent surface areas calculated for various conformers of the adsorptive are shown to provide insights into the packing of the adsorbate in the pores or channels of the solid.

Knowledge of the molecular dimensions of adsorptive molecules is crucial to the understanding of molecular exclusion, as well as shape and size selectivity. The critical molecular dimensions (Table 2-3) are used to explain molecular exclusions of adsorptives from a solid (*e.g.*, shape selectivity in the synthesis of alkyl-benzenes and exclusion of 2,6 di-*tert*-butylpyridine from HZSM-5) and diffusivity of alkanes in porous solids (*e.g.*, zeolites).

CHAPTER 3
A MULTIPLE-PROCESS EQUILIBRIUM ANALYSIS OF SILICA GEL AND HZSM-5

Introduction

Equation 3-1 describes the physisorption of a gas, $A_{(g)}$, by a solid surface, $S_{(s)}$.

$$S_{(s)} + A_{(g)} \rightleftharpoons SA_{(s)} \tag{3-1}$$

An adsorption equilibrium constant, K, for Equation 3-1 can be written and rearranged to give Equation 3-2[1,25]:

$$[SA]_s = \frac{nK[P]}{1+K[P]} \tag{3-2}$$

where n is the capacity for adsorption, $[SA]_s$ is the total amount of A adsorbed per gram of solid, and P is the equilibrium pressure, in atmospheres, of gaseous A in equilibrium with the solid. The novel feature of our approach is the treatment of non-specific adsorption by this distribution type of equilibrium constant (like a distribution coefficient) that refers to a process and not to a specific, isolated binding site on a planar surface. Thus, though Equation 3-2 is similar in form to the Langmuir equation, the MEA derivation, with n defined as a process capacity, leads to a conceptually different model and eliminates the assumptions required[1] to apply the Langmuir model to binding at a solid site. The n of Equation 3-2 provides the process capacity of an equilibrium process that involves adsorbate in *similar* size pores undergoing *similar* energies of interaction with the solid and neighbor adsorbate molecules.

In the first two papers of this series,[7,26] it has been shown that, for porous carbonaceous materials, a simple one-process model does not adequately describe adsorption isotherms for gases above their critical temperature and up to 1 atmosphere external pressure. Several equilibria like that in Equation 3-1 may be involved and summation of *i*-expressions like Equation 3-2, to accommodate *i*-multiple adsorption processes, leads to Equation 3-3.

$$[SA]_s = \sum_i \frac{n_i K_i [P]}{1 + K_i [P]} \tag{3-3}$$

Each of the *i*-adsorption processes is treated by a separate equilibrium constant, and the total adsorption isotherm is the sum of the individual isotherms for each *i*-process.

A novel feature of this multiple-process, equilibrium analysis, MEA, is the accurate definition of the K and n values by measuring adsorption isotherms at several temperatures. The values for $n_{i,ads}$, like solid densities, are essentially temperature independent; therefore, new temperatures introduce as unknowns only the new $K_{i,ads}$ for each process. Adsorption measurements at several temperatures not only provide meaningful equilibrium adsorption K and n values, by a better definition of the minimum in a least squares data fit, but also provide enthalpies of adsorption for each process via the van't Hoff equation. In contrast to the BET model, the MEA model fits the total adsorption isotherm at each temperature and provides equilibrium constants, capacities, and enthalpies for each adsorption process. The capacity of the solid for the various processes, $n_{i,ads}$, in moles g^{-1}, can be converted to accessible pore volumes for the different processes using the molar volume of the adsorbate, and for monolayer coverage, the corresponding surface areas utilized can be determined from adsorbate molecular areas.

The different equilibria correspond to adsorption in pores of different sizes. In the absence of donor-acceptor interactions, the smallest accessible pores are expected[27] to have the more

negative enthalpy and the largest pores the less negative enthalpy. In an amorphous solid containing a distribution of pore sizes, like carbon, the sizes of the pores utilized for the different processes will vary with the sorptive size. Studying a solid with regular, known pore dimensions will provide a test of the MEA by checking the relation between the structure and the number of processes needed to fit the isotherm. Such a porous, crystalline solid is provided by the aluminosilicate HZSM-5 which consists of straight channels and intersecting perpendicular zigzag channels.[28-31] The dimensions of the elliptical straight channel are reported as 5.4 x 5.6 Å and those of the intersecting, sinusoidal channel as 5.1 x 5.4 Å.[32] June *et al.*[33] calculate that the intersections of the zigzag and straight channels of silicalite will lead to roughly 9.0 Å voids. The different channel dimensions should lead to at least two different affinity adsorption processes and allow us to determine if MEA can distinguish them.

There are additional advantages to studying HZSM-5. Though applications of zeolites[34,35] as shape selective catalysts and adsorbents are related to zeolite porosity, determination of the pore volume is not straightforward and remains uncertain. Saito and Foley[36] reported adsorption isotherms for nitrogen and argon at 77 K on high alumina content HZSM-5 samples (Si/Al = 23). Using the Horvath-Kawazoe (H-K) model to calculate the pore size distribution, an observed single transition in the isotherm resulted in a calculated pore diameter of 5.5 Å. At higher Si/Al ratios (70 and >400), the 5.5 Å pore transition is also found, but in addition, a second transition is observed in the isotherm corresponding to a calculated pore diameter of 7.7 Å. This larger pore diameter was reported to be a nonexistent artifact. The defined porosity, H-K complications and extensive literature on theoretical modeling make the study of zeolites an important challenge for the development of our model.

For most adsorbates that do not undergo specific interactions, the extension of MEA to HZSM-5 requires two processes. The K and n values for various size probe molecules provide added insight regarding the influence of pore dimensions on adsorbent affinity and capacity. The

trends observed in the MEA parameters for different adsorptives show patterns expected for an adsorbent with defined porosity and in so doing support our claim that MEA is not meaningless data fitting with multiple parameters. Instead, the resulting thermodynamic data, pore volumes, and surface areas for the different adsorptives provide a characterization of adsorption by solids that is unique in the detail provided. The MEA characterization of microporous HZSM-5 and Fisher silica gel, materials of similar composition, affords a dramatic comparison of the influence of porosity on the adsorption process.

Experimental

Gases

The gases CH_4, CO, C_2H_6, C_3H_8, and DME (99.99%) were purchased from Matheson Gas. N_2 (99.99%) was purchased from Liquid Air, Inc. Sulfur hexafluoride (SF_6) was purchased from Aldrich Chemical. All gases were used as received without further purification.

Solid Characterization

Silica gel was purchased from Fisher Scientific (lot no. 934403), and HZSM-5 (Si/Al = 53) was donated by PQ Corporation. Carbon and nitrogen analyses were performed by the University of Florida elemental analysis laboratory. The HZSM-5 contained 0.61% carbon which corresponds to 0.05 millimoles of template or 0.5 millimoles of carbon from residual alkoxide. Nitrogen at 0.25% is within the 0.4% limit of the analysis. Silica gel gave no carbon or nitrogen. In view of the small amount of impurities, the solids, as received, were degassed under vacuum ($< 10^{-4}$ torr) for 8 hours at 200 °C and then studied. The infrared spectrum of HZSM-5 subjected to these drying conditions showed no bands from water or ammonium ions.

For comparative purposes, surface area and pore volume data were measured with N_2 adsorption at 77 K using a Micromeretics ASAP 2000 gas analyzer. Surface areas are reported using a five-point BET calculation.[37] Micropore volume was determined using the Harkins-Jura

t-plot model with thickness parameters from 5.0 to 10.0 Å.[38] Macro- and mesopore volumes were calculated using the Barrett-Joyner-Halenda (BJH) desorption curve.[39]

Adsorption Measurements

Gaseous uptake measurements on porous silica gel and HZSM-5 were performed on a Micromeretics ASAP 2000 instrument with chemisorption/physisorption software employing a 47-point pressure table ranging from 0.1 to 760 Torr on samples degassed for 8 hours. The system was considered to be at equilibrium when the pressure change was less than 1% of the selected pressure point in a 10-second equilibration time interval. Pressure tolerances were 1% with the 10 Torr transducer and 1 mmHg with the 1000 Torr transducer. Low-temperature baths, consisting of a solvent/liquid nitrogen mixture, were required to collect isotherms at low temperatures.[40] Studies involving condensable gases (ethane, propane, DME, and SF_6) required elevated temperatures that were obtained with insulated heating mantles which maintained the temperature to within ± 1 °C. All measurements are carried out at or above the critical temperatures.

Equilibrium Analysis

The measured isotherms were analyzed using Equation 3-3 by a procedure that was previously described.[7,26] In using this equation, the minimum number of processes required to obtain a good data fit are utilized. A detailed explanation of the criteria for selecting the correct number of processes is reported.[7b] One starts the MEA by taking each individual data set and graphing it as P_{atm} / moles adsorbed vs P_{atm}. For one adsorption process, Equation 3-3 reduces to a straight line with the slope of the line equal to $1/n$ and the intercept equal to $1/nK$. The graphs of the individual data sets are curved and not linear, indicating multiple processes. Linear regions can be found in the curved plot and a linear regression performed on these regions to obtain a rough estimate of n and K for the processes. The data sets at different temperatures introduce new $K_{i,ads}$ values for each process, but the $n_{i,ads}$ values from these plots remain fairly constant for the different

temperature data sets of a particular probe. The n and K values obtained for each process from the linear portion of the isotherm are then used as seed values in a modified least-squares minimization, simplex fitting program which has been designed to simultaneously fit the combined temperature sets of adsorption data for a particular adsorptive. Low-temperature data provide the most accurate n and $K_{1,ads}$ values for process 2, whereas higher temperatures provide more accurate values for process 1. This accuracy is reflected by examining the data fits where the process 1 capacity at low temperature is filled within the first two or three pressure measurements, providing little information to calculate the process 1 parameters. However, most of the isotherm at low temperature corresponds to process 2, leading to an accurate determination of these parameters. Experiments at higher temperature will not adsorb as much of the gas at or below 1 atmosphere leading to a more extensive data set for determination of the process 1 parameters.

Results and Discussion

Silica gel (amorphous) and HZSM-5 (crystalline) have similar compositions but different porosities. Fisher silica gel is reported to consist of a distribution of mainly mesopores. X-ray data indicate that the channels and voids from channel intersections in HZSM-5 have fixed dimensions and are microporous. In contrast to these conclusions from X-ray data, results from standard N_2 porosimetry would lead to the incorrect conclusion that our sample of HZSM-5 contains comparable volumes of micro- and mesopores (Table 3-1). The BET surface area of 402 m^2g^{-1} is also uncertain, for it is reported[25] that shortcomings of the BET model can lead to prediction of too large of a surface area for microporous solids. Thus, MEA of HZSM-5 using nonpolar adsorbates of varying dimensions and shapes above their critical temperatures not only will provide a test of the significance of the MEA parameters but also can offer an alternative to BET for surface areas and to the H-J t-plot and BJH for determining pore volumes of porous solids.

Table 3-1: Physical Properties of Adsorbents

	Fisher SG	PQ ZSM5
BET Surface Area ($m^2\ g^{-1}$)[a]	508	402
Pore Volume ($mL\ g^{-1}$)		
Micropore[b]	0.02	0.14
Mesopore[c]	0.33	0.17
Macropore[c]	-------	------

a. Surface Area and pore volume data are from N_2 porosimetry at 77 K.
b. Micropore volumes calculated from the Harkins-Jura *t*-plot model.
c. Meso- and Macropore volumes calculated from Barrett-Joyner-Halenda (BJH) desorption data.

Adsorption Isotherms

Experimental adsorption isotherms for HZSM-5 (Si/Al = 53) are given by the points in Figures 3-1 and 3-2, and sample data fits are illustrated by the solid lines. The physical properties of the adsorbates used are summarized in Table 3-2. The temperature dependent $K_{i,ads}$ values for all systems studied are listed in Table 3-3. The calculated $n_{i,ads}$ values are listed in Table 3-4. Measurements at several temperatures for most gases show that in the absence of donor-acceptor interactions two processes are able to fit the adsorption data to experimental accuracy. Criteria have been reported[7b] for determining the number of processes required. The existence of at least two processes is expected because two different channels exist, one straight and one zigzag, with different dimensions.

The temperature dependence of $K_{i,ads}$ gives the enthalpies ($-\Delta H_{i,ads}$) and entropies ($-\Delta S_{i,ads}$) for the processes via the van't Hoff equation. These results are summarized in Table 3-5, and the $\ln K_{1,ads}$ vs 1/T(K) plots for HZSM-5 are shown in Figure 3-3. The linearity of these and reported plots,[7] as well as resulting enthalpies whose magnitudes are those expected for physisorption processes,[41] support our contention that meaningful thermodynamic parameters result from the model.

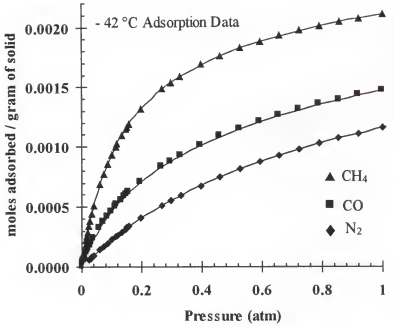

Figure 3-1: Adsorption isotherms for the small molecules at -42 °C on HZSM-5. The symbols are the experimental data points and the solid lines are the calculated isotherms from the MEA n and K values.

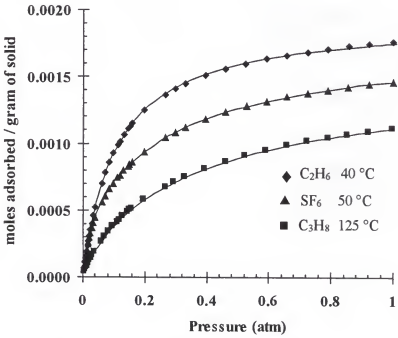

Figure 3-2: Adsorption isotherms for the larger molecules on HZSM-5. The symbols are the experimental data points and the solid lines are the calculated isotherms using the n and K values from the MEA.

Table 3-2: Summary of Gases and Physical Properties

Probe Gas[a]	MW (g mol^{-1})	Polarizability ($Å^3$)[b]	Dipole Moment Debye[c]	Molar Volume[d] (mL mole^{-1})	Critical Temp (°C)	Normal Boiling Point (°C)	ΔH°_{v} (kcal mole^{-1})	ΔS°_{v} (cal mole^{-1} K^{-1})	van der Waals Const. [*a*]	Molecular Area ($Å^2$)[d]	Molecular radius (Å)[d]
N_2	28.01	1.74	0	25.02	-146.9	-195.8	1.332	17.22	1.390	15.27[e]	2.149
CO	28.01	1.95	0.13	28.28	-140.2	-191.5	1.443	17.67	1.485	15.77[e]	2.238
CH_4	16.04	2.59	0	29.74	-82.60	-161.5	1.96	17.5	2.253	16.26[e]	2.276
C_2H_6	30.07	4.47	0	47.21	32.3	-88.65[b]	3.51	19.0	5.489	24.01[e]	2.655
C_3H_8	44.10	6.29	0.084	64.53	96.7	-42.1	4.54	19.6	8.664	28.27[e]	2.946
SF_6	146.05	6.54	0	77.04	45.55	-63.8$_{sub}$	4.08	19.5	7.365[f]	31.17[e]	3.126
DME	46.07	5.16	1.3	56.36	127	-24.9	5.13	20.7	8.073	26.16[e]	2.816

a. *Lange's Handbook of Chemistry*, 13th edition; McGraw-Hill: New York, 1985. All data is from this source unless otherwise specified.
b. *Handbook of Chemistry and Physics*, 71st edition; CRC Press: Boca Raton, Florida, 1991.
c. McClellan, A. L. *Tables of Experimental Dipole Moments*; W. H. Freeman and Company: San Francisco, 1963.
d. Due to contradictions in the literature values, molar volumes, surface areas, and molecular radii of the adsorbates are calculated using ZINDO[43]
e. N_2, CO, CH_4, and C_2H_6, z-axis parallel to plane. C_3H_8 and DME, z-axis perpendicular to plane. SF_6, F face on plane. Other orientations are possible: for CO, specific interaction, z perpendicular to plane: 11.31Å^2; for CH_4, 2 H's in contact with a plane: 15.35Å^2; for C_2H_6, 3 H's in contact with a plane, z perpendicular to plane: 19.32Å^2. See text and reference 43 for more discussion.
f. There is no literature *a* value for SF_6, so all van der Waals *a* parameters were recalculated[g] from critical constants.[a] A linear least squares regression was performed on the reported *a* values and those calculated from the critical constants giving an r^2 value of 0.999. The *a* value for SF_6 was interpolated from the least squares line.
g. Barrow, G.M. *Physical Chemistry*; McGraw Hill, New York, 1988, p 42.

Table 3-3: Equilibrium Constants and Total Amount Adsorbed at Lowest Temp

Temp °C (mmol)[a]	K_1[b]	K_2[b]	Temp °C (mmol)[a]	K_1[b]	K_2[b]
HZSM-5 / N_2			FSG / N_2		
-93 (2.4 mmol)	22.7 ± 0.3	2.26 ± 0.34	-93 (0.74 mmol)	4.9 ± 0.4	0.29 ± 0.03
-43	1.51 ± 0.01	0.214 ± 0. 009	-62	0.9 ± 0.4	0.09 ± 0.03
0	0.260 ± 0.002	0.084 ± 0.002	-44	0.5 ± 0.2	0.05 ± 0.01
25	0.0973 ± 0.0004	0.0791 ± 0.0005	-17	0.14 ± 0.09	0.028 ± 0.007
HZSM-5 / CH_4			FSG / CO		
-42 (1.54 mmol)	8.539 ± 0.016	1.080 ± 0.038	-93 (1.24 mmol)	7 ± 1	0.6 ± 0.2
-16	2.406 ± 0.013	0.366 ± 0.030	-62	1.4 ± 0.3	0.14 ± 0.05
0	1.323 ± 0.014	0.238 ± 0.034	-44	0.7 ± 0.1	0.06 ± 0.02
			-17	0.23 ± 0.09	0.03 ± 0.02
HZSM-5 / C_2H_6			FSG / CH_4		
40 (1.78 mmol)	9.504 ± 0.037		-93 (1.45 mmol)	20 ± 2	0.6 ± 0.2
50	5.221 ± 0.020		-62	2.8 ± 0.3	0.16 ± 0.03
75	2.544 ± 0.022		-44	1.3 ± 0.3	0.09 ± 0.03
			-17	0.4 ± 0.2	0.04 ± 0.02
HZSM-5 / C_3H_8			FSG / C_2H_6		
125 (1.11 mmol)	7.769 ± 0.083	1.760 ± 0.042	40 (0.308 mmol)	0.6 ± 0.3	0.08 ± 0.04
150	5.018 ± 0.021	0.881 ± 0.011	55	0.5 ± 0.2	0.05 ± 0.02
175	2.199 ± 0.029	0.322 ± 0.014	75	0.3 ± 0.1	0.03 ± 0.01
			100	0.19 ± 0.07	0.018 ± 0.008
HZSM-5 / SF6			FSG / C_3H_8		
50 (1.46 mmol)	34.1 ± 0.2	2.94 ± 0.09	75 (0.35)	2.9 ± 0.5	0.09 ± 0.02
65	19.56 ± 0.09	1.52 ± 0.04	125	1.0 ± 0.5	0.03 ± 0.02
80	12.57 ± 0.06	0.835 ± 0.029	150	0.9 ± 0.2	0.016 ± 0.009

Temp °C (mmol)[a]	K_1[b]	K_2[b]	K_3[b]
HZSM-5 / CO			
-93 (2.55 mmol)	414 ± 6	28 ± 3	2.4 ± 3.2
-42	8.69 ± 0.67	1.48 ± 0.33	0.21 ± 0.38
-16	2.56 ± 0.07	0.454 ± 0.036	0.149 ± 0.041
0	1.230 ± 0.004	0.182 ± 0.002	0.147 ± 0.003
HZSM-5 / DME			
150 (1.48mmol)	11546 ± 9.5	79 ± 37	1.5 ± 4.4
175	3731 ± 2.0	32.7 ± 8.0	0.83 ± 0.92
200	713 ± 1.6	11.8 ± 6.4	0.39 ± 0.74

a. Total experimental amount adsorbed (mmoles) at the lowest temperature analyzed is indicated in parentheses.

b. Gas-Solid Equilibrium Constant. The first digit of the uncertainty is the last significant figure.

Table 3-4: MEA Accessible Surface Areas (m^2g^{-1}) and Volumes ($mL\ g^{-1}$)

	ZSM-5 N_2			ZSM-5 CO			ZSM-5 DME		
process	mmol ads	mL ads	area	mmol ads	mL ads	area	mmol ads	mL ads	area
n_1	1.540 ± 0.015	0.039	141.6	0.612 ± 0.028	0.017	58.1	0.582 ± 0.005	0.033	91.7
n_2	1.29 ± 0.12	0.032	118.6	1.22 ± 0.17	0.035	115.9	0.147 ± 0.067	0.007	23.2
n_3	-	-	-	1.08 ± 1.3	0.031	102.6	1.2 ± 2.7	0.068	189
total	2.83 ± 0.14	0.071	260.2	2.9 ± 1.5	0.083	276.6	1.98 ± 2.8	0.109	303.9

	ZSM-5 CH_4			ZSM-5 C_2H_6			ZSM-5 C_3H_8		
process	mmol ads	mL ads	area	mmol ads	mL ads	area	mmol ads	mL ads	area
n_1	1.870 ± 0.013	0.0557	183.5	1.918 ± 0.016	0.091	277.3	0.514 ± 0.006	0.033	87.5
n_2	0.806 ± 0.075	0.0240	78.9	-	-	-	1.02 ± 0.03	0.066	173.6
total	2.68 ± 0.09	0.0797	262.4	1.918 ± 0.016	0.091	277.3	1.53 ± 0.04	0.099	261.1

	ZSM-5 SF_6			FSG N_2			FSG CO		
process	mmol ads	mL ads	area	mmol ads	mL ads	area	mmol ads	mL ads	area
n_1	0.556 ± 0.004	0.043	104.4	0.213 ± 0.001	0.0053	19.6	0.451 ± 0.002	0.013	42.8
n_2	1.230 ± 0.039	0.095	231	2.48 ± 0.07	0.062	228.1	2.2 ± 0.1	0.062	209
total	1.790 ± 0.043	0.138	335.4	2.69 ± 0.07	0.0674	247.7	2.6 ± 0.1	0.075	251.8

	FSG CH_4			FSG C_2H_6			FSG C_3H_8		
process	mmol ads	mL ads	area	mmol ads	mL ads	area	mmol ads	mL ads	area
n_1	0.330 ± 0.001	0.0098	32.3	0.284 ± 0.002	0.007	41.1	0.111 ± 0.0001	0.013	18.9
n_2	3.03 ± 0.14	0.0901	296.7	2.3 ± 0.2	0.18	332.6	2.8 ± 0.2	0.11	476.7
total	3.3 ± 0.1	0.0999	329	2.6 ± 0.2	0.19	373.6	2.9 ± 0.2	0.12	495.6

Note: Surface Areas in m^2g^{-1}; Process Volumes in $mL\ g^{-1}$. For Molecular Surface Areas and Volumes, see Table 3-2. The first digit of the uncertainty is the last significant figure.

Table 3-5: Enthalpies and Entropies of Adsorption for HZSM-5

		$-\Delta H_{1,2,3}$ (kcal mol^{-1})	$-\Delta S_{1,2,3}$ (cal mol^{-1} K^{-1})
N_2			
	A572	4.5±0.2, 4.1±0.2, 3.1±0.1	17.8±0.3, 19.6±0.8, 17.1±0.7
	HZSM5	4.9±0.2, 3.2±0.4	20±1, 16±2
	FSG	4.2±0.4, 2.9±0.1	20±1, 18.4±0.3
CO			
	A572	5.2±0.1, 4.7±0.3, 3.0±0.2	18±1, 18±1, 19±1
	HZSM5	6.11±0.09, 5.2±0.3, 3.1±0.5	22.0±0.4, 22±1, 16±2
	FSG	4.1±0.2, 3.6±0.2	18.7±0.7, 21.05±0.72
CH_4			
	A572	6.6±0.5, 5.6±0.1, 4.4±0.1	20±2, 20.2±0.9, 19±1
	HZSM5	5.1±0.1, 4.54±0.09	18.3±0.5, 20.9±0.4
	FSG	4.6±0.1, 3.2±0.1	19.5±0.3, 18.9±0.6
C_2H_6			
	A572	9.0±0.2, 7.7±0.1, 6.7±0.1	21±1, 20.01±0.82, 20.9±0.9
	HZSM5	8.159±0.001	21.580±0.004
	FSG	5.0±0.4, 5.6±0.3	16±1, 22.4±0.8
C_3H_8			
	A572	10±0.2, 9.1±0.1, 8.6±0.8	20.2±10.2 , 18.6±1.1, 20.5±1.1
	HZSM5	9±2, 12±2	18±5, 29±4
	FSG	4.9±0.8, 6.8±0.8	12±2, 24±1
SF_6			
	A572	8.6±0.7, 7.0±0.3, 6.6±1.2	16.4±2, 16.2±0.9, 19.6±3.6
	HZSM5	7.5±0.3, 9.52±0.02	16.4±0.9, 27.32±0.07
DME			
	HZSM5	22±3, 15±1, 10±1	33±7, 27±3, 24±3

Note: The first digit of the uncertainty is the last significant figure.

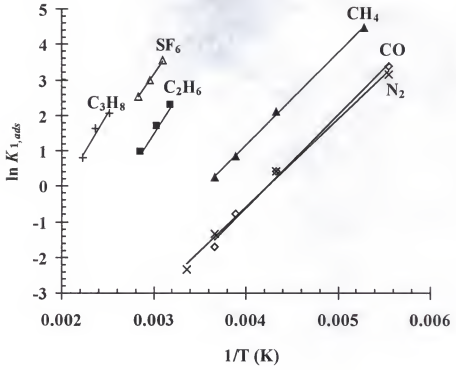

Figure 3-3: van't Hoff plots (ln $K_{1,ads}$ vs 1/T(K)) for various adsorptives with HZSM-5.

Summary of the HZSM-5 Thermodynamic Data

The process designation[7,25] gives the order of pore filling and assigns the lowest number to the process with the largest equilibrium constant. In earlier studies of amorphous carbons, the lower numbered processes also were more exothermic, corresponding to adsorption in the smaller pores of the solid. Process 1 corresponded to pores that are near the size of the gas adsorptive and had the greatest enthalpy of interaction ($-\Delta H_1$) because the adsorbed molecule interacts with both walls of the slit-shaped carbon pores. Process 2 pores are 1.2-1.4 times as large, and process 3 pores are above 1.4 and below 2 times the size of the gaseous adsorbate. Decreased interaction with the opposite wall accompanies increasing pore size. Comparison of the diameters of the probes (Table 3-2) suggests that the small channel diameter of HZSM-5 is large enough to accommodate SF_6 and 1.5 times larger than the diameter of the smaller gas molecules studied.

Thus, in contrast to carbon where the adsorbate selects those pores with comparable dimensions for process 1 from the distribution of pore sizes available in an amorphous solid, process 1 with pores of fixed dimensions, as in zeolites, will correspond to different types of adsorbate-wall interactions for different size adsorbates.

The diameter of the HZSM-5 channel does not allow two molecules to occupy positions adjacent to each other spanning the channel diameter, even for molecules as small as N_2. Therefore, a single molecule is expected to adsorb on the channel wall so as to provide the maximum interaction with the surface. As the adsorbates increase in size, interaction with the distant walls of the cylinder is expected to increase, becoming a maximum when the molecular diameter of the probe is that of the cylinder. Increasing adsorptive size not only leads to increased surrounding wall interaction but also parallels increased surface dispersion interaction for the larger, more polarizable molecules. Thus, the process nomenclature, used earlier for carbon, is incomplete because process 1 for a small molecule will involve pores larger than the adsorptive diameter if they are the smallest ones available. The term "process" will continue to designate the order of K values, with process 1 corresponding to the pore that fills first. The term "type" will be used to describe the matching of the adsorbate and pore dimensions. A type 1 adsorbate is one in which the molecular dimensions of the adsorbate match the pore. A type 2 adsorbate interacts strongly with one wall and appreciably with the rest of the pore surface, while a type 3 adsorbate interacts strongly with one wall and weakly with the rest of the pore surface or in larger pores with a molecule on the opposite surface.

The difference in the process and type designation is manifested in the thermodynamic data for adsorption. For the smaller adsorbates, N_2 and CH_4, the larger equilibrium constants for process 1 are also manifested in more negative enthalpies than those for process 2. However, for the larger adsorbates, SF_6 and propane, whose dimensions approach those of the channels, the

larger K values, at the temperatures studied, correspond to the processes with the less negative enthalpies. Stronger adsorptive-solid interactions will give rise to more negative enthalpies attributed to the smaller pores. However, the equilibrium constants contain entropic contributions,[27] and more negative entropy values in the smaller pores can cause the equilibrium constants for stronger adsorption processes to be smaller than those for weaker adsorption processes.

Adsorption of CO was best defined by a three-process interpretation of the adsorption data. Process 1 is attributed to weak hydrogen bonding with the acid sites of HZSM-5, *vide infra*. Comparison of the process 2 and 3 enthalpies for CO with 1 and 2, respectively, for N_2 indicates that similar nonspecific interactions are involved.

A plot of the enthalpy of adsorption vs the entropy gives a poor correlation when data for all the processes are combined. The larger -ΔH process for each adsorptive has a larger -ΔS value. This trend is expected except that the increases in -ΔS for the more negative enthalpy processes are too large to fall on the same line as those for the smaller enthalpy processes. When the data are divided into two different sets of large and small enthalpies for each adsorptive, better correlations are found for each set, Figure 3-4. The following adsorptives, with the process listed in parentheses, are assigned to the larger -ΔH line: $N_2(1)$, $CO(2)$, $CH_4(1)$, $C_3H_8(2)$, $SF_6(2)$. The following are assigned to the smaller -ΔH line: $N_2(2)$, $CO(3)$, $CH_4(2)$, $SF_6(1)$, and $C_3H_8(1)$. The K values for the two processes for ethane are too close to resolve, so the data fit to a single process. When ethane is fit to two processes, the process 1 capacity is the same as in the one-process fit. Process 2 is not distinguished from 1, and large errors result in the meaningless process 2 parameters. Thus, least-squares lines are constructed for these two assignments with ethane omitted and shown in Figure 3-4 for the larger enthalpies. The larger -ΔH plot gives an excellent correlation ($R^2 = 0.93$) even though the type of interaction changes as the adsorbate size increases

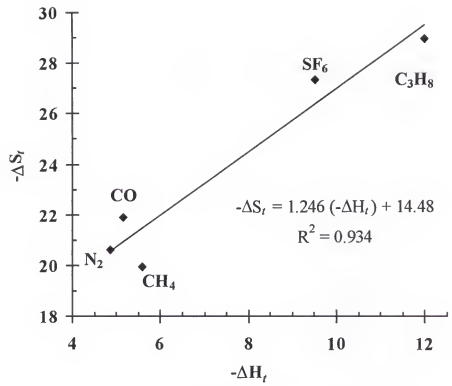

Figure 3-4: $-\Delta S_{small\ pore}$ vs $-\Delta H_{small\ pore}$ for HZSM-5. The gases are labeled.

on going from N_2 and CO to SF_6 and propane. Thus, the slope of the line contains an enthalpy and entropy component from the dispersion interaction to the bound surface and from changing the type of interaction with the remaining surface. Those processes assigned to the smaller -ΔH line span a range of only four entropy units and as a result give an entropy-enthalpy correlation with small deviations but a poor R^2. The main conclusion from this analysis is the existence of two different entropy-enthalpy plots which indicates two different fundamental groupings processes. A larger -ΔH and lower equilibrium constant for the second process is a result of the more negative entropy associated with adsorption of propane and SF_6 in the small channel. With this assignment, process 2 occurs in the small channel, and propane as well as SF_6 is well behaved in the entropy-enthalpy plots. The more exothermic process 1 for methane corresponds to the smaller -ΔS so the enthalpy criterion would assign this process to the small channel while the entropy criterion would assign

this process to the large channel. Also note that the difference in the enthalpies for the two processes is not very large. The single-process fit of ethane gives an average enthalpy value that falls below the large -ΔH plot.

Dimethyl ether was not included in these correlations because large, specific hydrogen bonding interactions are involved in processes 1 and 2. For specific interactions, the process designations depend on the strength of different groupings of specific donor-acceptor sites. The more negative enthalpies of processes 1 and 2 are consistent with a specific hydrogen bonding interaction. These conclusions will be discussed in more detail in the section on donor probes.

The cause of the two different enthalpy groupings for the processes is attributed to adsorption in the two different size channels of HZSM-5. The more negative enthalpy processes would be assigned to the smaller channels and the less negative enthalpy to the larger channels. Only a difference of 0.2 e.u. would result from confining an adsorbate in the smaller of the two volumes ($(-R \ln(\nu_{small}/\nu_{large}))$). Thus, the entropy differences for the two groupings could result from differing interactions with the distant wall and from more efficient packing of the adsorbate molecules for the more negative enthalpy process.

Figure 3-5 is a plot of the entropies of adsorption versus the entropies of vaporization of the liquids. The entropy for the small channel is more negative than the entropy of vaporization as expected for a more confined molecule. The increase in entropy for the larger molecules also has the contributions normally observed[42] from a more negative enthalpy of interaction. The entropies for the larger channel are less negative than the entropies of vaporization and indicate a weaker constraint in this channel than in the liquid. The errors are larger than those of the small channel, and the slope of the line is 0.05 ± 0.8. In addition, more ordering of the hydroxyl functionality or a greater loss of vibrational freedom for the silicon and aluminum atoms comprising the walls of the small channels than that for the large channel could lead to a more negative entropy for the small

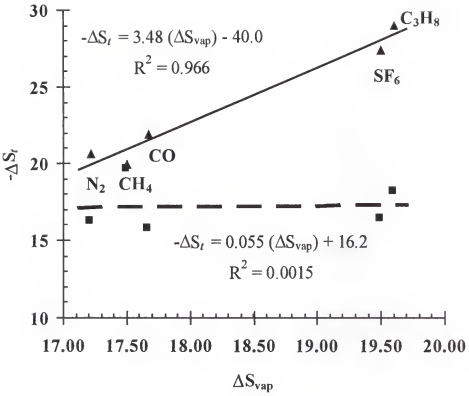

Figure 3-5: Plot of the entropy of adsorption vs the entropy of vaporization. The solid line is for the small pores, and the dashed line is for the large pores.

channel when adsorption occurs. Calorimetric analysis[19] of the acidity of HZSM-5 has shown that the small channel contains most of the hydroxyl functionality. These different entropy components for the two channels lead to the two different entropy-enthalpy plots.

The reversals in equilibrium constants and enthalpies observed in HZSM-5 are not observed in the carbon adsorbents studied to date. This observation is attributed to slit-shaped pores in carbon in contrast to those in HZSM-5 and other zeolites whose channels approximate cylinders. The slit-shaped pores lead to less molecular reorganization when a large molecule is adsorbed. Low-energy bending of the O-Si-O angles also leads to some flexibility in the channel dimensions of a zeolite which can lead to entropy contributions. Carbon entropies do not exceed -21 cal mol^{-1} deg^{-1} for the adsorptives studied here.

Further insights concerning adsorbent-adsorbate interactions arise from plots of the enthalpies vs the square root of the van der Waals *a* parameter. Figure 3-6 shows a good correlation ($R^2 = 0.96$) of the more negative enthalpy processes, and a better correlation ($R^2 = 0.99$) of the less negative enthalpy plots. Linear van der Waals plots $(R^2 = 0.99)^7$ for carbon adsorbents assumed that the type of interaction is the same for a given process for all molecules. The adsorptive selects pores from the distribution available to undergo similar adsorbate-wall interactions for all molecules involved in the i^{th} processes. For the fixed channel dimensions of HZSM-5, the slopes of the lines in Figure 3-5 have an additional contribution to these plots from a change in the type of interaction as the adsorbate size increases.

For ethane, the van der Waals plot indicates that the single-process enthalpy for ethane is less negative than expected for the more negative enthalpy processes and more negative than

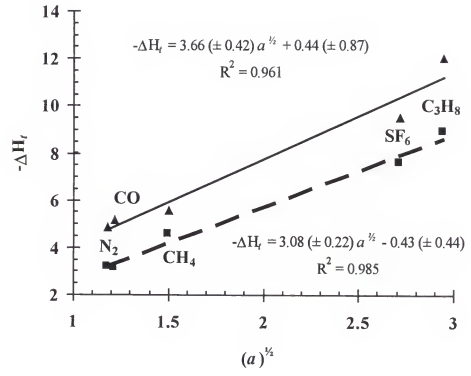

Figure 3-6: Enthalpy of adsorption vs van der Waals $(a)^{½}$ for the small pores (solid line) and large pores (dashed line) of HZSM-5.

expected from the smaller -ΔH plot. This behavior is expected if the MEA provides an average enthalpy because the two K values cannot be resolved.

Insights from the Process Capacities

As shown above, the multiple-equilibrium thermodynamic parameters provide unprecedented detail about the adsorption process. Even more detail results from the MEA capacities of the processes, $n_{i,ads}$. The capacities in moles and the equilibrium constants, $K_{i,ads}$, can be substituted into Equation 3-3 to resolve the total isotherm into the process 1 and 2 components. This resolution is shown in Figure 3-7 for CH_4 with HZSM-5 and shows that, at all measured pressures, adsorption occurs simultaneously in both channels of the solid during the adsorption process.

The process capacities (mmoles g^{-1}) (Table 3-4) decrease as the size of the gas molecules increases (Table 3-2). These capacities can be converted into the surface areas and pore volumes for the individual processes using the molecular areas and molar volumes of the adsorbates, respectively. Different literature reports give adsorbate molar volumes and molecular areas that vary considerably. Accordingly, these quantities were calculated using ZINDO[43] and the calculated values are given in Table 3-2. The calculated surface areas are based on the projected areas for orientations of the molecules that are expected to provide the maximum dispersion interaction with the surface of the solid. June *et al.*[33] report that the channels of the zeolite exhibit constraining effects upon long hydrocarbon chains, such that these molecules are forced to take on a more elongated shape. The orientations employed are given in the Table 3-2 footnotes. The calculated total MEA accessible surface areas reported in Table 3-4 for HZSM-5 are: N_2, 260 $m^2 g^{-1}$; CO, 277 $m^2 g^{-1}$; CH_4, 263 $m^2 g^{-1}$; C_2H_6, 278 $m^2 g^{-1}$; C_3H_8, 261 $m^2 g^{-1}$; and SF_6, 335 $m^2 g^{-1}$. For nitrogen, the milliliters of gas adsorbed in the two processes is low compared to other adsorbates, indicating that the N_2 molecules are not packed as closely to each other as they are in

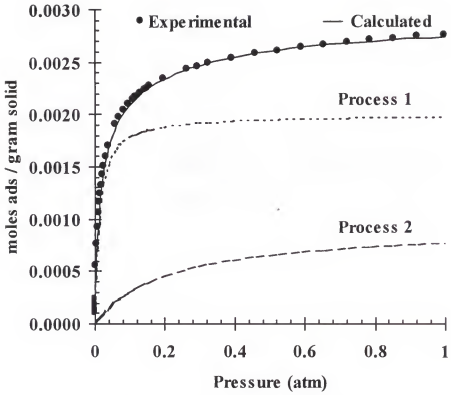

Figure 3-7: Process resolved isotherms for CH_4 adsorption by HZSM-5 calculated from the MEA n and K values. The solid circles are experimental data points, and the solid line is the sum of the two processes.

the liquid or that gaps exist in the extent of surface coverage near the channel intersections where 9 Å diameter voids exist.[33] The bond axis of CO is expected to be linear to the O-H bond for the specific interaction of process 1. CO is expected to adsorb parallel to the surface for the nonspecific dispersion interaction of processes 2 and 3. The area for CO, calculated assuming that the n_1 process is C bonded perpendicular to the surface and physisorption is parallel results in an area of 260 m^2g^{-1}. If the O-H bond is not perpendicular to the surface, a value approaching 277 m^2g^{-1} results. The propane molecule is assumed to have two hydrogens from each methyl and one from the methylene interacting with the surface. The more polarizable SF_6 has a stronger surface interaction and results in more effective coverage in the channels and into the intersections. Thus, surface area is adsorptive dependent, and for small molecular weight gases above the critical temperature a value around 270 m^2g^{-1} results.

In all instances, the process capacities for the small channels are greater than those of the large channel. These capacities are consistent with the small channels having a zigzag shape and the large ones being straight.

Ethane has dimensions that could permit it to span the diameter of the channel with the C-C bond perpendicular to the surface. In this orientation, ethane would have two sets of three hydrogens interacting with the solid surface of opposite walls. The molecular surface area per wall for ethane in this configuration is 19.32 $Å^2$, as calculated with ZINDO. If ethane lies flat, an eclipsed conformation, with four hydrogens interacting with the surface, is expected. The molecular surface area for ethane in this configuration is 24.01 $Å^2$. The calculated MEA surface area for ethane adsorbing parallel is 278 $m^2 g^{-1}$, and 223 $m^2 g^{-1}$ for ethane perpendicular to the surface in both channels. These considerations suggest that ethane is adsorbed with its bond axis parallel to the surface and illustrates the unparalleled, detailed insight available about adsorption from MEA.

Pore volumes from MEA can be compared to the micropore pore volume measured with the H-J *t*-plot for HZSM-5 at 77 K which was found to be 0.14 mL g^{-1}. Calculation of the total pore volume by MEA (Table 3-4) for N_2 indicates a total volume of 0.07 mL g^{-1} consistent with its low surface area. Adsorption on the surface of the 9 Å voids at liquid nitrogen temperatures normally used for N_2 porosimetry measurements could give rise to a third, lower enthalpy process, which accounts for the large volume from porosimetry. The equilibrium constant for this third process is too low to contribute above the critical temperature and at the pressures employed for the N_2 isotherms in this study.

The larger adsorbates give larger values for the accessible pore volume. Adsorption of SF_6 resulted in an MEA volume of 0.14 mL g^{-1} which is comparable to that from the *t*-plots. The other adsorbates give MEA volumes of 0.09 ± 0.01 mL g^{-1}. When the surface of a pore is completely covered by adsorbates of smaller dimensions than the channel, the area from the

adsorbate to the distant wall is empty space that is not calculated as pore volume. This empty space accounts for part of the lower volumes found for the other adsorbates than that found for SF_6. The most accurate assessment of the structural channel volume of the solid comes from adsorbates whose dimensions match that of the pore and which pack efficiently. When this is not the case, the adsorbent capacity is a utilized pore volume that is adsorptive dependent. At lower temperatures, condensable adsorptives are expected to reveal an additional process corresponding to adsorption on the surface of the channel intersections. The important point is that the structural pore volume of the solid is not as relevant a quantity for understanding adsorption as is the pore volume utilized by the particular adsorptive employed at the conditions of the experiment. Clearly, this detailed understanding of adsorption provided by MEA is relevant for interpreting results from applications of zeolites in gas separation or gas phase catalysis when carried out above the critical temperature of the gas.

For methane, the process capacities support the enthalpy conclusion and indicate that process 1 occurs in the smaller channel. However, the more negative methane enthalpy is comparable to that of N_2, falls on the entropy-enthalpy plot, but is low on the van der Waals plot. One possibility for a lower than expected enthalpy would involve interaction of the edge instead of the face of the tetrahedral methane molecule with the solid surface in the small channel. Interaction for this configuration would be mainly driven by entropy considerations with some stabilization from opposite wall interactions. Leaving methane out of the more negative entropy-enthalpy plot (Figure 3-4) gives the equation $-\Delta S_{small} = 1.15\ (-\Delta H) + 15.6$ and improves the R^2 to 0.973 from 0.934. The surface areas for methane packed in the manner proposed above is 248 compared to 263 m^2g^{-1} for adsorption with the three-fold axis perpendicular to the surface. Thus, areas might distinguish the adsorption mode. Futhermore, the process 2 enthalpy is well behaved in the van der Waals plot, suggesting that methane packs in the large channel with its three-fold axis perpendicular to the surface.

Interpretation of the Process Groupings for Donor Probes

In an earlier report from this laboratory,[19] it was shown that titration of HZSM-5 slurried in cyclohexane with pyridine revealed 0.042 millimoles of a very strong acid site and 0.53 millimoles g^{-1} of hydrogen bonding sites. Titrations with 2,6-lutidine and 2,6-di-*tert*-butylpyridine indicate that the strong sites were located in the small channels, 0.32 millimoles of hydrogen bond sites were located in the small channel, 0.18 millimoles g^{-1} of hydrogen bond sites were located in the large channels, and 0.034 millimoles were located on the exterior surface. It was also shown that when the solid was studied at elevated temperatures the strong and weak acid sites could not be resolved because the equilibrium constants approached one another. These conclusions are consistent with the dimethyl ether results from MEA. At the temperatures employed the strong acid n_1 sites are not distinguished from the weaker n_2 sites found by Cal-ad for pyridine, and an n_1 value of 0.58 millimoles g^{-1} results for $(CH_3)_2O$. The van der Waals plot suggests that about 11 kcal $mole^{-1}$ of the process 1 enthalpy for $(CH_3)_2O$ arises from the nonspecific component of the gas-solid interaction and 11 kcal $mole^{-1}$ from the average specific donor-acceptor interaction of the strong and weaker acid sites found in the pyridine titration. Process 2 has a 7 kcal $mole^{-1}$ more negative enthalpy than expected from the nonspecific interaction estimated from the van der Waals plot.

Comparison of n_1 for CO with n_1 for DME indicates that both gases are involved in a specific interaction with the same number of hydrogen bonding sites. CO is weakly basic compared to DME, and this is reflected in the magnitude of the enthalpies for the first process. The 0.6 millimoles g^{-1} capacity is the same as that for process 1 for $(CH_3)_2O$. This indicates that the density of acid sites is such that they are accessed by both molecules. This result occurs even though the surface area required to accommodate site 1 for $(CH_3)_2O$ is twice that of CO. The process 2 capacity in millimoles g^{-1} for dimethyl ether compared to 2,6-lutidine suggests that the weak hydrogen bond sites in the large channel are included in the process 2 capacities. Such a

conclusion is also suggested by the deviation of 5 kcal $mole^{-1}$ of process 2 for $(CH_3)_2O$ from the process 1 van der Waals plot.

With only specific interactions measured for the pyridine titration in hexane, the pore volumes required are 0.032 mL g^{-1} for the small pore and 0.012 mL g^{-1} for the large pore. Hexane fills the rest of the pore volume.

The bulk silica/alumina ratio of 53 corresponds to a Si/Al atom ratio of 23.5 which is used to calculate the mmoles of aluminum per gram of HZSM-5. The ~ 0.6 mmoles of n_1, acid sites of HZSM-5 from the MEA of CO and $(CH_3)_2O$ correspond to 0.58 mmoles g^{-1} of aluminum atoms giving rise to Si-O(H)-Al sites.

Adsorption by Silica Gel

Adsorption isotherms on Fisher silica gel, FSG, for nonspecific adsorbates, are also best fit by a two-process analysis of the adsorption data. This result is significant because the pores in FSG are not expected to be as homogeneous in size or shape as the channels of HZSM-5. Process 1 enthalpies for N_2, CO, and CH_4 on FSG are less negative than those for the small channel of HZSM-5 and comparable to the large channel enthalpies for HZSM-5, Table 3-5. This suggests that the small pores of silica gel are of comparable size to those of the large channel of HZSM-5. The more negative enthalpy, propane process (process 2) on FSG is also within experimental error of that for the large channel of HZSM-5. The capacities, Table 3-4, indicate that the volume of the FSG small pores is very low, about 0.01 mL g^{-1}. It is noteworthy that *t*-plots detect a small micropore capacity of 0.02 mL g^{-1}. Most of the adsorption capacity of FSG arises from larger pores. Comparison of the FSG less negative enthalpies with those for the larger channels of HZSM-5 indicate that these involve slightly larger channels in FSG which are not in the mesopore regime. The *t*-plots indicate 0.33 mL g^{-1} of mesopores. MEA indicates 0.10 mL g^{-1} for process 2 capacities which increase to 0.19 for propane. Apparently these large micropores are included in

the mesopores of the *t*-plot analysis. The remaining 0.14 mL g^{-1} of mesopores from the *t*-plot analysis are not accessed by any process for the adsorbates studied at these temperatures and pressures. Lower temperatures or higher pressures are needed to populate the weaker energy adsorption process that occurs in the mesopores. This emphasizes that porosity must be determined under conditions relevant to the application. For any applications involving gases similar to those studied, porosity that is not accessed is not relevant.

Since the bulk compositions of FSG and HZSM-5 are similar, the differences in the MEA results dramatically illustrate the influences of porosity on adsorption. One major difference in the reactivity of HZSM-5 and FSG is the strong acidity of the former. The two-process fit of CO with enthalpies that fit the van der Waals plot indicate the absence of acid sites strong enough to undergo a specific interaction with silica gel.

Reversals in process enthalpies and equilibrium constants are observed for propane with silica gel. Consistent with this reversal, process 2 for propane falls on the small pore van der Waals plot for other substrates and process 1 for propane falls on the large pore plot.

$$-\Delta H_{type\,1} = 1.458\ (\pm 0.098)\ a^{½} + 2.381\ (\pm 0.19) \qquad R^2 = 0.987 \qquad (3\text{-}4)$$

$$-\Delta H_{type\,2} = 1.138\ (\pm\ 0.30)\ a^{½} + 1.829\ (\pm 0.60) \qquad R^2 = 0.824 \qquad (3\text{-}5)$$

The entropy-enthalpy plots and the entropy of adsorption--entropy of vaporization plots show the same behavior as in the case of HZSM-5 for the small pore data. The large pore data are poorly behaved in both plots. This behavior suggests that the pores involved in the large pore processes involve a different distribution of pore sizes for N_2 and CO compared to ethane and propane.

The BET surface area of silica is reported to be 508 $m^2 g^{-1}$. The MEA results show a decided adsorptive dependence of the surface area. For example, methane gives an area of 329 $m^2 g^{-1}$ and the total area for propane is 496 $m^2 g^{-1}$ with 478 $m^2 g^{-1}$ arising from the more negative enthalpy process. This larger area is attributed to a better matching of the pore distribution to the propane dimensions.

Effective Pressure

In heterogeneous catalysis, porosity in supports enhances adsorption and concentrates reactants around catalytic sites, thereby increasing the reaction rate. The concept of effective pressure, P_{eff}, was introduced[78] as a way to compare the concentrating power of solid supports. Effective pressure is the pressure that would have to be applied to an ideal gas to obtain a concentration in the gas phase equal to the moles of gas adsorbed per mL of pore volume in the support. The moles of gas adsorbed by different adsorbents varies with the pressure of gas over the solid and the temperature. P_{eff} is defined at 25 °C so the number of moles adsorbed, $n_{ads,1atm}$ is calculated from the MEA K and n values at this temperature. Using the ideal gas law, the number of moles adsorbed is converted to P_{eff} using the total MEA volume, Σn_i (L g^{-1}) in Equation 3-6.

$$P_{eff} = \frac{n_{adx,1atm} RT}{\sum n_i (\text{L g}^{-1})} \tag{3-6}$$

P_{eff} indicates that 229 atmospheres would be required to match the effective pressure of methane in HZSM-5. This compares to 98 atmospheres for the carbonaceous adsorbent A572, and a P_{eff} of 21 atmospheres for silica gel. Thus, porosity permits one to carry out a reaction in the pores of HZSM-5 at 1 atmosphere external pressure which requires greater than 200 atmospheres of CH_4 in the gas phase.

Conclusions

Adsorption isotherms for several adsorptives were measured at multiple temperatures above their critical temperatures with a zeolite, HZSM-5, and silica gel. The MEA, which fits the isotherms simultaneously to a minimum number of processes (Table 3-3), provides process capacities (Table 3-4) and enthalpies and entropies (Table 3-5). In amorphous adsorbents the processes contain a distribution of pore dimensions. If this distribution is narrow enough to give the same thermodynamic interaction parameters within experimental error, it is reasonable to group them together in describing the adsorption process. HZSM-5 was selected for study because it contains two channels with slightly different, fixed dimensions. The adsorption data for HZSM-5 are fit with the MEA model using two adsorption processes, providing a check on the meaning of the model. Examination of a solid with fixed dimensions has provided not only a test of the applicability of the MEA model but also insights into the very complex energetics of adsorbate-adsorbent interactions. Unlike amorphous adsorbents, where an adsorptive can select pores of similar size from the distribution available for process 1, the first adsorption process that occurs in materials with uniform, fixed dimensions may not involve a pore of comparable size. Since the process designations for different size adsorbates correspond to different interaction potentials, a type designation is used to indicate the matching of adsorptive and pore dimensions. The correlations of enthalpies of adsorption to entropies and van der Waals constants reveal a specific interaction giving rise to one process for CO and two for dimethyl ether.

Reversals in the magnitude of the enthalpy (Table 3-5) and equilibrium constant (Table 3-3) are found for the processes corresponding to adsorption of propane and SF_6 by HZSM-5. Process 1 has the larger K and less negative enthalpy, indicating a type 2 interaction. A wide variety of probe molecules have been studied on carbonaceous adsorbents, and none show this reversal. In contrast to HZSM-5, the pores of the carbonaceous A-572 consist of parallel sheets or planes with localized graphitic domains. The adsorbate-adsorbent interactions occur along the

surfaces of these planes, and a large adsorbate is less constrained in a slit than it is in a cylinder. Reversals in K and ΔH can be expected in cylindrical-shaped pores.

The process capacities (Table 3-4) that result from the MEA are as significant as the thermodynamic data. Using calculated molar volumes (Table 3-2), one can calculate the accessible pore volume for an adsorbate (Table 3-4). When adsorptive dimensions match pore dimensions, structural pore volumes result. Comparison of these volumes with those from standard N_2 porosimetry (Table 3-1) shows important differences. For measurements above the adsorptive critical temperature, monolayer coverage is expected and conversion of the process capacities from MEA to molecular areas provides accessible surface areas. Significant differences result between the values obtained in this manner and those from BET on microporous solids.

The larger equilibrium constants obtained for HZSM-5 compared to silica gel indicate that the zeolite has a larger affinity for adsorbing these molecules as a result of the presence of smaller, defined channel dimensions with larger capacities. The credibility of the MEA model is enhanced by its ability to provide a rational explanation of adsorbent differences using thermodynamic and capacity criteria. Clearly much more useful information is obtained from an MEA characterization than other isotherm analyses.

CHAPTER 4
THE MULTIPLE EQUILIBRIUM ANALYSIS DESCRIPTION
OF ADSORPTION ON Na-MORDENITE AND H-MORDENITE

Introduction

Gas adsorption of a given adsorbate, $A_{(g)}$, by a solid adsorbent, $S_{(s)}$, is described by Equation 4-1,

$$S_{(s)} + A_{(g)} \rightleftharpoons SA_{(s)} \tag{4-1}$$

where $SA_{(s)}$ is the total amount of $A_{(g)}$ adsorbed per gram of solid. Rearrangement of the thermodynamic equilibrium expression describing Equation 4-1, assuming homogeneous energetic adsorption interactions, yields Equation 4-2,[1,44]

$$[SA]_s = \frac{nK[P]}{1+K[P]} \tag{4-2}$$

where n is the capacity of the solid for adsorption, K is the equilibrium constant, and P is the equilibrium pressure. Although Equation 4-2 is similar in form to the Langmuir equation,[45] the distribution type equilibrium constant (K) refers to a process, not a specific, isolated binding site on a planar surface. The conceptual basis of this process equilibrium analysis eliminates the assumptions required[1] to apply the Langmuir model to binding at a solid site.

As demonstrated in the first five papers of this series,[6,7,26,46] multiple adsorption processes are required to adequately describe a system with heterogeneous energetic interactions, such as

porous carbonaceous materials or zeolites (HZSM-5 and TS-1). The expansion of Equation 4-2 to include multiple processes yields Equation 4-3,

$$[\mathrm{SA}]_s = \sum_{i=1}^{i} \frac{n_i K_i [P]}{1+K_i [P]} \tag{4-3}$$

where n_i is the capacity of the solid for adsorption for the i^{th} process and K_i is the equilibrium constant for the i^{th} process. This expression is employed in the Multiple Equilibrium Analysis (MEA) of gas-solid interactions.[6,7,26,46]

An innovation of the MEA model is the resolution of adsorbate interactions with homogeneous regions of a heterogeneous solid and the definition of the n_i and K_i of these processes. This information is gathered through the measurement of adsorption isotherms at multiple temperatures measured above the critical temperature (T_c) of the adsorbate. The process capacities (n_i) are a characteristic of the solid and do not change with temperature, while the equilibrium constant (K_i) is temperature dependent. The resolvability of the different adsorbate-adsorbent interactions at a given temperature leads to the definition of processes. A process is defined by the order of pore filling, *i.e.*, the highest magnitude K_i is the first process. At equilibrium and excluding specific interactions, the first pores to fill will be those of similar size to the probe because these interactions have the most negative enthalpy and entropy of adsorption. The wide pore size distribution in amorphous solids allows for the pores used in a given process to vary with the probe size. A solid with limited pore dimensions (*e.g.*, mordenite or ZSM-5) does not possess the versatility of pore sizes encountered in amorphous solids. Heterogeneous solids sometimes undergo reversals in the enthalpy of adsorption (ΔH_i) and the order of pore filling (highest K_i).[6,46] The concept of a process, alone, is not an adequate descriptor of solids with a limited pore size distribution. The description of the different interactions encountered in heterogeneous solids with

crystalline frameworks (which have a limited pore size, *e.g.*, zeolites) requires the use of new terminology-process and type designation.[6] A type, as defined previously,[6] is a relationship between the molecular diameter of the adsorbate and the pore width of the adsorbent. A type 1 interaction defines the interaction of a probe with pores that are closest in size to itself, *i.e.*, a strong interaction with two opposing walls (a pore size of 1.0 to 1.2 molecular diameters). A type 2 interaction describes a probe adsorbed in a pore where the adsorbate is interacting strongly with one wall and weakly with the opposite (a pore size of 1.2 to 1.4 molecular diameters). An interaction with only one wall is the weakest, designated type 3 (a pore size greater than 1.4 molecular diameters). Considering a solid with a limited pore size distribution like mordenite, one can envision a smaller probe (*e.g.*, N_2) exhibiting the maximum interaction in a different region of the framework than a larger molecule (*e.g.*, SF_6) because the smaller molecule can access regions that the larger molecule can not.

Previous MEA studies have explored the porosity of carbons,[7,26] silica gel,[6] and other zeolites (HZSM-5,[6] TS-1,[46] and H-Y[47]). These other zeolites present an interesting comparison to the straight, intersecting, elliptical channels of mordenite. For instance, the zeolite, HZSM-5,[28,31] is comprised of the similar-sized straight channels (5.75 Å by 5.22 Å) and intersecting sinusoidal channels (5.55 Å by 5.29 Å).*[48] Mordenite is comprised of two different size channels (see Figure 4-1). The larger channel, commonly referred to as the "main channel," exists parallel to the *c* axis. The free aperture to the main channel is a 12 member oxygen ring with reported crystallographic dimensions of 6.69 Å by 7.05 Å.**[49] The smaller channels, often referred to as the "side-pockets," are a more complex series of offset channels that intersect the larger channel along the *b* symmetry

---

*These dimensions are based on an oxygen atom radii of 1.35 Å, with the fractional coordinates of reference 48.

**These dimensions are based on an oxygen atom radii of 1.35 Å, with the fractional coordinates of reference 49a.

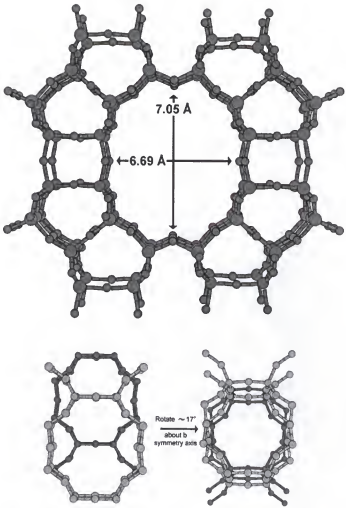

Figure 4-1: Schematic for the mordenite aluminosilicate framework. Based on fractional coordinates of reference 49a. The small channels have an opening of 4.82 Å 3.97 Å. When the structure is rotated ~ 17° about the *b* symmetry axis, the free aperture between two adjacent channels is ~3.4 Å by ~4.0 Å.

axis. The reported crystallographic dimensions for the small channel include an 8 member oxygen ring with an aperture of 4.82 Å by 3.97 Å.* The crystallographically determined values for the large channel aperture have been questioned.[50] From catalytic studies, Csicsery reports the presence of various molecules in the aluminosilicate framework of H-mordenite (H-MOR) that are

*Since "side-pockets" are offset, the opening to a small channel and the opening to the next consecutive small channel create an ~3.4 Å by ~4.0 Å "free aperture" between consecutive "side-pockets" (based on an oxygen atom radii of 1.35 Å).

larger than the reported crystallographic dimensions,[50] *e.g.*, 1,3,5-trimethylbenzene (MIN-2 of 8.3 Å) and 1,2,3-trimethylbenzene (MIN-2 of 7.9 Å), where MIN-2[43] is the second minimum larger dimension calculated from molecular dimensions that directly correlate with bulk molar volumes.[43] Csicsery concluded that these larger molecular species could not enter the structure if the aperture to the framework has the reported crystallographic dimensions.[50]

Since the acidic form of mordenite (H-MOR) is often utilized in catalytic industrial processes, the complete characterization of the acidic properties is of interest. Many techniques, such as Temperature Programmed Desorption,[51] various Nuclear Magnetic Resonance methods,[52] and Infrared Spectrocopy,[53] have been employed to study the interactions between a basic probe and H-MOR. Since the MEA model has the ability to characterize heterogeneous gas-solid interactions, it is interesting to explore the differences in gas adsorption between Na-mordenite (Na-MOR) and H-MOR. The analysis of the data gathered from Na-MOR and H-MOR (each with a limited pore size distribution) provides confirmation of the insights gained by the MEA model for gas adsorption.

Experimental

Gases

The gases CH_4, C_2H_6, C_3H_8, *i*-C_4H_{10}, *n*-C_4H_{10}, and Xe were purchased from Matheson. N_2 and CO were purchased from BITEC. O_2 was purchased from Alphagaz, SF_6 was purchased from Aldrich, and Ar was purchased from AIRCO. All gases are 99.99% pure and were used as received. Pertinent physical and molecular properties of the above gases can be found in Table 4-1.

Solid Preparation

Na-mordenite (Si/Al = 39.5, Lot #1716-23) was donated by Zeolyst International. The sample was degassed under vacuum for 8 hours at 200 °C. The IR spectrum of the degassed

Table 4-1: Summary of Physical and Molecular Properties of Adsorbates

Probe Gas[a]	MW	polarizability[b]	dipole moment[c]	MVL[d]	critical temp	boiling point	ΔH°_{v}	ΔS°_{v}	van der Waals	molecular area[d]	molecular radius[d]	molecular dimensions[d] (Å)	
	(g mol^{-1})	(Å^3)	(Debye)	(mL mol^{-1})	(°C)	(°C)	(kcal mol^{-1})	(cal mol^{-1} K^{-1})	const. *a*	(Å^2)	(Å)	MIN-1	MIN-2
O_2	32.00	1.58	0	23.55	-118.4	-183.0	1.63	18.08	1.360	14.66	2.106	2.93	2.99
N_2	28.01	1.74	0	25.02	-146.9	-195.8	1.332	17.22	1.390	15.27	2.149	2.99	3.05
CO	28.01	1.95	0.13	28.28	-140.2	-191.5	1.443	17.67	1.485	15.77	2.238	3.28	3.34
Ar	39.95	1.64	0	29.05	-122.4	-185.9	1.56	17.88	1.345	15.17	2.258	3.51	3.63
CH_4	16.04	2.59	0	29.74	-82.6	-161.5	1.96	17.5	2.253	16.26	2.276	3.83	3.94
Xe	131.29	4.04	0	44.06	16.9	-107.1	3.02	18.18	4.194	18.18	2.594	4.04	4.17
C_2H_6	30.07	4.47	0	47.21	32.3	-88.65[b]	3.51	19.0	5.489	24.01	2.655	3.81	4.08
SF_6	146.05	6.54	0	77.04	45.55	-63.8$_{sub}$	4.08	19.5	7.365[e]	31.17	3.126	4.87	5.27
C_3H_8	44.1	6.29	0.084	64.53	96.7	-42.1	4.54	19.6	8.664	28.27	2.946	4.02	4.52
i-C_4H_{10}	58.12	-	0.132	82.03	134.7	-11.63	5.089	19.46	12.870	35.27	3.184	4.63	6.00
n-C_4H_{10}	58.12	8.20	<0.05	81.40	152	-0.05	5.035	18.44	14.470	38.37	3.192	4.01	4.52

a. *Lange's Handbook of Chemistry*, 14th ed; McGraw-Hill: New York, 1992. All data is from this source unless otherwise specified.
b. *Handbook of Chemistry and Physics*, 71st ed; CRC Press: Boca Raton, FL, 1991.
c. McClellan, A. L. *Tables of Experimental Dipole Moments*; W. H. Freeman and Company, San Francisco, 1963.
d. Due to contradictions in the literature values, molar volumes (*MVL*), excluded molecular areas, and molecular dimensions of the adsorbates are calculated using ZINDO.[43,12] See text of reference 43 for more discussion.
e. Reference 4c, Table 2.

Na-MOR demonstrated no ammonium ions or water. H-MOR was prepared by exchanging Na^+ for NH_4^+ via soaking the Na-MOR in a solution of NH_4Cl, then filtering, and followed by calcining the sample at 400 °C. $NH_{3\,(g)}$ was released during the calcination, thereby producing H-mordenite. The resulting solid was stored under an inert atmosphere to prevent degradation from moisture.

Using a Micromeritics ASAP 2000 gas analyzer, the Brunauer-Emmett-Teller (BET) surface area[37] and pore volume data were measured with N_2 at 77 K. This information was gathered for a comparison to the analysis by the MEA model. The BET surface areas are reported using a 5 point BET calculation.[37] The MEA accessible surface area was calculated with CH_4 analysis at -63 °C. The micropore volume was determined using the Harkins-Jura *t*-plot model[38] with thickness parameters from 5.0 Å to 10.0 Å. Macro- and mesopore volumes were calculated using the Barrett-Joyner-Halenda (BJH) desorption curve.[39] The conclusions of the standard literature methods for characterizing the porosity of a solid are presented in Table 4-2.

Table 4-2: Physical Properties of Na-mordenite and H-mordenite

	Na-MOR	H-MOR
surface area ($m^2\ g^{-1}$)		
MEA[a]	265	342
BET[b]	458	462
pore volume ($\mu L\ g^{-1}$)		
micropore[c]	175	171
mesopore[d]	97	88
macropore[d]	-	-

a. MEA accessible surface area from CH_4 porosimetry.
b. BET surface area from N_2 porosimetry at 77 K.[37]
c. Micropore volume calculated from the Harkins-Jura *t*-plot model.[38]
d. Meso- and macropore volumes calculated from Barrett-Joyner-Halenda (BJH) desorption data.[39]

Adsorption measurements

Gas adsorption isotherms on Na-MOR and H-MOR were measured using the ASAP 2000 gas analyzer with the chemisorption/physisorption software employing a 47-point pressure table from 0.1 to 760 Torr. The system was determined to have reached equilibrium when the pressure change was less than 1% of the desired pressure point in a 15-sec equilibration time interval. Pressure tolerances were set to 1% for the 10 Torr transducer and 1 Torr with the 1000 Torr transducer. Low-temperature baths, consisting of liquid nitrogen/solvent mixtures,[40] were utilized to maintain a constant temperature for low temperature experiments. For higher temperature experiments, an insulated heating mantle was used to maintain the temperature. All experiments were carried out above the critical temperature of the adsorbate--this precaution inhibits the formation of multilayers. All temperatures were maintained to within ±1 °C.

Equilibrium analysis

The acquired isotherms were analyzed by using Equation 4-3. When applying this equation, the minimum number of processes needed to attain a fit of the experimental data were utilized. Detailed criteria for selecting the correct number of processes[7b] and proper application of the multiple-process equilibrium analysis[7] have been reported. For each data set, the graph of P_{atm} ÷ (mols adsorbed g^{-1}) vs P_{atm} produced a curved plot with linear regions. If Equation 4-3 describes a one-process adsorption equilibrium, the transformation would produce a linear plot, with the slope equal to $1/n_1$ and the intercept equal to $1/(n_1K_1)$. The seed values for n_i and K_i were obtained for each process from the linear regression of the linear regions of the curved transformation plot. These seed values were employed in a program utilizing a non-linear least-squares constrained modified simplex minimization algorithm designed to simultaneously fit the combined adsorption isotherm data of all the temperature sets for a particular adsorbate, allowing for better characterization of the processes and the total capacity of the solid. At lower temperatures, a

greater proportion of the capacity of the solid is utilized, leading to a better definition of the final processes. At higher temperatures, gas uptake is significantly reduced, improving the characterization of the initial processes.

Results and Discussion

Mordenite is a microporous zeolite with fixed channel dimensions (Figure 4-1). This zeolite, with reported crystallographic dimensions of 6.7 Å by 7.0 Å[49] for the large channel, is of interest because of its utilization in catalytic processes, such as hydrocarbon cracking.[34,35] The BET surface area of Na-MOR (458 $m^2 g^{-1}$) and H-MOR (462 $m^2 g^{-1}$) is an inaccurate measurement of the accessible surface area because of the inherent flaws in the BET method.[44] For microporous solids, the BET model leads to a measurement that is an over estimation of the surface area.[44] Utilization of the MEA model for the analysis of gas adsorption systems with Na- and H-mordenite, above the critical temperatures of the adsorbate, yields meaningful thermodynamic parameters for the interaction of a probe with the solid and offers an alternative to the common methods of microporous solid characterization.

Gas Adsorption on Na-Mordenite

Na-MOR was investigated with a variety of small and large adsorbates. The smaller probe gases (O_2, N_2, CO, Ar, and CH_4), whose experimental and calculated isotherms at -63 °C are plotted in Figure 4-2, were used to better characterize the smaller channels that cannot be accessed by the larger probes. The experimental and calculated isotherms of the larger probe gases (C_2H_6, C_3H_8, *n*-C_4H_{10}, *i*-C_4H_{10}, Xe, and SF_6) at various temperatures are plotted in Figure 4-3. A variety of gases were used to better characterize the channels by gradually increasing the size of the probe in an effort to approach the channel size. The appropriate physical and molecular properties of the adsorptives can be found in Table 4-1. The number of processes was determined from the acquired gas adsorption isotherms. The temperature dependent K_i are listed in Table 4-3, and the process

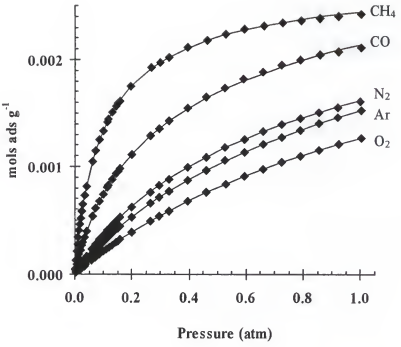

Figure 4-2: Adsorption isotherms at -63 °C for the small adsorbates (O_2, CO, N_2, Ar, and CH_4) on Na-mordenite. The ◆ represent the experimental data, and the solid lines are the calculated isotherms using the n_i and K_i values from the MEA description of adsorption.

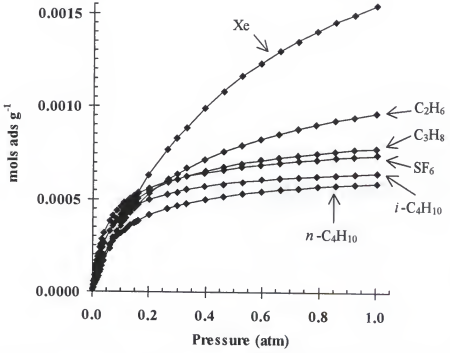

Figure 4-3: Adsorption isotherms at various temperatures for the large adsorbates Xe (30 °C), C_2H_6 (40 °C), C_3H_8 (100 °C), SF_6 (50 °C), i-C_4H_{10} (140 °C), and n-C_4H_{10} (165 °C) on Na-mordenite. The ◆ represent the experimental data, and the solid lines are the calculated isotherms using the n_i and K_i values from the MEA description of adsorption.

capacities (n_i), along with the accessible surface areas and pore volumes associated with each process, are reported in Table 4-4. The process designations emphasize the order of pore filling, with the largest K_i assigned to the first process, the next largest K_i assigned to second process, and so on. Except for the weak interactions of CO and N_2, the work on Na-MOR lacked specific acid-base interactions, further limiting the existing number of processes. Since the smaller probes can access the small channel (while the larger probes cannot) more processes are expected for the smaller gases.

For N_2 and CO adsorption of Na-MOR, the extension of MEA describes three processes. N_2 and CO possess very specific molecular properties (*i.e.*, size, shape, and polarizability) that enable these adsorbates to resolve two heterogeneous interactions in the large channel. CO and N_2 are also capable of acid-base interactions[53]--CO is weak and N_2 is an even weaker base. These donor-acceptor interactions allow for characterization of acidic properties of Na-MOR. Only two processes are required to describe O_2, Ar, and CH_4 adsorption in Na-MOR. The low polarizability (along with very little basic character) and small size of O_2 and Ar result in their inability to distinguish two processes for adsorption in the large channel and lead to one process for the small channel and one for the large channel. It follows that if Ar requires two processes to describe adsorption, then O_2 would require no more than two processes because O_2 has a lower polarizability than Ar. Even though CH_4 is more polarizable and capable of strong interactions with the solid, CH_4 requires two processes to describe adsorption--one process for the small channel and one for the large channel. Interestingly, while CH_4 only demonstrates two processes in Na-MOR, it is capable of distinguishing four processes in H-MOR, *vide infra*. The large adsorbates (C_2H_6, C_3H_8, *n*-C_4H_{10}, *i*-C_4H_{10}, Xe, and SF_6) are restricted from the small channel and are able to distinguish two heterogeneous interactions in the large channel; thereby, requiring two processes to describe adsorption.

Table 4-3: MEA Equilibrium Constants and Total Amount (mmol) adsorbed at Lowest Temperature for Na-mordenite

	temp °C (mmol)[a]	K_1 [b]	K_2 [b]	K_3 [b]
N_2	-93 (2.67 mmol)	38.69 ± 0.05	8.376 ± 0.019	0.835 ± 0.019
	-63	3.510 ± 0.031	1.371 ± 0.011	0.200 ± 0.011
	-43	1.490 ± 0.041	0.542 ± 0.014	0.107 ± 0.014
	-19	0.401 ± 0.011	0.1902 ± 0.0039	0.0442 ± 0.0039
Ar	-93 (2.72 mmol)	17.58 ± 0.07	1.87 ± 0.02	
	-63	2.55 ± 0.03	0.43 ± 0.01	
	-43	1.009 ± 0.003	0.2220 ± 0.0008	
	-19	0.342 ± 0.006	0.0901 ± 0.0018	
CH_4	-63 (2.41 mmol)	31.1 ± 0.2	6.46 ± 0.09	
	-43	7.98 ± 0.17	2.812 ± 0.066	
	-19	2.023 ± 0.018	0.7340 ± 0.0071	
C_3H_8	100 (0.78 mmol)	17.07 ± 0.13	1.78 ± 0.22	
	120	8.59 ± 0.06	0.776 ± 0.096	
	140	5.14 ± 0.03	0.435 ± 0.053	
	160	3.213 ± 0.037	0.249 ± 0.061	
i-C_4H_{10}	140 (0.64 mmol)	22.55 ± 0.14	3.00 ± 0.39	
	155	16.16 ± 0.07	1.51 ± 0.20	
	170	11.28 ± 0.05	1.02 ± 0.14	
	185	6.733 ± 0.017	0.408 ± 0.047	
SF_6	50 (0.74 mmol)	24.56 ± 0.20	1.39 ± 0.45	
	80	9.316 ± 0.051	0.58 ± 0.11	
	90	5.54 ± 0.03	0.306 ± 0.078	
CO	-93 (3.17 mmol)	267.1 ± 3.7	24.6 ± 1.2	1.6 ± 1.2
	-63	14.40 ± 0.61	3.06 ± 0.19	0.29 ± 0.19
	-43	5.422 ± 0.099	1.09 ± 0.03	0.15 ± 0.03
	-19	1.290 ± 0.010	0.305 ± 0.003	0.062 ± 0.003
O_2	-93 (1.68 mmol)	5.622 ± 0.097	0.97 ± 0.01	
	-63	2.24 ± 0.01	0.572 ± 0.001	
	-43	1.051 ± 0.014	0.3455 ± 0.0015	
C_2H_6	40 (0.96 mmol)	7.420 ± 0.036	0.883 ± 0.035	
	55	4.347 ± 0.015	0.470 ± 0.015	
	70	2.94 ± 0.01	0.31 ± 0.01	
	85	1.92 ± 0.01	0.20 ± 0.01	
	100	1.317 ± 0.008	0.114 ± 0.008	
n-C_4H_{10}	165 (0.59 mmol)	18.09 ± 0.18	2.52 ± 0.26	
	175	12.57 ± 0.07	1.63 ± 0.10	
	185	9.82 ± 0.13	1.253 ± 0.185	
Xe	30 (1.54 mmol)	2.411 ± 0.011	0.976 ± 0.014	
	45	1.490 ± 0.009	0.530 ± 0.011	
	60	0.972 ± 0.003	0.290 ± 0.004	
	75	0.6689 ± 0.0036	0.1888 ± 0.0047	

a. Total experimental amount adsorbed (mmol) at the lowest temperature analyzed is indicated in parentheses.
b. Gas-Solid Equilibrium Constant. The first digit of the uncertainty is the last significant figure.

Table 4-4: MEA Accessible Surface Areas ($m^2\ g^{-1}$) and Volumes ($\mu L\ g^{-1}$) of Na-mordenite

	N_2			CO		
	mmols ads	area	μL ads	mmols ads	area	μL ads
n_1	0.548 ± 0.011	50.4 ± 1.0	13.7 ± 0.3	0.530 ± 0.015	50.3 ± 1.4	15.0 ± 0.4
n_2	1.587 ± 0.027	146.0 ± 2.4	39.7 ± 0.7	1.672 ± 0.073	158.8 ± 6.9	47.3 ± 2.1
n_3	1.59 ± 0.13	145.9 ± 12.0	39.7 ± 3.3	1.66 ± 0.86	157.7 ± 81.5	46.9 ± 24.3
total	3.72 ± 0.17	342.3 ± 15.5	93.1 ± 4.2	3.86 ± 0.95	366.8 ± 89.9	109.2 ± 26.8

	Ar			O_2		
	mmols ads	area	μL ads	mmols ads	area	μL ads
n_1	0.91 ± 0.01	82.8 ± 0.9	26.3 ± 0.3	0.322 ± 0.005	28.4 ± 0.4	7.6 ± 0.1
n_2	2.87 ± 0.05	262.6 ± 4.6	83.5 ± 1.5	2.85 ± 0.02	251.4 ± 1.9	67.1 ± 0.5
total	3.78 ± 0.06	345.3 ± 5.5	109.8 ± 1.7	3.17 ± 0.03	279.8 ± 2.3	74.7 ± 0.6

	CH_4			C_2H_6		
	mmols ads	area	μL ads	mmols ads	area	μL ads
n_1	0.766 ± 0.014	75.0 ± 1.4	22.8 ± 0.4	0.712 ± 0.004	103.0 ± 0.6	33.6 ± 0.2
n_2	1.945 ± 0.035	190.5 ± 3.5	57.9 ± 1.1	0.714 ± 0.035	103.3 ± 5.0	33.7 ± 1.6
total	2.71 ± 0.05	265.5 ± 4.9	80.6 ± 1.5	1.43 ± 0.04	206.2 ± 5.6	67.3 ± 1.8

	C_3H_8			n-C_4H_{10}		
	mmols ads	area	μL ads	mmols ads	area	μL ads
n_1	0.5845 ± 0.0056	99.51 ± 0.96	37.72 ± 0.36	0.410 ± 0.005	87.1 ± 1.0	33.6 ± 0.4
n_2	0.350 ± 0.056	59.6 ± 9.6	22.6 ± 3.6	0.278 ± 0.031	59.0 ± 6.7	22.8 ± 2.6
total	0.93 ± 0.06	159.1 ± 10.6	60.3 ± 4.0	0.688 ± 0.036	146.1 ± 7.7	56.4 ± 3.0

	i-C_4H_{10}			SF_6		
	mmols ads	area	μL ads	mmols ads	area	μL ads
n_1	0.522 ± 0.004	120.7 ± 0.8	42.5 ± 0.3	0.6059 ± 0.0045	113.7 ± 0.9	46.7 ± 0.4
n_2	0.186 ± 0.025	42.9 ± 5.8	15.1 ± 2.0	0.267 ± 0.072	50.2 ± 13.4	20.6 ± 5.5
total	0.708 ± 0.028	163.6 ± 6.6	57.6 ± 2.3	0.873 ± 0.076	163.9 ± 14.3	67.3 ± 5.9

	Xe		
	mmols ads	area	μL ads
n_1	1.406 ± 0.007	159.4 ± 0.8	63.1 ± 0.4
n_2	1.101 ± 0.021	124.8 ± 2.4	49.3 ± 1.0
total	2.51 ± 0.03	284.2 ± 3.3	112.4 ± 1.3

Note: For excluded molecular areas and calculated molar volumes, see Table 4-1. The first digit of the uncertainty is the last significant figure.

Substitution of the calculated n_i and K_i into Equation 4-3 generates the process resolved isotherm. Figure 4-4 depicts a N_2 resolved adsorption isotherm at -93 °C on Na-MOR. The calculated isotherm (solid line) reflects the summation of the three component processes, demonstrating the energetically unique interactions that occur between N_2 and Na-MOR, and accurately generates the experimentally determined isotherm (points).

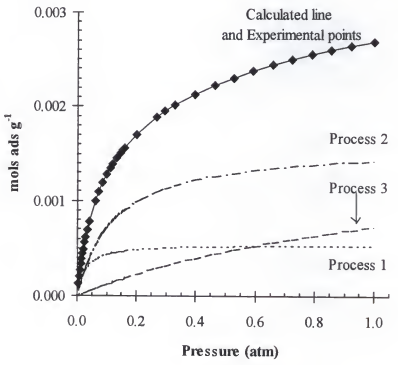

Figure 4-4: Resolved adsorption isotherm for N_2 on Na-mordenite at -93 °C. The ◆ represent the experimental data, the solid line is the MEA calculated total isotherm, and the three dashed lines represent the component processes.

Gas Adsorption on H-Mordenite

The adsorption isotherms for H-MOR have been determined for O_2, N_2, CO, CH_4, and Xe at various temperatures. N_2 and CH_4 were chosen because they are the adsorbate standards for the BET and MEA gas adsorption models, respectively. CO was chosen because of its ability to undergo specific donor-acceptor interactions. Xe is of interest because it is slightly larger than methane and is easily polarizable. Since adsorption of the smaller and less polarizable O_2 on Na-

MOR required only two processes (but still enters both channels), the adsorption of O_2 on H-MOR presents an interesting contrast to the other adsorbates. The H-MOR adsorption isotherms for Xe at 45 °C, O_2 and CH_4 at -63 °C, N_2 and CO at -93 °C are plotted in Figure 4-5, with calculated line and experimental points. The interaction of CH_4 with H-MOR is interesting because of the stark differences from the results of CH_4 with Na-MOR. The exchange of Na^+ for H^+ eliminates any occlusion due to the larger Na^+ and increases the charge to size ratio of the cation. These changes allow greater access and increased interactions in the small channel for CH_4. These added interactions are due to the high polarizability of CH_4, the size of CH_4, and the increased charge to size ratio of the cation from Na-MOR to H-MOR.

Replacement of Na^+ with the much smaller H^+ should yield an increase in the accessible surface area of the adsorbent. The BET model finds an apparent increase in the surface area from

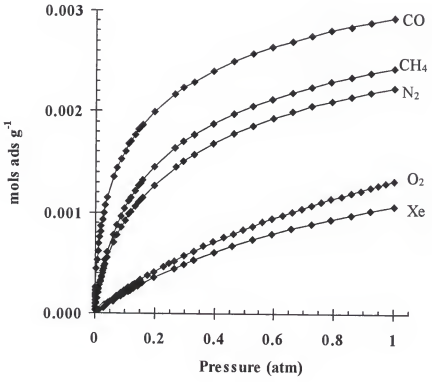

Figure 4-5: Adsorption isotherms at various temperatures for the adsorbates (O_2, N_2, CO, CH_4, and Xe) on H-mordenite. The ◆ represent the experimental data, and the solid lines are the calculated isotherms using the *n*, and *K*, values from the MEA description of adsorption.

458 $m^2 g^{-1}$ (Na^+ form) to 462 $m^2 g^{-1}$ (H^+ form). This small increase demonstrates the ineffectiveness of the BET model to determine an accessible surface area of a microporous solid. This inaccuracy exists because the experiment of the BET model fills a microporous structure with liquid nitrogen and designates the result as a surface area measurement. Therefore, the slight differences in the BET surface areas can be attributed to the difference in volume between Na^+ and H^+ cations. In contrast, MEA determined the accessible surface area of Na-MOR to be 265 $m^2 g^{-1}$ and H-MOR to be 337 $m^2 g^{-1}$. These values are significantly different because of the increased interactions of CH_4 in both channels of H-MOR. The temperature dependent thermodynamic equilibrium constants (K_i) for the adsorbates with H-MOR are listed in Table 4-5; process capacities (n_i), accessible process surface areas, and pore volumes for the adsorbates with H-MOR are tabulated in Table 4-6.

Summary of Na-Mordenite and H-Mordenite Thermodynamic Data

A solid with a limited pore size distribution undergoes different types of adsorbate-adsorbent interactions than does an amorphous solid. The distinction between interactions is clarified through the use of the process and type terminology.[6] A type 1 interaction arises when the probe undergoes strong interactions with all sides of the pore, *i.e.*, when the probe size most closely matches the pore size. A type 2 is an interaction with one wall and a significant, yet smaller, interaction with the opposite wall. A type 3 is adsorption on a surface with no significant interaction from the opposing wall. The difference between process and type designation is that processes describe the order of pore filling, while types classify the interactions of a probe with the adsorbent.* A process is determined simply by ordering the K_i from largest to smallest, with the

*In an effort to avoid confusion, ΔH_i and ΔS_i have been used to represent process-designated enthalpies and entropies, while ΔH_i and ΔS_i represent type-designated enthalpies and entropies.

largest K_i corresponding to the first process, *etc*. In general, the order of the enthalpies of adsorption follows the order of the process designations--no reversal of ordering of K_i and ΔH_i. If there is a reversal, in general, to determine the type designation for a given process, one orders the entropies of adsorption for the processes and assigns the most negative entropy to the type 1, the next most negative entropy to type 2, and so on. This type designation may be complicated by a probe that does not undergo a particular type interaction with the adsorbent, *e.g.*, no type 1 interaction, *vide infra*. The ΔH_i vs $a^{\frac{1}{2}}$ (square root of the van der Waals a parameter) plots are also utilized to help distinguish type designations in a given adsorbate-adsorbent system.

Previous studies have explored porous carbons where process and type designations are indistinguishable.[7,26,54] The similarity of process and type designations is a result of the wide pore size distribution that allows the probe gas to "choose" the most thermodynamically favored pore. In amorphous solids, gas adsorption occurs in pores of similar size to the probe gas, necessarily leading to the largest K_i and most negative ΔH_i corresponding to the same process.[7,26] A study of the zeolite, HZSM-5,[6] found that there is no direct correlation between types and processes because, in contrast to amorphous carbons, zeolites have fixed pore sizes. The probe adsorbs in the limited pore structure of the zeolite, which is not necessarily the "ideal" size for the adsorbate--*e.g.*, mordenite offers two unique channels for gas adsorption. Since crystalline solids have a limited pore structure that dictates where and how gas adsorption will occur, types and processes need not correlate.

Recall that type 1 is defined as a strong interaction with two opposing walls. The small gases (O_2, N_2, CO, Ar, and CH_4) are of an appropriate size to enter the small channel of mordenite, where the strongest interactions for the smaller probes can occur. For the small probes in the resolved isotherm, the first process corresponds most closely to type 1 adsorption in the small channel. The resolved isotherm illustrates two processes for N_2 and CO occurring in the

Table 4-5: MEA Equilibrium Constants and Total Amount (mmol) adsorbed at Lowest Temperature for H-mordenite

	temp °C (mmol)[a]	K_1 [b]	K_2 [b]	K_3 [b]	K_4 [b]
O_2	-93 (2.57 mmol)	21.8 ± 0.3	2.20 ± 0.04		
	-63	1.043 ± 0.004	0.2324 ± 0.0007		
	-43	2.61 ± 0.04	0.450 ± 0.005		
	-19	0.305 ± 0.001	0.1029 ± 0.0002		
N_2	-93 (2.22 mmol)	143 ± 3	17.3 ± 0.4	1.75 ± 0.15	
	-63	11.3 ± 0.3	2.476 ± 0.036	0.521 ± 0.014	
	-43	3.500 ± 0.065	1.020 ± 0.007	0.228 ± 0.003	
	-19	1.398 ± 0.021	0.248 ± 0.002	0.1068 ± 0.0009	
CO	-93 (2.91 mmol)	2078 ± 7	114.9 ± 3.7	15.0 ± 1.4	1.6 ± 0.9
	-63	114.6 ± 0.4	9.4 ± 0.2	1.97 ± 0.08	0.35 ± 0.05
	-43	29.71 ± 0.16	3.24 ± 0.08	0.87 ± 0.03	0.18 ± 0.02
	-19	2.81 ± 0.03	0.249 ± 0.015	0.193 ± 0.006	0.137 ± 0.004
CH_4	-63 (2.41 mmol)	54.6 ± 0.6	10.6 ± 0.1	4.5 ± 0.1	0.58 ± 0.09
	-43	13.4 ± 0.1	4.57 ± 0.03	1.82 ± 0.02	0.29 ± 0.02
	-19	2.83 ± 0.03	1.109 ± 0.006	0.514 ± 0.005	0.077 ± 0.004
Xe	30 (1.27 mmol)	1.977 ± 0.004	0.370 ± 0.006		
	45	1.268 ± 0.007	0.27 ± 0.01		
	60	0.810 ± 0.004	0.154 ± 0.006		
	75	0.551 ± 0.004	0.069 ± 0.007		

a. Total experimental amount adsorbed (mmoles) at the lowest temperature analyzed is indicated in parentheses.
b. Gas-Solid Equilibrium Constant. The first digit of the uncertainty is the last significant figure

large channel of mordenite, corresponding to two unique adsorbate-adsorbent interactions in the large channel. As discussed earlier, O_2 and Ar can not distinguish heterogeneous interactions in the large channel. Most of the larger probes (C_3H_8, *n*-C_4H_{10}, *i*-C_4H_{10}, Xe, and SF_6) can not fit adjacent to each other in the large channel of mordenite. The larger probes studied cannot access the small channel and are too small to undergo more than moderate interactions with the opposing wall of the large channel. For these molecules, the absence of strong interactions with two opposing walls leads to no type 1 interactions. However, by default, there is a first process because there is a

Table 4-6. MEA Accessible Surface Areas ($m^2\ g^{-1}$) and Volumes ($\mu L\ g^{-1}$) of H-mordenite

	O_2			N_2			Xe		
	mmols ads	area	μL ads	mmols ads	area	μL ads	mmols ads	area	μL ads
n_1	0.470 ± 0.008	41.5 ± 0.7	11.1 ± 0.2	0.094 ± 0.003	8.67 ± 0.25	2.359 ± 0.069	1.547 ± 0.009	175.4 ± 1.0	69.4 ± 0.4
n_2	3.12 ± 0.04	275.2 ± 3.4	73.4 ± 0.9	0.82 ± 0.01	75.9 ± 1.2	20.6 ± 0.3	0.92 ± 0.05	103.9 ± 6.0	41.1 ± 2.4
n_3	–	–	–	2.12 ± 0.11	195.1 ± 9.8	53.1 ± 2.7	–	–	–
total	3.59 ± 0.05	316.7 ± 4.1	84.5 ± 1.1	3.04 ± 0.12	279.6 ± 11.3	76.1 ± 3.1	2.46 ± 0.06	279.3 ± 7.0	110.5 ± 2.8

	CO			CH_4		
	mmols ads	area	μL ads	mmols ads	area	μL ads
n_1	0.231 ± 0.002	22.0 ± 0.2	6.54 ± 0.05	0.191 ± 0.002	18.7 ± 0.2	5.67 ± 0.07
n_2	0.45 ± 0.02	42.5 ± 1.6	12.6 ± 0.5	0.932 ± 0.008	91.3 ± 0.8	27.7 ± 0.2
n_3	1.20 ± 0.07	114.1 ± 6.7	34.0 ± 2.0	1.07 ± 0.02	105.2 ± 1.8	31.9 ± 0.6
n_4	1.8 ± 0.6	170 ± 56	51 ± 17	1.34 ± 0.14	130.9 ± 13.6	39.7 ± 4.1
total	3.7 ± 0.7	349 ± 64	104 ± 19	3.53 ± 0.17	346 ± 16	105 ± 5

Note: For excluded molecular areas and calculated molar volumes, see Table 4-1. The first digit of the uncertainty is the last significant figure.

largest K_i. In general, as the size of a given adsorbate increases, the excluded molecular area and the interactions with the channel increase, leading to a more negative ΔH_i. The resolved isotherms for the large probes illustrate two different processes. Since the dimensions of the larger molecules are larger than the free aperture of the small channel, these two distinct processes must occur in the main channel.

The enthalpies and entropies of adsorption for each process and adsorbate are determined from a van't Hoff plot with a weighted linear regression (*e.g.*, Figure 4-6 for the first process of the adsorbates interacting with Na-MOR). The thermodynamic parameters for each adsorbate and process can be found in Table 4-7 (Na-MOR) and Table 4-8 (H-MOR). For each of the adsorptives, the experiments are performed above the critical temperature of the gas. One should remember that the enthalpy of vaporization of a liquid becomes zero (as does the entropy of vaporization) as the temperature of the liquid approaches its critical temperature.

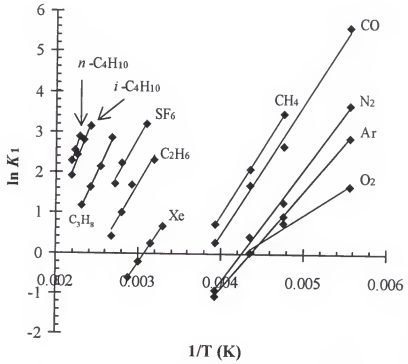

Figure 4-6: Example of van't Hoff plots (ln K_i vs 1/T (K)) for the various adsorbates on Na-mordenite.

Table 4-7. Enthalpies and Entropies of Adsorption with Na-mordenite

	$-\Delta H_1$	$-\Delta S_1$	$-\Delta H_2$	$-\Delta S_2$	$-\Delta H_3$	$-\Delta S_3$
N_2	5.67 ± 0.38	24.3 ± 2.0	4.59 ± 0.11	21.3 ± 0.6	3.56 ± 0.18	20.1 ± 0.9
CO	6.46 ± 0.33	24.8 ± 1.5	5.37 ± 0.11	23.4 ± 0.5	3.93 ± 0.12	20.9 ± 0.5
Ar	4.7 ± 0.1	20.7 ± 0.5	3.60 ± 0.17	18.7 ± 0.8		
O_2	2.71 ± 0.47	11.4 ± 2.3	1.75 ± 0.41	9.6 ± 1.9		
CH_4	6.46 ± 0.52	24.0 ± 2.3	5.18 ± 0.23	20.9 ± 1.0		
C_2H_6	6.60 ± 0.12	17.14 ± 0.36	7.53 ± 0.40	24.3 ± 1.2		
C_3H_8	8.92 ± 0.34	18.34 ± 0.84	10.52 ± 0.48	27.1 ± 1.2		
n-C_4H_{10}	12.4 ± 1.5	22.5 ± 3.3	14.2 ± 2.3	30.7 ± 5.0		
i-C_4H_{10}	10.4 ± 1.0	18.7 ± 2.3	16.1 ± 1.9	36.7 ± 4.5		
Xe	5.995 ± 0.067	18.04 ± 0.21	7.82 ± 0.26	25.85 ± 0.81		
SF_6	7.4 ± 1.3	16.5 ± 3.7	7.3 ± 2.0	21.8 ± 5.7		

Note: Enthalpies in kcal mol^{-1} and entropies in eu (cal mol^{-1} K^{-1}). The first digit of the uncertainty is the last significant figure.

Table 4-8. Enthalpies and Entropies of Adsorption with H-mordenite

	$-\Delta H_1$	$-\Delta S_1$	$-\Delta H_2$	$-\Delta S_2$	$-\Delta H_3$	$-\Delta S_3$	$-\Delta H_4$	$-\Delta S_4$
O_2	5.2 ± 0.2	22.8 ± 0.8	3.7 ± 0.1	19.2 ± 0.5				
N_2	5.70 ± 0.31	22.0 ± 1.4	5.17 ± 0.33	22.8 ± 1.5	3.59 ± 0.19	18.6 ± 0.8		
CO	7.6 ± 0.7	26.8 ± 3.5	6.8 ± 1.1	28.0 ± 5.2	5.3 ± 0.4	24.0 ± 1.8	2.6 ± 0.6	14.1 ± 2.6
CH_4	7.1 ± 0.2	25.99 ± 0.97	5.7 ± 0.9	22.0 ± 3.7	5.4 ± 0.5	22.5 ± 2.3	5.3 ± 1.0	25.6 ± 4.4
Xe	5.96 ± 0.09	18.3 ± 0.3	6.8 ± 1.5	24.2 ± 4.8				

Note: Enthalpies in kcal mol^{-1} and entropies in eu (cal mol^{-1} K^{-1}). The first digit of the uncertainty is the last significant figure.

One might expect that the difference between the process entropies for the small adsorptives would result from simply confining the adsorbate to the smaller of the two channels (resulting from a change in volume). This difference in volume would produce a difference of 2.9 eu (2.9 eu = $-R \ln (v_{small}/v_{large}) = R \ln (26.3/112.4)$; 26.3 μL from the first Ar process with Na-MOR, and 112.4 μL from the total of the Xe processes with Na-MOR). However, the largest observed difference is 13.9 eu. Therefore, the difference in the process entropies results from the differing interactions of the adsorbate with the solid.

One might note that, in general, the entropy of adsorption is relatively constant, ≈ -22 eu. One can compare the magnitude of this average of the entropies of adsorption (22 eu) to Trouton's constant (21-22 eu). With Trouton's Rule, the relationship comes from the similarity of the dispersion interaction of the molecules at the phase transition. The phase transition produces a change in the environment of a molecule from the gas phase, where it has free motion, to the liquid phase, where it has restricted motion. One would expect that a physisorption interaction would also produce a similar restrictive motion due to the dispersion interaction, more specifically, the interaction of the molecule with a homogeneous portion of the solid. This constancy of the entropy of adsorption is analogous to Trouton's Rule, *i.e.*, for a given molecule interacting with a solid, the entropy of adsorption remains approximately constant, as for a pseudo-phase change of the adsorptive. The variation of the entropy from 22 eu is due to the influence of the solid on the adsorbate.

For the smaller adsorbates (O_2, N_2, CO, Ar, and CH_4), the process designations are in the same order as the type designations (Tables 4-7 and 4-8). With most of the larger probes (C_2H_6, C_3H_8, *n*-C_4H_{10}, *i*-C_4H_{10}, and Xe), a more negative ΔH_2 and ΔS_2 (the second process) is found when compared to those determined for the first process for Na-MOR (Table 4-7). For the large adsorbates, the reversal of the order of the enthalpy and entropy of adsorption for the first and

second process occurs because of the different interaction types between the adsorbate and adsorbent. This reversal is also found for Xe on H-MOR (Table 4-8).

An increase in magnitude of the entropy is generally observed[42,55] with a more negative enthalpy of interaction. This relationship has also been reported for solubility data and was first compiled by Barclay and Butler.[55] Figures 4-7a and 4-7b represent the linearity of the entropy-enthalpy plots ($-\Delta S_i$ vs $-\Delta H_i$) for CO and C_2H_6 on a variety of solids, which illustrates process and type designations. Error bars are included for the parameters derived for the carbonaceous solids; where no error bars are visible, they are present underneath the symbol for that particular data point. For the carbonaceous solids (A572, A600, A563, F300, and BPL),[54] the process and type designations concur on both CO and C_2H_6. For the zeolitic solids (HZSM-5 and Na-MOR)--where process and type designations need not correspond--the first process for C_2H_6 on Na-MOR is a type 3 interaction, the C_2H_6 second process on Na-MOR is a type 2, and the first C_2H_6 process on HZSM-5 is a type 2 interaction. For all of the CO systems (except TS-1 with no type 1 interaction), the process and type designations coincide. One should note that the separation of the types is derived from the enthalpy data, which have significantly lower errors than the entropy data. While the CO and C_2H_6 plots best represent the difference in type and process designations, equivalent plots can be made for other adsorbates and show similar trends.

It is also interesting to note that for the adsorbates interacting with both Na- and H-MOR, the enthalpy of adsorption (ΔH_i) is directly proportional to the temperature dependent change in free energy (ΔG_i). Of course this linear relationship can only be observed for adsorbates that require more than two processes. The highest enthalpy process for N_2 and CO interacting with H-MOR and the lowest process enthalpy for CH_4 interacting with H-MOR deviate from this relationship, and this departure is an indication of a non-similar adsorption process, when compared to the

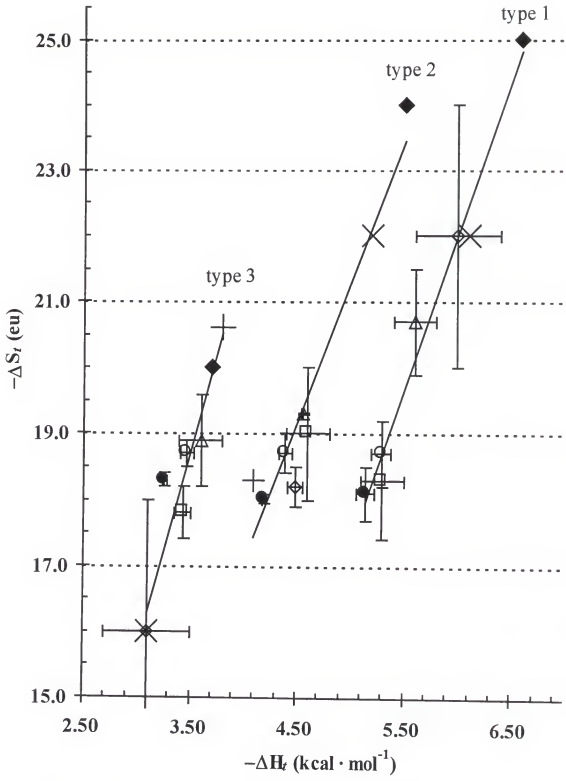

Figure 4-7a: CO entropy-enthalpy plot. When the adsorption processes are grouped according to the interaction type, the graph of the entropy vs the enthalpy of adsorption ($-\Delta S_t$ vs $-\Delta H_t$) results in a linear correlation. (a) CO type plot and (b) C_2H_6 type plot. The symbols represent: ● (BPL), ○ (A572), △ (A600), □ (F300), ◇ (A563), ◆ (Na-MOR), × (HZSM-5), + (TS-1).

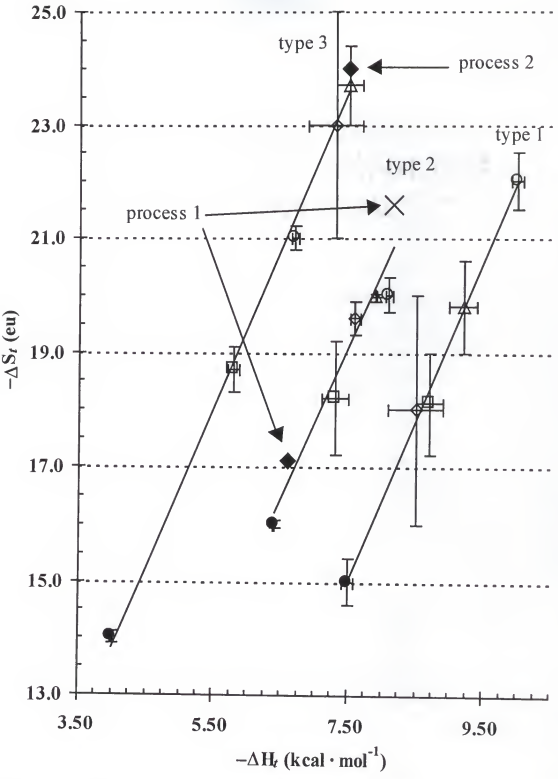

Figure 4-7b: C_2H_6 entropy-enthalpy plot. When the adsorption processes are grouped according to the interaction type, the graph of the entropy vs the enthalpy of adsorption ($-\Delta S_f$ vs $-\Delta H_f$) results in a linear correlation. (a) CO type plot and (b) C_2H_6 type plot. The symbols represent: ● (BPL), ○ (A572), △ (A600), ◘ (F300), ◇ (A563), ◆ (Na-MOR), × (HZSM-5).

other processes. The deviation of the strongest interaction of N_2 and CO might be expected since these processes are most likely the interaction with the most acidic acid site of H-MOR.

An increase in K_i (Table 4-5) and ΔH_i (Table 4-8) is observed for the interactions of the adsorbate with H-MOR when compared to those with Na-MOR. These changes indicate that while the H^+ in H-MOR is not able to significantly hinder adsorption (as did the Na^+), the proton influences the adsorbate-adsorbent interactions considerably. The value of ΔH_1 and ΔH_3 for N_2 remain constant (within error) for the interaction with H-MOR and Na-MOR (Tables 4-7 and 4-8). Geobaldo *et al.* conclude that the strongest interaction of N_2 with H-MOR is with the Lewis acid site.[53e] The ΔH_1 for N_2 represents an interaction with the Lewis acid site, and the exchange of the Na^+ for the H^+ does not significantly effect the strength of the Lewis site. Geobaldo *et al.* also conclude that, while N_2 can access the small channel, N_2 does not interact with the small channel Brönsted acid site.[53e] These conclusions[53e] confirm our findings with MEA--no fourth process for the interaction of N_2 with H-MOR, *vide infra*. For N_2 interacting with Na-MOR and H-MOR, the low heat and constant value of ΔH_3 indicate that the third process (type 3) is a simple physisorption interaction with the solid. The conclusions of Geobaldo *et al.* concur with this simple physisorption assignment.[53e]

For a given type of interaction, ΔH_i is directly proportional to the square root of the van der Waals *a* constant.[6,7,26,46] Figures 4-8 demonstrates the correlation that exists when the types are grouped and then plotted enthalpy of adsorption ($-\Delta H_i$) vs $a^{½}$. The lack of correlation between the process designated enthalpies and $a^{½}$ is due to the fact that processes are not a measure of adsorbate-adsorbent interactions. The first process for the small adsorbates does not involve the same interactions as the first process for the larger adsorbates; *e.g.*, N_2 (smaller adsorbate) is capable of entering the small channel, while the larger *i*-C_4H_{10} is restricted from those pores. The type designation groups similar interactions and allows for the correlation with the $a^{½}$. Poorer

correlations can arise because of a finite pore size of a given adsorbent, *e.g.*, in mordenite each probe adsorbs with the strongest possible interaction, which is not necessarily the most "ideal" interaction type, changing the expected magnitude of the enthalpy.

Each probe will maximize its interaction with one wall, and as the probe size increases, the adsorbate will begin to interact with the opposing wall. For example, a steady increase of the $-\Delta H_{t,ads}$ for type 2 on Na-MOR is observed from CH_4 (6.3 kcal mol^{-1}), C_2H_6 (7.5), C_3H_8 (10.4) *n*-C_4H_{10} (14) to *i*-C_4H_{10} (16). This trend demonstrates the gradual increase of adsorbate-adsorbent interactions as a probe increases the interactions with the opposite wall of the large channel. The weighted-linear regression of the type 2 enthalpies for the adsorbates interacting with Na-MOR yields a reasonable correlation, $-\Delta H_2 = 3.61(a^{½}) + 0.35$, $R^2 = 0.924$. As one might expect, there also exists a correlation between the excluded molecular area and the enthalpy of adsorption for a

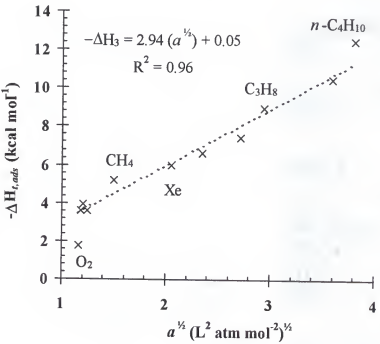

Figure 4-8: Enthalpy of Adsorption vs $a^{½}$. The type-grouped enthalpies of adsorption ($-\Delta H_{t,ads}$) for the adsorbates on Na-mordenite vs the square root of the van der Waals *a* parameters ($a^{½}$) of the adsorbates. This weighted-linear correlation is for a type 3 interaction of the adsorbate with the solid.

given type of interaction, as the excluded molecular area increases so does the enthalpy of adsorption.

Comparison of MEA Results with IR Studies, Simulations, and Adsorption Studies

Since the acidic form of mordenite (H-MOR) is often utilized in catalytic industrial processes, the complete characterization of its acidic properties is useful. Many techniques, such as Temperature Programmed Desorption,[51] various Nuclear Magnetic Resonance methods,[52] and Infrared Spectrocopy,[53] have been employed to study the interactions between a probe molecule and mordenite. Since the MEA model has the ability to characterize heterogeneous gas-solid interactions, it is interesting to explore the differences in gas adsorption between Na-MOR and H-MOR. In addition, it is useful to compare the MEA interpretation to the pertinent results from the above mentioned spectroscopic techniques.

Geobaldo *et al.* and Wakabayashi *et al.* have studied H-MOR and the Group IA cation exchanged forms of mordenite and found results that depend on the cation.[53a-g] The exchange of the H^+ with an alkali metal cation will lead to two differences in the gas-solid interactions. First, the H^+ will occupy considerably less space than the akali cation, thereby significantly reducing the occlusion of the small channel produced by the Group IA cations. Excluding specific interactions, this feature will lead to increased accessible surface areas. Second, the proton, with its larger charge to size ratio, will increase the strength of the specific interactions of the adsorbate with the solid, *i.e.*, increased equilibrium constants (K_i) and enthalpies of adsorption (ΔH_i).

Since both the fundamental infrared stretching frequency of the adsorbed molecule and the change in free energy upon adsorption are proportional to the strength of the interaction (between the adsorbate and the adsorbent), one might expect a linear relationship between the free energy change associated with adsorption and the infrared stretching frequency of the adsorbed molecule. A comparison of the findings of Geobaldo *et al.* and Wakabayashi *et al.* (fundamental infrared

stretching frequencies associated with the adsorbed molecule) with the MEA results (change in free energy upon adsorption) yields reasonable agreement. If one compares the N_2 stretching frequencies ($\nu_{N\equiv N}$) of the adsorbed N_2 on H-MOR[53a,e] to the natural log of the MEA derived process equilibrium constant ($\ln K_i$, which is directly proportional to ΔG_i) for N_2 adsorbed on H-MOR, one finds a linear correlation (see Figure 4-9a). This linear correlation is the expected linear free energy relationship for the simple adduct formation of a given molecule and a series of acids.[56]

Again, a linear correlation is found if one compares the analogous CO data of Bordiga *et al.*[53d] ($\nu_{C\equiv O}$ for the interaction of CO with H-MOR) to the MEA results ($\ln K_i$), see Figure 4-9b. The IR spectrum of CO adsorbed on H-MOR contains three bands (one band at ~2223 cm^{-1}, one asymmetric band at 2172 cm^{-1}, and one band at 2138 cm^{-1}).[53d] Although Bordiga *et al.* do not assign the broad peak centered at ~2223 cm^{-1}, the peak assignment follows from the conclusions of Geobaldo *et al.*[53e] and the conclusions of Gruver and Fripiat[53h]--this peak is the interaction of CO with the Lewis acid site. Bordiga *et al.* note that the 2172 cm^{-1} band is asymmetric on the low frequency side and attribute this band to the two types of bridged (Brönsted) OH groups (main channel and small channel location).[53d] While "the perturbation of the C-O stretching vibration does not seem to be sensitive enough to discriminate between the two [Brönsted sites],"[53d] MEA can resolve this slight difference in interaction. Since the 2172 cm^{-1} asymmetric peak is comprised of the two unresolved interactions, Figure 4-9b includes the shift of this asymmetric peak once--speculation about the deconvolution of this 2172 cm^{-1} band is erroneous. In order to match the 2172 cm^{-1} shift, the value for the $\ln K_i$ used in Figure 4-9b is the capacity-weighted free energy change for the second and third process, $\ln K_{2\text{-}3\ \text{weighted}} = (n_2/(n_2 + n_3) \times \ln K_2 + (n_3/(n_2 + n_3) \times \ln K_3$. From the process capacities, one can conclude that the second CO process on H-MOR is for the interaction with the Brönsted sites in the small channel, while the third CO process is the interaction with the large channel Brönsted acid site.

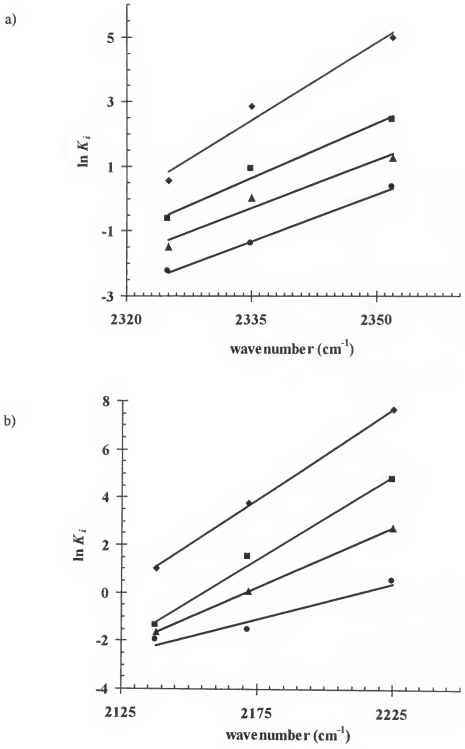

Figure 4-9: Linear free energy relationship between the temperature-dependent free energy (ln K_i) and the Infrared stretching frequency (v) for (a) N_2 adsorbed on H-mordenite at -93 °C (◆), -63 °C (■), -43 °C (▲), and -19 °C (●); and (b) CO adsorbed on H-mordenite at -93 °C (◆), -63 °C (■), -43 °C (▲), and -19 °C (●).

The restrictive size and geometry of the mordenite large channel requires the probe molecules to encounter different gas-solid interactions in the same channel. In the large channel, adsorption at adjacent walls is eliminated for the large probes, and the structure of the large channel forces adsorbate-adsorbent interactions that are energetically unique. The MEA description of adsorption distinguishes between two unique interactions in the large channel for Xe (5.995 ± 0.067 kcal mol^{-1} for the first process [type 3] and 7.82 ± 0.26 kcal mol^{-1} for the second process [type 2]), and this finding is in agreement with the Monte Carlo simulations of Xe adsorption on Na-MOR.[57] From Monte Carlo simulations, Nivathi *et al.* conclude that there are two heterogeneous adsorption processes--one process at the opening to the side-pockets in the main channel (two "sites") with an enthalpy of 10.7 kcal mol^{-1} and the other process in the main channel (six "sites") with an enthalpy of 7.2 kcal mol^{-1}.[57] The authors state that two of the six "sites" of the main channel have a slightly different adsorption potential, a difference of 0.09 kcal mol^{-1} for a Si/Al ratio of 5, which is within two standard deviations of the MEA enthalpy for the first process (type 3). Since there exists an "inaccurate estimation of the polarization energy component of the total adsorption potential energy,"[57] the ratio of the enthalpies from the simulation ($\Delta H_{\text{Side-pocket}}$ / $\Delta H_{\text{Main}} = 0.67$) and the ratio of the MEA enthalpies ($\Delta H_{\text{process 1}}$ / $\Delta H_{\text{process 2}} = 0.77$) should be used for a comparison. This comparison of the relative values demonstrates modest agreement between the two. For a comparison of the amount of Xe adsorbed by Na-MOR for a given process, a ratio of the process capacity to the total capacity should be used. This comparison yields 0.37 ± 0.1* for the second MEA process capacity and 0.25** for the "side-pocket site" capacity.

*The ratio of the MEA process 2 capacity to the total capacity is $0.37 \pm 0.1 = (0.93 \pm 0.09$ mmol / $(0.93 \pm 0.09$ mmol + 1.57 ± 0.01 mmol)).

**The ratio of the "side-pocket site" capacity (per unit cell) to the total "site" capacity (per unit cell) is 0.25 = (2 molecules / (2 molecules + 6 molecules)).[57]

Ohgushi and Yokoyama have reported the heat of adsorption for Xe in Na-MOR (Si/Al = 9.43) to be ~7.6 kcal mol^{-1},[58] and this value is in good agreement with the weighted average of the MEA enthalpies (7.14 ± 0.42 kcal mol^{-1})* for Xe adsorption on Na-MOR (Si/Al = 39.5).

Insights from the Process Capacities of Na-Mordenite and H-Mordenite

The process capacities are converted into accessible adsorbent surface areas (using the excluded molecular areas[43]) and pore volumes (using the calculated molar volumes, *MVL*[43]). Different literature reports give adsorbate molar volumes (used for molecular volume) and molecular areas that vary considerably. Generally, these molecular properties have been estimated from bulk properties, but many assumptions are required. The calculation of these properties eliminates the need to assume spherical symmetry of the adsorbate and a molecular packing in the structure.[43] Molecular properties, calculated molar volumes, and excluded molecular areas were determined previously[43] for the adsorptives utilizing ZINDO,[12] a series of molecular electronic structure programs from the Quantum Theory Project at the University of Florida, and are presented in Table 4-1.

The calculated MEA capacities (n_i), accessible surface areas, and pore volumes for Na-MOR can be found in Table 4-4 and Table 4-6 for H-MOR. In general, the total process capacities decrease as the size of the probe increases. The fact that both N_2 and CO, which are larger than O_2, yield a total accessible adsorbent surface area greater than that of O_2 is caused by their electron donor properties and higher polarizability, which permit specific donor-acceptor interactions with the solid.

---

*$-\Delta H_{\text{weighted MEA}}$ = (7.14 ± 0.42 kcal mol^{-1}) = (n_1/n_{tot}) × $-\Delta H_1$ + (n_2/n_{tot}) × $-\Delta H_2$
= (0.627 ± 0.013)×(7.82 ± 0.26) + (0.373 ± 0.022)×(5.995 ± 0.067);
n_1/n_{tot} = 0.627 ± 0.013 = (1.547 ± 0.009 mmol) ÷ (2.467 ± 0.051 mmol);
n_2/n_{tot} = 0.373 ± 0.022 = (0.92 ± 0.05 mmol) ÷ (2.467 ± 0.051 mmol);
$n_{\text{tot}} = n_1 + n_2$ = 2.467 ± 0.051 mmol = (1.547 ± 0.009) + (0.92 ± 0.05)

As expected, the pore volume of the small channel is significantly less than the volume of the large channel. This difference aids in the distinction between the types of interactions. For Na-MOR, the type 1 accessible surface areas for N_2 and CO are lower than their type 2 and type 3 accessible surface areas. The type 1 accessible surface areas for both N_2 and CO are identical within error, and the type 2 value is equal (within error) to the type 3 value for both N_2 and CO. This information indicates that both N_2 and CO have similar interactions with the small channel, and the volume of the small channel is a minor proportion of the total pore volume; *i.e.*, the large channel is the majority of the structural pore volume (structural porosity volume of the solid). Since the larger probes are excluded from the small channel, they may only be used to determine information about the large channel and the aperture of the small channel and yield no information about the small channel directly.

Conclusions

Adsorption isotherms for eleven adsorptives were measured at multiple temperatures above their critical temperatures with the zeolite Na-mordenite and five representative adsorptives with H-mordenite. The Multiple Equilibrium Analysis (MEA), which fits the adsorption isotherms simultaneously to a minimum number of processes (Tables 4-3 and 4-5), provides process capacities, accessible surface areas, and pore volumes (Tables 4-4 and 4-6) and enthalpies and entropies of adsorption for each process (Tables 4-7 and 4-8). The adsorption process contains a narrow distribution of the same thermodynamic interaction parameters (within experimental error) and groups them together in describing the adsorption process (an interaction type). Mordenite was selected for study because it contains two channels with very different, fixed dimensions. The examination of Na-MOR and H-MOR has provided insights into the very complex energetics of adsorbate-adsorbent interactions. Unlike amorphous adsorbents, where for the first process an

adsorptive can select pores of similar size from the distribution available, the first adsorption process that occurs in materials with uniform, fixed dimensions may not involve a pore of comparable size. This difference leads to the type designation terminology, used to indicate the degree of matching of adsorptive and pore dimensions.

Reversals in the magnitude of the enthalpy of adsorption ($-\Delta H_i$) and equilibrium constant (K_i) are found for the processes corresponding to adsorption of the larger adsorbates in the large channel of Na-MOR and H-MOR. The larger adsorbates studied did not exhibit any type 1 interactions with Na-MOR or H-MOR. The first process of the larger adsorbates has the larger K and less negative enthalpy, and the $-\Delta H_i$ vs $a^{½}$ plot indicates a type 3 interaction for the first process and a type 2 interaction for the second process. A wide variety of probe molecules have been studied on carbonaceous adsorbents, and none show this reversal. In contrast to zeolites, the pores of the carbonaceous A-572 consist of parallel sheets or planes with localized graphitic domains. The adsorbate-adsorbent interactions occur along the surfaces of these planes, and a large adsorbate is less constrained in a slit-shaped pore than it is in a cylindrical pore. Reversals in K_i and ΔH_i can be expected for some adsorbates in cylindrical-shaped pores.

The process capacities that result from MEA are as significant as the thermodynamic data. Using calculated molar volumes (*MVL*), one can calculate the accessible pore volume for an adsorbate. When adsorptive dimensions match pore dimensions, structural pore volumes result. A comparison of these volumes with those from standard N_2 porosimetry shows important differences. For measurements above the adsorptive critical temperature, monolayer coverage is expected and conversion of the MEA process capacities (with excluded molecular areas) provides probe dependent, accessible surface areas. Significant differences result between the values obtained in this manner and those from BET on microporous solids.

The larger equilibrium constants obtained for H-MOR compared to Na-MOR (Tables 4-5 and 4-3) indicate that H-MOR has a larger affinity for adsorbing the molecules studied due to the stronger interactions induced by the proton of H-MOR. The MEA description of adsorption provides a rational explanation of adsorbent differences using thermodynamic parameters and probe dependent adsorbent capacities. The MEA method produces insight and a useful overall characterization of gas-solid interactions.

CHAPTER 5
A METHOD FOR CHARACTERIZING EFFECTIVE PORE SIZES OF CATALYSTS

Introduction

Zeolites have played a major role in shape and size selective catalysis. The properties of these heterogeneous catalysts and other solid adsorbents have been widely studied and discussed.[59-61] The selectivity of these structures has been a major concern since the first use of zeolite Y as an isomerization catalyst in 1959.[62] The zeolite's inherent control over a reaction within the internal constraints of the structure directs this selectivity at the molecular level. Selectivity in heterogeneously catalyzed reactions arises from reactant selectivity, two types of product selectivity, and restricted transition-state selectivity.

Reactant selectivity is a case in which potential reactants are excluded based upon their size compared to that of the pore dimensions. Different zeolites have distinct window openings to their channel system. There are more than 50 different available aluminosilicate zeolites with pore openings ranging from less than 5 Å to larger than 10 Å,[63] and silicoaluminophosphates extend this upper limit to 13 Å.[64] This selectivity and a wide number of zeolites give the potential to preferentially use certain reactants in a catalytic reaction within a multiple reactant system. Many examples of this type of selectivity are found in the literature.[63] A simple diagrammatic representation of reactant selectivity is shown in Figure 5-1a.

Product selectivity may be obtained by two different means--preferential diffusion and size exclusion. Preferential-diffusion product selectivity appears when two or more reaction products made within the confines of the structure have apparent diffusivities, which sufficiently differ to

allow one product to preferentially diffuse out of the structure. Often, the smaller diffusivity of the larger isomer allows for isomerization to the diffusion preferred (smaller) product. One must recall that a reaction product is a molecule formed within the structure by the reaction, but that not all reaction products necessarily appear in the product stream. Preferential-diffusion product selectivity, which has been referred to as configurational diffusion controlled selectivity,[67] is represented in Figure 5-1b. The second type of product selectivity, size-exclusion, arises from an actual confinement of a reaction product within the structure of the solid. Exclusion product selectivity had been hypothesized, and the work of Anderson and Klinowski[17] demonstrated the experimental evidence. This type of selectivity is represented in Figure 5-2a.

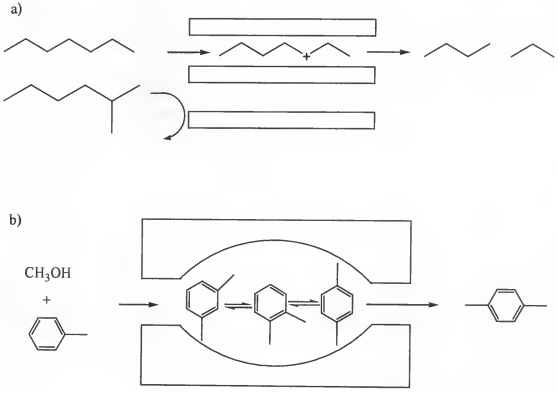

Figure 5-1: Selectivity in zeolites. (a) Representation of reactant shape selectivity in zeolite channnels (rejection of branched chain hydrocarbons). After reference 65. (b) Representation of preferential-diffusion product shape selectivity (*p*-xylene diffuses preferentially out of the channels). After reference 66.

The final type of selectivity to be discussed is restricted transition-state selectivity. For this type of selectivity, certain types of transition states are too large to be contained within the pores (or, if present, intersections) of the structure. Experimental evidence for transition-state selectivity comes from low temperature cyclization of dienes inside H-mordenite (H-MOR, a large pore zeolite) and HZSM-5 (a medium pore zeolite.) Using electron paramagnetic resonance (EPR) spectroscopy, one can observe the formation of cyclo-olefinic radical species inside the structure of H-MOR compared to HZSM-5 where no cyclo-olefinic radicals are formed.[66] Figure 5-2b is a

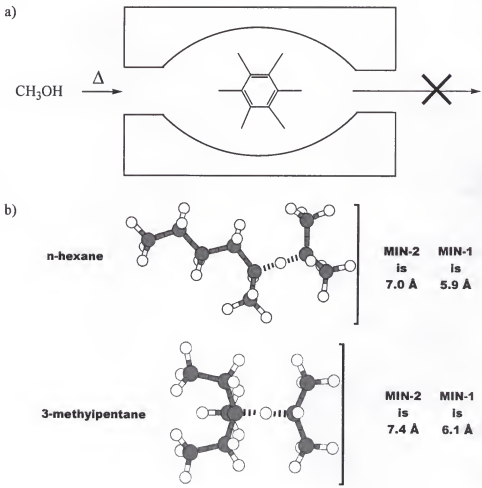

Figure 5-2: Selectivity in zeolites. (a) Representation of size-exclusion shape selectivity (hexamethylbenzene cannot diffuse out of the intersection). (b) 3-Methylpentane is a bulkier molecule than *n*-hexane, therefore its transition state has a larger cross section. The transition states and their sizes were calculated using ZINDO.[12]

representation of different sized transition states. In this case, 3-methylpentane has a bulkier transition state than does *n*-hexane (determined by calculated minimum dimensions).

To date, the investigation and subsequent reporting of the effective pore size of zeolite catalysts has not been systematic with respect to the reactions catalyzed by a particular solid. The literature values, determined from crystallographic measurements, for the window size of the straight (large) channel of HZSM-5 are 5.6 Å by 5.4 Å and for the zigzag (small) channel of HZSM-5 are 5.5 Å by 5.1 Å.[32] Figure 5-3 is a representation of the crystallographically determined pore size compared to the oxygen atom center-to-center distances of the large channel of HZSM-5. While these quoted aperture sizes are used throughout the literature, it is well-known that large aromatic molecules (>7 Å) are readily formed in catalytic reactions involving these materials and are found in the product stream at mild reaction conditions (*i.e.*, 300 °C and atmospheric pressure).[68]

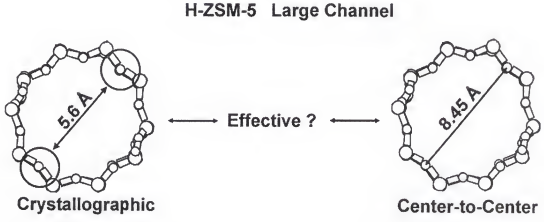

Figure 5-3: Crystallographic pore size vs center-to-center distance. Crystallographic pore size based on oxygen atom radius of 1.35 Å. The values used for the center-to-center oxygen distances were obtained from the fractional coordinates of the van Koningsveld *et al.* (*Acta. Crystallogr.* **1987**, *B43*, 127-132) which had improved framework accuracy over previous reports. The oxygen atoms used were those chosen by Olson *et al.*;[32] for the straight channel, the largest (8.449 Å) and smallest (7.922 Å) center-to-center oxygen atom distances give rise to 5.75 Å by 5.22 Å dimensions of the large channel based on an oxygen atom radius of 1.35 Å.

Many authors ascribe this discrepancy between reported crystallographic pore sizes of zeolites and catalytic reaction products to thermal vibrations as well as the distortion of the crystal lattice and the adsorbate molecule. This "movement" is said to account for changes of 0.4 Å in the oxygen window sizes.[69]

The early studies of Barrer first noted this discrepancy.[70] Csicsery concluded from the selective disproportionation of ethyltoluene over H-MOR that the effective pore dimensions were somewhere between 8.2 Å and 8.6 Å.[50] These dimensions are 1.2 Å to1.6 Å greater than the largest dimension of the reported crystallographic measurements (6.7 Å by 7.0 Å). Dwyer *et al.* determined an elliptical catalytic pore size for HZSM-5 of approximately 5.5 Å by 7 Å on the basis of dewaxing of distillate charge stocks and noted that HZSM-5 can discriminate both molecular size and shape.[71] This report also concluded that H-MOR has a "catalytic pore size" between 9 Å to 10 Å and ZSM-23 (crystallographic: 4.5 Å by 5.6 Å) has a catalytic pore size of 4.5 Å by 6.5 Å.[71]

Many studies have been conducted on the attractive and repulsive interactions between molecules and solids. A commonly used potential for studying these interactions is the Lennard-Jones (LJ) 12-6 potential, which has several assumptions. The main premise is that a spherically symmetric potential is assumed with an r^{-6} dependence on attractive forces and an r^{-12} dependence on repulsive forces. The minimum allowed separation (σ_{sep}) of two approaching species can be calculated from the LJ 12-6 potential and the equilibrium position (r_{sep}) with Equation 5-1.

$$\sigma_{sep} = 2^{1/6} r_{sep} \tag{5-1}$$

This equation may be applied to calculate the minimum approachable distance for any system that follows an r^{-12} dependence on repulsive forces. Most systems are well defined by an r^{-12} dependence though r^{-9} to r^{-15} has been used--the "harder" the molecule, the larger the exponent.[72]

Another important consideration in heterogeneously catalyzed reactions is the relationship between exterior shape selectivity and the surface activity of the solid. The shape selectivity of external surface sites of a zeolite has been termed the *nest effect*.[73] Fraenkel *et al.* proposed that "half cavities" which contained the acid site were responsible for the selective formation of 2,6- and 2,7-dimethylnaphthalene in the HZSM-5 catalyzed methylation of naphthalene.[74]

Calculations

Molecular Dimensions

ZINDO, a series of molecular electronic structure programs from the Quantum Theory Project at the University of Florida,[12] was used to calculate molecular dimensions for both the lowest energy molecular structure and other relevant molecular conformations tabulated in Table 5-1. Implementation of the subroutine GEPOL (GEometria POLihedro, 1993) calculates the molecular surface area and the molecular volume of a molecule from the calculated structure.[13]

Results and Discussion

Choice of Oxygen Atom Radii

The discrepancy in the literature between pore sizes from refined crystallographic data and catalytic reaction products is related to the value for the framework oxygen atom radius used to determine the pore window opening. Values of 1.3 Å, 1.35 Å, 1.40 Å, and 1.575 Å have all been used in the zeolite field.[32,75]

With the commonly used value of 1.35 Å, one obtains 5.75 Å by 5.22 Å for the calculated window size of the large channel of HZSM-5.* This calculated window size is not large enough to

*The values used for the center-to-center oxygen distances were obtained from the fractional coordinates of the van Koningsveld *et al.* paper,[48] which had improved framework accuracy over previous reports. The oxygen atoms used were those of Olson *et al.*,[32] the largest (8.449 Å) and smallest (7.922 Å) center-to-center oxygen atom distances for the straight channel.

Table 5-1. Molecular *x*, *y*, *z*, MIN-1, and MIN-2 Dimensions

Molecule	*x* (Å)	*y* (Å)	*z* (Å)	MIN-1 (Å)	MIN-2 (Å)
benzene	6.628	7.337	3.277	3.277	6.628
2,6-di-*tert*-butylpyridine	11.344	6.454	8.294	6.454	8.294
cyclohexane	7.168	6.580	4.982	4.982	6.580
ethylbenzene	6.625	5.285	9.361	5.285	6.625
hexamethylbenzene	9.089	9.079	4.027	4.027	9.079
hexane	10.344	4.536	4.014	4.014	4.536
2,6-lutidine	8.927	4.127	6.957	4.127	6.957
2-methylnaphthalene	10.294	7.354	3.967	3.967	7.354
pentamethylbenzene	9.094	4.029	8.223	4.029	8.223
propylbenzene	6.625	5.277	10.274	5.277	6.625
1,2,3,4-tetramethybenzene	7.646	4.117	9.099	4.034	7.646
1,2,3,5-tetramethybenzene	8.549	4.034	9.152	4.034	8.174
1,2,4,5-tetramethybenzene	7.377	4.034	9.072	4.034	7.377
toluene	6.625	4.012	8.252	4.012	6.625
1,2,3-trimethybenzene	9.058	4.062	8.227	4.062	7.635
1,2,4-trimethybenzene	7.576	4.024	9.145	4.024	7.251
1,3,5-trimethybenzene	8.276	8.553	4.062	4.062	8.178
m-xylene	8.994	3.949	7.314	4.012	7.258
o-xylene	7.269	3.834	7.826	3.834	7.269
p-xylene	6.618	3.810	9.146	3.810	6.618

Note: MIN-1, the minimum dimension through a molecule, and MIN-2, the second minimum dimension through a molecule perpendicular to MIN-1. MIN-1 will determine if the molecule can enter a slit-shaped pore, while MIN-1 and MIN-2 will determine if a molecule can enter a cylindrical pore, Figure 5-4. Minimum Dimensions are meant to be used as a direct comparison of molecular sizes and have no temperature dependence (as do kinetic diameters) and have been determined from calculated molecular structures, which have dimensions shown to correlate well with the bulk density of the molecule[43] (unlike kinetic diameters). See text and reference 43.

allow for the nonrestricted diffusion of *o*-xylene, which is necessary for the 0.0 kcal mol^{-1} activation energy for its steady-state diffusion (*vide infra*).

In fairness, one should also consider the application of the Lennard-Jones (LJ) 12-6 potential to the oxygen radii of the zeolite window. The "minimum radius" of the oxygen atom can be calculated from the relationship of the LJ diameter (σ_{LJ}) and the equilibrium diameter (r_e) by

Equation 5-1 assuming a static situation. After this correction is performed for the van der Waals radii of 1.40 Å, the large channel's pore size increases to 5.95 Å by 5.43 Å, which is again too small a pore diameter to allow these large aromatics to diffuse in the HZSM-5 structure. If one applies the correction to the O^{2-} radii of 1.32 Å,[76] one obtains a pore size of 6.10 Å by 5.57 Å--still too small.

While the radius of the oxygen atoms of a zeolite could be thought of as a radial distribution function describing the extension of the electron probabilities of the orbitals (increasing the "sponginess" of the oxygen atoms), the unhindered diffusion of the larger aromatic molecules precludes the necessity of such an argument (except for the largest molecules at 370 °C which could possibly have an activation energy for steady-state diffusion). The omission of a discussion of a radial distribution describing the oxygen atom radius does not detract from the validity of such an argument, when found necessary by the experimental conclusions. Larger molecules are allowed to diffuse through a more restricted opening if the oxygen atoms are considered "spongy."

Minimum Dimensions

The concept of effective minimum dimensions of molecules has been set forth in a previous paper.[43] MIN-1, the minimum dimension through a molecule, and MIN-2, the second minimum dimension through a molecule perpendicular to MIN-1, determine whether or not a molecule can enter a pore. MIN-1 will determine if the molecule can enter a slit-shaped pore, while MIN-1 and MIN-2 will determine if a molecule can enter a cylindrical pore (Figure 5-4).

Minimum dimensions are meant to be used as a direct comparison of molecular sizes and have no temperature dependence (as do kinetic diameters) and have been determined from calculated molecular structures, which have dimensions shown to correlate well with the bulk density of the molecule[43] (unlike kinetic diameters). Minimum dimensions are static descriptors of a dynamic process.

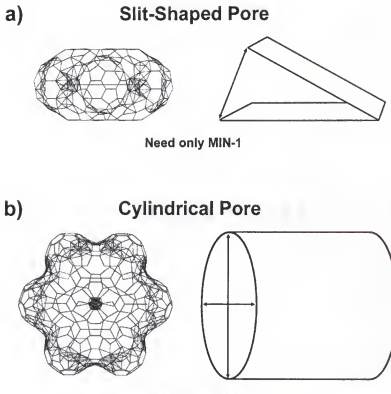

Figure 5-4: Application of the MIN-1 and MIN-2 of a benzene molecule to pore access. The minimum dimensions of the adsorptive dictate pore access. In (a), MIN-1 less than the dimension of a slit-shaped pore is required for access. In (b), MIN-1 and MIN-2 less than the two dimensions of a cylindrical pore is required for access.

Effective Catalytic Pore Size

The apparent change in size of the HZSM-5 channel and the intersection, realized from a change in temperature, can be determined from the analysis of the ^{13}C MAS NMR spectra of HZSM-5 catalyzed, shape-selective conversion of methanol to gasoline[17] and data collected from GC analysis of the product stream of the same reaction at two temperatures.[68,77a] The products of this conversion for the two temperatures and the relevant adsorbed specie for the two temperatures are tabulated in Table 5-2. It should be noted that the intensities quoted in the adsorbed phase are only a rough estimate of their concentration[17] due to the nuclear Overhauser effect (nOe).

At 300 °C, the product stream of the HZSM-5 catalyzed conversion of methanol to higher molecular weight alkanes and aromatics (*i.e.*, gasoline) contains aromatic molecules as large as

Table 5-2. Distribution of Aromatics in the Product Stream and in the Adsorbed Phase from Methanol Conversion over HZSM-5

Compound	MIN-2 (Å)	Distribution		Product Stream by Gas Chromatography				Adsorbed Phase by ^{13}C MAS NMR [17]	
				300 °C [68]		370 °C [77a]			
		Statistical[b]	Thermodynamic[c]	dist (%)[d]	wt %[e]	dist (%)[d]	wt %[f]	300 °C[g]	370 °C[g]
benzene	6.63	-	-	-	-	-	1.0	-	w
toluene	6.63	-	-	-	-	-	11.6	w	m
xylenes									
p-	6.62	10.0%	23.5%	100%[g]	1.6[g]	38.5%	21.1	s	m
m-	7.26	40.0%	52.7%			43.5%	23.8	w	s
o-	7.27	40.0%	23.8%	0%	0	18.0%	9.9	s	s
trimethylbenzenes									
1,2,4-	7.25	63.2%	66.0%	-	-	93.5%	20.1	m	m
1,2,3-	7.64	26.3%	7.8%	-	-	6.5%	1.4	w	m
1,3,5-	8.18	10.5%	26.2%	-	-	0.0%	0.0	w	w
tetramethylbenzenes									
1,2,4,5-	7.38	10.0%	33.4%	-	-	100%	1.0	s	w
1,2,3,4-	7.65	40.0%	16.0%	-	-	0.0%	0.0	w	vw
1,2,3,5-	8.17 × 8.88[a]	40.0%	50.6%	-	-	0.0%	0.0	m	vw
pentamethylbenzene	8.22 × 9.09[a]	-	-	-	-	-	-	-	w
hexamethylbenzene	9.08 × 9.09[a]	-	-	-	-	-	-	-	w

a. The second quoted dimension is MIN-3

b. Expected for random methyl substitution on the benzene ring.

c. Thermodynamic Equilibrium Distributions at 371 °C.[78] Values for the xylenes at 300 °C are *p*:*m*:*o*::24.1%:54.4%:21.5%[82]

d. Normalized isomer distribution.

e. Weight percent of (total normalized, hydrocarbon) product stream. 1.24 LHSV (Liquid Hourly Space Velocity); 45 minutes TOS (Time on Stream); 82.4% COM (Conversion of Methanol); Aromatics were 9.2 wt% of hydrocarbon products.

f. Weight percent of (normalized, total collected organic liquid) product stream. 1.5 WHSV (Weight Hourly Space Velocity); 105 minutes TOS; 100% COM; The organic liquid does not contain the lighter hydrocarbons (smaller than pentane and with some pentane loss). Aromatics were 86.5 wt% of collected organic liquid products.

g. s = strong, m = medium, w = weak, and vw = very weak intensity. TOS of 35 minutes for 300 °C and 33 minutes for 370 °C.

h. *m*- and *p*-xylene were reported together, not individually

m-xylene (Tables 5-1 and 5-2). The next larger aromatic molecules in the adsorbed phase, as determined from the ^{13}C MAS NMR, *o*-xylene and 1,2,4-trimethylbenzene, are not found in the products. This product exclusion places the effective catalytic pore size between 7.26 Å (MIN-2 of *m*-xylene, Table 5-1) and 7.27 Å (MIN-2 of *o*-xylene, Table 5-1). This fine resolution of the effective catalytic pore size is an artifact of the data because the *m*- and *p*-xylene are reported together. The effective catalytic pore size is better realized as being between 6.62 Å (MIN-2 of *p*-xylene, Table 5-1) and 7.27 Å (MIN-2 of *o*-xylene, Table 5-1). These results are consistent with a previous study[19] which finds that neither channel is accessible to 2,6-di-*tert*-butylpyridine (MIN-2 of 8.29, Table 5-1) at 25 °C. It should be noted that preferential-diffusion product selectivity can be induced by increasing the Liquid Hourly Space Velocity (LHSV [flow rate]) of the feed stock through the reaction apparatus over the catalyst bed.

At 370 °C, the product stream of the HZSM-5 catalyzed conversion of methanol to gasoline contains aromatic molecules no larger than 1,2,3-trimethylbenzene (Table 5-2). This reaction product requires the effective catalytic pore size to be at least 7.64 Å (Table 5-1). 1,2,4-trimethylbenzene is the next smaller isomer and is therefore allowed to exit the structure. The possibility that 1,2,3-trimethylbenzene is a product of the isomerization of 1,2,4-trimethylbenzene from exterior surface activity is unlikely. The thermodynamically favored isomer is 1,3,5-trimethylbenzene, and the favored isomerization product is 1,2,3-trimethylbenzene by the nest effect. An isomerization of 1,2,4-trimethylbenzene would produce both of the other two isomers (favoring the 1,2,3-), but no 1,3,5-trimethylbenzene was observed. Although molecules ranging in size from 1,2,3,4-tetramethylbenzene to hexamethylbenzene (MIN-2 of 7.65 Å to MIN-2 to 9.08 Å, Table 5-1) are in the adsorbed phase, they do not show up in the product stream. More temperature studies on this catalytic reaction would be required to ascertain an exact temperature at which the larger molecules would not be selected against in the product stream (overcoming an

activation energy for diffusion), but these studies could be complicated by surface activity isomerization.

The channel intersection allows for the formation of molecules greater in size than 1,2,4-trimethylbenzene at 300 °C and larger than 1,2,3-trimethylbenzene at 370 °C. At 300 °C, the largest molecule formed at the intersection is 1,2,3,5-tetramethylbenzene (MIN-2 of 8.17 Å by MIN-2 of 8.88 Å). At 370 °C, the intersection allows for the formation of molecules as large as pentamethylbenzene and hexamethylbenzene. This formation of larger sized products at 370 °C indicates an increase in the apparent size of the intersection from 8.17 Å by 8.88 Å to at least 9.08 Å by 9.09 Å (MIN-2 by MIN-3 for hexamethylbenzene).

Fraenkel and Levy concluded that neither pentamethyl- nor hexamethylbenzene are found in the product stream of the methanol conversion catalyzed by HZSM-5[77a] at reaction conditions similar to those of Chang and Silvestri.[78] Fraenkel and Levy do not report production of 1,3,5-trimethylbenzene, 1,2,3,4-tetramethyl-, or 1,2,3,5-tetramethylbenzene.[77a] The crystal size of the HZSM-5 catalyst used in the investigation was between 5 and 10 μm.[77b] Along with the crystal size of the catalyst, the absence of the third trimethylbenzene isomer as well as the other two tetramethylbenzene isomers leads to the conclusion that the exterior surface activity of the particular HZSM-5 catalyst was minimal.

At the proper conditions, the selectivity of the MTG process (with "equilibrium MTG catalyst") is essentially exclusive to the 1,2,4-trimethylbenzene isomer (over the two other trimethyl isomers) and to the 1,2,4,5-tetramthylbenzene (over the two other tetramethyl isomers).* The MTG process uses HZSM-5 crystals which are of submicron size.* Such particles would be expected to have a large ratio of exterior surface activity compared to larger crystals (>1 micron).

---

*C. D. Chang, Personal Communication.

It should be noted that, if present, exterior surface acidity of the zeolite could isomerize the alkyl-substituted benzenes to near equilibrium distributions. As a catalytic reaction progresses, if present, the surface activity is quenched, and slight coking of the pore structure could lead to greater selectivity based on size.

A previous study[19] reported that the sinusoidal (small) channel of HZSM-5 contains the strong Brønsted acid site. It is reported that small channel acid site is accessed by pyridine (MIN-2 of 6.48 Å) but not by 2,6-lutidine (MIN-2 of 6.96 Å) at 25 °C. This would set the difference in the effective catalytic pore size of the two channels at room temperature to be no greater than 0.48 Å. One should not conclude that the catalytic formation of aromatic compounds in the conversion of methanol to gasoline must always occur at the strongest Brønsted site because the dimensions of the largest formed molecules are larger than allowed in either of the channels (when formed inside the structure opposed to formed on the exterior of the structure).

Product Selectivity

While the product distribution of the xylenes at 300 °C demonstrates preferential-diffusion product selectivity, this distribution is not the only evidence. The activation energy of diffusion for a probe molecule in a given structure reflects the extent of interaction of the probe with the walls of the structure itself. If the probe molecule can freely diffuse without hindrance (repulsion) from the structure, the activation energy for diffusion is zero. Since the non-steady-state (apparent) diffusivity of a probe molecule reflects thermodynamic properties in addition to characteristics of the stochastic process, the temperature dependence of the steady-state diffusivities must be determined in order to examine if the diffusing molecule experiences any repulsion with the framework structure. The observation that the steady-state diffusivity (D_{ss}) of *o*-xylene in HZSM-5 has an activation energy of 0.0 kcal mol^{-1} [79] explicitly states that an *o*-xylene molecule does not experience any repulsions from the framework structure of HZSM-5 (Figure 5-5). This D_{ss} was

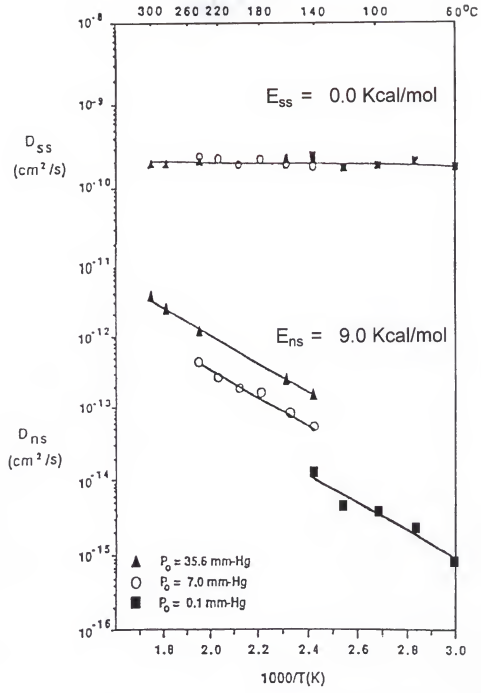

Figure 5-5: Determination of the activation energy for steady-state diffusivity (E_{ss}) and uptake diffusivity (E_{ns}) at various pressures over a given temperature range. A uniform value of the steady-state diffusivity is attained for all cases of pressure and temperature. A steady-state diffusion activation energy (E_{ss}) of 0.0 kcal mol^{-1} requires that *o*-xylene (MIN-2 of 7.27 Å) be able to "freely diffuse" through the HZSM-5 structure. The steady-state diffusion activation energy for *p*-xylene (MIN-2 of 6.62 Å) and 2-methylnaphthalene (MIN-2 of 7.35 Å) also have E_{ss} = 0.0 kcal mole^{-1}. Used with permission from reference 79.

determined over a wide range of temperatures (60 to 315 °C) and loadings (pressures), and this result can be extended to the other molecules of lesser size in the HZSM-5 structure. In this same study,[79] consistent with the findings for *o*-xylene, the steady-state diffusivity determined activation energy of *p*-xylene (smaller than *o*-xylene, MIN-2 of 6.62 Å) and 2-methylnaphthalene (slightly larger than *o*-xylene, MIN-2 of 7.35 Å) were also found to be 0.0 kcal mol^{-1}. As expected, although *p*-xylene has 0.0 kcal mol^{-1} activation energy for diffusion, it still diffuses at a much higher rate than does the larger *o*-xylene molecule.

Preferential-diffusion product selectivity may also be achieved with the increase of the flow velocity (*e.g.*, LHSV) of the reactant feedstock through the catalyst bed.[68] While the conversion of the reactant feed is decreased and the selectivity to aromatics products is decreased, the products with smaller minimum dimensions will be favored (Table 5-3). It should be noted that at the slowest flow rate, the xylene isomer distribution is essentially that of the thermodynamic distribution at the same temperature. This correspondence of the distributions is expected because the stochastic contribution to the product distribution is removed at low space velocities.

Various investigators have demonstrated size-exclusion product selectivity, simply by digesting spent catalyst and determining the reaction products not allowed to exit the structure.[80] Large molecules (biphenyls, alkylnaphthalenes, etc.) are among the retained residue from the catalyzed reaction of benzene and toluene.

Nest Effect

In the HZSM-5 catalyzed conversion of methanol to gasoline over small crystal catalyst, the distribution of the poly-substituted methylbenzenes in the product stream should be the same as that of a nonselective catalyst (the thermodynamic distribution) if no nest effect is present. The smallest isomer would be produced, and in the case of a nest effect (by isomerization), would produce the other isomers, with the less steric attack selected over the more steric.

Chang concluded that trace amounts of pentamethylbenzene can be found in the product stream of the MTG process at the proper conditions (*e.g.*, elevated temperatures, etc.), but that "it is not possible either to quantify or pinpoint [pentamethylbenzene's] origin."* The question arises as to the source of the pentamethylbenzene. Exterior surface activity of the zeolite can isomerize and even methylate substituted benzenes. Chang believes that "if [one] looked hard enough, [one] could even find hexamethylbenzene."* The crystallite size of HZSM-5 used in studies of Chang and Silvestri[78] was <0.05 micron.*

Chen reports that surface activity can be neglected when the crystal size is greater than 1 micron because the external surface area relative to the intracrystalline surface area is less than one percent.[74]

> One should exercise caution in assuming that external surface sites can be neglected with large crystals of ZSM-5. All things being equal, this might be true; however, many preparations of large crystal material tend to exhibit Al zoning (gradient), *i.e.*, a higher concentration of Al at or near the crystal surface (R. von Ballmoos and W. M. Meier, *Nature* **1981**, *289*, 782), thus actually increasing external site density.*

For the xylenes at 371 °C in the methanol conversion over HZSM-5, the largest isomer (*o*-xylene) is decreased from its thermodynamic equilibrium amount, while the two smaller isomers (*m*- and *p*-xylene) are increased. For the trimethylbenzenes at 371 °C, the largest isomers (1,2,3- and 1,3,5-trimethylbenzene) are decreased from their thermodynamic equilibrium amount, while the smallest isomer (1,2,4-trimethylbenzene) is increased. For the tetramethylbenzenes at 371 °C, again the two largest isomers (1,2,3,5-tetramethylbenzene and 1,2,3,4-tetramethylbenzene) are decreased, while the smallest isomer (1,2,4,5-tetramethylbenzene) is increased from its thermodynamic equilibrium amount. (See Table 5-4.)

---

*C. D. Chang, Personal Communication.

Table 5-3. Comparison of Space Velocity Effects on Distribution of Xylenes in the Product Stream from Methanol Conversion over HZSM-5 at 300 °C

			Product Stream by Gas Chromotagraphy[68]							
		Thermodynamic	LHSV[b] = 0.15[c]		LHSV = 0.31[d]		LHSV = 0.62[e]		LHSV = 1.24[f]	
Compound	MIN-2 (Å)	Distribution[a]	dist (%)[g]	wt%[h]	dist (%)[g]	wt%[h]	dist (%)[g]	wt%[h]	Dist (%)[g]	wt %[h]
xylenes										
p-	6.62	24.1%	} 78.9%[i]	} 7.1[i]	} 87.9%[i]	} 9.4[i]	} 93.2%[i]	} 4.1[i]	} 100%[i]	} 1.6[i]
m-	7.26	54.4%								
o-	7.27	21.5%	21.1%	1.9	12.1%	1.3	6.8%	0.3	0%	0.0
trimethylbenzene										
1,2,4-	7.25	67.7%	100%	4.5	100%	4.0	100%	2.6	0%	0.0

a. Thermodynamic Equilibrium Distributions at 300 °C.[82]
b. LHSV (Liquid Hourly Space Velocity [$mL \cdot hr^{-1}$])
c. 45 minutes TOS (Time on Stream); 100% COM (Conversion Of Methanol); aromatics were 16.9 wt% of HP (Hydrocarbon Products). Xylenes were 53.2% of AP (Aromatic Products).
d. 45 minutes TOS; 100% COM; aromatics were 21.9 wt% of HP. Xylenes were 48.8% of AP.
e. 45 minutes TOS; 90.5% COM; aromatics were 9.2 wt% of HP. Xylenes were 47.8% of AP.
f. 45 minutes TOS; 82.4% COM; aromatics were 1.6 wt% of HP. Xylenes were 100% of AP.
g. Normalized isomer distribution.
h. Weight percent of (total normalized, hydrocarbon) product stream
i. *m*- and *p*-xylene were reported together, not individually.

Table 5-4. Distribution of Aromatics in the Product Stream from Methanol Conversion over small crystal HZSM-5 at 371 °C

Compound	MIN-2 (Å)	Thermodynamic Product Distribution[a]	Product Stream by Gas Chromatography[78]	
			dist (%)[b]	wt %[c]
benzene	6.63	-	-	1.7
toluene	6.63	-	-	10.5
xylenes				
p-	6.62	23.5%	23.9%	4.09
m-	7.26	52.7%	54.6%	9.06
o-	7.27	23.8%	21.5%	4.04
trimethylbenzenes				
1,2,4-	7.25	66.0%	78.7%	4.57
1,2,3-	7.64	7.8%	6.4%	0.37
1,3,5-	8.18	26.2%	14.9%	0.87
tetramethylbenzenes				
1,2,4,5-	7.38	33.4%	46.5%	0.82
1,2,3,4-	7.65	16.0%	9.3%[d]	0.16
1,2,3,5-	8.17 × 8.88[e]	50.6%	44.2%	0.78
pentamethylbenzene	8.22 × 9.09[e]	-	-	< 0.2[f]

a. Thermodynamic Equilibrium Distributions at 371 °C.[78]
b. Normalized isomer distribution.
c. Weight percent of (total normalized, hydrocarbon) product stream. 1.0 LHSV (Liquid Hourly Space Velocity); 60 minutes TOS* (Time on Stream); 100% COM (Conversion of Methanol); Aromatics were 41.2 wt% of hydrocarbon products.
d. Reported incorrectly in reference 78.
e. The second quoted dimension is MIN-3.
f. 0.2 weight percent of the (total normalized, hydrocarbon) product stream was C_{11}^{+}. Only trace amounts of pentamethylbenzene are found, and it is not possible to either quantify or pinpoint its origin.*

*C. D. Chang, Personal Communication.

The distributions of the isomers of the poly-substituted methylbenzenes represent the nest effect from the activity of the exterior surface of the HZSM-5 catalyst. One should consider the results of the 371 °C reaction catalyzed with small crystal HZSM-5 interesting from the point that the final distribution of dimethyl-substituted products is close to the thermodynamic distribution, but slightly favors the nonsteric product (*m*-xylene favored over *o*-xylene, see Table 5-4).

The nest effect could be indicated by the ratio of the isomeric distributions of the tetramethylbenzenes (see Table 5-4 and Figure 5-6). The exterior surface shape selectivity would isomerize 1,2,4,5-tetramethylbenzene selecting towards the less steric isomer (of the two larger isomers). Since the production of 1,2,3,4-tetramethylbenzene by the isomerization of

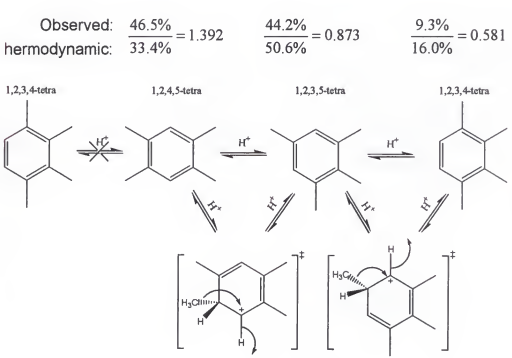

Figure 5-6: Illustration of the isomerization of 1,2,4,5-tetramethylbenzene. While the isomerization of 1,2,4,5-tetramethylbenzene to 1,2,3,5-tetramethylbenzene may occur by a one-step process (1,2-methyl shift), the 1,2,4,5- cannot directly isomerize to the 1,2,3,4-tetramethylbenzene. However, the 1,2,3,5-tetramethylbenzene can isomerize directly to the 1,2,4,5-tetramethylbenzene.

1,2,4,5-tetramethylbenzene would have to occur via a 1,3-methyl shift, the 1,2,3,4-tetramethylbenzene cannot give direct experimental observation of the exterior surface activity's shape selectivity (nest effect).

The trimethylbenzene isomeric group can give a direct experimental observation of the exterior surface activity's shape selectivity because the isomerization of 1,2,4-trimethylbenzene could produce either the 1,2,3-trimethylbenzene isomer or the 1,3,5-trimethylbenzene isomer via a 1,2-methyl shift (Figure 5-7). Since either isomer can be produced independent from the other, the ratio of each isomer's observed value compared with its thermodynamic equilibrium value demonstrates a selectivity towards the less steric attack (1,2,3-trimethyl isomer), even though this isomer is thermodynamically unfavored compared to the 1,3,5-trimethyl isomer (Table 5-4).

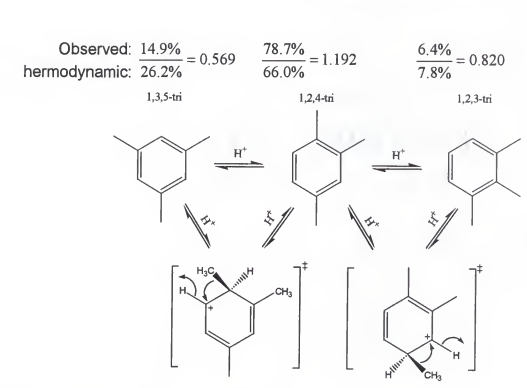

Figure 5-7: Illustration of the isomerization of 1,2,4-trimethylbenzene. The isomerization of 1,2,4-trimethylbenzene can occur directly to either the 1,2,3- or 1,3,5-trimethylbenzene through a 1,2-methyl shift. The nest effect can be directly observed by comparing the ratios of the observed to thermodynamic distributions of 1,2,3- and 1,3,5-trimethylbenzene. Even though the isomerization thermodynamically favors 1,3,5-trimethylbenzene, the 1,2,3-trimethylbenzene has a higher ratio of observed product.

Conclusions

The temperature dependent effective catalytic pore size of HZSM-5 is concluded to be between 6.62 Å (MIN-2 of *p*-xylene) and 7.27 Å (MIN-2 of *o*-xylene) at 300 °C. The effective pore size is increased to a minimum of 7.64 Å (MIN-2 of 1,2,3-trimethylbenzene) at 370 °C. The increase in temperature effectively increases the channel intersection from 8.17 Å by 8.88 Å to 9.08 Å by 9.09 Å.

Minimum dimensions (MIN-1 and MIN-2) are a scale of particle size based on calculations using geometries obtained from quantum chemistry, and volumes and projected dimensions calculated from these geometries using our model. This model yields dimensions that are reasonable, that are uniquely defined, and that are not inconsistent with molar volumes, for example. All of the calculated dimensions suggest these molecules are too big to fit in the pores suggested from the static structures of the zeolites. Nevertheless, we have generated a very reasonable, first principles, measurement of relative sizes, although this particular choice of calculation is, admittedly, arbitrary. We have then calibrated the effective size of the pore using a combination of experiment and our calculated results, and this is independent of the real or imagined pore size of the zeolite.

When one uses the van der Waals radii of oxygen or the oxide ion radius to calculated a window size of the large channel of HZSM-5 (or their LJ corrected radii), neither produce a pore of the necessary dimensions to allow for the entry or exit of these large aromatic molecules. These calculated window sizes do not allow for the nonrestricted diffusion of *o*-xylene, demonstrated by the 0.0 kcal mol^{-1} activation energy for steady-state diffusion.

The distribution of the poly-substituted methylbenzenes in the product stream of the HZSM-5 catalyzed conversion of methanol to gasoline are what one would expect, the largest isomer of each group is selected against (Table 5-2). For the xylenes at 300 °C, the largest isomer

(*o*-xylene) is completely selected against, while the amounts of the two smaller isomers (*m*- and *p*-xylene) are increased from that expected from thermodynamic equilibrium. For the xylenes at 370 °C, the amount of the largest isomer (*o*-xylene) is decreased from that expected at thermodynamic equilibrium, while the two smaller isomers (*m*- and *p*-xylene) are increased. At 300 °C, the trimethylbenzenes and tetramethylbenzenes are entirely selected against. For the trimethylbenzenes at 370 °C, the largest isomer (1,3,5-trimethylbenzene) is entirely selected against, the middle-sized isomer is decreased from its thermodynamic equilibrium, and the smallest isomer (1,2,4-trimethylbenzene) is highly favored. For the tetramethylbenzenes at 370 °C, the two largest isomers (1,2,3,5-tetramethylbenzene and 1,2,3,4-tetramethylbenzene) are completely selected against, while the smallest isomer (1,2,4,5-tetramethylbenzene) is favored and is thus increased from its thermodynamic equilibrium amount.

The nest effect (shape selectivity of the exterior surface activity of the zeolite) has been demonstrated by the distribution of the trimethylbenzene isomers produced from the conversion of methanol (and isomerization of 1,2,4-trimethylbenzene) over small crystal HZSM-5 (Table 5-4). Since either isomer can be produced independent from the other (Figure 5-7), a comparison of the ratio of the trimethylbenzene isomer's observed value with its thermodynamic equilibrium value demonstrates selectivity towards the less steric attack (1,2,3-trimethylbenzene), even though the 1,3,5-trimethyl isomer is thermodynamically favored.

The species found in the adsorbed phase reaction products demonstrate the second type of product selectivity, size-exclusion. The adsorbed phase contains molecules that cannot diffuse though either channel of the zeolite. This type of pore-confinement product selectivity excludes the reaction product from the product stream, contrary to the classically described, preferential-diffusion product selectivity, which allows for diffusion of all reaction products.

While limited selectivity towards *p*-xylene (two-fold increase in distribution compared to thermodynamic equilibrium) over *o*- and *m*-xylene is achieved by HZSM-5 in the methanol alkylation of toluene,[81] increased selectivity for *p*-xylene (>97%) can be attained by modified ZSM-5.[81] Increased flow rates over HZSM-5 can increase selectivity towards the elongated products (*i.e.*, *p*-xylene, see Table 5-3).[68] These results, as well as the 0.0 kcal mol^{-1} activation energy for the steady-state diffusion of *o*-xylene, show that the often cited, preferred alkylation of toluene to *p*-xylene over HZSM-5[65] is governed by the retarded diffusion of the other two larger isomers (*o*- and *m*-). Therefore, this selectivity is from purely kinetic considerations--kinetic transport (*i.e.*, increased diffusivity) of *p*-xylene is the reason for the increased selectivity over HZSM-5.

The discussion of dimensions for the determination of actual pore sizes should be put in perspective. The dimensions one chooses are quite arbitrary; it is the consistency with which measurements are determined which is important. Since crystallographic derived pore sizes are well below those expected from experimentally derived chemical correlations and the portability of probe based measurements are more convenient for comparison of different structures, this method for determining the temperature dependent, effective catalytic pore size has worked well with this HZSM-5 catalyzed methanol conversion and has great potential for further study.

CHAPTER 6
THE MULTIPLE EQUILIBRIUM ANALYSIS QUANTITATIVE PREDICTION OF SINGLE AND MULTI-COMPONENT ADSORPTION ISOTHERMS ON CARBONACEOUS AND ZEOLITIC SOLIDS

Introduction

Surface catalyzed reactions play a major role in current chemical production technology.[83] Currently, 90% of all chemicals are produced by heterogeneously catalyzed reactions.[83a] Most of these catalyzed reactions involve adsorption, concentrating the substrate(s) (the adsorbate) on the surface of the solid (the adsorbent).

Various adsorbents are available, including activated carbonaceous adsorbents (powdered and granular activated carbons) and zeolitic solids. Carbonaceous adsorbents, which are amorphous and have a wide pore size distribution, are prepared by condition-specific pyrolysis of various synthetic polymers and a wide variety of naturally occurring carbon-containing materials, including petroleum coke, coal, wood, coconut shell, peat moss, and lignite.[84-86]

Zeolitic solids are crystalline mineral oxides, typically containing tetrahedral silicon with bridging oxygen and various silicon atom substitutions.[60] While many naturally occurring zeolites can be synthesized, there are a few examples of synthetic zeolites that have no known naturally occurring counterpart, such as zeolite A (Linde Corporation, now part of Union Carbide) and HZSM-5 (Mobil Corporation). There are more than 50 different available aluminosilicate zeolites with pore openings ranging from less than 5 Å to larger than 10 Å,[63] and silicoaluminophosphates extend this upper limit to 13 Å.[64] Porous crystalline solids synthesized similarly to zeolites that contain polyhedra of elements other than both aluminum and silicon are known as "zeotypes," *e.g.*, silicates, phosphates, and other heteropoly acids (and their salts).[87]

The porosity of a solid is induced by activation. Physical activation reactions of carbon-containing solids involve the use of gases (such as carbon dioxide, air, and/or steam) during the higher temperatures of pyrolysis.[84-86,88] Another route by which the porosity of a solid can be changed is chemical activation, the treatment of the adsorbents with various chemical agents before pyrolysis.[84] These activation techniques lead to increased internal accessible surface areas and pore volumes of the solids, depending on the activation conditions.[84-85] Typical adsorbent surface areas range from ~300 to 3,000 $m^2 g^{-1}$ depending on the solid and the controlling factors of the activation technique[84,85,89]--the macroscopic area of a football field is ~ 4,180 m^2.

The prediction of adsorption isotherms would be of great utility to material and environmental scientists. The process of adsorption plays a key role in environmental (cleanup) applications. Carbonaceous adsorbents and zeolitic solids can be utilized in liquid-phase adsorption, water purification,[85,89] waste stream separation[85,89,90] as well as gas adsorption,[84,90,91] separation (such as pressure-swing adsorption) and purification techniques,[84,92] and catalyst supports.[84] Carbonaceous materials have also been suggested for natural gas fuel storage.[84,91] There is great potential for a method that could accurately predict adsorption isotherms for microporous solids, and such a method would lead to an increased understanding of the adsorbent behavior in catalysis and adsorption procedures.

Means of Prediction: Simulations

Many investigators have utilized statistical mechanics (*e.g.*, Monte Carlo and molecular dynamics simulations using intermolecular potentials) in the qualitative and quantitative description of adsorption[93-94] as well as fluid mechanics (phase transitions,[95] solubilities,[96] liquid structure,[97] etc.). These methods are very powerful tools for probing intermolecular interactions. Simulations have also been used to predict adsorption capacities, but these studies are limited to known or predicted structures.[98] The crystallinity of zeolitic solids produces a regular array of apertures that "presents a periodic potential energy field" to an adsorbate molecule.[94] Many

studies of molecular interactions with graphite have been reported.[93e-j] With amorphous solids, assumptions about the structure, such as pore size distribution and the density of available pores, must be made in order to simulate adsorption. While the investigation of adsorption on solids will lead to a greater understanding of the nature of the interaction of a probe molecule with a given type of pore, these studies do not easily allow for a direct determination of adsorption of a probe with a given amorphous solid, whose structure is not known exactly.

Means of Prediction: Empirical Relationships

Several previous attempts to predict adsorption capacities and isotherms empirically have been reported. Some reports are rather limited in their scope in trying to understand the fundamental nature of the adsorption process, while others have a strong theoretical background. Prediction studies can be limited to similarly functionalized derivatives, or can be more general, and apply to a variety of adsorbate-adsorbent systems.

Dubinin and coworkers first suggested the use of a "characteristic curve" with which one could predict adsorption isotherms[99] (from Polanyi-Dubinin potential theory also known as Polanyi adsorption potential theory[100]). In principle, each adsorbent system has a characteristic curve that describes the adsorbate-adsorbent interactions regardless of the temperature at which the experiment was performed. In practice, there are a few discrepancies: (1) not every adsorbate always follows this adsorbent characteristic curve at all temperatures, (2) various modifications must be applied to the equation to model adsorbents that are very different (*e.g.*, carbons and zeolites), and (3) this equation cannot be used to describe adsorption isotherms that are concave to the ordinate (*i.e.*, isotherms below the critical temperature that have adsorbate-adsorbate interactions dominating at lower partial pressures).[101,102a] Since the early work of Maslan *et al.* and Lewis *et al.*, who first applied modified Dubinin-Polanyi adsorption equations to the prediction of adsorption isotherms, many investigators have applied various modifications of this equation in order to predict single component[102,103] and multicomponent[103,104] adsorption

isotherms. Noll *et al.* presented an interesting comparison of three parameter-based methods (molar volume, molecular parachor, and polarizability) for isotherm prediction with a characteristic curve derived from a Dubinin-Polanyi type equation.[102e] John *et al.* proposed an isotherm equation, but it is fundamentally the same as a Dubinin-Polanyi equation.[105] A major disadvantage when considering the description of adsorption is that Polanyi-Dubinin adsorption equations do not follow Henry's Law at low pressures, and their empirical nature does not allow for a statistical thermodynamics treatment.[101,106]

Chen *et al.* proposed an empirical method for isotherm prediction that employs (1) physical constants of a particular adsorbate (including the critical temperature, critical pressure, normal boiling point temperature, and Pizter's acentric factor), (2) four characteristic parameters for each adsorbent that relate to the volume of a "pseudo-liquid" phase, (3) and four characteristic parameters that are identified with each adsorbent that account for the density of the adsorbed phase.[107] In order to predict the amount of adsorption six more parameters are required, three derived from the experimental data of one reference adsorption system and three obtained from an equation of state (such as the Redlich-Kwong equation) for the adsorbate. While the average error of the experimental and predicted values is 9.3%, the prediction procedure is used for only two adsorbates (N_2 and CH_4) at a few temperatures (one for N_2 and two for CH_4) on the zeolite 13X. The experimental data utilized for the reference system in the prediction was for the adsorption of CO_2.

While ideal adsorbed solution theory (IAST) has been used quite effectively to predict multicomponent competitive adsorption systems, IAST does not have the inherent ability to predict single component adsorption isotherms.[108] IAST uses an empirical isotherm equation (such as the Freundlich equation that does not have parameters with a high physical significance) to represent the single component isotherms. Crittenden *et al.* have presented a comparison between the prediction of multicomponent adsorption equilibira by IAST and Polanyi-Dubinin potential theory.[108b]

Huggahalli and Fair have presented an interesting approach for the prediction of water adsorption onto activated carbon with parameters that have "a clear cut physical significance," but again these parameters must be estimated from pure-component isotherms.[109] Their study deals with the physical displacement of an organic adsorbate by water with increasing partial pressure of water. Several studies have been published which propose methods for predicting multicomponent adsorption equilibria utilizing parameters from an empirical isotherm equation (such as the Langmuir-Freundlich equation, etc.) that characterize single component adsorption equilibria[110] and comparisons with other methods (such as IAST, Polanyi-Dubinin theory, and the vacancy solution model).[111]

Multiple Equilibrium Analysis Description of Adsorption

Insights into the adsorption process can be obtained through the modeling of the species involved in a catalytic system. The previously introduced Multiple Equilibrium Analysis (MEA) model,[6,7,14,26,46] although simple, has the ability to make distinctions and interpretations not found in previous models; including adsorbent surface areas and pore volumes from process capacities (n_i), as well as enthalpies (ΔH_i) and entropies (ΔS_i) of adsorption derived from the temperature dependence of the thermodynamic equilibrium constant (K_i) for distinct pore régimes of the solid. Adsorption on variety of carbonaceous[7,26] and zeolitic solids[6,14,46] has been described by the MEA.

Prediction of Isotherms by MEA

Single Component

In order to predict adsorption isotherms with the MEA, the adsorbate dependent n_i and K_i values for each process are required. The n_i values are a property of the solid and are not temperature dependent, while the thermodynamic K_i values have a temperature dependence. There are two methods to predict K_i values and two to predict the n_i values.

The adsorbate dependent n_i values for each process can be predicted from either the probe dependent surface areas or the probe dependent pore volumes of the solid. One may use the weighted average of the next smaller and next larger adsorbates to interpolate the surface area (m^2 g^{-1}) or pore volume (mL g^{-1}) for a given probe, and this value can be converted to the required units (mol g^{-1}). For the smallest and largest adsorbates, the n_i values for each process must be extrapolated from the values of the other probes. (Another way the n_i values could be predicted involves plotting the calculated n_i values of the probe molecules vs the excluded molecular area or the calculated molar volume and interpolating (or extrapolating, if necessary) the desired n_i.)

Since a linear relationship exists between ln K_i and $a^{½}$ (square root of the van der Waals a parameter),[6,7,14] a method for predicting K_i involves interpolating (or extrapolating, if necessary) the desired K_i from the plot of the ln K_i vs the corresponding $a^{½}$ of the other molecules. There also exists a linear relationship between $-\Delta H_t$ (enthalpy for a given type interaction) and $a^{½}$.[6,7,14] Therefore, the enthalpy of adsorption can be predicted. To date, no direct empirical relationship has been observed for ΔS_t (entropy for a given type interaction) that would allow for its prediction. The linear relationship between $-\Delta H_t$ and $a^{½}$ allows for the prediction of $-\Delta S_t$. If one plots ($-\Delta H_t/-\Delta S_t$) vs $a^{½}$, the desired $-\Delta S_t$ may be interpolated (or, if necessary, extrapolated). The value of $-\Delta S_t$ has been determined to be approximately constant (~ 22 cal mol^{-1} K^{-1}),[14] and this could allow for the use of a single ΔS value to predict the temperature dependent K_i values. While this constant value could be used, the linear relationship between ($-\Delta H_t/-\Delta S_t$) vs $a^{½}$ provides for a more accurate prediction of the MEA K_i values.

Multicomponent

Multicomponent adsorption isotherms (a mixture of gases with one solid) could be predicted with MEA. In order to determine the amount of gas adsorbed on the solid, one could

use the weighted average of the fraction of the total process capacities of the solid at a given pressure as well as the weighted average of the additive volume of the gas mixture.

$$\sum_j \frac{V_j}{V_T}(n_{j,P}) = n_{ads,P}$$

V_j is the volume of jth gas in a gas mixture, V_T is the total volume of the gas mixture, $n_{j,P}$ is the total adsorption process quantity ($\Sigma\, n_{i,ads,P}$) at a given pressure (P), and $n_{ads,P}$ is the total predicted moles adsorbed at a given pressure (P). By combining $n_{ads,P}$ with the component K_i for each adsorbate, the adsorption at a given temperature and pressure can be predicted. The assumption is that the other component gases do not effect the thermodynamics for the individual adsorbate-adsorbent interactions, but that only the capacity of the solid is effected by the occupancy of the available pores. The prediction of multicomponent adsorption isotherms with MEA has not been tested because of a lack of available experimental data and will not be further discussed.

Results and Discussion

The prediction of adsorption isotherms on five carbonaceous solids [Rohm and Haas Ambersorb 572 (A-572), Rohm and Haas Ambersorb 563 (A-563), Rohm and Haas Ambersorb 600 (A-600), Calgon Carbon Company BPL (BPL), and Calgon Carbon Company Filtrasorb 300 (F300)] and one zeolitic solid (HZSM-5) with five adsorbates (N_2, CO, CH_4, C_2H_6, SF_6) are reported. The Ambersorb series are derived from the controlled pyrolysis of polysulfanated polystyrene resins. BPL and F300 are coal-derived materials. All of the experimental and predicted data are above the adsorbate critical temperature.

Figures 6-1 through 6-3 give a comparison of some of the predicted and experimental isotherms. The predictions of the adsorption isotherm for the smaller adsorbates (N_2, CO, and CH_4) tend to be more accurate than those for the larger adsorbates (C_2H_6 and SF_6). Tables 6-1

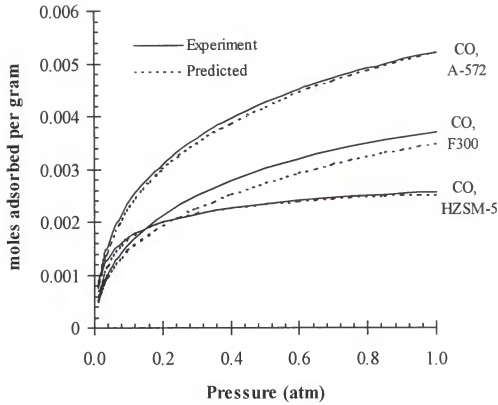

Figure 6-1: Experimental and predicted adsorption isotherms for CO on three solids.

through 6-5 give the comparison of the total experimental and predicted adsorption capacity (mmols g^{-1}) of the six solids for each of the adsorbates. The column headings Method *K* and Method $\Delta H/\Delta S$ are for the two K_i prediction procedures, and the columns subheadings with Area and Volume are for the two n_i prediction methods. The column labeled Δs indicates the amount that the prediction either overestimated or underestimated the experimental value, Δs = (experimental mols ads – predicted mols ads) ÷ experimental mols ads.

Table 6-6 gives the average error (and the standard deviation) of the predicted adsorption capacity for each of the probes with the solids at all the measured temperatures for all prediction methods. The total average error and standard deviation is given for all the solids. (It should be noted that the average error and standard deviation for "all solids" is from all of the predicted

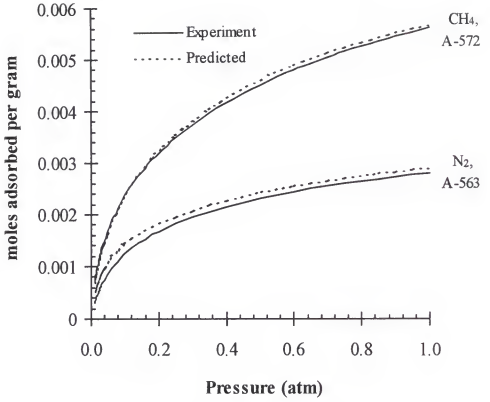

Figure 6-2: Experimental and predicted adsorption isotherms for CH_4 and N_2.

capacities, not from the average values from the adsorbate with each solid.) Tables 6-7 and 6-8 give the average error (and the standard deviation) of the predicted adsorption capacity for the two n_t and two K_t prediction methods.

From Table 6-6, in can be determined that the isotherms of CO are the best predicted. The accuracy and precision of this prediction is most likely from the fact that the pore size distributions realized by the two closest sized adsorbates (N_2 and CH_4) used to predict the CO isotherms are very similar to the pore size distribution detected by CO. The total capacity for CH_4 and C_2H_6 are both under predicted, while on average the capacity for SF_6 is over predicted and the standard deviation is quite large.

From Table 6-7, it can be observed that for the smaller adsorbates, either method for the prediction of n_t (from area or volume) works equally well. For the two larger adsorbates, the

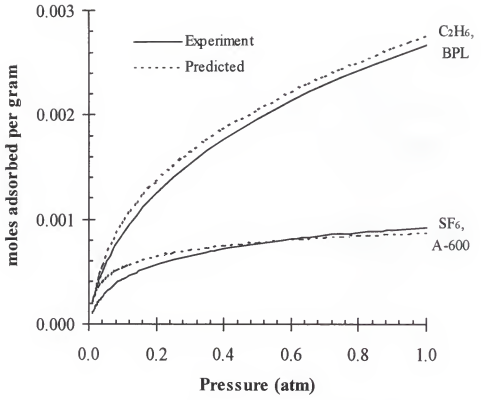

Figure 6-3: Experimental and predicted adsorption isotherms for C_2H_6 and SF_6.

volume method is slightly better. In general, for SF_6 the volume method underestimates the adsorption capacity, while the area method overestimates the adsorption capacity.

The data tabulated concerning the two K_i prediction methods in Table 6-8 demonstrates that the K method predicts adsorption capacity better for N_2, CH_4, and C_2H_6, about the same for CO, and slightly worse for SF_6. In both cases, the values of K_i are under predicted for C_2H_6 and mostly over for SF_6.

In order to illustrate the predictive power of the MEA description of adsorption, presented here is an attempt to predict literature adsorbate-adsorbent data. The high-pressure gas adsorption data of Reich *et al.* for CH_4 on BPL was utilized for the prediction.[103c] Figure 6-4 is a graph of the literature data compared to the prediction data with the Volume method for n_i and both methods for K_i. There is excellent agreement between the experimental and the predicted

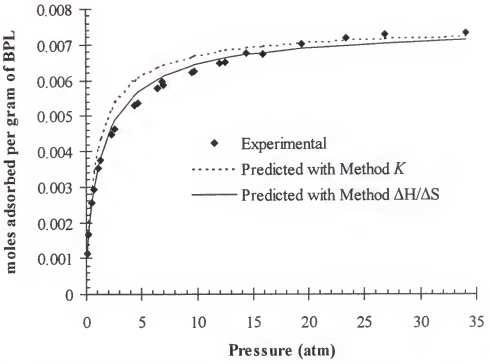

Figure 6-4: Experimental and predicted CH_4 isotherm. The high-pressure experimental data of Reich *et al.*[103c] and predicted adsorption isotherms for CH_4 on BPL at -60.5 °C.

adsorption isotherm. The adsorption of CH_4 on BPL was performed at a different temperature than the studies used to determine the prediction parameters. Also, the experimental BPL data includes very high pressures--the data used to determine the prediction parameters was below one atmosphere.

Conclusions

The described method for the prediction of adsorption isotherms for N_2, CO, CH_4, C_2H_6, and SF_6 has been applied to one zeolitic and five carbonaceous solids. Various degrees of accuracy have been obtained; the adsorption of CO is best reproduced on each of the solids. In general, the adsorption of N_2 has been accurately predicted, while CH_4 and C_2H_6 are under predicted and SF_6 is over predicted.

Utilizing the volume method for estimate the n_i and both the K and $\Delta S/\Delta H$ methods to estimate the K_i, the MEA prediction reproduced the data over the entire pressure range for the adsorption of CH_4 on BPL reported by Reich *et al.* It is interesting to note that the high-pressure portion of the isotherm was reproduced, even though the parameters were derived from relatively low-pressure data. (The highest pressure used in the parameter estimation was one atmosphere.)

The application of the MEA prediction of adsorption behavior has quite a potential for a variety of applications. Adsorbents can be used for catalyst supports, gas separation, respiratory protection, environmental applications, and even have the potential for fuel storage capabilities. The prediction of adsorption performance will lead a greater understanding of the fundamental interactions involved in these systems and will help create new and better systems.

Table 6-1: Prediction of N_2 Adsorption Capacity for Solids at Various Temperatures

A-572			Method *K*				Method ΔH/ΔS			
Temp (°C)	Exp (mmol)	Area (mmol)	Δs (%)	Volume (mmol)	Δs (%)	Area (mmol)	Δs (%)	Volume (mmol)	Δs (%)
-93.0	4.35	4.77	9.5	4.77	9.6	5.25	20.6	5.25	20.7
-43.0	1.66	2.00	20.6	2.01	20.7	2.33	40.1	2.33	40.2
0.0	0.67	0.83	23.0	0.83	23.2	1.01	49.8	1.01	50.0

A-563			Method *K*				Method ΔH/ΔS			
Temp (°C)	Exp (mmol)	Area (mmol)	Δs (%)	Volume (mmol)	Δs (%)	Area (mmol)	Δs (%)	Volume (mmol)	Δs (%)
-93.0	2.79	2.88	3.4	2.88	3.4	3.12	11.7	3.12	11.7
-62.0	1.66	1.90	14.0	1.90	14.0	2.08	25.2	2.08	25.2
-43.0	1.15	1.39	20.6	1.39	20.6	1.53	32.6	1.53	32.6

A-600			Method *K*				Method ΔH/ΔS			
Temp (°C)	Exp (mmol)	Area (mmol)	Δs (%)	Volume (mmol)	Δs (%)	Area (mmol)	Δs (%)	Volume (mmol)	Δs (%)
-93.0	4.93	3.27	-33.6	3.27	-33.6	3.27	-33.6	3.27	-33.6
-62.0	2.60	1.54	-40.6	1.54	-40.6	2.15	-17.4	2.15	-17.4
-43.0	1.77	0.62	-64.8	0.62	-64.8	1.56	-11.7	1.56	-11.7

F300			Method *K*				Method ΔH/ΔS			
Temp (°C)	Exp (mmol)	Area (mmol)	Δs (%)	Volume (mmol)	Δs (%)	Area (mmol)	Δs (%)	Volume (mmol)	Δs (%)
-93.0	3.07	2.75	-10.2	2.75	-10.2	3.57	16.3	3.57	16.3
-62.0	1.73	1.53	-11.7	1.53	-11.7	2.08	20.3	2.08	20.3
-43.0	1.23	1.04	-15.1	1.04	-15.1	1.42	16.0	1.42	16.0

BPL			Method *K*				Method ΔH/ΔS			
Temp (°C)	Exp (mmol)	Area (mmol)	Δs (%)	Volume (mmol)	Δs (%)	Area (mmol)	Δs (%)	Volume (mmol)	Δs (%)
-93.0	3.48	3.61	3.7	3.61	3.7	4.18	20.1	4.18	20.1
-62.0	1.70	2.00	17.9	2.00	17.9	2.53	49.1	2.53	49.1
-43.0	1.17	1.37	16.9	1.37	16.9	1.81	54.9	1.81	54.9

HZSM-5			Method *K*				Method ΔH/ΔS			
Temp (°C)	Exp (mmol)	Area (mmol)	Δs (%)	Volume (mmol)	Δs (%)	Area (mmol)	Δs (%)	Volume (mmol)	Δs (%)
-93.0	2.37	1.82	-23.1	1.85	-22.0	1.68	-29.0	1.71	-27.9
-43.0	1.15	0.89	-22.9	0.90	-21.8	0.97	-15.7	0.99	-14.5
0.0	0.42	0.32	-23.3	0.33	-22.2	0.44	6.2	0.45	7.7
25.0	0.23	0.17	-26.2	0.17	-25.1	0.26	14.3	0.27	16.0

Table 6-2: Prediction of CO Adsorption Capacity for Solids at Various Temperatures

A-572			Method *K*			Method ΔH/ΔS			
Temp (°C)	Exp (mmol)	Area (mmol)	Δs (%)	Volume (mmol)	Δs (%)	Area (mmol)	Δs (%)	Volume (mmol)	Δs (%)
-93.0	5.19	5.19	0.1	5.10	-1.7	5.39	3.9	5.29	2.1
-62.0	3.19	3.13	-1.8	3.41	6.9	3.29	3.1	3.24	1.6
-43.0	2.27	2.19	-3.5	2.48	9.3	2.31	1.7	2.28	0.4

A-563			Method *K*			Method ΔH/ΔS			
Temp (°C)	Exp (mmol)	Area (mmol)	Δs (%)	Volume (mmol)	Δs (%)	Area (mmol)	Δs (%)	Volume (mmol)	Δs (%)
-93.0	2.92	3.31	13.5	3.25	11.3	3.35	14.6	3.28	12.4
-62.0	2.15	2.16	0.6	2.13	-1.0	2.20	2.1	2.16	0.5
-43.0	1.56	1.56	0.0	1.54	-1.4	1.59	1.8	1.57	0.3

A-600			Method *K*			Method ΔH/ΔS			
Temp (°C)	Exp (mmol)	Area (mmol)	Δs (%)	Volume (mmol)	Δs (%)	Area (mmol)	Δs (%)	Volume (mmol)	Δs (%)
-93.0	3.15	3.42	8.7	3.35	6.4	3.35	6.3	3.28	4.1
-62.0	2.13	2.24	5.0	2.20	3.2	2.15	0.8	2.11	-0.9
-43.0	1.54	1.61	4.7	1.58	3.1	1.53	-0.2	1.51	-1.7

F300			Method *K*			Method ΔH/ΔS			
Temp (°C)	Exp (mmol)	Area (mmol)	Δs (%)	Volume (mmol)	Δs (%)	Area (mmol)	Δs (%)	Volume (mmol)	Δs (%)
-93.0	3.67	3.42	-6.8	3.38	-8.0	3.46	-5.8	3.41	-7.1
-62.0	2.20	1.94	-11.9	1.91	-13.0	2.02	-8.0	2.00	-9.1
-43.0	1.59	1.32	-17.0	1.31	-18.0	1.45	-9.1	1.43	-10.2

BPL			Method *K*			Method ΔH/ΔS			
Temp (°C)	Exp (mmol)	Area (mmol)	Δs (%)	Volume (mmol)	Δs (%)	Area (mmol)	Δs (%)	Volume (mmol)	Δs (%)
-93.0	3.91	4.03	3.1	3.97	1.6	4.37	11.9	4.31	10.3
-62.0	2.08	2.20	5.7	2.17	4.3	2.57	23.5	2.53	21.9
-43.0	1.52	1.48	-3.0	1.46	-4.2	1.79	17.9	1.77	16.4

HZSM-5			Method *K*			Method ΔH/ΔS			
Temp (°C)	Exp (mmol)	Area (mmol)	Δs (%)	Volume (mmol)	Δs (%)	Area (mmol)	Δs (%)	Volume (mmol)	Δs (%)
-93.0	2.55	2.39	-6.3	2.33	-8.5	2.50	-1.8	2.44	-4.2
-42.0	1.46	1.31	-10.4	1.29	-12.1	1.48	1.0	1.45	-1.1
-16.0	0.96	0.74	-22.6	0.73	-24.0	0.89	-7.7	0.87	-9.5
0.0	0.66	0.50	-24.4	0.49	-25.8	0.62	-6.9	0.61	-8.7

Table 6-3: Prediction of CH_4 Adsorption Capacity for Solids at Various Temperatures

A-572		Method *K*				Method ΔH/ΔS			
Temp (°C)	Exp (mmol)	Area (mmol)	Δs (%)	Volume (mmol)	Δs (%)	Area (mmol)	Δs (%)	Volume (mmol)	Δs (%)
-62.0	5.59	5.41	-3.2	5.65	1.2	4.26	-23.7	4.45	-20.3
-43.0	3.91	4.19	7.1	4.37	11.9	3.10	-20.6	3.24	-17.1
0.0	2.09	2.08	-0.8	2.16	3.5	1.38	-33.9	1.44	-31.1

A-563		Method *K*				Method ΔH/ΔS			
Temp (°C)	Exp (mmol)	Area (mmol)	Δs (%)	Volume (mmol)	Δs (%)	Area (mmol)	Δs (%)	Volume (mmol)	Δs (%)
-62.0	3.34	3.10	-7.3	3.23	-3.1	2.67	-20.0	2.80	-16.3
-43.0	2.72	2.56	-5.9	2.68	-1.5	2.07	-23.7	2.17	-19.9
-16.0	1.84	1.80	-2.1	1.89	2.7	1.35	-26.8	1.42	-23.0

A-600		Method *K*				Method ΔH/ΔS			
Temp (°C)	Exp (mmol)	Area (mmol)	Δs (%)	Volume (mmol)	Δs (%)	Area (mmol)	Δs (%)	Volume (mmol)	Δs (%)
-62.0	3.28	3.05	-6.9	3.17	-3.1	2.66	-18.9	2.77	-15.5
-43.0	2.57	2.47	-3.9	2.58	0.1	2.05	-20.3	2.14	-17.0
-16.0	1.84	1.33	-27.7	1.38	-24.7	1.32	-28.1	1.37	-25.1

F300		Method *K*				Method ΔH/ΔS			
Temp (°C)	Exp (mmol)	Area (mmol)	Δs (%)	Volume (mmol)	Δs (%)	Area (mmol)	Δs (%)	Volume (mmol)	Δs (%)
-62.0	3.93	3.30	-16.0	3.47	-11.6	3.34	-14.8	3.52	-10.3
-43.0	2.97	2.45	-17.6	2.57	-13.3	2.42	-18.4	2.55	-14.1
-16.0	1.87	1.58	-15.5	1.66	-11.1	1.48	-21.1	1.55	-17.0

BPL		Method *K*				Method ΔH/ΔS			
Temp (°C)	Exp (mmol)	Area (mmol)	Δs (%)	Volume (mmol)	Δs (%)	Area (mmol)	Δs (%)	Volume (mmol)	Δs (%)
-62.0	4.32	3.88	-10.3	4.05	-6.2	3.35	-22.5	3.50	-19.0
-43.0	3.35	2.84	-15.3	2.97	-11.6	2.38	-29.1	2.48	-26.0
-16.0	2.04	1.81	-11.6	1.89	-7.8	1.44	-29.6	1.50	-26.6

HZSM-5		Method *K*				Method ΔH/ΔS			
Temp (°C)	Exp (mmol)	Area (mmol)	Δs (%)	Volume (mmol)	Δs (%)	Area (mmol)	Δs (%)	Volume (mmol)	Δs (%)
-42.0	2.26	1.89	-16.5	2.00	-11.7	1.36	-40.0	1.44	-36.6
-16.0	1.66	1.31	-20.9	1.38	-16.4	1.02	-38.2	1.08	-34.7
0.0	1.31	0.98	-25.7	1.03	-21.4	0.80	-39.2	0.84	-35.8

Table 6-4: Prediction of C_2H_6 Adsorption Capacity for Solids at Various Temperatures

A-572			Method *K*				Method ΔH/ΔS			
Temp (°C)	Exp (mmol)	Area (mmol)	Δs (%)	Volume (mmol)	Δs (%)	Area (mmol)	Δs (%)	Volume (mmol)	Δs (%)
40.0	3.78	2.85	-24.8	3.23	-14.7	2.28	-39.8	2.58	-31.9
55.0	3.16	2.40	-24.2	2.71	-14.2	1.89	-40.1	2.14	-32.4
70.0	2.78	2.00	-27.9	2.26	-18.6	1.57	-43.5	1.77	-36.4

A-563			Method *K*				Method ΔH/ΔS			
Temp (°C)	Exp (mmol)	Area (mmol)	Δs (%)	Volume (mmol)	Δs (%)	Area (mmol)	Δs (%)	Volume (mmol)	Δs (%)
40.0	1.99	1.32	-33.9	1.44	-27.8	1.12	-43.5	1.23	-38.4
55.0	1.75	1.13	-35.2	1.23	-29.3	0.95	-45.7	1.03	-40.8
70.0	1.49	0.67	-55.1	0.73	-51.2	0.79	-47.1	0.86	-42.4

A-600			Method *K*				Method ΔH/ΔS			
Temp (°C)	Exp (mmol)	Area (mmol)	Δs (%)	Volume (mmol)	Δs (%)	Area (mmol)	Δs (%)	Volume (mmol)	Δs (%)
40.0	2.01	1.21	-39.7	1.30	-35.3	1.12	-44.4	1.20	-40.4
55.0	1.78	1.06	-40.2	1.14	-36.0	0.97	-45.6	1.03	-41.9
70.0	1.56	0.92	-40.8	0.99	-36.9	0.83	-47.1	0.88	-43.7
100.0	1.14	0.68	-40.2	0.72	-36.6	0.59	-48.6	0.62	-45.7

F300			Method *K*				Method ΔH/ΔS			
Temp (°C)	Exp (mmol)	Area (mmol)	Δs (%)	Volume (mmol)	Δs (%)	Area (mmol)	Δs (%)	Volume (mmol)	Δs (%)
40.0	2.69	2.01	-25.3	2.34	-13.0	1.99	-25.9	2.32	-13.8
55.0	2.30	1.71	-25.6	1.99	-13.4	1.61	-29.9	1.88	-18.4
70.0	1.91	1.47	-23.4	1.71	-10.9	1.29	-32.5	1.50	-21.6

BPL			Method *K*				Method ΔH/ΔS			
Temp (°C)	Exp (mmol)	Area (mmol)	Δs (%)	Volume (mmol)	Δs (%)	Area (mmol)	Δs (%)	Volume (mmol)	Δs (%)
40.0	2.65	2.35	-11.6	2.74	3.4	1.75	-34.2	2.04	-23.1
55.0	2.24	1.97	-12.0	2.30	2.9	1.40	-37.4	1.63	-27.0
70.0	1.82	1.66	-8.4	1.94	7.0	1.12	-38.3	1.31	-28.1
100.0	1.52	1.20	-21.4	1.39	-8.4	0.71	-53.2	0.83	-45.6

HZSM-5			Method *K*				Method ΔH/ΔS			
Temp (°C)	Exp (mmol)	Area (mmol)	Δs (%)	Volume (mmol)	Δs (%)	Area (mmol)	Δs (%)	Volume (mmol)	Δs (%)
40.0	1.74	1.55	-10.6	1.55	-10.6	1.55	-10.6	1.55	-10.6
50.0	1.61	1.40	-13.0	0.19	-37.3	1.40	-13.0	1.40	-13.0
75.0	1.38	1.05	-23.9	1.05	-23.9	1.05	-23.9	1.05	-23.9

Table 6-5: Prediction of SF_6 Adsorption Capacity for Solids at Various Temperatures

		Method *K*				Method ΔH/ΔS			
A-572	Temp	Exp	Area	Δs	Volume	Δs	Area	Δs	Volume	Δs
	(°C)	(mmol)	(mmol)	(%)	(mmol)	(%)	(mmol)	(%)	(mmol)	(%)
	50.0	2.59	3.48	34.6	1.70	-34.4	2.76	6.6	1.35	-48.0
	65.0	2.38	3.14	32.0	1.53	-35.6	2.32	-2.6	1.13	-52.5
	80.0	2.03	2.77	36.7	1.35	-33.3	1.92	-5.1	0.94	-53.7
A-563			Method *K*				Method ΔH/ΔS			
	Temp	Exp	Area	Δs	Volume	Δs	Area	Δs	Volume	Δs
	(°C)	(mmol)	(mmol)	(%)	(mmol)	(%)	(mmol)	(%)	(mmol)	(%)
	50.0	1.00	1.71	71.3	0.83	-16.4	1.47	47.3	0.72	-28.2
	65.0	0.89	1.55	73.2	0.75	-15.6	1.28	43.0	0.62	-30.3
	80.0	0.78	1.38	75.9	0.67	-14.2	1.09	39.5	0.53	-32.0
A-600			Method *K*				Method ΔH/ΔS			
	Temp	Exp	Area	Δs	Volume	Δs	Area	Δs	Volume	Δs
	(°C)	(mmol)	(mmol)	(%)	(mmol)	(%)	(mmol)	(%)	(mmol)	(%)
	50.0	0.92	1.77	93.3	0.87	-5.7	1.49	62.6	0.73	-20.7
	65.0	0.84	1.62	93.8	0.79	-5.5	1.30	55.5	0.64	-24.1
	80.0	0.75	1.46	94.5	0.71	-5.1	1.13	50.3	0.55	-26.7
	95.0	0.67	1.30	95.9	0.64	-4.5	0.97	45.9	0.47	-28.8
F300			Method *K*				Method ΔH/ΔS			
	Temp	Exp	Area	Δs	Volume	Δs	Area	Δs	Volume	Δs
	(°C)	(mmol)	(mmol)	(%)	(mmol)	(%)	(mmol)	(%)	(mmol)	(%)
	50.0	1.98	2.47	24.9	1.21	-39.1	2.72	37.6	1.33	-32.9
	65.0	1.65	2.27	37.3	1.11	-33.0	2.45	48.5	1.20	-27.6
	80.0	1.47	2.06	40.5	1.01	-31.5	2.16	47.1	1.05	-28.3
BPL			Method *K*				Method ΔH/ΔS			
	Temp	Exp	Area	Δs	Volume	Δs	Area	Δs	Volume	Δs
	(°C)	(mmol)	(mmol)	(%)	(mmol)	(%)	(mmol)	(%)	(mmol)	(%)
	50.0	2.35	2.80	18.9	1.36	-42.0	1.88	-20.1	0.92	-61.0
	65.0	1.96	2.55	29.8	1.24	-36.7	1.65	-16.2	0.80	-59.1
	80.0	1.64	2.31	41.2	1.13	-31.2	1.44	-11.9	0.70	-57.1
	95.0	1.39	2.08	50.0	1.01	-26.9	1.26	-9.4	0.61	-55.8
HZSM-5			Method *K*				Method ΔH/ΔS			
	Temp	Exp	Area	Δs	Volume	Δs	Area	Δs	Volume	Δs
	(°C)	(mmol)	(mmol)	(%)	(mmol)	(%)	(mmol)	(%)	(mmol)	(%)
	50.0	1.46	1.67	14.4	2.05	40.6	2.36	61.8	2.90	98.8
	65.0	1.27	1.49	17.1	1.83	43.9	2.26	78.1	2.78	118.9
	80.0	1.07	1.36	26.7	1.67	55.6	2.14	98.7	2.62	144.1

Table 6-6: Average Error and Standard Deviation of Predicted Adsorption Capacity for All Solids over All Temperatures for All Methods

Solid	N_2 Δs (%) ± σ (%)	CO Δs (%) ± σ (%)	CH_4 Δs (%) ± σ (%)	C_2H_6 Δs (%) ± σ (%)	SF_6 Δs (%) ± σ (%)
A-572	27 ± 14	2 ± 4	-11 ± 16	-30 ± 10	-12 ± 35
A-563	18 ± 10	5 ± 6	-12 ± 10	-41 ± 9	18 ± 44
A-600	-34 ± 18	3 ± 3	-16 ± 10	-41 ± 4	29 ± 49
F300	3 ± 16	-10 ± 4	-15 ± 3	-22 ± 9	6 ± 38
BPL	27 ± 19	9 ± 9	-18 ± 9	-21 ± 18	-18 ± 36
HZSM-5	-14 ± 16	-11 ± 9	-28 ± 10	-16 ± 9	67 ± 42
all solids	4 ± 27	-1 ± 10	-17 ± 12	-29 ± 14	13 ± 48

Table 6-7: Average Error and Standard Deviation of Predicted Adsorption Capacity for All Solids over All Temperatures for the Two n_i Methods

	N_2		CO		CH_4	
	Δs (%) ± σ (%)		Δs (%) ± σ (%)		Δs (%) ± σ (%)	
Solid	Area	Volume	Area	Volume	Area	Volume
A-572	27 ± 15	27 ± 15	1 ± 3	3 ± 4	-13 ± 16	-9 ± 17
A-563	18 ± 10	18 ± 10	5 ± 7	4 ± 6	-14 ± 10	-10 ± 11
A-600	-34 ± 19	-34 ± 19	4 ± 3	2 ± 3	-18 ± 10	-14 ± 11
F300	3 ± 16	3 ± 16	-10 ± 4	-11 ± 4	-17 ± 2	-13 ± 2
BPL	27 ± 20	27 ± 20	10 ± 10	8 ± 10	-20 ± 9	-16 ± 9
HZSM-5	-15 ± 16	-14 ± 16	-12 ± 9	-14 ± 9	-31 ± 10	-27 ± 11
all solids	3 ± 27	4 ± 27	0 ± 10	-1 ± 10	-19 ± 11	-15 ± 12

	C_2H_6		SF_6	
	Δs (%) ± σ (%)		Δs (%) ± σ (%)	
Solid	Area	Volume	Area	Volume
A-572	-34 ± 9	-26 ± 10	18 ± 21	-43 ± 10
A-563	-43 ± 9	-38 ± 10	59 ± 19	-23 ± 9
A-600	-43 ± 4	-40 ± 4	74 ± 22	-15 ± 11
F300	-28 ± 6	-17 ± 7	43 ± 9	-30 ± 5
BPL	-27 ± 16	-15 ± 19	10 ± 28	-46 ± 14
HZSM-5	-18 ± 6	-20 ± 11	49 ± 35	84 ± 43
all solids	-33 ± 13	-26 ± 15	42 ± 32	-16 ± 44

Table 6-8: Average Error and Standard Deviation of Predicted Adsorption Capacity for All Solids over All Temperatures for the Two K_i Methods

	N_2		CO		CH_4	
	Δs (%) $\pm \sigma$ (%)		Δs (%) $\pm \sigma$ (%)		Δs (%) $\pm \sigma$ (%)	
Solid	K	$\Delta H/\Delta S$	K	$\Delta H/\Delta S$	K	$\Delta H/\Delta S$
A-572	18 ± 6	37 ± 13	2 ± 5	2 ± 1	3 ± 5	-24 ± 7
A-563	13 ± 8	23 ± 9	4 ± 7	5 ± 6	-3 ± 4	-22 ± 4
A-600	-46 ± 15	-21 ± 10	5 ± 2	1 ± 3	-11 ± 12	-21 ± 5
F300	-12 ± 2	18 ± 2	-12 ± 5	-8 ± 2	-14 ± 3	-16 ± 4
BPL	13 ± 7	41 ± 17	1 ± 4	17 ± 5	-10 ± 3	-25 ± 4
HZSM-5	-24 ± 2	2 ± 14	-20 ± 7	-5 ± 4	-21 ± 4	-37 ± 2
all solids	-7 ± 24	14 ± 26	-4 ± 10	2 ± 9	-9 ± 9	-24 ± 8

	C_2H_6		SF_6	
	Δs (%) $\pm \sigma$ (%)		Δs (%) $\pm \sigma$ (%)	
Solid	K	$\Delta H/\Delta S$	K	$\Delta H/\Delta S$
A-572	-21 ± 6	-38 ± 5	2 ± 38	-27 ± 27
A-563	-36 ± 11	-45 ± 5	31 ± 48	5 ± 39
A-600	-38 ± 2	-45 ± 3	45 ± 53	14 ± 42
F300	-18 ± 7	-27 ± 9	3 ± 39	9 ± 40
BPL	-6 ± 10	-36 ± 10	0 ± 38	-36 ± 24
HZSM-5	-25 ± 10	-18 ± 6	36 ± 17	110 ± 28
all solids	-23 ± 14	-35 ± 12	18 ± 43	7 ± 53

APPENDIX A
FORTRAN 77 CODE FOR 421.EXE AND COMMENTS ON INPUT AND OUTPUT FILES

The code for 421.exe implements a non-linear least-squares constrained modified simplex minimization algorithm designed to simultaneously fit the combined adsorption isotherm data of all the temperature sets for a particular adsorbate. Many different modifications and improvements have been made since the first version of the code. The initial version was 411 named for the telephone directory information line, 4-1-1. In order to accommodate any desired changes, the code is commented. The program has automated the process of fitting the adsorption data and made the procedure much easier and faster. The program also performs weighted (or unweighted) linear regressions of the natural log of the thermodynamic equilibrium constant ($\ln K_i$) vs reciprocal absolute temperature (T^{-1}) and calculates the enthalpy (ΔH_i) and entropy (ΔS_i) of adsorption (along with their errors). The output file also contains the calculated process accessible surface areas and pore volumes. The input and output files are described. A new input file is also generated at the end of the fitting routine and has the same format as the original input file. The new input file and the output file are designed so that one may paste them space-delimited into a spreadsheet.

```
c ------------------------------------------------------------------
c -- Title          : 421.exe
c -- Description    : This program implements NELDER and MEADE's
c --                  Modified Simplex Method. It is set up
c --                  to contrain the simplex to positive space
c --                  but not allowing any of the parameters to
c --                  become less than 0.
c --
c --                  The comments in this code assume the reader
c --                  has some knowledge of the simplex algorithm.
c --                  The comments should be sufficient to determine
c --                  flow and allow cross reference between the
c --                  code and the following references.
c --
c --                  References:
c --                  A Simplex Method for Function Minimization by
c --                  J. A. Nelder and R. Mead in The Computer
c --                  Journal, 1965, pp 308-313
c --
c --                  Fitting Curves to Data by Marco S. Caceci and
c --                  William P. Cacheris in Byte, May 1984,
c --                  pp 340-362
c --
c --                  Simplex Optimization of Variables in Analytical
c --                  Chemistry by Stanley N. Deming and Stephen L.
c --                  Morgan in Analytical Chemistry, Vol 45,
c --                  March 1973, pp 278-283
c --
c -- Author         : Charles Edwin Webster
c -- Revision History :
c --                  1.Added comments throughout the simplex portion
c --                  of the code.
c --                  2.Constrained the simplex to positive space.
c --                  (the parameters will always come out non-negative)
c --                  Note that the "magic" number is set to 1.0E+1
c --                  If that number is too small, it may be changed
c --                  to a max of 1.0E+308.
c --                  3.Used the SAVE compiler directive to make sure
c --                  that when this code is moved to another
c --                  compiler, the centroid variable in VERTEX will
c --                  keep it's value from function call to function
c --                  call. The code had assumed that the compiler
c --                  (in this case Microsoft) automatically saves
c --                  the value.
c --                  4.Got rid of the last compiler warnings.
c ------------------------------------------------------------------

      IMPLICIT NONE

      INTEGER MAXNTEMP,MAXNPOINT,MAXNSITE
      PARAMETER (MAXNTEMP=5)
      PARAMETER (MAXNSITE=5)
      PARAMETER (MAXNPOINT=200)

      CHARACTER*60 INFILE, OUTFILE, NEWINFILE

      DOUBLE PRECISION B(MAXNTEMP,MAXNPOINT)
      DOUBLE PRECISION H(MAXNTEMP,MAXNPOINT)
      DOUBLE PRECISION P(MAXNTEMP**2*MAXNSITE)
      DOUBLE PRECISION DUP(MAXNTEMP**2*MAXNSITE)
      DOUBLE PRECISION DDOWN(MAXNTEMP**2*MAXNSITE)
      DOUBLE PRECISION DIF(MAXNTEMP,MAXNPOINT)
      DOUBLE PRECISION HH(MAXNTEMP,MAXNPOINT)
      DOUBLE PRECISION SD(MAXNTEMP,MAXNSITE,2),BR
      DOUBLE PRECISION AVGE(MAXNTEMP),GE(MAXNTEMP),EP,DEVN,BI,HCAL
      DOUBLE PRECISION PER,TOT_SQ, SQUARE(MAXNTEMP)
      DOUBLE PRECISION CAL, N_TOT, N_SD
      DOUBLE PRECISION TEMP(MAXNTEMP)
      DOUBLE PRECISION SX(MAXNTEMP), SX2(MAXNTEMP)
      DOUBLE PRECISION SXY(MAXNTEMP), SY(MAXNTEMP)
```

```
      DOUBLE PRECISION SLOPE(MAXNTEMP), YINTER(MAXNTEMP)
      DOUBLE PRECISION RBX(MAXNTEMP), RBY(MAXNTEMP)
      DOUBLE PRECISION RT(MAXNTEMP), R(MAXNTEMP)
      DOUBLE PRECISION AREA, MVL
      DOUBLE PRECISION WGT(MAXNTEMP, MAXNSITE), T_WGT(MAXNSITE)
      DOUBLE PRECISION SD_Y(MAXNTEMP), DY(MAXNTEMP,MAXNSITE),D
      DOUBLE PRECISION SD_M(MAXNTEMP), SD_B(MAXNTEMP)
      INTEGER I, IS, K, NT, N(MAXNTEMP), NE(MAXNTEMP), NS(MAXNTEMP)
      INTEGER TOTAL_NS, FIXEDN, L1, L2, UPORDWN, IP, KX
      INTEGER TOTAL_NP, MAXNS,TOT_N
      INTEGER COUNT, M, CALC_DIM, WEIGHT

c Get name of data file
      WRITE (6,10)
   10 FORMAT (5X,'Name of Data File? ')
      READ (5,'(A)') INFILE
c Get name of output file
      WRITE (6,20)
   20 FORMAT (/5X,'Name of Output File? ')
      READ (5,'(A)') OUTFILE
c Get name of new input file
      WRITE (6,30)
   30 FORMAT (/5X,'Name of New Input File? ')
      READ (5,'(A)') NEWINFILE
c Open the data file
      OPEN (8,FILE=INFILE,STATUS='OLD')
c get accuracy bound, max iterations
      CALL GETLINE(8)
      READ (8,*) EP, KX, FIXEDN
        PRINT *,'Read in EP(convergence), KX(loops), Fixedn(0,1)'
        PRINT *, EP, KX, FIXEDN
      CALL GETLINE(8)
      READ (8,*) UPORDWN, COUNT, CALC_DIM, WEIGHT
        PRINT *,'Read in Uporddown(0,1,2,3,4,5,10,15) Count(External Loo
     *ps)'
        PRINT *, UPORDWN, COUNT
        PRINT *,'Read in Calc Dimensions?(0,1), Weighted Regression?(0,
     *1)'
        PRINT *, CALC_DIM, WEIGHT
      IF (CALC_DIM.EQ.1) THEN
        CALL GETLINE(8)
        READ (8,*) AREA, MVL
          PRINT *,'Read in AREA/Molecule (A^2), Molar Vol (mL/mole)'
          PRINT *, AREA, MVL
      ENDIF
c get number of temperature sets
      CALL GETLINE(8)
      READ (8,*) NT
        PRINT *,'Read in NT(number of temperature sets)'
        PRINT *, NT
c make sure use has not requested too many temperature sets
c if so, tell the user and quit
      IF (NT.GT.MAXNTEMP) THEN
        PRINT 100,NT,MAXNTEMP
        STOP
  100 FORMAT(5X,'Sorry. You asked for ',I3,
     *       ' temperature sets. The maximum number is ',I3)
      ENDIF
c set counter IP = 1
      IP = 1
c max number of sites
      MAXNS = 0
c total number of points
      TOT_N = 0
      DO 1000 K=1,NT
        AVGE(K) = 0.00
c get number of data points (pressure ratio, moles abs)
c NE is the number of data points, and GE is the grams of solid
        CALL GETLINE(8)
        READ (8,*) NE(K),GE(K)
```

```
        PRINT *, 'This is NE(k)[number of data points]',
     *       ' GE(k)[grams of solid]'
        PRINT *, NE(K), GE(K)
c make sure the user has not requested too many points
c if so, tell the user and quit
        IF (NE(K).GT.MAXNPOINT) THEN
          PRINT 120,NE(K),MAXNPOINT
          STOP
  120 FORMAT(5X,'Sorry. You asked for ',I3,
     *    ' data points. The maximum number is ',I3)
        ENDIF
        N(K) = NE(K)
        TOT_N = TOT_N + N(K)
c read the data points
      DO 150 I=1,N(K)
       CALL GETLINE(8)
       READ (8,*) B(K,I),H(K,I)
       PRINT *, B(K,I),H(K,I)
  150 CONTINUE
c get the number of sites for this temp set
      CALL GETLINE(8)
       READ (8,*) NS(K), TEMP(K)
       PRINT 160,NS(K),K,TEMP(K)
       IF (NS(K).GT.MAXNSITE) THEN
         PRINT 170,NS(K),MAXNSITE
         STOP
  160 FORMAT('Number of Sites [NS(K)]:',I2,5X,'Temp',I2,':',F7.2)
  170 format(5X,'Sorry. You asked for ',I3,
     *    ' sites. The maximum number is ',I3)
       ENDIF
      IF (NS(K).GT.MAXNS) MAXNS = NS(K)
      DO 180 I=1,2*NS(K)
        CALL GETLINE(8)
      IF (UPORDWN.LT.0) THEN
        UPORDWN=0
      ENDIF
      IF (UPORDWN.EQ.0) THEN
        READ (8,*) P(IP),DDOWN(IP),DUP(IP)
        PRINT *, P(IP), DDOWN(IP), DUP(IP)
      ENDIF
      IF (UPORDWN.EQ.15) THEN
        READ (8,*) P(IP)
          DDOWN(IP)=1E-15*P(IP)
          DUP(IP)=1E-15*P(IP)
        PRINT *, P(IP), DDOWN(IP), DUP(IP)
      ENDIF
      IF (UPORDWN.EQ.10) THEN
        READ (8,*) P(IP)
          DDOWN(IP)=1E-10*P(IP)
          DUP(IP)=1E-10*P(IP)
        PRINT *, P(IP), DDOWN(IP), DUP(IP)
      ENDIF
      IF (UPORDWN.EQ.5) THEN
        READ (8,*) P(IP)
          DDOWN(IP)=1E-5*P(IP)
          DUP(IP)=1E-5*P(IP)
        PRINT *, P(IP), DDOWN(IP), DUP(IP)
      ENDIF
      IF (UPORDWN.EQ.4) THEN
        READ (8,*) P(IP)
          DDOWN(IP)=1E-4*P(IP)
          DUP(IP)=1E-4*P(IP)
        PRINT *, P(IP), DDOWN(IP), DUP(IP)
      ENDIF
      IF (UPORDWN.EQ.3) THEN
        READ (8,*) P(IP)
          DDOWN(IP)=1E-3*P(IP)
          DUP(IP)=1E-3*P(IP)
        PRINT *, P(IP), DDOWN(IP), DUP(IP)
      ENDIF
```

```
      IF (UPORDWN.EQ.2) THEN
        READ (8,*) P(IP)
          DDOWN(IP)=.01*P(IP)
          DUP(IP)=.01*P(IP)
        PRINT *, P(IP), DDOWN(IP), DUP(IP)
      ENDIF
      IF (UPORDWN.EQ.1) THEN
        READ (8,*) P(IP)
          DDOWN(IP)=.1*P(IP)
          DUP(IP)=.1*P(IP)
        PRINT *, P(IP), DDOWN(IP), DUP(IP)
      ENDIF
        IP = IP + 1
  180   CONTINUE
        DO 190 I=1,N(K)
          AVGE(K) = AVGE(K) + H(K,I) / NE(K)
  190   CONTINUE
        IF (AVGE(K).EQ.0) AVGE(K) = 1.00
        DO 200 I=1,N(K)
          HH(K,I) = H(K,I) / GE(K)
  200   CONTINUE
        DO 210 I=1,MAXNSITE
          SD(K,I,1)=0.0
          SD(K,I,2)=0.0
  210   CONTINUE
 1000 CONTINUE
c Close the input file.
      CLOSE(8)
      TOTAL_NP = IP - 1
      TOTAL_NS = TOTAL_NP / 2
c same n's for diff temps, so the rest of the n's are dummies
c they should not be variable
      IF (FIXEDN.NE.0) THEN
        DO 500 I = 2*MAXNS + 1, TOTAL_NP-1,2
          DDOWN(I) = 0.0
          DUP(I)   = 0.0
  500   CONTINUE
      ENDIF
c this loop sets up the inner_loop run for the program
      DO 5000 M = 0, COUNT-1
        DO 1020 K=1,NT
          DO 1010 I=1,MAXNSITE
            SD(K,I,1)=0.0
            SD(K,I,2)=0.0
 1010     CONTINUE
 1020   CONTINUE
c set value tot_sq = 0.0
        TOT_SQ = 0.0
c Do the filling now
        WRITE (6,1050)
 1050 FORMAT(//5X,'WORKING')
      CALL SIMPLEX(NT,EP,TOTAL_NP,N,KX,P,DDOWN,DUP,HH,B,NS,FIXEDN,
     *COUNT,M,BR)
c All done
      WRITE (6,1060)
 1060 FORMAT (/5X,'Fitting Routinue Completed')
c OPEN THE OUTPUT FILES
      OPEN (7,FILE=OUTFILE)
      OPEN (10,FILE=NEWINFILE)
      OPEN (9,FILE='BEST.BR')
      PRINT 1070, OUTFILE,NEWINFILE
      WRITE (7,1080) BR
      WRITE (9,1090) COUNT-M, BR
      WRITE (10,1100)
 1070 FORMAT (/,'Writing    ',1A12,', '1A12', and Best.BR')
 1080 FORMAT ('BR = ',E25.17)
 1090 FORMAT ('The Best Residual for count',i3,' is',e25.17,' .')
 1100 FORMAT ('#',1X,'ep(convergence)',1X,'kx(loops)',1X,'Fixedn(0/1)')
      IF (UPORDWN.GT.2) THEN
        UPORDWN = 5
```

```
      WRITE (10,1110) EP, KX, FIXEDN
      WRITE (10,1120)
      WRITE (10,1130) UPORDWN, COUNT, CALC_DIM, WEIGHT
     IF (CALC_DIM.EQ.1) THEN
      WRITE (10,1140)
      WRITE (10,1150) AREA, MVL
     ENDIF
    ELSE
      WRITE (10,1110) EP, KX, FIXEDN
      WRITE (10,1120)
      WRITE (10,1130) UPORDWN, COUNT, CALC_DIM, WEIGHT
     IF (CALC_DIM.EQ.1) THEN
      WRITE (10,1140)
      WRITE (10,1150) AREA, MVL
     ENDIF
    ENDIF
1110 FORMAT (E16.4,3X,I10,3X,I1)
1120 FORMAT ('#',1X,'Upordown(0,1,2,3,4,5,10,15)',1X,
   *'Count(ext_loops) Calc_Dim(0,1) Weight(0,1)')
1130 FORMAT (I2,3X,I2,3X,I2,3X,I2)
1140 FORMAT ('#',' AREA(A^2), MVL(mL/mole)')
1150 FORMAT (F7.3,3X,F7.3)
    WRITE (7,1160) COUNT-M
    WRITE (10,1170)
    WRITE (10,1180) NT
1160 FORMAT(1X,'Count_is: ',I2)
1170 FORMAT ('#_number_of_temperature_sets')
1180 FORMAT (I3)
    IP = 1
    DO 2010 K=1,NT
     DEVN=0.00
     SQUARE(K) = 0.0
     DO 1190 I=1,N(K)
      DIF(K,I) = H(K,I) - GE(K) * CAL(K,I,IP,P,B,NS,FIXEDN)
      SQUARE(K) = SQUARE(K) + DIF(K,I)**2
1190  CONTINUE
     DO 2000 I=1,N(K)
      DEVN=DIF(K,I)**2
      DO 2000 IS=0,NS(K)-1
       IF (FIXEDN.EQ.0) THEN
        L1 = IP + 2*IS
       ELSE
        L1 = 2*IS + 1
       ENDIF
       L2 = IP + 2*IS + 1
       B1 = P(L2)*B(K,I)
       IF (FIXEDN.EQ.0) THEN
        SD(K,IS+1,1)=SD(K,IS+1,1)+(((1.0+B1)/B1)**2)*DEVN
       ELSE
        SD(1,IS+1,1)=SD(1,IS+1,1)+(((1.0+B1)/B1)**2)*DEVN
       ENDIF
       SD(K,IS+1,2)=SD(K,IS+1,2)+(DIF(K,I)/(B(K,I)*
   *    (P(L1)-DIF(K,I))))**2
2000  CONTINUE
    IP = IP + 2*NS(K)
2010 CONTINUE
    IP = 1
    DO 2030 K=1,NT
     DO 2020 IS=0,NS(K)-1
      IF (FIXEDN.EQ.0) THEN
       L1 = IP + 2*IS
      ELSE
       L1 = 2*IS + 1
      ENDIF
      L2 = IP + 2*IS + 1
      IF (FIXEDN.EQ.0) THEN
       SD(K,IS+1,1) = SQRT(SD(K,IS+1,1)/N(K))
       IF ((DDOWN(L1).EQ.0.0).AND.(DUP(L1).EQ.0.0)) THEN
        SD(K,IS+1,1)=-1.00
       ENDIF
```

```
      ENDIF
      SD(K,IS+1,2) = SQRT(SD(K,IS+1,2)/N(K))
      IF ((DDOWN(L2).EQ.0.0).AND.(DUP(L2).EQ.0.0)) THEN
        SD(K,IS+1,2)=-1.00
      ENDIF
2020  CONTINUE
    IP = IP + 2*NS(K)
2030 CONTINUE
   IF (FIXEDN.NE.0) THEN
   DO 2040 IS=0,MAXNS-1
     L1 = 2*IS + 1
     SD(1,IS+1,1) = SQRT(SD(1,IS+1,1)/TOT_N)
     IF ((DDOWN(L1).EQ.0.0).AND.(DUP(L1).EQ.0.0)) THEN
       SD(1,IS+1,1)=-1.00
     ENDIF
2040  CONTINUE
   ENDIF
   IP = 1
   DO 2260 K=1,NT
    WRITE (10,2050)
    WRITE (10,2060) NE(K), GE(K)
    WRITE (7,2070) K, TEMP(K)
    WRITE (10,2080) K, TEMP(K)
    IF (NE(K).GT.0) WRITE (7,2090)
    WRITE (10,2100)
2050 FORMAT ('#_No._of Data_Points, No._of grams_ of_solid')
2060 FORMAT (I4,2X,F5.3)
2070 FORMAT ('Data_for temp_set ',I3,5X,'Temp(K): ',f7.2)
2080 FORMAT ('#_Data_for temp_set ',I3,5X,'Temp(K): ',f7.2)
2090 FORMAT (3X,'#',6X,'Eq_press',6X,'Exp_Ads',9X,'Calc_Ads',12X,
   *       'Err',15X,'Per')
2100 FORMAT ('#',3X,'Eq_press',5X,'Exp_Ads',8X,'Calc_Ads',10X,
   *       'Err',17X,'Per')
    DO 2150 I=1,N(K)
     HCAL=GE(K) * CAL(K,I,IP,P,B,NS,FIXEDN)
     PER = DABS(100.0*DIF(K,I)/HH(K,I))
     IF (B(K,I).LT.1E-9) THEN
      WRITE (7,2110) I,B(K,I),H(K,I),HCAL,DIF(K,I),PER
      WRITE (10,2120) B(K,I),H(K,I),HCAL,DIF(K,I),PER
     ELSE
      WRITE (7,2130) I,B(K,I),H(K,I),HCAL,DIF(K,I),PER
      WRITE (10,2140) B(K,I),H(K,I),HCAL,DIF(K,I),PER
     ENDIF
2150  CONTINUE
2110 FORMAT (1X,I3,3X,E14.8,3X,E14.8,2(3X,E14.8),3X,F9.4)
2120 FORMAT (1X,E14.8,3X,E14.8,2(3X,E14.8),1X,F9.4)
2130 FORMAT (1X,I3,3X,F11.9,3X,E14.8,2(3X,E14.8),5X,F9.4)
2140 FORMAT (1X,F11.9,3X,E14.8,2(3X,E14.8),3X,F9.4)
    WRITE (7,2160) K, SQUARE(K)
    TOT_SQ = SQUARE(K) + TOT_SQ
    WRITE (7,*)
    WRITE (10,2170)
    WRITE (10,2180) NS(K), TEMP(K)
2160 FORMAT ('/3X,'The_sum_of squares_for temp_set',I2,' is ',E14.8)
2170 FORMAT ('# number of sites above with: n1,K1, n2,K2...; Temp(K)')
2180 FORMAT (I2,F7.2)
    DO 2240 IS=1,NS(K)
     IF (FIXEDN.EQ.0) THEN
      L1 = IP + 2*IS - 2
     ELSE
      L1 = 2*IS - 1
     ENDIF
     L2 = IP + 2*IS - 1
     IF (FIXEDN.EQ.0) THEN
      WRITE (7,2200) IS,P(L1),SD(K,IS,1),IS,P(L2),SD(K,IS,2)
     ELSE
      WRITE (7,2210) IS,P(L2),SD(K,IS,2)
     ENDIF
2200 FORMAT (2X,'n',I1,'_is ',E20.11,2X,' +/- ',2X,E15.5,2X,
   *       'in_mole/g',
```

```
     *      /2X,'K',I1,'_ is ',E20.11,2X,' +/- ',2X,E15.5)
2210 FORMAT (2X,'K',I1,'_ is ',E20.11,2X,' +/- ',2X,E15.5)
       IF (UPORDWN.LE.3) THEN
         IF ((DDOWN(L1).EQ.0.0).AND.(DUP(L1).EQ.0.0)) THEN
           WRITE (10,2220)  P(L1),0,0
         ELSE
           WRITE (10,2230) P(L1),P(L1)*.01,P(L1)*.01
         ENDIF
         IF ((DDOWN(L2).EQ.0.0).AND.(DUP(L2).EQ.0.0)) THEN
           WRITE (10,2220)  P(L2),0,0
         ELSE
           WRITE (10,2230) P(L2),P(L2)*.01,P(L2)*.01
         ENDIF
       ELSE
         IF ((DDOWN(L1).EQ.0.0).AND.(DUP(L1).EQ.0.0)) THEN
           WRITE (10,2220)  P(L1),0,0
         ELSE
           WRITE (10,2230) P(L1),P(L1)*1E-10,P(L1)*1E-10
         ENDIF
         IF ((DDOWN(L2).EQ.0.0).AND.(DUP(L2).EQ.0.0)) THEN
           WRITE (10,2220)  P(L2),0,0
         ELSE
           WRITE (10,2230) P(L2),P(L2)*1E-10,P(L2)*1E-10
         ENDIF
       ENDIF
2240  CONTINUE
2220 FORMAT (E21.15,15X,I1,25X,I1)
2230 FORMAT (E21.15,5X,E21.5,5X,E21.5)
     IF (NE(K).GT.0) WRITE (7,2250) GE(K)
2250 FORMAT(/3X,'Grams of_Solid for_equilibrium data_is ',
     *      F5.3,3X/)
     IP = IP + 2*NS(K)
2260 CONTINUE
     IF (FIXEDN.NE.0) THEN
       N_TOT = 0.0
       N_SD = 0.0
       DO 2280 IS=1,MAXNS
         L1 = 2*IS - 1
         WRITE (7,2270) IS,P(L1),SD(1,IS,1)
         N_TOT = P(L1) + N_TOT
         N_SD = SD(1,IS,1) + N_SD
2270 FORMAT (2X,'n',I1,'_ is ',E20.11,2X,' +/- ',2X,
     *      E15.5,' in_mole/g')
2280  CONTINUE
       WRITE (7,*)
       WRITE (7,2300) N_TOT, N_SD
2290    FORMAT (/)
2300  FORMAT (3X,'The_total n_is ',E16.10,' +/- ',3X,
     *      E11.5,' in_mole/g')
     ENDIF
     WRITE (7,2310) TOT_SQ
2310  FORMAT (/3X,'The_total sum_of_sq is_ ',E16.10)
     IF (CALC_DIM.EQ.1) THEN
       WRITE (7,2290)
       WRITE (7,2320) AREA, MVL
       WRITE (7,*)
       DO 2340 IS=1,MAXNS
         L1 = 2*IS - 1
         WRITE (7,2330) IS,AREA*P(L1)*1000*6.023,
     *              AREA*SD(1,IS,1)*1000*6.023
2340  CONTINUE
       WRITE (7,2350) AREA*N_TOT*1000*6.023, AREA*N_SD*1000*6.023
       WRITE (7,*)
       DO 2370 IS=1,MAXNS
         L1 = 2*IS - 1
         WRITE (7,2360) IS,MVL*P(L1), MVL*SD(1,IS,1)
2370  CONTINUE
       WRITE (7,2380) MVL*N_TOT, MVL*N_SD
     ENDIF
2320 FORMAT ('  The_AREA_per_mole_is ', F7.3,' The_MVL_is ', F7.3)
```

```
2330 FORMAT (2X,'n',11,'_area_is ',7X,F10.3,2X,' +/- ',2X,
     *       F10.4,' in_meters^2/g')
2350 FORMAT (2X,'Total_area_is ',4X,F10.3,2X,' +/- ',2X,
     *       F10.4,' in_meters^2/g')
2360 FORMAT (2X,'n',11,'_pore_vol_is ',3X,F10.7,2X,' +/- ',2X,
     *       F10.7,' in_mL/g')
2380 FORMAT (2X,'Total_pore_vol_is ',F10.7,2X,' +/- ',2X,
     *       F10.7,' in_mL/g')
     WRITE (7,*)
     WRITE (7,2400)
2400 FORMAT (/,' Temp:',4X,'Temp_#',3X,'K',12X,'K',14X,
     *       'SD(K)')
       IP = 1
     DO 2560 K=1, NT
       DO 2550 IS=1,MAXNS
         L2 = IP + 2*IS - 1
         SX(IS)  = 0
         SX2(IS) = 0
         SXY(IS) = 0
         SY(IS)  = 0
         WGT(K,IS) = 0
         T_WGT(IS) = 0
         WRITE (7,2500) TEMP(K),K,IS,P(L2),SD(K,IS,2)
2550   CONTINUE
       IP = IP + 2*NS(K)
2560 CONTINUE
2500 FORMAT (F7.2,4X,I2,6X,I1,4X,F16.9,1X,F16.9)
     IF (WEIGHT.EQ.0) WRITE (7,2570)
2570 FORMAT (/,' Temp:',4X,'Temp_#',3X,'K',7X,'1/Temp',11X,'ln(K)',8X,
     *       'Weight(K)')
     IF (WEIGHT.EQ.1) WRITE (7,2580)
2580 FORMAT (/,' Temp:',4X,'Temp_#',3X,'K',7X,'1/Temp',11X,'ln(K)',8X,
     *       'Weight(K)',8X,'Wgt_Factor')
       IP = 1
     IF (WEIGHT.EQ.0) THEN
       DO 2670 K=1, NT
         DO 2650 IS=1,MAXNS
           L2 = IP + 2*IS - 1
         SX(IS)  = 1/TEMP(K) + SX(IS)
         SX2(IS) = (1/TEMP(K))**2 + SX2(IS)
         SY(IS)  = LOG(P(L2)) + SY(IS)
         SXY(IS) = 1/TEMP(K)*LOG(P(L2)) + SXY(IS)
         WRITE (7,2600)  TEMP(K),K,IS,1/TEMP(K),LOG(P(L2)),
     *                   P(L2)/SD(K,IS,2)
2650     CONTINUE
       IP = IP + 2*NS(K)
2670   CONTINUE
     ENDIF
2600 FORMAT (F7.2,4X,I2,6X,I1,4X,F11.8,2X,F14.7,2X,F14.7)
     IF (WEIGHT.EQ.1) THEN
       DO 2700 K=1, NT
         DO  2690 IS=1,MAXNS
           L2 = IP + 2*IS - 1
         WGT(K,IS) = P(L2)/SD(K,IS,2)
         T_WGT(IS) = T_WGT(IS) + WGT(K,IS)
2690     CONTINUE
       IP = IP + 2*NS(K)
2700   CONTINUE
     ENDIF
     IF (WEIGHT.EQ.1) THEN
       DO 2710 IS=1,MAXNS
         T_WGT(IS) = T_WGT(IS)/NT
2710   CONTINUE
     ENDIF
     IF (WEIGHT.EQ.1) THEN
       IP = 1
       DO 2770 K=1, NT
         DO 2750 IS=1,MAXNS
           L2 = IP + 2*IS - 1
         SX(IS) = (WGT(K,IS)/T_WGT(IS))*(1/TEMP(K)) + SX(IS)
```

```
      SX2(IS) = (WGT(K,IS)/T_WGT(IS))*(1/TEMP(K))**2 + SX2(IS)
       SY(IS) = (WGT(K,IS)/T_WGT(IS))*LOG(P(L2)) + SY(IS)
      SXY(IS) = (WGT(K,IS)/T_WGT(IS))*1/TEMP(K)*LOG(P(L2)) + SXY(IS)
      WRITE (7,2730) TEMP(K),K,IS,1/TEMP(K),LOG(P(L2)),
     *            P(L2)/SD(K,IS,2),(WGT(K,IS)/T_WGT(IS))
 2750  CONTINUE
     IP = IP + 2*NS(K)
 2770  CONTINUE
     ENDIF
 2730 FORMAT (F7.2,4X,I2,6X,I1,4X,F11.8,2X,F14.7,2X,F14.7,2X,F14.7)
     IF (NT.EQ.1) THEN
      GOTO 5010
     ELSE
      WRITE (7,*)
      IF (WEIGHT.EQ.0) WRITE (7,2790)
      IF (WEIGHT.EQ.1) WRITE (7,2800)
 2790 FORMAT (' These_are_the unweighted_regression_parameters')
 2800 FORMAT (' These_are_the weighted_regression_parameters')
      DO 2830 IS=1, MAXNS
      SLOPE(IS) = (NT*SXY(IS)-SX(IS)*SY(IS))/(NT*SX2(IS)-SX(IS)**2)
      YINTER(IS) = (SX2(IS)*SY(IS)-SXY(IS)*SX(IS))
     *          /(NT*SX2(IS)-SX(IS)**2)
 2830  CONTINUE
      DO 2840 IS=1,MAXNS
       SD_Y(IS) = 0
 2840  CONTINUE
      IP = 1
      DO 2860 K=1, NT
       DO 2850 IS=1,MAXNS
         L2 = IP + 2*IS - 1
       DY(K,IS) = LOG(P(L2)) - (SLOPE(IS)*1/TEMP(K)+YINTER(IS))
       SD_Y(IS) =  DY(K,IS)**2 + SD_Y(IS)
 2850  CONTINUE
      IP = IP + 2*NS(K)
 2860  CONTINUE
       IS=1
      D = SX2(IS)*NT-SX(IS)**2
      IF (NT.GT.2) THEN
       DO 2880 IS=1,MAXNS
        SD_M(IS) = SQRT((SD_Y(IS)/(NT-2))*NT/D)*1.987/1000
        SD_B(IS) = SQRT((SD_Y(IS)/(NT-2))*SX2(IS)/D)*1.987
       WRITE (7,2820) IS,SLOPE(IS)*1.987/1000,SD_M(IS),
     *            IS,-YINTER(IS)*1.987,SD_B(IS)
 2880  CONTINUE
      ENDIF
      IF (NT.LE.2) THEN
       DO 2890 IS=1,MAXNS
        SD_M(IS) = SQRT(((SD_Y(IS)/(NT-1))*NT/D)**2)*1.987/1000
        SD_B(IS) = SQRT(((SD_Y(IS)/(NT-1))*SX2(IS)/D)**2)*1.987
       WRITE (7,2820) IS,SLOPE(IS)*1.987/1000,SD_M(IS),
     *          IS,-YINTER(IS)*1.987,SD_B(IS)
 2890  CONTINUE
      ENDIF
 2820 FORMAT ('-dH',I1,',',F10.4,' +/- ',F8.5,' kCal/mole',3X,
     * '-dS',I1,',',F10.4,' +/- ',F8.5,' Cal/(mol*K)')
      IP = 1
      DO 2940 IS=1,MAXNS
       SX(IS) = SX(IS)/NT
       SY(IS) = SY(IS)/NT
       RT(IS) = 0
       RBX(IS) = 0
       RBY(IS) = 0
 2940  CONTINUE
      DO 2970 K=1, NT
       DO 2950 IS=1,MAXNS
         L2 = IP + 2*IS - 1
       RT(IS) = (1/TEMP(K) - SX(IS))*(LOG(P(L2)) - SY(IS)) + RT(IS)
       RBX(IS) = (1/TEMP(K) - SX(IS))**2 + RBX(IS)
       RBY(IS) = (LOG(P(L2)) - SY(IS))**2 + RBY(IS)
 2950  CONTINUE
```

```
      IP = IP + 2*NS(K)
 2970  CONTINUE
       DO 2990 IS=1,MAXNS
         R(IS) = RT(IS)/SQRT(RBX(IS)*RBY(IS))
         WRITE (7,2980) IS, R(IS)**2
 2990  CONTINUE
 2980 FORMAT ('R^2(',I1,')= ',F7.5)
 5010 ENDIF
      CLOSE (7)
      CLOSE (10)
 5000 CONTINUE
      CLOSE (9)
      STOP
      END
C -------------------------------------------------------------------------
C
C FUNK: Computes the standard error for the experimental
C       and the computed variables. (sum of the squares of
C       the residuals)
C
C  The sum of squares equation that is computed is:
C
C    SQRT{summation( Y - f(x) )**2/n}
C
C    where Y    = dependent variable (moles adsorbed) from data file
C          f(x) = dependent variable computed using the independent
C                 variables from data file and the computed
C                 constants/parameters (n and K) from the simplex.
C          n    = total number of parameters.
C
C  The equation to solve for f(x) is:
C
C    summation ( (ni*Ki*Bi) / (1.0+Ki*Bi) )
C      for each set of n's and K's in the temp set.
C
C H  contains the array of moles adsorbed
C P  is the array of computed data points (n & K)
C B  contains the array of equil conc
C N  contains the number of data points per temp set.
C NT contains the number of temperature sets.
C NS contains the number of sites
C
C -------------------------------------------------------------------------
      DOUBLE PRECISION FUNCTION FUNK(H,P,B,N,NT,NS,FIXEDN)

      IMPLICIT NONE

      INTEGER   MAXNTEMP,MAXNPOINT,MAXNSITE
      PARAMETER (MAXNTEMP=5)
      PARAMETER (MAXNSITE=5)
      PARAMETER (MAXNPOINT=200)

      DOUBLE PRECISION H(MAXNTEMP,MAXNPOINT),P(MAXNTEMP*2*MAXNSITE)
      DOUBLE PRECISION B(MAXNTEMP,MAXNPOINT),F,B2
      INTEGER NT,N(MAXNTEMP),NS(MAXNTEMP),I,K,IS,IP,N_TOT,FIxedn

C L1 contains the location of n for a particular site
C L2 contains the location of K for a particular site
      INTEGER L1,L2
      FUNK = 0.0
      N_TOT = 0
      B2 = 0.0
      IP = 1
C solve - summation( Y - f(x) )**2 for all temp sets.
      DO 20 K=1,NT
C solve the part of -> summation( Y - f(x) )**2 for this particular
C temp set
        DO 10 I=1,N(K)
          F=0.0
C solve f(x)
```

```
      DO 15 IS=0,NS(k)-1
c   P(IP)   = the N(IS)
c   P(IP+1) = the K(IS)
c get the location of n (I1) and K (I2) in the data point array
        IF (FIXEDN.EQ.0) THEN
          L1 = IP + 2*IS
        ELSE
          L1 = 1 + 2*IS
        ENDIF
        L2 = IP + 2*IS + 1
c ( solve f(x) )  (moles adsorbed), then add that result to the previous
c result (f) to build upon the summation.
        B2 = P(L1)*P(L2)*B(K,I)/(1.0+P(L2)*B(K,I))
        F = F + B2
  15    CONTINUE
c do the partial summation (if this is not the last go around in the
c loop) of the sum of the squares of the residuals
        FUNK=FUNK+(H(K,I)-F)**2
  10  CONTINUE
      IP = IP + 2*NS(K)
      N_TOT = N_TOT + N(K)
  20 CONTINUE
c all through with the intermediate calculations so can now perform
c the last part of the equation.
      FUNK=SQRT(FUNK/(N_TOT-1))
      RETURN
      END

c -------------------------------------------------------------------------
c Calculate the value of the function at the i-th point in the
c k-th temp set, using ns(k) sites that have parameters
c starting at offset ip in the P array.
c
c The equation is:
c    summation ( (ni*Ki*Bi) / (1.0+Ki*Bi) )
c       for each set of n's and K's in the temp set.
c
c -------------------------------------------------------------------------
      DOUBLE PRECISION FUNCTION CAL(K,I,IP,P,B,NS,FIXEDN)
      IMPLICIT NONE

      INTEGER MAXNTEMP,MAXNPOINT,MAXNSITE
      PARAMETER (MAXNTEMP=5)
      PARAMETER (MAXNSITE=5)
      PARAMETER (MAXNPOINT=200)

      DOUBLE PRECISION P(MAXNTEMP*2*MAXNSITE),B(MAXNTEMP,MAXNPOINT),B3
      INTEGER IS,I,NS(MAXNTEMP),K,IP,FIXEDN,L1,L2

      CAL = 0.0
      B3 = 0.0
c do the summation from 1 to the number of sites
      DO 10 IS=1,NS(K)
c Find the index to the N (L1) and K (L2)
        IF (FIXEDN.EQ.0) THEN
          L1 = IP + 2*IS - 2
        ELSE
          L1 = 2*IS - 1
        ENDIF
        L2 = IP + 2*IS - 1
c Do the calulation of the equation then add the result to
c the partial summation (CAL), unless of course, this is the
c last site.
        B3 = P(L1)*P(L2)*B(K,I)/(1.0+P(L2)*B(K,I))
        CAL = CAL + B3
  10 CONTINUE
      RETURN
      END

c -------------------------------------------------------------------------
```

```
c
c  This subroutine is used to fit non-linear equations,
c  the subroutine uses a Simplex Routine to solve the
c  the equation.
c
c  The program the number of parameters, NP, the
c  convergence factor, EP, the variables, B, the number
c  of points, N, the maximum number of loops, KX, the
c  measured value, H, initial guesses for parameter, T,
c  and the interval for varying the parameters, D.
c  Set D equal to zero to fix parameter.
c
c  This is a sample of what the function FUNK looks like
c
c     FUNCTION FUNK(H,P,B,N)
c     DIMENSION H(250),P(10),B(10,250)
c     FUNK=0.0
c     DO 10 I=1,N
c     FUNCTION=function you wish to solve parameters for
c     FUNK=FUNK+(H(I)-FUNCTION)**2
c   10 CONTINUE
c     FUNK=SQRT(FUNK/(N-1))
c     RETURN
c     END
c
c  This function is where the function that you wish to
c  solve the parameters for will go in.
c
c  Attach this function to the main part of the program
c  that you write for input and output of your data
c
c ---------------------------------------------------------------------
      SUBROUTINE SIMPLEX(NT,EP,NP,N,KX,T,DDOWN,DUP,H,B,NS,FIXEDN,COUNT,
     *M,BR)
      IMPLICIT NONE

      INTEGER MAXNTEMP,MAXNSITE
      PARAMETER (MAXNTEMP=5)
      PARAMETER (MAXNSITE=5)
      DOUBLE PRECISION RI(MAXNTEMP*2*MAXNSITE),T(MAXNTEMP*2*MAXNSITE)
      DOUBLE PRECISION TT(MAXNTEMP*2*MAXNSITE)
      DOUBLE PRECISION S(MAXNTEMP*2*MAXNSITE,MAXNTEMP*2*MAXNSITE + 1)
      DOUBLE PRECISION H(MAXNTEMP,MAXNSITE),B(MAXNTEMP,MAXNSITE)
      DOUBLE PRECISION DDOWN(MAXNTEMP*2*MAXNSITE)
      DOUBLE PRECISION DUP(MAXNTEMP*2*MAXNSITE)
      DOUBLE PRECISION EP,BR,WR,F,RT,R
      INTEGER NP,N(MAXNTEMP),NS(MAXNTEMP),KX,KI,JW,JB,I,J,NV,NT
      INTEGER FIXEDN, COUNT, M
c Initialize the vertices of the simplex.
      CALL PARMAT(NT,NP,S,T,RI,DDOWN,DUP,B,H,N,NS,FIXEDN)
      NV = NP+1
      IF (RI(1).EQ.0.0) THEN
        GO TO 110
      ENDIF
      KI = 0
c initialize BR to 0, just to make sure it has a value before the
c following conditional statement.
      BR = 0.0
c initialize the Worst vertex (WR), Best vertex (BR), R in the
c variable name is for Response (error response).
c the index for the worst vertex (JW), and the best vertex (JB)
   20 WR = RI(1)
      BR = WR
      JW = 1
      JB = 1
c find the best and worst vertex by the value of the their error
c response.
      DO 30 I = 2,NV
        IF (RI(I).GE.WR) THEN
          WR = RI(I)
```

```
      JW = I
     ENDIF
     IF (RI(I).LT.BR) THEN
      BR = RI(I)
      JB = I
     ENDIF
  30 CONTINUE
     IF (KI.EQ.500) PRINT 131, BR, KI, COUNT-M
     IF (KI.EQ.1000) PRINT 131, BR, KI, COUNT-M
     IF (KI.EQ.2000) PRINT 131, BR, KI, COUNT-M
     IF (KI.EQ.3000) PRINT 131, BR, KI, COUNT-M
     IF (KI.EQ.4000) PRINT 131, BR, KI, COUNT-M
     IF (KI.EQ.5000) PRINT 131, BR, KI, COUNT-M
     IF (KI.EQ.6000) PRINT 131, BR, KI, COUNT-M
     IF (KI.EQ.7000) PRINT 131, BR, KI, COUNT-M
     IF (KI.EQ.8000) PRINT 131, BR, KI, COUNT-M
     IF (KI.EQ.9000) PRINT 131, BR, KI, COUNT-M
     IF (KI.EQ.10000) PRINT 131, BR, KI, COUNT-M
     IF (KI.EQ.15000) PRINT 131, BR, KI, COUNT-M
     IF (KI.EQ.20000) PRINT 131, BR, KI, COUNT-M
     IF (KI.EQ.25000) PRINT 131, BR, KI, COUNT-M
     IF (KI.EQ.30000) PRINT 131, BR, KI, COUNT-M
     IF (KI.EQ.35000) PRINT 131, BR, KI, COUNT-M
     IF (KI.EQ.45000) PRINT 131, BR, KI, COUNT-M
     IF (KI.EQ.50000) PRINT 131, BR, KI, COUNT-M
     IF (KI.EQ.55000) PRINT 131, BR, KI, COUNT-M
     IF (KI.EQ.KX) PRINT 131, BR, KI, COUNT-M
c test to see if we are finished according to max allowed loop
c iterations. KX = max allowed as defined by user, KI, number
c of times this loop has executed.
     IF (KI.GE.KX) THEN
      GO TO 110
     ENDIF
c if the best response is less than the convergence factor, then
c stop. (test for convergence)
     IF (BR.LT.EP) THEN
      PRINT *,'Best Test within acceptable limits.'
      GO TO 110
     ENDIF
c keep track how how many loops are performed.
     KI = KI+1
c Start moving the simplex by first performing REFLECTION. This is
c specified to VERTEX by setting F to 1.0.
     F = 1.0
     CALL VERTEX(NT,S,T,JW,NP,F,H,B,R,N,NS,FIXEDN)
c If the new vertex is worse than the best vertex, go perform a check
c at 40 to see if this new vertex is at least better than the current
c worse vertex.
c Otherwise, we have a really good one, so, let's press our luck and
c search for an even better one. Save the new vertex's error response
c in RT and it's parameter's in TT just in case we have to backtrack
c and accept this new vertex for the simplex.
     IF (R.GT.BR)  GO TO 40
     RT = R
     DO 50 I = 1,NP
      TT(I) = T(I)
  50 CONTINUE
c Since we have a good new vertex from reflection, perform
c EXPANSION on the simplex to see if going further in this direction
c would improve the new vertex's location in the factor space.
     F = 2.0
     CALL VERTEX(NT,S,T,JW,NP,F,H,B,R,N,NS,FIXEDN)
c if the expanded vertex is not better than the reflected one then go
c to 60 in order to restore the reflected vertex as the new vertex for
c the simplex.
c Otherwise, the expanded is good so, go ahead and replace the worse
c vertex of the simplex with the new (expanded) one.
     IF (R.GT.RT) GO TO 60
c This is where the new vertex is placed in the simplex, replacing
c the worst one.
```

```
  90 DO 70 I = 1,NP
     S(I,JW) = T(I)
  70 CONTINUE
c Replace the error response for the worst vertex with the error
c response of the new vertex.
     RI(JW) = R
c Finished adding the new vertex to the simplex so, start the search
c process all over again.
     GO TO 20
c If execution has reached here then the expanded vertex did not
c improve upon the reflected, so, reset the error response and
c the paramter array to the reflected vertex's values and
c go to 90 to store the reflected vertex in the simplex.
  60 R = RT
     DO 80 I = 1,NP
       T(I) = TT(I)
  80 CONTINUE
     GO TO 90
c If the reflected (step 1) vertex is at least better than the worst,
c go ahead to 90 to accept it into the simplex, replacing the worst
c vertex.
  40 IF (R.LE.WR)  GO TO 90
c Otherwise, try CONTRACTION on the simplex.
     F = -0.5
     CALL VERTEX(NT,S,T,JW,NP,F,H,B,R,N,NS,FIXEDN)
c If contraction produced a better vertex, got to 90 and accept it
c into the simplex, replacing the worst vertex.
     IF (R.LE.WR)  GO TO 90
c Otherwise, just shrink the whole simplex.
     DO 100 I = 1,NP
       DO 100 J = 1,NV
         IF (J.NE.JB)  S(I,J) = (S(I,JB)+S(I,J))/2
 100 CONTINUE
c Go to 20 to test for & possibly to continue looking for convergence
     GO TO 20
c Determine if convergence was reached or the maximum number of loops
c allowed was reached and spit out a message accordingly.
  110 IF (KI.GE.KX) WRITE (6,120)
     IF (KI.LT.KX) WRITE (6,130)
c Could be used for another test for convergence...
  110  IF (BR.GT.EP) THEN
         PRINT *,'  Best test improves less than acceptable limits.'
         PRINT 31,BR,EP
   31   FORMAT('   Best test=',E21.15,'   Acceptable limit=',E8.2)
       ENDIF
  120 FORMAT (/5X,'Maximum Number of Loops (KX) Exceeded')
  130 FORMAT (/5X,'Convergence Reached, Best Residual will not improve'
     *' in this count.'/)
  131 FORMAT ('BR = ',E25.17,3X,'Loops = ',I11,2X,'Count = ',I2)
     RETURN
     END

c ---------------------------------------------------------------------
c
c  PARMAT:
c
c  Sets up the parameter matrix
c
c Build the parameter matrix, (a table containing all the vertices
c of the simplex). This is done by adding dup or subtracting ddown
c from t (named p in the top part of this program) depending on
c if the outer loop's counter (i) is >= to the inner loops' counter
c (j).
c
c example :
c if the data file looks like this:
c
c #t    ddown   dup
c 3     2       2
c 6     2       2
```

```
c 4     2     2
c 5     2     2
c
c The parameter matrix (array S) will look like this:
c
c       Vertex (j)
c       1 2 3 4 5
c (i) +----------
c  P 1| 5 1 1 1 1
c  a 2| 8 8 4 4 4
c  r 3| 6 6 6 2 2
c  m 4| 7 7 7 7 3
c
c ---------------------------------------------------------------------
      SUBROUTINE PARMAT(NT,NP,S,T,RI,DDOWN,DUP,B,H,N,NS,FIXEDN)
      IMPLICIT NONE

      INTEGER MAXNTEMP,MAXNPOINT,MAXNSITE
      PARAMETER (MAXNTEMP=5)
      PARAMETER (MAXNSITE=5)
      PARAMETER (MAXNPOINT=200)

      DOUBLE PRECISION T(MAXNTEMP*2*MAXNSITE)
      DOUBLE PRECISION S(MAXNTEMP*2*MAXNSITE,MAXNTEMP*2*MAXNSITE+1)
      DOUBLE PRECISION RI(MAXNTEMP*2*MAXNSITE)
      DOUBLE PRECISION DDOWN(MAXNTEMP*2*MAXNSITE)
      DOUBLE PRECISION DUP(MAXNTEMP*2*MAXNSITE),B(MAXNTEMP,MAXNPOINT)
      DOUBLE PRECISION H(MAXNTEMP,MAXNPOINT)
      INTEGER NV,NP,I,J,N(MAXNTEMP),NS(MAXNTEMP),NT,FIXEDN
      DOUBLE PRECISION FUNK

c NV = Number of vertices of the simplex
      NV=NP+1
c Build the parameter matrix
      DO 30 I=1,NP
        DO 30 J=1,NV
          IF (I.GE.J) THEN
            S(I,J) = T(I)+DUP(I)
          ELSE
            S(I,J) = T(I)-DDOWN(I)
c if the parameter is negative then just take 10% of the T(i)
c (the P column data point).  This does assume that T(i) is
c non-negative.
            IF (S(I,J) .LT. 0.0) THEN
              S(I,J) = T(I) * 0.1
            ENDIF
          ENDIF
   30 CONTINUE
c build the array of error responses for all vertices of the simplex
c for later use.
      DO 40 I=1,NV
        DO 50 J=1,NP
          T(J)=S(J,I)
   50   CONTINUE
        RI(I) = FUNK(H,T,B,N,NT,NS,FIXEDN)
   40 CONTINUE
      RETURN
      END

c ---------------------------------------------------------------------
c
c   VERTEX: Find a new vertex
c
c   Finds the new vertex of the simplex. It will do either
c   reflection, expansion, of contraction based on the
c   coefficient F.
c
c   C is the centroid of the simplex face containing all
c   vertices but the worst.
c
```

```
c  T is the array that holds the paramters for the new
c  vertex.
c
c  R contains the error response for the new vertex.
c
c -------------------------------------------------------------------
      SUBROUTINE VERTEX(NT,S,T,JW,NP,F,H,B,R,N,NS,FIXEDN)
      IMPLICIT NONE

      INTEGER MAXNTEMP,MAXNPOINT,MAXNSITE
      PARAMETER (MAXNTEMP=5)
      PARAMETER (MAXNSITE=5)
      PARAMETER (MAXNPOINT=200)

      DOUBLE PRECISION T(MAXNTEMP*2*MAXNSITE)
      DOUBLE PRECISION S(MAXNTEMP*2*MAXNSITE,MAXNTEMP*2*MAXNSITE+1)
      DOUBLE PRECISION C(MAXNTEMP*2*MAXNSITE),B(MAXNTEMP,MAXNPOINT)
      DOUBLE PRECISION H(MAXNTEMP,MAXNPOINT)
      DOUBLE PRECISION F,R,SU
      INTEGER NP,N(MAXNTEMP),NS(MAXNTEMP),NV,I,J,JW,NT,FIXEDN
      DOUBLE PRECISION FUNK

c Added SAVE command because, this code assumes the compiler will
c save the values of the variables from subroutine call to subroutine
c call automatically. Specifically, the centroid variable.
c So, if this code is ported to a compiler that does not do so, the
c SAVE command will force it to for this subroutine.  -AR
      SAVE
      NV = NP + 1
c For each paramter in the vertex, do the following:
c 1. Reset the parameter sum (SU) to 0,
c 2. If the coefficient is 1 then this is a reflection which is
c    only done at the beginning of the search for a new vertex.
c    So get the centroid, otherwise, skip the computation as we
c    already have the centroid from the reflection we did earlier.
c 3. Assign the new parameter to the vertex's array (T).
c    Depending on the value of the coefficient F, the formula
c    T(I) = C(I) * (1.0 + F) - F * S(I,JW) will provide either
c    reflection  : T(I) = C(I) + ( C(I) - S(I,J) )
c    expansion   : T(I) = C(I) + 2( C(I) - S(I,J) )
c    contraction : T(I) = C(I) - .5( C(I) - S(I,J) )
c    (in Deming and Morgan's representation of the formulas)
c 4. Perform the test on the new parameter to ensure it is in
c    positive factor space.
c 5. Lastly, get the error response for the new vertex (R)
      DO 10 I = 1,NP
        SU = 0.0
        IF (F.NE.1.0) GO TO 30
        DO 20 J = 1,NV
          IF (J.NE.JW) SU = SU + S(I,J)
   20   CONTINUE
        C(I) = SU / NP
   30   T(I) = C(I) * (1.0 + F) - F * S(I,JW)
c If the parameter is out of bounds, give it a very undesirable
c number in order to ensure the vertex will be forced back inside.
c NELDER&MEADE rule 5, the "magic" number
        IF ( T(I) .LT. 0.0 ) THEN
          T(I) = 1.0D+1
        ENDIF
   10 CONTINUE
c get the error response of the new vertex
      R = FUNK(H,T,B,N,NT,NS,FIXEDN)
      RETURN
      END

c -------------------------------------------------------------------
c
c  GETLINE: gets a line from the data file.
c
c -------------------------------------------------------------------
```

```
      SUBROUTINE GETLINE(U)
      IMPLICIT NONE

      INTEGER      U
      CHARACTER*78 BUF

   10 READ (U,'(A)') BUF
c  Read in the file a line at a time until a non-comment line is read
c  in.
      IF (BUF(1:1).EQ.'#') THEN
        PRINT *, BUF
        GOTO 10
      ENDIF
c     At this point we have a potential line with data so
c     backup the file pointer to the beginning of the line
c     to allow the caller to parse it with the READ command.
      BACKSPACE(U)
      RETURN
      END
```

Example of standard input file for 421.exe

```
# Methane adsorption on HZSM-5
# ep(convergence) kx(loops) Fixedn(0/1)
    0.1000E-11      8000   1
# Upordown(0,1,2,3,4,5,10,15) Count(ext_loops)
# Calc_Dim(0,1) Weight(0,1)
 2   1   1   0
# AREA(A^2), MVL(mL/mole)
 16.261    29.740
#_number_of_temperature_sets
  3
#_No._of Data_Points, No._of grams_ of_solid
 35  1.000
#_Data_for temp_set  1    Temp(K):  231.15
#  Eq_press      Exp_Ads
0.003997760  0.64856800E-04
0.006669870  0.10701800E-03
0.009119470  0.14371800E-03
0.011841300  0.18300200E-03
0.014563200  0.22043400E-03
0.017217000  0.25596900E-03
0.020006800  0.29113300E-03
0.023749500  0.33662900E-03
0.027968300  0.38578600E-03
0.033207900  0.44175500E-03
0.039672200  0.50707600E-03
0.060494300  0.68789100E-03
0.072266300  0.77410500E-03
0.085127000  0.85702200E-03
0.098600100  0.93479100E-03
0.112005000  0.10034500E-02
0.117993000  0.10318500E-02
0.131671000  0.10919600E-02
0.145008000  0.11447400E-02
0.151132000  0.11669700E-02
0.158004000  0.11907600E-02
0.197675000  0.13161400E-02
0.267150000  0.14827300E-02
0.295661000  0.15365200E-02
0.327779000  0.15906900E-02
0.395553000  0.16873500E-02
0.460809000  0.17623800E-02
0.526814000  0.18260300E-02
0.591866000  0.18791400E-02
0.657734000  0.19257600E-02
0.723671000  0.19666500E-02
0.789472000  0.20025300E-02
0.855204000  0.20349000E-02
0.921141000  0.20640000E-02
1.000140000  0.20949400E-02
# number of sites above with: n1,K1, n2,K2...; Temp(K)
 2 231.15
0.173E-02
0.901E+01
0.868E-03
0.157E+01
#_No._of Data_Points, No._of grams_ of_solid
 31  1.000
#_Data_for temp_set  2    Temp(K):  257.15
#  Eq_conc      Exp_Ads
0.014341400  0.65749100E-04
0.017675700  0.80726300E-04
0.019785100  0.89586900E-04
0.023595700  0.10644700E-03
0.028086700  0.12574700E-03
0.033054100  0.14615000E-03
0.039722500  0.17392700E-03
0.060204500  0.25312300E-03
0.072044500  0.29622100E-03
0.085177400  0.34159900E-03
0.098718600  0.38666000E-03
0.112056000  0.42888400E-03
0.118316000  0.44813500E-03
0.131789000  0.48794500E-03
0.144990000  0.52473500E-03
0.151250000  0.54167900E-03
0.157987000  0.55984200E-03
0.197045000  0.65679000E-03
0.265023000  0.80113800E-03
0.295372000  0.85805300E-03
0.328646000  0.91513300E-03
0.395331000  0.10166000E-02
0.460860000  0.11030600E-02
0.526048000  0.11781800E-02
0.591712000  0.12455300E-02
0.657921000  0.13056900E-02
0.723517000  0.13592400E-02
0.789386000  0.14079700E-02
0.855323000  0.14521000E-02
0.920987000  0.14924600E-02
1.000060000  0.15369700E-02
# number of sites above with: n1,K1, n2,K2...; Temp(K)
 2 257.15
0.173E-02
0.252E+01
0.868E-03
0.523E+00
#_No._of Data_Points, No._of grams_ of_solid
 26  1.000
#_Data_for temp_set  3    Temp(K):  273.15
#  Eq_conc      Exp_Ads
0.033908700  0.83773500E-04
0.039148300  0.96529000E-04
0.059017800  0.14413800E-03
0.072082500  0.17465000E-03
0.085283400  0.20442600E-03
0.099028800  0.23414800E-03
0.111005000  0.25939600E-03
0.118626000  0.27519400E-03
0.130466000  0.29931700E-03
0.145028000  0.32813000E-03
0.151424000  0.34060400E-03
0.158093000  0.35326600E-03
0.196471000  0.42317300E-03
0.262611000  0.53153800E-03
0.295274000  0.58059700E-03
0.328956000  0.62830400E-03
0.393668000  0.71212600E-03
0.460762000  0.79078700E-03
0.526494000  0.86008700E-03
0.591954000  0.92370400E-03
0.658095000  0.98230100E-03
0.723624000  0.10357000E-02
0.789628000  0.10849000E-02
0.855156000  0.11304800E-02
0.921229000  0.11730600E-02
1.000090000  0.12201300E-02
# number of sites above with: n1,K1, n2,K2...; Temp(K)
 2 273.15
0.174E-02
0.192E+01
0.868E-03
0.607E+00
```

Example of standard input file for 421.exe--explained

```
# Methane adsorption on HZSM-5
# ep(convergence) kx(loops) Fixedn(0/1)
    0.1000E-11        8000   1
# Upordown(0,1,2,3,4,5,10,15) Count(ext_loops)
# Calc_Dim(0,1) Weight(0,1)
 2   1   1   0
# AREA(A^2), MVL(mL/mole)
 16.261   29.740
# _number_of_temperature_sets
 3
# No. of Data_Points, No._of grams_ of_solid
 35  1.000
# _Data_for temp_set_1    Temp(K):  231.15
#  Eq_press       Exp_Ads
0.003997760  0.64856800E-04
0.006660870  0.10701800E-03
0.009119470  0.14371800E-03
0.011841300  0.18300200E-03
0.014563200  0.22043400E-03
0.017217000  0.25596900E-03
0.020006800  0.29115300E-03
0.023749500  0.33662900E-03
0.027968300  0.38538600E-03
0.033207900  0.44175500E-03
0.039672200  0.50707600E-03
0.060494300  0.68789100E-03
0.072266300  0.77410500E-03
0.085127000  0.85702200E-03
0.098600100  0.93479100E-03
0.112005000  0.10034500E-02
0.117993000  0.10318500E-02
0.131671000  0.10919600E-02
0.145008000  0.11447400E-02
0.151132000  0.11669700E-02
0.158004000  0.11907600E-02
0.197675000  0.13161400E-02
0.267150000  0.14827300E-02
0.295661000  0.15365200E-02
0.327779000  0.15906900E-02
0.395553000  0.16873500E-02
0.460809000  0.17623800E-02
0.526814000  0.18260300E-02
0.591866000  0.18791400E-02
0.657734000  0.19257600E-02
0.723671000  0.19666500E-02
0.789472000  0.20025300E-02
0.855204000  0.20349000E-02
0.921141000  0.20640000E-02
1.000140000  0.20949400E-02
# number of sites above with: n1,K1, n2,K2...;
Temp(K)
 2 231.15
0.173E-02
0.901E+01
0.868E-03
0.157E+01
```

Convergence factor (set very low for best convergence)
Number of internal loops
Fixed n_i values for each temperature?

Variance of initial guesses
Number of external loops
Calculate surface areas and pore volumes from n_i values?
Weighted linear regressions for van't Hoff plots?

Values for molecular area and *MVL* (calculated molar volume)

Total number of temperature sets

Number of data points for this temperature set
Grams of solid (experimental mols ads usually normalized to 1 gram)

Experimental mols ads per gram

Pressure (usually in atm)

Data for first temperature set

Number of processes
Temperature of experiment (in K)

Initial guesses for solid pore capacities (in mols)
Initial guesses for temperature dependent equilibrium constants

Example of standard output file of 421.exe

```
BR =  0.1180499051183799E-05
Count_is:  1
Data_for temp_set  1    Temp(K)  231.15

#   Eq_press        Exp_Ads          Calc_Ads          Err              Per
1   0.0039977760    0.6485680E-04    0.6530902E-04     -4.5222012E-06   0.6973
2   0.0066698670    0.1070180E-03    0.1067177E-03      3.0021808E-06   0.2806
3   0.0091194470    0.1437180E-03    0.1432119E-03      5.0605078E-06   0.3521
4   0.0111643300    0.1783020E-03    0.1822163E-03     -3.9114263E-06   0.4293
5   0.0145635200    0.2204540E-03    0.2196914E-03      7.6251558E-06   0.3368
6   0.0172170000    0.2559690E-03    0.2548434E-03      1.1125122E-05   0.4396
7   0.0200068000    0.2911530E-03    0.2904103E-03      7.4266957E-06   0.2551
8   0.0237037000    0.3662950E-03    0.3630359E-03      3.2659178E-05   0.8919
9   0.0279683300    0.3857860E-03    0.3848061E-03      9.7981975E-06   0.2540
10  0.0330207900    0.4417550E-03    0.4417948E-03     -3.9885514E-07   0.0090
11  0.0390772000    0.5070760E-03    0.5071853E-03     -1.0918449E-06   0.0215
12  0.0460493000    0.6878910E-03    0.6875669E-03      0.3240471E-06   0.0471
13  0.0772266300    0.7741050E-03    0.7732818E-03      0.8231259E-06   0.1063
14  0.0851270000    0.8570220E-03    0.8566479E-03      0.5401104E-06   0.0646
15  0.0986001000    0.9347910E-03    0.9339365E-03      0.8544348E-06   0.0914
16  0.1120050000    0.1003450E-02    0.1002853E-02      0.5961104E-06   0.0594
17  0.1179930000    0.1031850E-02    0.1031368E-02      0.4813976E-06   0.0467
18  0.1316710000    0.1091960E-02    0.1091923E-02      0.3635492E-07   0.0033
19  0.1450080000    0.1144740E-02    0.1145585E-02     -8.4533932E-06   0.0738
20  0.1511320000    0.1669770E-02    0.1669576E-02      0.1945765E-06   0.0117
21  0.1580040000    0.1907660E-02    0.1934816E-02     -2.7216207E-05   0.2286
22  0.1976750000    0.1316140E-02    0.1318297E-02     -2.1577307E-05   0.1639
23  0.2671500000    0.1481730E-02    0.1482195E-02     -2.6586109E-06   0.0179
24  0.2956610000    0.1536520E-02    0.1537034E-02     -5.1480603E-06   0.0335
25  0.3277790000    0.1590690E-02    0.1591606E-02     -3.7045399E-06   0.0233
26  0.3955590000    0.1687350E-02    0.1686789E-02      0.5610402E-06   0.0332
27  0.4608090000    0.1762380E-02    0.1761691E-02      0.6886013E-06   0.0391
28  0.5268140000    0.1826030E-02    0.1825061E-02      0.9688354E-06   0.0531
29  0.5918660000    0.1879140E-02    0.1878345E-02      0.7945315E-06   0.0423
30  0.6577340000    0.1925760E-02    0.1925106E-02      0.6534542E-06   0.0339
31  0.7236710000    0.1966650E-02    0.1966152E-02      0.4974859E-06   0.0253
32  0.7894720000    0.2002530E-02    0.2002450E-02      0.8000009E-07   0.0040
33  0.8552040000    0.2034990E-02    0.2034869E-02      0.1203489E-07   0.0015
34  0.9211410000    0.2064000E-02    0.2064160E-02     -1.6093484E-06   0.0078
35  1.0001400000    0.2094940E-02    0.2095678E-02     -7.3786451E-06   0.0353

The_sum_of_squares_for temp_set 1 is 0.2698086E-10

K1_is   0.8538906458E+01  +/-     0.1647Z-01
K2_is   0.1079616778Z+01  +/-     0.3828E-01

Grams of_Solid for_equilibrium data_is 1.000

Data_for temp_set  2    Temp(K)  257.15

#   Eq_press        Exp_Ads          Calc_Ads          Err              Per
1   0.0114341400    0.6576910E-04    0.6669023Z9E-04   -9.4113930E-06   1.4314
2   0.0176575700    0.8072630E-04    0.8159662Z9E-04   -8.7032895E-06   1.0781
3   0.0197851000    0.8958690E-04    0.9091555Z-04     -1.3286518E-05   1.4831
4   0.0235977000    0.1064470E-03    0.1075357E-03     -1.0887788E-05   1.0228
5   0.0280867000    0.1254770E-03    0.1267776E-03     -1.0306565E-05   0.8196
6   0.0330541000    0.1461500E-03    0.1476375E-03     -1.4875448E-05   1.0178
7   0.0397225500    0.1779270E-03    0.1749602E-03      1.0391968E-05   0.5975
8   0.0602045000    0.2531230E-03    0.2543961E-03     -1.2731592E-05   0.5030
9   0.0720445000    0.2962210E-03    0.2974539Z-03     -1.2329175E-05   0.4162
10  0.0885177000    0.3631300E-03    0.3629836Z-03      1.3840825E-06   0.0381
11  0.0987186600    0.3866600E-03    0.3876552E-03     -9.9524326E-06   0.2574
12  0.1210560000    0.4288840E-03    0.4295636Z-03     -6.6836092E-06   0.1591
13  0.1383160000    0.4481350E-03    0.4485668Z-03     -4.3182360E-06   0.0964
14  0.1317890000    0.4879450E-03    0.4880931E-03     -1.4813948E-06   0.0304
15  0.1449900000    0.5247350E-03    0.5251156Z-03     -3.8062748E-06   0.0725
16  0.1512500000    0.5416770E-03    0.5421154Z-03     -4.3644213E-06   0.0806
17  0.1579870000    0.5598420E-03    0.5600286Z-03     -1.8662515E-06   0.0333
18  0.1970450000    0.6567900E-03    0.6567297Z-03      0.6026534E-07   0.0092
19  0.2650230000    0.8011380E-03    0.8007186Z-03      0.4193648Z5E-06   0.0523
20  0.2953720000    0.8580530E-03    0.8569196Z-03      0.1133387E-05   0.1321
21  0.3286440000    0.9151330E-03    0.9137930Z-03      0.1339059Z5E-05   0.1464
22  0.3953310000    0.1016600E-02    0.1015173Z-02      0.1426670Z5E-05   0.1403
23  0.4608600000    0.1030600E-02    0.1031420Z-02     -0.1639538Z5E-05   0.1486
24  0.5260480000    0.1178180E-02    0.1176728E-02      0.1451179Z5E-05   0.1232
25  0.5917120000    0.1245300E-02    0.1243992E-02      0.1537387Z5E-05   0.1234
26  0.6579210000    0.1305690E-02    0.1304615E-02      0.1075541Z5E-05   0.0824
27  0.7235170000    0.1359240E-02    0.1358720Z7E-02    0.5192633E-06   0.0382
28  0.7893860000    0.1407970E-02    0.1408139Z-02     -4.9873798E-07   0.0031
29  0.8553230000    0.1452100E-02    0.1453040Z-02     -9.4007861E-06   0.0647
30  0.9209870000    0.1492460E-02    0.1491480Z-02      1.7159893E-05   0.1152
31  1.0000600000    0.1536970E-02    0.1539495E-02     -2.5249435E-05   0.1646

The_sum_of_squares_for temp_set 2 is 0.4016292Z9E-10

K1_is   0.2405520949Z+01  +/-     0.1309Z-01
K2_is   0.3661987728E+00  +/-     0.3041Z-01

Grams of_Solid for_equilibrium data_is 1.000

Data_for temp_set  3    Temp(K)  273 15

#   Eq_press        Exp_Ada          Calc_Ads          Err              Per
1   0.0339087000    0.8377350E-04    0.8691384Z2E-04   -3.1403415Z-05   3.7486
2   0.0391483000    0.9652900E-04    0.9972234Z1E-04   -3.1934122Z-05   3.3082
3   0.0590178000    0.1441380E-03    0.1468910Z1E-03   -2.7530118E-05   1.9100
4   0.0720825000    0.1746500E-03    0.1767502E-03     -2.1002350E-05   1.2026
5   0.0852834000    0.2044260E-03    0.2060403E-03     -1.6143563E-05   0.7897
6   0.0990288800    0.2341480E-03    0.2356413Z0E-03   -1.4932977E-05   0.6378
7   0.1110050000    0.2593960E-03    0.2607190E-03     -1.3230639E-05   0.5101
8   0.1180260000    0.2751940E-03    0.2763444E1E-03   -1.1504094E-05   0.4180
9   0.1304660000    0.2993170E-03    0.3001245E0-03    -1.8075044E-05   0.2698
10  0.1450280800    0.3281300E-03    0.3285776E-03     -4.4456241E-06   0.1358
11  0.1514240000    0.3406040E-03    0.3408044E-03     -2.0043888E-06   0.0588
12  0.1580930000    0.3532660E-03    0.3533864E1-03    -1.2040745E-06   0.0341
13  0.1964710000    0.4231730E-03    0.4222620E-03     0.5526362Z2E-06   0.1306
14  0.2626110000    0.5313580E-03    0.5306170E-03     0.9209436Z5E-06   0.1733
15  0.2952740000    0.5805970E-03    0.5793431E-03     0.1253827Z8E-05   0.2160
16  0.3289560000    0.6283040E-03    0.6267606Z5E-03   0.1523779Z5E-05   0.2425
17  0.3496680800    0.7122260E-03    0.7108096E-03     0.1316542Z5E-05   0.1849
18  0.4607620000    0.7907870E-03    0.7893643Z0E-03   0.1420695Z8E-05   0.1797
19  0.5264940000    0.8600870E-03    0.8591408Z5E-03   0.9461533Z7E-06   0.1100
20  0.5919540000    0.9237040E-03    0.9225666Z8E-03   0.1137374Z7E-05   0.1231
21  0.6580950000    0.9823010E-03    0.9813397E1-03    0.9612892Z4E-06   0.0979
22  0.7236240000    0.1035700E-02    0.1034979Z8E-02   0.7201943Z5E-06   0.0695
23  0.7896280000    0.1084900E-02    0.1084991Z8E-02   -9.0951139E-07   0.0084
24  0.8551560000    0.1130480E-02    0.1131029Z0E-02   -5.4898754E-06   0.0486
25  0.9212290000    0.1173060E-02    0.1174304E-02     -1.2447802E-05   0.1061
26  1.0009900000    0.1220130E-02    0.1222256E-02     -2.1267201E-05   0.1743

The_sum_of_squares_for temp_set 3 is 0.5967181Z0E-10

K1_is   0.1323228211E+01  +/-     0.1449Z1-01
K2_is   0.2382465128E+00  +/-     0.3360Z7-01

Grams of_Solid for_equilibrium data_is 1.000

n1_is   0.1873501206Z-06  +/-     0.1344E-04 in_mole/g
n2_is   0.8061476844E-03  +/-     0.7012E-04 in_mole/g

The_total n_is 0.2679677805E-02 +/-  0.8845E-04 in_mole/g

The_total sum_of_sq_is  0.1268155989E-09

The_AREA_per_mole_is 16.261 The_MVL_is 29.740

n1_area_is      183.494  +/-     1.3169 in_meters**2/g
n2_area_is      78 954  +/-     7.3467 in_meters**2/g
Total_area_is   262.448  +/-     8.6636 in_meters**2/g

n1_pore_vol_is  0.0557188  +/-   0.0003999 in_mL/g
n2_pore_vol_is  0.0239748  +/-   0.0022309 in_mL/g
Total_pore_vol_is 0.0796936  +/-  0.0026307 in_mL/g

Temp    Temp_# K        K               SD(K)
231.15  1   1   8 538906406     0.0164717S8
231 15  1   2   1 079616778     0.0382875S5
257.15  2   1   2 405529949     0.0130976S4
257.15  2   2   0 366198772     0.0304153S9
273.15  3   1   1 323228211     0.0144908T0
273 15  3   2   0 238246513     0.0336071Z9

Temp    Temp_# K        1/Temp          ln(K)       Weight(K)
231.15  1   1   0 00432620      2.1446329   518.3967952
231 15  1   2   0 00432620      0.0766061   28 1975693
257 15  2   1   0 00388878      0.8777665   183.6631035
257.15  2   2   0 00388878      -1.0045790  12.0400165
273 15  3   1   0 00366099      0.2800744   91.3146132
273.15  3   2   0 00366099      -1.4344494  7.0891660

These_are_the unweighted_regression_parameters
-dH1:   5.9543 +/-  0.13621 kCal/mole  -dS1:  19 9587 +/-  0.54052 Cal/(mol*K)
-dH2:   4.5668 +/-  0.29236 kCal/mole  -dS2:  19 6431 +/-  1.16015 Cal/(mol*K)
R^2(1)= 0.99941
R^2(2)= 0.99592
```

Example of standard output file of 421.exe--explained

BR = 0.11804990511837590E-05
Count_is: 1
Data_for temp_set 1 Temp(K): 231.15

#	Eq_press	Exp_Ads	Calc_Ads	Err	Per
1	0.003997760	0.54435800E-03	0.65209894E-04	0.6973
2	0.006669870	0.14443800E-03	0.48771771E-03	0.2939380E-04	0.6806
3	0.008319470	0.14171800E-03	0.14211799E-03	0.06007783E-06	0.0421
4	0.011641300	0.18302000E-03	0.18211635E-03	0.83653590E-06	0.2293
5	0.014563200	0.22843400E-03	0.22669148E-03	0.74251550E-06	0.3368
6	0.017217000	0.25296900E-03	0.25184388E-03	0.11251226E-05	0.4396
7	0.020496800	0.28153000E-03	0.28134033E-03	0.18426957E-06	0.5551
8	0.022749500	0.33426900E-03	0.33293591E-03	0.39309307E-06	0.7162
9	0.025968300	0.38728600E-03	0.38486618E-03	0.97981975E-06	0.2540
10	0.031207900	0.44656500E-03	0.44798489E-03	0.19819514E-07	0.0309
11	0.036672200	0.50707600E-03	0.50718518E-03	0.10918449E-06	0.0215
12	0.040459300	0.68389100E-03	0.67556685E-03	0.82404711E-05	0.8471
13	0.044	0.85	0.82	0.32315299E-04	0.3926
14	0.047	0.85	0.85	0.55401104E-05	0.0650
15	0.051	0.93	0.93	0.45443488E-06	0.0049
16	0.054	0.10	0.10	0.89611004E-04	0.8961
17	0.117993000	0.10118500E-02	0.10313686E-02	0.84819676E-06	0.0467
18	0.131671000	0.10919600E-02	0.10919236E-02	0.36354920E-07	0.0033
19	0.145908300	0.11585800E-02	0.11579717E-02	0.60858E-06	0.0738
20	0.151132000	0.12	0.12	0.86576E-02	0.1446
21	0.158004900	0.12	0.12	0.93481E-02	0.2286
22	0.197917000	0.14	0.14	0.29717E-02	0.2039
23	0.267150000	0.14827300E-02	0.14829959E-02	-0.26586029E-06	0.0179
24	0.295661000	0.15365200E-02	0.15370348E-02	-0.51480603E-06	0.0335
25	0.327710000	0.15906900E-02	0.15910605E-02	-0.37045599E-06	0.0233
26	0.395553000				0.0332
27	0.460809000				0.0391
28	0.528618000				0.0531
29	0.591866000	0.18791800E-02	0.18783455E-02	0.79453155E-06	0.0423
30	0.657734000	0.19257600E-02	0.19251006E-02	0.65345427E-06	0.0339
31	0.723671000	0.19665200E-02	0.19661525E-02	0.49748356E-06	0.0253
32	0.789472000	0.20025300E-02	0.20024500E-02	0.80000099E-07	0.0040
33	0.855204000	0.20349000E-02	0.20348697E-02	0.30343832E-07	0.0015
34	0.921141000	0.20640000E-02	0.20641609E-02	-0.16093484E-06	0.0078
35	1.000140000	0.20949400E-02	0.20956788E-02	-0.73884651E-06	0.0353

The_sum_of squares_for temp_set 1 is 0.26980860E-10

K1_is	0.85389064058E+01	+/-	0.16472E-01
K2_is	0.10796167782E+01	+/-	0.38288E-01

Grams of_Solid for_equilibrium data_is 1.000

Data_for temp_set 2 Temp(K): 257.15

#	Eq_press	Exp_Ads	Calc_Ads	Err	Per
1	0.014341400	0.65749100E-04	0.66690239E-04	-0.94113930E-06	1.4314
2	0.017675700	0.80726300E-04	0.81596629E-04	-0.87032895E-06	1.0782
3	0.019785100	0.89586900E-04	0.90915552E-04	-0.13286518E-05	1.4831
4	0.023595700	0.10664700E-03	0.10753576E-03	-0.10887588E-05	1.0228
5	0.028086700	0.12574700E-03	0.12677166E-03	-0.10265466E-05	0.8196
6	0.0			-0.12044848E-05	1.0178
7	0.0	Data for second temperature set		-0.36868E-05	0.5975
8	0.0			-0.[illegible]2E-05	0.5030
9	0.072044500	0.29622100E-03	0.29745392E-03	-0.12329125E-05	0.4162
10	0.085177400	0.34159900E-03	0.34298381E-03	-0.13848472E-05	0.4054
11	0.098715600	0.38726300E-03	0.38875257E-03	-0.14895744E-05	0.3574
12	0.112056600	0.42888400E-03	0.42956636E-03	-0.6823609[illegible]E-06	0.1591
13	0.118316000	0.44813500E-03	0.44856681E-03	-0.43183260E-06	0.0964
14	0.131789000	0.48574500E-03	0.48609819E-03	-0.35319384E-06	0.0727
15	0.144990000	0.52473500E-03	0.52511563E-03	-0.38062748E-06	0.0725
16	0.151250000	0.54167900E-03	0.54211544E-03	-0.43644213E-06	0.0806
17	0.157987000	0.55964200E-03	0.56002884E-03	-0.38625115E-06	0.0333
18	0.197045000	0.65679000E-03	0.65672815E-03	0.60265345E-07	0.0092
19	0.265023000	0.80113800E-03	0.80072665E-03	0.41936826E-06	0.0523
20	0.295372000	0.85905300E-03	0.85919862E-03	-0.14533787E-06	0.0121
21	0.328646000	0.91513300E-03	0.91379309E-03	0.13390959E-05	0.1464
22	0.395331000	0.10166600E-02	0.10151735E-02	0.14264706E-05	0.1403
23	0.460806000	0.11030600E-02	0.11014205E-02	0.16393582E-05	0.1486
24	0.526048000	0.11781800E-02	0.11767288E-02	0.14451796E-05	0.1232
25	0.591712000	0.12455300E-02	0.12439926E-02	0.15373873E-05	0.1234
26	0.657921000	0.13056200E-02	0.13040145E-02	0.10755341E-05	0.0824
27	0.723517000	0.13592800E-02	0.13587207E-02	0.51926333E-06	0.0382
28	0.789386000	0.14079700E-02	0.14080139E-02	-0.43873798E-07	0.0031
29	0.855323000	0.14521100E-02	0.14530401E-02	-0.94007861E-06	0.0647
30	0.920987000	0.14924600E-02	0.14941800E-02	-0.17196893E-05	0.1152
31	1.000060000	0.15369700E-02	0.15394895E-02	-0.25294935E-05	0.1646

The_sum_of squares_for temp_set 2 is 0.40162929E-10

K1_is	0.24005209492E+01	+/-	0.13097E-01
K2_is	0.36619877228E+00	+/-	0.30415E-01

Grams of_Solid for_equilibrium data_is 1.000

Data_for temp_set 3 Temp(K): 273.15

#	Eq_press	Exp_Ads	Calc_Ads	Err	Per
1	0.033908700	0.83773500E-04	0.86913842E-04	-0.31403415E-05	3.7486
2	0.039148300	0.96529000E-04	0.99722341E-04	-0.31933412E-05	3.3082
3	0.059017900	0.14413800E-03	0.14689101E-03	-0.27530118E-05	1.9100
4	0.072082500	0.17465000E-03	0.17675032E-03	-0.21032508E-05	1.2026
5	0.085283400	0.20442600E-03	0.20604036E-03	-0.16143563E-05	0.7897
6	0.099028800	0.23414800E-03	0.23564130E-03	-0.14932977E-05	0.6378
7	0.111005000	0.25939600E-03	0.26071906E-03	-0.13230639E-05	0.5101
8	0.118626000	0.27519400E-03	0.27634641E-03	-0.11540944E-05	0.4180
9	0.130466000				0.2698
10	0.145028000	Data for third temperature set			0.1358
11	0.151424000				0.0588
12	0.158093000	0.35326600E-03	0.35338641E-03	-0.12040745E-06	0.0341
13	0.196471000	0.42317500E-03	0.42362036E-03	-0.44526036E-06	0.1306
14	0.262611000	0.53153800E-03	0.53061705E-03	0.92094505E-06	0.1733
15	0.295274000	0.58059700E-03	0.57934371E-03	0.12538278E-05	0.2160
16	0.328956000	0.62830400E-03	0.62678062E-03	0.15233759E-05	0.2425
17	0.393668000	0.71212600E-03	0.71080946E-03	0.13165425E-05	0.1849
18	0.460762000	0.79078700E-03	0.78936630E-03	0.14206595E-05	0.1797
19	0.526494000	0.86908700E-03	0.85914385E-03	0.98615337E-06	0.1100
20	0.591954000	0.92370400E-03	0.92256663E-03	0.11373747E-05	0.1231
21	0.658095000	0.98230100E-03	0.98133971E-03	0.96128924E-06	0.0979
22	0.723624000	0.10357000E-02	0.10349798E-02	0.72019635E-06	0.0695
23	0.789628000	0.10849900E-02	0.10845951E-02	0.59095139E-07	0.0054
24	0.855156000	0.11304800E-02	0.11312096E-02	-0.54898754E-06	0.0486
25	0.921229000	0.11730400E-02	0.11743048E-02	-0.12647802E-05	0.1061
26	1.000090000	0.12201300E-02	0.12222567E-02	-0.21267201E-05	0.1743

The_sum_of squares_for temp_set 3 is 0.59671810E-10

K1_is	0.13232282111E+01	+/-	0.14691E-01
K2_is	0.23824651284E+00	+/-	0.33607E-01

Grams of_Solid for_equilibrium data_is 1.000

n1_is	0.18735301206E-02	+/-	0.13446E-04 in_mole
n2_is	0.80614763444E-03	+/-	0.75011594 in_mole/g

The_total n_is 0.2679677805E-02 +/- 0.38458E-04 in_mole/g

The_total sum_of_sq is_ 0.12681559989E-09

The_AREA_per_mole_is 16.261 The_MVL_is 29.740

n1_area_is	183.494	+/-	1.3169 in_meters**2/g
n2_area_is	78.954	+/-	7.3467 in_meters**2/g
Total_area_is	262.448	+/-	8.6636 in_meters**2/g

n1_pore_vol_is	0.0557188	+/-	0.0003999 in_ml/g
n2_pore_vol_is	0.0239748	+/-	0.0022309 in_ml/g
Total_pore_vol_is	0.0796936	+/-	0.0026307 in_ml/g

Temp:	Temp_#	K	K	SD(K)
231.15	1	1	8.538906406	0.(
231.15	1	2	1.079616778	0.(
257.15	2	1	2.405520949	0.(
257.15	2	2	0.366198772	0.(
273.15	3	1	1.323228211	0.(
273.15	3	2	0.238246513	0.(

Temp:	Temp_#	K	1/Temp	ln(K)	Weight(K)
231.15	1	1	0.00432620	2.1446329	518.3967952
231.15	1	2	0.00432620	0.0766061	28.1973693
257.15	2	1	0.00388878	0.8777665	183.6631035
257.15	2	2	0.00388878	-1.0045790	12.0400165
273.15	3	1	0.00366099	0.2800744	91.3146132
273.15	3	2	0.00366099	-1.4344494	7.0891660

These_are_the unweighted_regression_parameters

-dH1: 5.5943 +/- 0.13621 kCal/mole -dS1: 19.9587 +/- 0.54052 Cal/(mol*K)
-dH2: 4.5664 +/- 0.29236 kCal/mole -dS2: 19.6431 +/- 1.16015 Cal/(mol*K)
R^2(1)= 0.99941
R^2(2)= 0.99592

Pressure (atm)

Calculated mols ads

% error in mols ads

Experimental mols ads

Error in mols ads

Best residual of output file, indicates "goodness of fit"

Temperature dependent equilibrium constants

Total sum of squares of errors

Solid dependent pore capacities, accessible surface areas, and pore volumes

Enthalpy and entropy of adsorption from linear regression parameters for van't Hoff plot

APPENDIX B
FORTRAN 77 CODE FOR AREA.EXE AND COMMENTS ON INPUT AND OUTPUT FILES

The code for area.exe implements the computation of the excluded molecular area of a molecule. The excluded molecular areas are calculated by projecting the shadow of the three-dimensional molecule onto a plane and connecting the outermost points. From these outermost points, an area is calculated from summing the areas of small-inscribed rectangles, similar to the application of the Trapezoidal Rule. The input and output files are described, and the output file is designed so that one may paste it space-delimited into a spreadsheet.

```
c ------------------------------------------------------------------------
c -- Title       : area.exe
c -- Description : This program computes the area of a
c --               molecule in a specified orientation projected
c --               onto a planar surface.
c --
c --               This program uses an approximation of the
c --               area of rectangles to estimate the area,
c --               similar to the Trapezoidal Rule.
c -- Author      : Charles Edwin Webster
c -- Comment:    If the number of data points is larger than
c --               600, then the MAXNPOINT will need to be
c --               increased.
c ------------------------------------------------------------------------

      IMPLICIT NONE
c FOR FMAIN
      CHARACTER*60 INFILE, OUTFILE
      INTEGER*2 MAXNPOINT
      PARAMETER (MAXNPOINT=600)
      INTEGER CHOICE,COMBO,DT,QUAD,I,J,K
      PARAMETER (QUAD=4)
      DOUBLE PRECISION X(MAXNPOINT),Y(MAXNPOINT),Z(MAXNPOINT), DIV
      DOUBLE PRECISION M(MAXNPOINT),N(MAXNPOINT),O(MAXNPOINT)
      DOUBLE PRECISION RMAXA(QUAD,MAXNPOINT/4), RMAXB(QUAD,MAXNPOINT/4)

c FOR MINMAX
      DOUBLE PRECISION MINX, MINY, MINZ, MAXX, MAXY, MAXZ
      DOUBLE PRECISION DISTX, DISTY, DISTZ
c FOR QUADMINMAX
      INTEGER DTA1, DTA2, DTA3, DTA4
      INTEGER DTB1, DTB2, DTB3, DTB4
      DOUBLE PRECISION A(MAXNPOINT), B(MAXNPOINT)
      DOUBLE PRECISION C(QUAD,MAXNPOINT)
      DOUBLE PRECISION D(QUAD,MAXNPOINT)
      DOUBLE PRECISION P(QUAD,MAXNPOINT)
      DOUBLE PRECISION Q(QUAD,MAXNPOINT)
      DOUBLE PRECISION MINA(QUAD),MAXA(QUAD)
      DOUBLE PRECISION MINB(QUAD),MAXB(QUAD)
c FOR SIZE
      DOUBLE PRECISION SZ,SQU
c FOR BOUNDARY
c     INTEGER PIE
      DOUBLE PRECISION PIE(QUAD)
      DOUBLE PRECISION DEGREE(QUAD,MAXNPOINT),R(QUAD,MAXNPOINT)
      DOUBLE PRECISION MAXR(QUAD,MAXNPOINT)
      REAL INDEX(QUAD,MAXNPOINT)
c FOR CONCAT
      DOUBLE PRECISION BDTA(QUAD)
      DOUBLE PRECISION TOT_AREA
c Get name of data file
      WRITE (6,5)
    5 FORMAT (5X,'Name of Data File? ')
      READ (5,'(A)') INFILE
c Get name of output file
      WRITE (6,20)
   20 FORMAT (/5X,'Name of Output File? ')
      READ (5,'(A)') OUTFILE
c Open the data file
      OPEN (8,FILE=INFILE,STATUS='OLD')
c get number of data points, number for division of distance to approximate rectangles
      CALL GETLINE(8)
      READ (8,*) DT, DIV, CHOICE
      IF (DT.GT.MAXNPOINT) THEN
        PRINT 50,DT,MAXNPOINT
        STOP
   50   FORMAT(/1X,'Sorry. You asked for ',I6,
     *       ' data points. The maximum number is ',I4'.')
      ENDIF
c     PRINT *,'Read in DT(number of data points), DIV(factor for square
```

```
c     *creation)'
c     PRINT *,'Choice (0/1), 0: set size, 1: calculate size.'
      IF (CHOICE.EQ.0) PRINT *,'# data pts, area calc factor, set size'
      IF (CHOICE.EQ.1) PRINT *,'# data pts, area calc factor, calculate
     *size'
      PRINT 55, DT, DIV, CHOICE
   55 FORMAT (3X,I5,3X,E12.5,3X,I1)
c find which combo of data points user wants
      CALL GETLINE(8)
      READ (8,*) COMBO, SZ
c     PRINT *,'Which combonation does user want?'
c     PRINT *,'1 for X*Y, 2 for X*Z, 3 for Y*Z'
      print 60, combo,sz
   60 FORMAT (3X,'User has chosen combo: ',I1,','3X,' SiZe: ',
     *f10.8)
      PRINT *,'     combo: 1 for X*Y, 2 for X*Z, 3 for Y*Z'
      CALL GETLINE(8)
      READ (8,*) PIE(1),PIE(2),PIE(3),PIE(4)
      PRINT 70, PIE(1),PIE(2),PIE(3),PIE(4)
   70 FORMAT (3X,'PIE_1:',F4.0,'  PIE_2:',F4.0,'  PIE_3:',F4.0,
     *'  PIE_4:',F4.0)
c GET THE DATA POINTS (X, Y, Z)
      DO 80 I=1,DT
       CALL GETLINE(8)
       READ (8,*) X(I),Y(I),Z(I)
       M(I) = X(I)
       N(I) = Y(I)
       O(I) = Z(I)
   80 CONTINUE
      CLOSE (8)
      CALL MINMAX(M,N,O,DT,MINX,MINY,MINZ,MAXX,MAXY,MAXZ,DISTX,DISTY,
     *DISTZ)
      CALL QUADMINMAX(X,Y,Z,COMBO,DT,A,B,C,D,P,Q,MINA,MAXA,MINB,
     *MAXB,DTA1,DTA2,DTA3,DTA4,DTB1,DTB2,DTB3,DTB4)
      IF (CHOICE.EQ.1) THEN
       CALL SIZE(COMBO,DIV,DT,DISTX,DISTY,DISTZ,SZ,SQU)
      ENDIF
      CALL BOUNDARY(PIE,C,D,DT,DTA1,DTA2,DTA3,DTA4,DEGREE,R,MAXR,
     *INDEX,BDTA)
       DO 100 J=1, QUAD
          DO 5000 J=2, BDTA(I)
            K = INDEX(I,J)
            RMAXA(I,J) = C(I,K)
            RMAXB(I,J) = D(I,K)
 5000       CONTINUE
  100   CONTINUE
      CALL CONCAT(DT,BDTA,MAXA,MINA,SZ,RMAXA,RMAXB,TOT_AREA)
 OPEN (10,FILE=OUTFILE)
      PRINT *, 'The area is ',tot_area,' '
      WRITE (10,*) 'The_uncorrected area_is_(A^2) ',tot_area,' .'
      WRITE (10,*) 'Parameters:'
      WRITE (10,*) 'No._of_Data Points, Division_Factor, Choice'
      WRITE (10,2) dt,div,choice
      WRITE (10,*) 'Combo, SiZe'
      WRITE (10,3) combo,sz
      WRITE (10,*) 'Pie_1, Pie_2, Pie_3, Pie_4'
      WRITE (10,4) PIE(1),PIE(2),PIE(3),PIE(4)
       DO 110 I=1, QUAD
          DO 5100 J=1, BDTA(I)
           IF (I.EQ.1) WRITE (10,116) I,J,MAXR(I,J),RMAXA(I,J),RMAXB(I,J)
           IF (I.EQ.2) WRITE (10,116) I,J,MAXR(I,J),RMAXA(I,J),RMAXB(I,J)
           IF (I.EQ.3) WRITE (10,116) I,J,MAXR(I,J),RMAXA(I,J),RMAXB(I,J)
           IF (I.EQ.4) WRITE (10,116) I,J,MAXR(I,J),RMAXA(I,J),RMAXB(I,J)
 5100   CONTINUE
  110   CONTINUE

  116   FORMAT ('Quad: ',i1,' Point:',i3,' Distance:',F10.6,'  Max_A:'
     *,F10.6,'  Max_B:',F10.6)
      WRITE (10,*) '                    X        Y        Z'
      WRITE (10,*) 'DT is',DT
```

```
      WRITE (10,1000) I, X(1), Y(1), Z(1)
       DO 300 J=2,DT-1
        WRITE (10,1010) J, X(J), Y(J), Z(J)
  300  CONTINUE
      WRITE (10,1020) DT, X(DT), Y(DT), Z(DT)
      CLOSE (10)
    2  FORMAT(I5,2X,E11.5,2X,I1)
    3  FORMAT(I1,2X,E13.7)
    4  FORMAT(F5.0,F5.0,F5.0,F5.0)
 1000 FORMAT(I3,' The_first_set_is ',F9.3', ',F9.3', ',F9.3'.')
 1010 FORMAT(I3,'  The_next_set_is ',F9.3', ',F9.3', ',F9.3'.')
 1015 FORMAT(I3, '  The_next_set_is ',F9.3', ',F9.3'.')
 1020 FORMAT(I3, ' The_last_ set_is ',F9.3', ',F9.3', ',F9.3'.')
 1025 FORMAT(I3,'  The_last_set_is ',F9.3', ',F9.3'.')
      END

c ------------------------------------------------------------------------
c
c  MINMAX: 1. Determines minimum and maximum X, Y, and Z
c            coordinates of molecule.
c        2. Determines distance in X, Y, and Z direction.
c
c ------------------------------------------------------------------------

      SUBROUTINE MINMAX(M,N,O,DT,MINX,MINY,MINZ,MAXX,MAXY,MAXZ,
     *DISTX,DISTY,DISTZ)
      IMPLICIT NONE
      INTEGER DT, I, J
      DOUBLE PRECISION M(DT), N(DT), O(DT), T
      DOUBLE PRECISION MINX, MINY, MINZ, MAXX, MAXY, MAXZ
      DOUBLE PRECISION DISTX, DISTY, DISTZ

c for X
      DO 50 J=1, DT-1
        DO 40 I=1, DT-1
          IF (M(I).LT.M(I+1)) GOTO 40
           T = M(I)
          M(I) = M(I+1)
          M(I+1) = T
   40   CONTINUE
   50 CONTINUE
c for Y
      DO 100 J=1, DT-1
        DO 90 I=1, DT-1
          IF (N(I).LT.N(I+1)) GOTO 90
           T = N(I)
          N(I) = N(I+1)
          N(I+1) = T
   90   CONTINUE
  100 CONTINUE
c for Z
      DO 200 J=1, DT-1
        DO 190 I=1, DT-1
          IF (O(I).LT.O(I+1)) GOTO 190
           T = O(I)
          O(I) = O(I+1)
          O(I+1) = T
  190   CONTINUE
  200 CONTINUE
      MINX = M(1)
      MINY = N(1)
      MINZ = O(1)
      MAXX = M(DT)
      MAXY = N(DT)
      MAXZ = O(DT)
      IF (MINX.LT.0) THEN
        DISTX = ABS(ABS(M(1))+M(DT))
      ELSE
        DISTX = ABS(M(1))+ABS(M(DT))
      ENDIF
```

```
      IF (MINY.LT.0) THEN
        DISTY = ABS(ABS(N(1))+N(DT))
      ELSE
        DISTY = ABS(N(1))+ABS(N(DT))
      ENDIF
      IF (MINZ.LT.0) THEN
        DISTZ = ABS(ABS(O(1))+O(DT))
      ELSE
        DISTZ = ABS(O(1))+ABS(O(DT))
      ENDIF
      END

c -------------------------------------------------------------------
c
c  QUADMINMAX:  Determines minimum and maximum X, Y, and Z
c          coordinates of molecule in specific quadrant
c
c -------------------------------------------------------------------

      SUBROUTINE QUADMINMAX(X,Y,Z,COMBO,DT,A,B,C,D,P,Q,MINA,MAXA,MINB,
     *MAXB,DTA1,DTA2,DTA3,DTA4,DTB1,DTB2,DTB3,DTB4)
      IMPLICIT NONE
      INTEGER COMBO, DT, I, J
      INTEGER DTA1, DTA2, DTA3, DTA4
      INTEGER DTB1, DTB2, DTB3, DTB4
      INTEGER QUAD
      PARAMETER (QUAD=4)
      DOUBLE PRECISION A(DT), B(DT), X(DT), Y(DT), Z(DT)
      DOUBLE PRECISION C(QUAD,DT),D(QUAD,DT)
      DOUBLE PRECISION P(QUAD,DT),Q(QUAD,DT)
      DOUBLE PRECISION T
      DOUBLE PRECISION MINA(QUAD),MAXA(QUAD)
      DOUBLE PRECISION MINB(QUAD),MAXB(QUAD)

      IF (COMBO.EQ.1) THEN
       DO 50 I=1, DT
         A(I) = X(I)
         B(I) = Y(I)
   50  CONTINUE
      ENDIF
      IF (COMBO.EQ.2) THEN
       DO 100 I=1, DT
         A(I) = X(I)
         B(I) = Z(I)
  100  CONTINUE
      ENDIF
      IF (COMBO.EQ.3) THEN
       DO 200 I=1, DT
         A(I) = Y(I)
         B(I) = Z(I)
  200  CONTINUE
      ENDIF
c for a
c for quad1 a values
      DTA1 = 2
      DO 1000 I=1, DT
       IF (A(I).GE.0.AND.B(I).GE.0) THEN
        DTA1 = DTA1 + 1
        C(1,DTA1) = A(I)
        P(1,DTA1) = A(I)
       ENDIF
 1000 CONTINUE
c for quad2 a values
      DTA2 = 2
      DO 1100 I=1, DT
       IF (A(I).LE.0.AND.B(I).GE.0) THEN
        DTA2 = DTA2 + 1
        C(2,DTA2) = A(I)
        P(2,DTA2) = A(I)
       ENDIF
```

```
1100 CONTINUE
c for quad3 a values
     DTA3 = 2
     DO 1200 I=1, DT
     IF ( A(I).LE.0.AND.B(I).LE.0) THEN
      DTA3 = DTA3 + 1
      C(3,DTA3) = A(I)
      P(3,DTA3) = A(I)
     ENDIF
1200 CONTINUE
c for quad4 a values
     DTA4 = 2
     DO 1300 I=1, DT
     IF ( A(I).GE.0.AND.B(I).LE.0) THEN
      DTA4 = DTA4 + 1
      C(4,DTA4) = A(I)
      P(4,DTA4) = A(I)
     ENDIF
1300 CONTINUE
c sorting
     IF (DTA1.GT.2) THEN
     DO 1400 J=3, DTA1-1
       DO 1390 I=3, DTA1-1
         IF (P(1,I).LE.P(1,I+1)) GOTO 1390
          T = P(1,I)
          P(1,I) = P(1,I+1)
          P(1,I+1) = T
1390     CONTINUE
1400  CONTINUE
     ENDIF
     IF (DTA2.GT.2) THEN
     DO 1500 J=3, DTA2-1
       DO 1490 I=3, DTA2-1
         IF (P(2,I).LE.P(2,I+1)) GOTO 1490
          T = P(2,I)
          P(2,I) = P(2,I+1)
          P(2,I+1) = T
1490     CONTINUE
1500  CONTINUE
     ENDIF
     IF (DTA3.GT.2) THEN
     DO 1600 J=3, DTA3-1
       DO 1590 I=3, DTA3-1
         IF (P(3,I).LE.P(3,I+1)) GOTO 1590
          T = P(3,I)
          P(3,I) = P(3,I+1)
          P(3,I+1) = T
1590     CONTINUE
1600  CONTINUE
     ENDIF
     IF (DTA4.GT.2) THEN
     DO 1700 J=3, DTA4-1
       DO 1690 I=3, DTA4-1
         IF (P(4,I).LE.P(4,I+1)) GOTO 1690
          T = P(4,I)
          P(4,I) = P(4,I+1)
          P(4,I+1) = T
1690     CONTINUE
1700  CONTINUE
     ENDIF
     MINA(1) = P(1,3)
     MINA(2) = P(2,3)
     MINA(3) = P(3,3)
     MINA(4) = P(4,3)
     MAXA(1) = P(1,DTA1)
     MAXA(2) = P(2,DTA2)
     MAXA(3) = P(3,DTA3)
     MAXA(4) = P(4,DTA4)
c for b
c for quad1 b values
```

```
      DTB1 = 2
      DO 2000 I=1, DT
       IF (B(I).GE.0.AND.A(I).GE.0) THEN
        DTB1 = DTB1 + 1
        D(1,DTB1) = B(I)
        Q(1,DTB1) = B(I)
       ENDIF
 2000 CONTINUE
c for quad2 b values
      DTB2 = 2
      DO 2100 I=1, DT
       IF (B(I).GE.0.AND.A(I).LE.0) THEN
        DTB2 = DTB2 + 1
        D(2,DTB2) = B(I)
        Q(2,DTB2) = B(I)
       ENDIF
 2100 CONTINUE
c for quad3 b values
      DTB3 = 2
      DO 2200 I=1, DT
       IF (B(I).LE.0.AND.A(I).LE.0) THEN
        DTB3 = DTB3 + 1
        D(3,DTB3) = B(I)
        Q(3,DTB3) = B(I)
       ENDIF
 2200 CONTINUE
c for quad4 b values
      DTB4 = 2
      DO 2300 I=1, DT
       IF (B(I).LE.0.AND.A(I).GE.0) THEN
        DTB4 = DTB4 + 1
        D(4,DTB4) = B(I)
        Q(4,DTB4) = B(I)
       ENDIF
 2300 CONTINUE
c sorting
      IF (DTB1.GT.2) THEN
       DO 2400 J=3, DTB1-1
         DO 2390 I=3, DTB1-1
          IF (Q(1,I).LE.Q(1,I+1)) GOTO 2390
           T = Q(1,I)
           Q(1,I) = Q(1,I+1)
           Q(1,I+1) = T
 2390    CONTINUE
 2400  CONTINUE
      ENDIF
      IF (DTB2.GT.2) THEN
       DO 2500 J=3, DTB2-1
         DO 2490 I=3, DTB2-1
          IF (Q(2,I).LE.Q(2,I+1)) GOTO 2490
           T = Q(2,I)
           Q(2,I) = Q(2,I+1)
           Q(2,I+1) = T
 2490    CONTINUE
 2500  CONTINUE
      ENDIF
      IF (DTB3.GT.2) THEN
       DO 2600 J=3, DTB3-1
         DO 2590 I=3, DTB3-1
          IF (Q(3,I).LE.Q(3,I+1)) GOTO 2590
           T = Q(3,I)
           Q(3,I) = Q(3,I+1)
           Q(3,I+1) = T
 2590    CONTINUE
 2600  CONTINUE
      ENDIF
      IF (DTB4.GT.2) THEN
       DO 2700 J=3, DTB4-1
         DO 2690 I=3, DTB4-1
          IF (Q(4,I).LE.Q(4,I+1)) GOTO 2690
```

```
        T = Q(4,I)
        Q(4,I) = Q(4,I+1)
        Q(4,I+1) = T
2690    CONTINUE
2700  CONTINUE
      ENDIF
      MINB(1) = Q(1,3)
      MINB(2) = Q(2,3)
      MINB(3) = Q(3,3)
      MINB(4) = Q(4,3)
      MAXB(1) = Q(1,DTB1)
      MAXB(2) = Q(2,DTB2)
      MAXB(3) = Q(3,DTB3)
      MAXB(4) = Q(4,DTB4)
      IF (DTA1.NE.DTB1) THEN
       PRINT *,'Warning!! There is at least one unmatched data point bet
     *ween a1 and b1.'
       PRINT *,'This could be an error.'
      ENDIF
      IF (DTA2.NE.DTB2) THEN
       PRINT *,'Warning!! There is at least one unmatched data point bet
     *ween a2 and b2.'
       PRINT *,'This could be an error.'
      ENDIF
      IF (DTA3.NE.DTB3) THEN
       PRINT *,'Warning!! There is at least one unmatched data point bet
     *ween a3 and b3.'
       PRINT *,'This could be an error.'
      ENDIF
      IF (DTA4.NE.DTB4) THEN
       PRINT *,'Warning!! There is at least one unmatched data point bet
     *ween a4 and b4.'
       PRINT *,'This could be an error.'
      ENDIF
      END

C -------------------------------------------------------------------
C
C  SIZE: 1. Determines the size of the squares to determine
C        area of molecule.
C     2. Makes square to estimate area of molecule.
C -------------------------------------------------------------------

      SUBROUTINE SIZE(COMBO,DIV,DT,DISTX,DISTY,DISTZ,SZ)
      IMPLICIT NONE
      INTEGER COMBO, DT
      DOUBLE PRECISION DISTX, DISTY, DISTZ, DIV, SZ

      IF (COMBO.EQ.1) SZ = ((DISTX+DISTY)/DT)*DIV
      IF (COMBO.EQ.2) SZ = ((DISTX+DISTZ)/DT)*DIV
      IF (COMBO.EQ.3) SZ = ((DISTY+DISTZ)/DT)*DIV

      END

C -------------------------------------------------------------------
C
C  Boundary: gets the outer most points of each quadrant.
C
C -------------------------------------------------------------------

      SUBROUTINE BOUNDARY(PIE,C,D,DT,DTA1,DTA2,DTA3,DTA4,DEGREE,R,
     *MAXR,INDEX,BDTA)
      IMPLICIT NONE
      INTEGER QUAD, MAXNPOINT
      DOUBLE PRECISION PI
      PARAMETER (QUAD=4, PI=3.141592653589793, MAXNPOINT=600)
      INTEGER DT, TEMP
      INTEGER I, J, K, L, M, N
      INTEGER DTA1, DTA2, DTA3, DTA4
      DOUBLE PRECISION BDTA(QUAD)
```

```
      DOUBLE PRECISION C(QUAD,DT),D(QUAD,DT)
      DOUBLE PRECISION R(QUAD,DT)
      DOUBLE PRECISION DEGREE(QUAD,DT)
      DOUBLE PRECISION TMP, T
      DOUBLE PRECISION MAXR(QUAD,DT)
      DOUBLE PRECISION TMPR(QUAD,MAXNPOINT)
      DOUBLE PRECISION PIE(QUAD)
      REAL INDEX(QUAD,DT)

c quad1
      DO 500 I=1, QUAD
       IF (I.EQ.1) THEN
         DO 490 J=1, DTA1
          IF (C(I,J).GT.0.AND.D(I,J).GE.0) THEN
           DEGREE(I,J) = ATAN(D(I,J)/C(I,J))*(360/(2*PI))
           R(I,J) = SQRT(C(I,J)**2+D(I,J)**2)
          ENDIF
  490     CONTINUE
        BDTA(I) = 1
        TMP = -90/PIE(I)
c 90/5 = 18. 18, b/c we need to go 18 times for 5 degree increments.
        DO 400 N=1, PIE(I)+1
          TMP = TMP + 90/PIE(I)
       IF (TMP.GE.90) GOTO 400
c bdta(1) = bdta(1) + 1, total 18
          BDTA(I) = BDTA(I) + 1
         M = 0
         DO 390 J=1, DTA1
          IF (C(I,J).GT.0.AND.D(I,J).GE.0) THEN
           IF (DEGREE(I,J).GE.TMP.AND.DEGREE(I,J).LE.TMP+90/
     *          PIE(I)) THEN
            IF (R(I,J).NE.0) THEN
             M = M + 1
             TMPR(I,M) = R(I,J)
            ELSE
             M = M - 1
             BDTA(I) = BDTA(I) - 1
            ENDIF
           ENDIF
          ENDIF
  390     CONTINUE
         DO 2000 K=1, M-1
          DO 1990 L=1, M-1
           IF (TMPR(I,L).LT.TMPR(I,L+1)) GOTO 1990
            T = TMPR(I,L)
            TMPR(I,L) = TMPR(I,L+1)
            TMPR(I,L+1) = T
 1990      CONTINUE
 2000     CONTINUE
       IF (M.EQ.0) M = 1
         TEMP = BDTA(I)
        MAXR(I,TEMP) = TMPR(I,M)
  400   CONTINUE
c index quadrant1 points to find maxr1 points.
       DO 15 J=1, DTAI
         DO 10 K=2, BDTA(I)
          IF (MAXR(I,K).EQ.R(I,J)) THEN
           INDEX(I,K) = J
          ENDIF
   10    CONTINUE
   15  CONTINUE
      ENDIF
c quad2
      IF (I.EQ.2) THEN
        DO 1480 J=1, DTA2
         IF (C(I,J).LT.0.AND.D(I,J).GE.0) THEN
          DEGREE(I,J) = ATAN(D(I,J)/C(I,J))*(360/(2*PI))
          R(I,J) = SQRT(C(I,J)**2+D(I,J)**2)
         ENDIF
 1480     CONTINUE
```

```
          BDTA(I) = 1
          TMP = 90/PIE(I)
c 90/5 = 18. 18, b/c we need to go 18 times for 5 degree increments.
        DO 1400 N=1, PIE(I)+1
            TMP = TMP - 90/PIE(I)
      IF (TMP.LE.-90) GOTO 1400
c bdta(2) = bdta(2) + 1, total 18
            BDTA(I) = BDTA(I) + 1
           M = 0
          DO 1390 J=1, DTA2
            IF (C(I,J).LT.0.AND.D(I,J).GE.0) THEN
              IF (DEGREE(I,J).LE.TMP.AND.DEGREE(I,J).GE.TMP-90/
     *            PIE(I)) THEN
                IF (R(I,J).NE.0) THEN
                  M = M + 1
                  TMPR(I,M) = R(I,J)
                ELSE
                  M = M - 1
                  BDTA(I) = BDTA(I) - 1
                ENDIF
              ENDIF
            ENDIF
 1390     CONTINUE
          DO 3000 K=1, M-1
            DO 2990 L=1, M-1
              IF (TMPR(I,L).LT.TMPR(I,L+1)) GOTO 2990
                T = TMPR(I,L)
                TMPR(I,L) = TMPR(I,L+1)
                TMPR(I,L+1) = T
 2990         CONTINUE
 3000       CONTINUE
        IF (M.EQ.0) M = 1
          TEMP = BDTA(I)
          MAXR(I,TEMP) = TMPR(I,M)
 1400   CONTINUE
c index quadrant2 points to find maxr2 points.
        DO 25 J=1, DTA2
          DO 20 K=2, BDTA(I)
            IF (MAXR(I,K).EQ.R(I,J)) THEN
              INDEX(I,K) = J
            ENDIF
   20     CONTINUE
   25   CONTINUE
      ENDIF
c quad3
      IF (LEQ.3) THEN
        DO 1470 J=1, DTA3
          IF (C(I,J).LT.0.AND.D(I,J).LE.0) THEN
            DEGREE(I,J) = ATAN(D(I,J)/C(I,J))*(360/(2*PI))
            R(I,J) = SQRT(C(I,J)**2+D(I,J)**2)
          ENDIF
 1470     CONTINUE
          BDTA(I) = 1
          TMP = -90/PIE(I)
        DO 2400 N=1, PIE(I)+1
          TMP = TMP + 90/PIE(I)
      IF (TMP.GE.90) GOTO 2400
          BDTA(I) = BDTA(I) + 1
          M = 0
        DO 2390 J=1, DTA3
          IF (C(I,J).LT.0.AND.D(I,J).LE.0) THEN
            IF (DEGREE(I,J).GE.TMP.AND.DEGREE(I,J).LE.TMP+90/
     *          PIE(I)) THEN
              IF (R(I,J).NE.0) THEN
                M = M + 1
                TMPR(I,M) = R(I,J)
              ELSE
                M = M - 1
                BDTA(I) = BDTA(I) - 1
              ENDIF
```

```
            ENDIF
           ENDIF
2390      CONTINUE
         DO 4000 K=1, M-1
           DO 3990 L=1, M-1
             IF (TMPR(L,L).LT.TMPR(I,L+1)) GOTO 3990
               T = TMPR(I,L)
               TMPR(I,L) = TMPR(I,L+1)
               TMPR(I,L+1) = T
3990         CONTINUE
4000      CONTINUE
       IF (M.EQ.0) M = 1
          TEMP = BDTA(I)
        MAXR(I,TEMP) = TMPR(I,M)
2400    CONTINUE
c index quadrant3 points to find maxr points.
       DO 35 J=1, DTA3
         DO 30 K=2, BDTA(I)
           IF (MAXR(I,K).EQ.R(I,J)) THEN
             INDEX(I,K) = J
           ENDIF
  30     CONTINUE
  35   CONTINUE
     ENDIF
c quad4
       IF (I.EQ.4) THEN
         DO 1460 J=1, DTA4
           IF (C(I,J).GT.0.AND.D(I,J).LE.0) THEN
            DEGREE(I,J) = ATAN(D(I,J)/C(I,J))*(360/(2*PI))
            R(I,J) = SQRT(C(I,J)**2+D(I,J)**2)
           ENDIF
1460     CONTINUE
         BDTA(I) = 1
         TMP = 90/PIE(I)
        DO 3400 N=1, PIE(I)+1
          TMP = TMP - 90/PIE(I)
       IF (TMP.LE.-90) GOTO 3400
          BDTA(I) = BDTA(I) + 1
          M = 0
         DO 3390 J=1, DTA4
           IF (C(I,J).GT.0.AND.D(I,J).LE.0) THEN
             IF (DEGREE(I,J).LE.TMP.AND.DEGREE(I,J).GE.TMP-90/
     *         PIE(I)) THEN
              IF (R(I,J).NE.0) THEN
                M = M + 1
                TMPR(I,M) = R(I,J)
              ELSE
                M = M - 1
                BDTA(I) = BDTA(I) - 1
              ENDIF
             ENDIF
           ENDIF
3390     CONTINUE
        DO 5000 K=1, M-1
          DO 4990 L=1, M-1
            IF (TMPR(I,L).LT.TMPR(I,L+1)) GOTO 4990
              T = TMPR(I,L)
              TMPR(I,L) = TMPR(I,L+1)
              TMPR(I,L+1) = T
4990        CONTINUE
5000      CONTINUE
c to fix this m=0 shit, this means that there was only one data point
c in the piece of pie.
       IF (M.EQ.0) M = 1
          TEMP = BDTA(I)
        MAXR(I,TEMP) = TMPR(I,M)
3400    CONTINUE
c index quadrant4 points to find maxr points.
       DO 45 J=1, DTA4
         DO 40 K=2, BDTA(I)
```

```
          IF (MAXR(I,K).EQ.R(I,J)) THEN
            INDEX(I,K) = J
          ENDIF
   40     CONTINUE
   45   CONTINUE
      ENDIF
  500  CONTINUE
      END

c ---------------------------------------------------------------------
c
c  concat:
c
c ---------------------------------------------------------------------

      SUBROUTINE CONCAT(DT,BDTA,MAXA,MINA,SZ,RMAXA,RMAXB,TOT_AREA)
      IMPLICIT NONE

      INTEGER QUAD
      INTEGER*4 MAXBOX
      PARAMETER (QUAD=4, MAXBOX=100000)
      INTEGER DT, I, K, M, TEMP
      DOUBLE PRECISION BDTA(QUAD)
      DOUBLE PRECISION SZ
      DOUBLE PRECISION RMAXA(QUAD,DT),RMAXB(QUAD,DT)
      DOUBLE PRECISION MAXA(QUAD),MINA(QUAD)
      DOUBLE PRECISION BOXA(MAXBOX,QUAD)
      DOUBLE PRECISION AREA, TOT_AREA, QUAD_AREA

        DO 1010 I=1, QUAD
           TEMP = BDTA(I)
           RMAXA(I,TEMP+1) = 0
         IF (RMAXB(I,TEMP).NE.0) THEN
           TEMP = BDTA(I)
           RMAXB(I,TEMP+1) = RMAXB(I,TEMP)
         ELSE
           TEMP = BDTA(I)
           RMAXB(I,TEMP+1) = RMAXB(I,TEMP-1)
         ENDIF
         RMAXB(I,1) = 0
         IF (RMAXB(I,2).NE.0) THEN
         RMAXA(I,1) = RMAXA(I,2)
          ELSE
         RMAXA(I,1) = RMAXA(I,3)
         ENDIF
       BDTA(I) = BDTA(I) + 1
 1010    CONTINUE
       BOXA(1,1) = 0
       BOXA(1,2) = SZ
       DO 3 I=1, QUAD
         AREA = 0
         QUAD_AREA = 0
 ccc
       IF (I.EQ.1.OR.I.EQ.4) THEN
         DO 5000 K=1, BDTA(I)
           DO 4000 M=1, MAXA(I)/SZ + 1
             BOXA(M,2) = BOXA(M-1,2) + SZ
             IF (BOXA(M,2).LE.RMAXA(I,K)) THEN
           AREA = BOXA(M,2) * (RMAXB(I,K)-RMAXB(I,K-1))
             ENDIF
 4000        CONTINUE
         QUAD_AREA = QUAD_AREA + AREA
 5000    CONTINUE
       ENDIF
 ccc
       IF (I.EQ.2.OR.I.EQ.3) THEN
         DO 7000 K=1, BDTA(I)
           DO 6000 M=1, ABS(MINA(I)/SZ) + 1
             BOXA(M,2) = BOXA(M-1,2) - SZ
             IF (BOXA(M,2).GE.RMAXA(I,K)) THEN
```

```
          AREA = ABS(BOXA(M,2)) * (RMAXB(I,K)-RMAXB(I,K-1))
            ENDIF
 6000       CONTINUE
          QUAD_AREA = QUAD_AREA + AREA
 7000     CONTINUE
        ENDIF
ccc
        PRINT *, 'The quadrant',I,' area is',ABS(QUAD_AREA),' .'
        TOT_AREA = TOT_AREA + ABS(QUAD_AREA)
    3   CONTINUE
      END

c ------------------------------------------------------------------------
c
c  GETLINE: gets a line from the data file.
c
c ------------------------------------------------------------------------

      SUBROUTINE GETLINE(U)
      IMPLICIT NONE

      INTEGER      U
      CHARACTER*79 BUF

    10 READ (U,'(A)') BUF
c  Read in the file a line at a time until a non-comment line is read
c  in.
      IF (BUF(1:1).EQ.'#') THEN
        PRINT *, BUF
        GOTO 10
      ENDIF
c     At this point we have a potential line with data so
c     backup the file pointer to the beginning of the line
c     to allow the caller to parse it with the READ command.
      BACKSPACE(U)
      RETURN
      END
```

Example input file for Area exe--benzene molecule

400 4e-4 1
1 0.01
12 12 12 12

x	y	z	a	b	c	x	y	z	x	y	z
-1.207431	0.697412	0.000000	-0.186679	-1.968750	-1.589042	-1.158759	1.018203	0.619491	2.669991	-0.724680	0.951150
-1.207442	-0.697121	0.000000	-0.186681	-1.968751	-1.589253	-2.259296	1.268593	0.619491	2.407491	-2.017044	0.883038
0.000000	-1.394211	0.000000	1.811546	-0.697120	1.589042	-1.158759	1.472119	0.619491	2.388557	-0.526300	0.627730
1.207440	-0.697120	0.000000	1.436549	-0.253074	1.589092	-0.969100	0.478491	0.586751	2.062503	-2.268592	0.619491
1.207442	0.697120	0.000000	0.764042	-0.360949	1.606901	-1.704280	1.342177	0.175555	3.100728	-1.630717	0.619491
0.000001	1.394212	0.000000	0.841353	-0.963097	1.638669	-2.945544	1.128325	0.193063	3.100728	-0.819603	0.619491
-2.156402	1.245160	0.000000	1.941338	-1.271660	1.589042	-3.260200	0.767554	0.193063	1.733186	-2.235062	0.507439
-2.156404	-1.245157	0.000000	2.320563	-0.683372	1.284841	-2.037082	2.425101	0.193063	2.853919	-2.017944	0.619491
-0.000002	-2.490161	0.000000	0.277756	-0.688809	1.284718	-3.249199	1.722748	0.193063	2.951264	-0.371814	0.512203
2.156399	-1.245160	0.000000	1.563154	-1.791898	1.259971	-3.006644	0.418672	0.184396	2.273718	-2.425501	0.193063
2.156403	1.245159	0.000000	1.419350	-1.141108	0.871375	-3.271732	2.423502	0.193063	3.313964	-1.498809	0.193063
0.000002	2.490161	0.000000	2.181399	-1.305759	1.253380	-3.313043	1.493809	0.193063	3.313940	-0.994312	0.193063
-0.630047	0.623930	1.604355	2.535257	-0.199400	0.937634	-2.931207	1.731814	-0.213103	1.479926	-2.324287	0.220225
-1.349021	1.309830	1.604355	1.986150	-0.751504	1.084619	-1.679393	2.324268	-0.220225	2.752478	-2.268592	0.193065
-1.696173	1.052505	1.582442	1.533152	-2.345375	0.256625	-2.753982	2.282549	0.193065	3.340197	-0.767553	0.193063
-1.702746	0.376137	1.594253	2.788409	-0.170864	0.336653	-3.313943	0.994513	0.193063	1.704276	-2.342277	0.175353
-0.980333	0.250976	1.618990	2.780087	-0.116762	-0.282777	-2.062506	2.268593	-0.619491	2.943541	-2.128324	-0.193063
-0.283121	-0.253260	1.547463	1.475996	-2.347604	0.507383	-1.109728	1.650718	-0.619491	3.906643	-0.418671	-0.184396
-1.194845	1.753606	1.330204	2.581972	-2.362133	-0.942573	-2.885580	0.526301	-0.625730	2.037079	-2.425502	-0.193063
-2.054037	1.330693	1.331113	0.166864	-0.089837	-1.491973	-1.753189	2.255065	-0.507459	3.340196	-1.722727	-0.619491
-2.170676	0.618714	1.298966	1.763635	-1.921025	-1.042128	-2.853922	2.017945	-0.619491	3.158726	-1.582202	-0.619491
-1.760636	1.921025	1.042128	1.458943	-2.117085	-0.903247	-1.109729	0.838604	-0.619491	1.734994	-2.317038	-0.563765
-2.581973	0.562133	0.942573	2.604253	-0.817455	-1.193937	-2.407494	2.017945	-0.883038	2.681994	-2.128324	-0.619491
-0.166866	0.098837	1.193937	2.178873	-0.187814	-1.298666	-2.969855	1.345161	-0.883038	2.569097	-0.478489	-0.506731
-1.458804	2.117085	0.903247	0.280522	-0.251248	1.347463	-2.969855	0.730671	-0.619491	2.250202	-2.268592	-0.619491
-2.406233	0.817455	1.193937	2.194844	-1.755508	-1.330204	-2.204543	1.637016	-1.113624	3.158756	-1.472119	-0.619491
-2.780088	0.116762	0.282777	2.054035	-1.330693	-1.331113	-2.603417	2.345510	-1.113624	3.948293	-0.791396	-0.868987
-1.473907	2.347605	0.507383	1.702745	-0.376137	-1.594233	-2.571276	0.865481	-1.060058	2.008936	-2.064659	-0.864104
-1.553154	2.343575	-0.256625	0.980331	-0.250976	-1.618990	-2.608233	1.059075	-1.060058	2.811768	-1.722746	-0.868104
-2.780490	0.170863	-0.336653	1.650046	-0.623950	-1.644355	-2.518065	1.567919	-1.113624	2.608248	-1.058670	-1.064102
-1.419353	1.141108	-0.871375	1.104802	-1.249850	-1.604355	-2.193842	-1.753738	1.054529	2.151837	-1.737539	-1.113624
-2.181400	1.305759	-1.253380	1.696172	-1.057205	1.589042	-2.384810	-0.794356	0.868987	2.518038	-1.507921	-1.113624
-1.984540	1.750551	-1.086619	1.811550	0.697118	1.589042	-2.813774	-1.722785	0.883038	2.003439	-1.241516	-1.113624
-2.535291	1.694990	-0.937643	1.394122	1.271658	1.589042	-2.908942	-2.064656	0.864104	2.294545	-2.470114	-1.113624
-1.563153	1.791898	-1.259971	0.841356	0.963097	1.638669	-2.869102	-0.478486	0.586731	2.572697	0.865479	1.060038
-2.026505	0.485572	-1.259971	0.764055	1.540400	1.606901	-3.115781	-1.472116	0.619491	2.608936	1.245157	1.060038
-0.277757	0.088809	-1.286718	1.434551	2.320973	1.618990	-2.259300	-2.268589	0.619491	2.407497	2.017942	0.883038
-0.841335	0.963097	-1.638669	2.180257	0.683370	1.284841	-2.158760	-1.018198	0.619491	2.669996	0.724667	0.951150
-1.394211	1.636901	-1.589042	1.563158	1.791897	1.259971	-2.682000	-2.128321	0.619491	2.831925	2.017942	0.619491
-1.811547	0.697120	-1.589042	0.277757	0.688809	1.284718	-1.753502	-2.211707	0.563765	2.170863	2.351055	0.507459
-1.434550	2.025774	-0.618990	1.254067	1.755508	1.284619	-1.006645	-0.418667	0.586996	2.310737	0.619650	0.619491
-0.744054	0.360449	-1.604601	2.335229	0.199397	0.937643	-1.260202	-1.722745	0.193063	3.100711	1.650713	0.619491
-0.650868	-0.623932	1.604355	2.181403	1.305756	1.084619	-2.037082	-2.425498	0.193063	2.022611	2.268590	0.619491
-0.980333	-0.250975	1.618990	1.419353	2.141106	0.871375	-3.249201	-0.767549	0.193063	2.885581	0.526297	0.627731
-1.702747	0.376137	1.594253	1.788491	2.117085	0.903253	-2.945547	-1.128321	0.193063	2.752484	2.268590	0.619491
-1.694174	-1.052205	1.582442	2.535191	2.345374	0.256625	-1.704283	-2.342773	0.175555	2.677393	2.324267	0.220225
-1.104015	-2.249150	0.604355	1.475911	2.347603	0.507383	-3.313944	-0.994510	0.193063	3.313944	0.994510	0.193063
-0.280525	-2.253263	1.547463	2.780099	0.116759	0.282777	-2.752485	-2.268589	0.193063	3.313945	1.493806	0.193063
-2.179876	-0.187813	1.298666	2.604237	0.817452	-1.193937	-1.679933	-2.324265	-0.220225	2.273734	2.423499	0.193063
-2.054038	-1.330693	1.331113	1.458804	2.117084	-0.903247	-2.951267	-0.371810	-0.220203	2.951267	0.371811	0.193063
-1.194847	-1.775609	1.330204	1.760640	1.921023	-1.042128	-1.313945	-1.493805	-0.193063	3.240202	1.722744	-0.193063
-2.406236	-0.867453	1.193937	1.166866	0.089838	-1.491973	-0.275724	-2.425499	-0.185068	2.037085	2.423499	-0.193063
-1.458948	-2.117085	0.902247	2.581974	0.562130	-0.942573	-1.100750	-0.835599	-0.619491	3.006645	0.418668	-0.184396
-1.168645	-0.698581	1.193937	2.054039	1.330691	-1.331113	-2.831922	-2.017941	-0.619491	2.945547	1.128322	-0.193063
-2.581973	-0.562133	0.942573	1.194848	1.755607	-1.330204	-1.753189	-2.255060	-0.507459	1.704283	2.342776	-0.175353
-1.760640	-1.921030	1.042128	0.280524	0.253262	-1.347463	-2.885581	-0.526296	-0.625730	3.240201	0.767550	-0.193063
-1.473910	-2.347604	0.507383	2.178876	1.187812	-1.298666	-1.109731	-1.650714	-0.619491	3.158781	1.472117	-0.619491
-2.780088	-0.116760	0.282777	1.696175	2.057204	1.589042	-2.062510	-2.268589	-0.619491	2.250299	2.268590	-0.619491
-0.768991	-0.117682	-0.336653	1.104800	1.249849	-1.604355	-2.669996	-2.724666	-0.951150	2.869101	0.478487	-0.506731
-1.353157	-2.343573	-0.256625	0.650049	0.623931	-1.604355	-2.969857	-1.345156	-0.883038	2.602000	2.128322	-0.619491
-2.533230	-0.199598	-0.937643	0.980334	0.250974	-1.618990	-2.407497	-2.017941	-0.883038	2.715092	2.717858	-0.563765
-1.196543	-1.750551	0.086619	1.702748	0.376135	-1.594253	-2.571278	-0.865474	-1.060058	2.158760	1.058199	-0.619491
-2.181402	-1.305757	-1.253380	0.557395	1.467400	1.604355	-2.603439	-1.245157	-1.113624	2.813774	1.722764	-0.883038
-1.413854	-2.025773	-0.871375	0.929020	1.870785	1.589042	-2.294546	-1.670314	-1.113624	2.608247	1.058667	-1.064102
-2.127757	-0.088810	-1.286718	-0.458130	1.766086	1.594233	-0.629654	-2.692223	-1.102298	1.848358	0.791384	-0.868987
-2.320504	-0.483753	-1.284841	-0.366086	2.128234	1.618990	-0.932701	-2.801486	-1.113616	2.518065	1.567918	-1.113624
-1.563158	-1.791898	-1.259971	0.102638	0.864182	0.604355	0.138140	-2.562569	1.113624	2.193862	1.753739	-1.094500
-0.764054	-1.636905	-1.589042	0.929020	1.870785	1.589042	0.138140	-2.702722	0.974722	2.026503	1.059676	-1.113624
-1.434550	-2.025774	-0.618990	0.349298	2.428137	1.503310	-0.657372	-2.967719	0.883038	0.429058	2.692228	1.102298
-1.811548	-0.697119	-1.589042	-0.897439	2.129233	1.228858	0.241099	-2.801486	0.883038	0.138144	2.915272	1.113624
-1.394122	-1.271639	-1.589042	0.012595	0.335734	1.320204	-0.979851	-2.820817	-0.605380	-0.132864	2.915272	1.113624
-0.841356	-0.963098	-1.638669	1.009507	0.428138	0.895279	-0.093897	-1.913545	0.619491	0.704047	2.692227	0.876722
0.277757	-0.088809	-1.286718	1.702745	1.501752	1.594233	-0.979852	-2.191270	0.952586	0.251095	2.902000	0.619491
0.102638	-0.864181	-1.604355	1.135817	2.094402	1.053401	-0.525599	-3.172277	0.619491	-0.657367	2.967724	0.883038
-0.366086	-2.128233	-0.618990	-0.277977	2.508582	1.053401	-0.657719	-3.262897	0.619491	0.677385	2.902000	0.619491
-0.458331	-1.766081	1.594233	1.265150	2.508581	0.811966	-1.083800	-2.967719	0.193063	-0.525594	2.737280	0.619491
0.186670	-1.968750	1.589042	1.257118	2.501750	0.288118	-0.911916	-3.669454	0.193063	-0.593972	2.915271	-0.621586
0.926918	-1.858070	1.347645	1.257118	2.501750	-0.288118	1.141703	-2.801487	0.193884	-0.093892	3.513148	0.619491
0.012596	-0.335722	1.330204	-1.245326	2.508581	-0.811966	-0.789146	-3.373276	0.193063	-0.973847	3.026121	0.605380
-0.897431	-2.152237	1.228826	0.277881	2.508582	0.811966	0.789146	-3.513546	0.193063	0.395083	3.513548	0.619491
0.349296	-2.428314	1.303310	-1.135814	2.094403	-1.053401	-0.596083	-3.313545	-0.193063	-0.789141	3.373280	0.193063
-0.271780	-2.508341	1.253380	-0.897440	2.129232	-1.228858	0.7891.40	-3.373278	-0.193063	1.141707	2.801488	0.193884
1.133814	-2.094402	1.053401	-1.009503	2.428138	-0.895279	-1.141707	-2.801485	-0.193884	0.113922	3.668457	0.193063
-0.819042	-2.501750	1.053401	0.897432	2.152238	1.228858	-0.119152	-3.669455	-0.193063	-1.083795	2.967722	0.193063
1.009504	-2.428317	0.895279	-0.349295	2.428138	-1.503310	1.083795	-2.967721	-0.193063	1.083799	2.967722	0.193063
-1.257317	-2.347603	0.507383	-0.978917	2.187813	1.347643	-0.657719	-3.262897	-0.619491	-0.119916	3.668457	-0.193063
1.243327	-2.508582	0.811966	-0.012595	0.335735	-1.320204	0.525593	-3.172277	-0.619491	1.141703	2.801490	0.193884
-1.265229	-2.508580	-0.811966	0.458133	1.766085	-1.594253	-0.934278	-2.912588	-0.621586	0.789146	3.373280	-0.193063
1.257113	-2.501750	-0.288118	-1.166867	1.887751	-1.589042	-0.093897	-1.913545	-0.619491	-0.596077	3.513549	-0.193063
-1.009506	-2.428315	-0.895279	-0.557393	1.467401	-1.604353	0.979846	2.820318	-0.605380	0.979850	2.820520	-0.605380
0.819699	-2.501750	-0.895548	0.102637	0.841482	-1.604355	-0.979847	-2.692225	-0.876722	-0.093897	3.513548	-0.619491
-1.137816	-2.094400	-1.053401	0.366087	1.128234	-1.618969	-0.251096	-3.262897	-0.883038	-0.934275	2.915273	-0.621586
0.277878	-2.508581	-1.253380	-1.253380	1.753740	-1.594253	0.657368	-2.967721	-0.883038	0.525596	3.373280	-0.619491
-0.012595	-0.335725	-1.330204	-0.518042	1.307921	1.615624	-0.429058	-2.692223	-1.102298	-0.677519	2.282500	-0.619491
-0.926919	-1.858069	-1.347643	-0.205823	1.930678	1.595482	-0.138143	-2.915270	-1.113624	0.657371	2.967722	-0.883038
-0.349298	-2.428316	-1.503310	-2.008930	2.064460	0.864104	0.332696	-2.801487	-1.113616	-0.251091	3.162699	-1.113624
0.897429	-2.152238	-1.228826	-2.813771	1.722768	0.883038	2.603434	-1.245160	1.113624	-0.794043	1.693229	-0.876722
0.366086	-2.128233	-1.638669	-2.848396	1.791588	0.860987	2.571272	-0.865481	1.060058	-0.132707	2.801489	-1.113616
-0.102637	-0.841481	-1.604355	-1.734999	2.217859	0.563765	2.294540	-1.670316	1.113624	-0.138140	2.915272	-1.113624
0.277878	-2.508583	-1.253380	-2.681997	2.130725	0.251469	2.968852	-1.245161	0.883038	-0.429054	2.692229	-1.102298

Example input file for Area.exe--benzene molecule explained

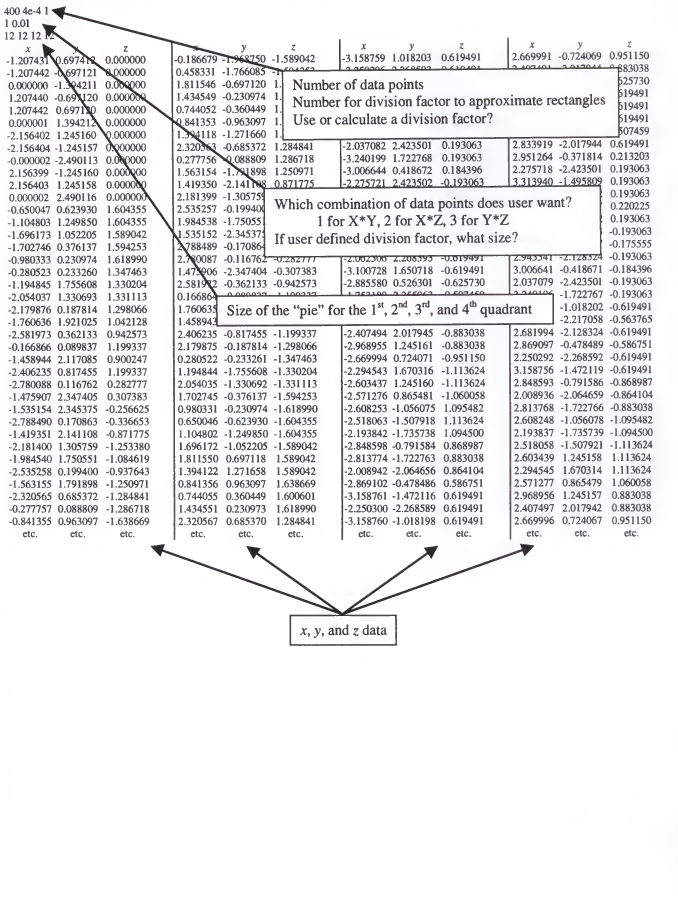

Example output file for Area.exe--benzene molecule
The_uncorrected area_is_(A^2) 33.413748775776020 .
Parameters:
No._of_Data Points, Division_Factor, Choice
400 0.40000E-03 1
Combo, SiZe
1 0.1396480E-04
Pie_1, Pie_2, Pie_3, Pie_4
12. 12. 12. 12.

Quad: 1	Point: 1	Distance: 0.000000	Max_A: 2.951267	Max_B: 0.000000
Quad: 1	Point: 2	Distance: 2.974596	Max_A: 2.951267	Max_B: 0.371811
Quad: 1	Point: 3	Distance: 3.329870	Max_A: 3.240201	Max_B: 0.767550
Quad: 1	Point: 4	Distance: 3.459953	Max_A: 3.313944	Max_B: 0.994510
Quad: 1	Point: 5	Distance: 3.669717	Max_A: 3.240202	Max_B: 1.722764
Quad: 1	Point: 6	Distance: 3.634006	Max_A: 2.945547	Max_B: 2.128322
Quad: 1	Point: 7	Distance: 3.566885	Max_A: 2.752484	Max_B: 2.268590
Quad: 1	Point: 8	Distance: 3.324495	Max_A: 2.275724	Max_B: 2.423499
Quad: 1	Point: 9	Distance: 2.897099	Max_A: 1.704283	Max_B: 2.342776
Quad: 1	Point: 10	Distance: 2.800683	Max_A: 1.245330	Max_B: 2.508581
Quad: 1	Point: 11	Distance: 3.159429	Max_A: 1.083799	Max_B: 2.967722
Quad: 1	Point: 12	Distance: 3.563753	Max_A: 0.596083	Max_B: 3.513548
Quad: 1	Point: 13	Distance: 3.670397	Max_A: 0.119322	Max_B: 3.668457
Quad: 1	Point: 14	Distance: 0.000000	Max_A: 0.000000	Max_B: 3.668457
Quad: 2	Point: 1	Distance: 0.000000	Max_A: -2.951267	Max_B: 0.000000
Quad: 2	Point: 2	Distance: 2.974596	Max_A: -2.951267	Max_B: 0.371814
Quad: 2	Point: 3	Distance: 3.329870	Max_A: -3.240200	Max_B: 0.767554
Quad: 2	Point: 4	Distance: 3.459953	Max_A: -3.313943	Max_B: 0.994513
Quad: 2	Point: 5	Distance: 3.669716	Max_A: -3.240199	Max_B: 1.722768
Quad: 2	Point: 6	Distance: 3.634006	Max_A: -2.945544	Max_B: 2.128325
Quad: 2	Point: 7	Distance: 3.566886	Max_A: -2.752482	Max_B: 2.268594
Quad: 2	Point: 8	Distance: 3.324495	Max_A: -2.275721	Max_B: 2.423502
Quad: 2	Point: 9	Distance: 2.897098	Max_A: -1.704280	Max_B: 2.342777
Quad: 2	Point: 10	Distance: 2.800683	Max_A: -1.245326	Max_B: 2.508583
Quad: 2	Point: 11	Distance: 3.159429	Max_A: -1.083795	Max_B: 2.967723
Quad: 2	Point: 12	Distance: 3.563753	Max_A: -0.596077	Max_B: 3.513549
Quad: 2	Point: 13	Distance: 3.670397	Max_A: -0.119316	Max_B: 3.668457
Quad: 2	Point: 14	Distance: 0.000000	Max_A: 0.000000	Max_B: 3.668457
Quad: 3	Point: 1	Distance: 0.000000	Max_A: -2.951267	Max_B: 0.000000
Quad: 3	Point: 2	Distance: 2.974596	Max_A: -2.951267	Max_B: -0.371810
Quad: 3	Point: 3	Distance: 3.329870	Max_A: -3.240201	Max_B: -0.767549
Quad: 3	Point: 4	Distance: 3.459953	Max_A: -3.313944	Max_B: -0.994509
Quad: 3	Point: 5	Distance: 3.669717	Max_A: -3.240202	Max_B: -1.722763
Quad: 3	Point: 6	Distance: 3.634006	Max_A: -2.945547	Max_B: -2.128321
Quad: 3	Point: 7	Distance: 3.566885	Max_A: -2.752485	Max_B: -2.268589
Quad: 3	Point: 8	Distance: 3.324494	Max_A: -2.275724	Max_B: -2.423498
Quad: 3	Point: 9	Distance: 2.897098	Max_A: -1.704283	Max_B: -2.342775
Quad: 3	Point: 10	Distance: 2.800682	Max_A: -1.245329	Max_B: -2.508580
Quad: 3	Point: 11	Distance: 3.159427	Max_A: -1.083800	Max_B: -2.967719
Quad: 3	Point: 12	Distance: 3.563750	Max_A: -0.596083	Max_B: -3.513545
Quad: 3	Point: 13	Distance: 3.670395	Max_A: -0.119322	Max_B: -3.668455
Quad: 3	Point: 14	Distance: 0.000000	Max_A: 0.000000	Max_B: -3.668455
Quad: 4	Point: 1	Distance: 0.000000	Max_A: 2.951264	Max_B: 0.000000
Quad: 4	Point: 2	Distance: 2.974593	Max_A: 2.951264	Max_B: -0.371814
Quad: 4	Point: 3	Distance: 3.329867	Max_A: 3.240197	Max_B: -0.767553
Quad: 4	Point: 4	Distance: 3.459950	Max_A: 3.313940	Max_B: -0.994512
Quad: 4	Point: 5	Distance: 3.669713	Max_A: 3.240196	Max_B: -1.722767
Quad: 4	Point: 6	Distance: 3.634003	Max_A: 2.945541	Max_B: -2.128324
Quad: 4	Point: 7	Distance: 3.566882	Max_A: 2.752478	Max_B: -2.268592
Quad: 4	Point: 8	Distance: 3.324492	Max_A: 2.275718	Max_B: -2.423501
Quad: 4	Point: 9	Distance: 2.897095	Max_A: 1.704276	Max_B: -2.342777
Quad: 4	Point: 10	Distance: 2.800683	Max_A: 1.245327	Max_B: -2.508582
Quad: 4	Point: 11	Distance: 3.159427	Max_A: 1.083795	Max_B: -2.967721
Quad: 4	Point: 12	Distance: 3.563750	Max_A: 0.596078	Max_B: -3.513546
Quad: 4	Point: 13	Distance: 3.670394	Max_A: 0.119316	Max_B: -3.668454
Quad: 4	Point: 14	Distance: 0.000000	Max_A: 0.000000	Max_B: -3.668454

Example output file for Area.exe--benzene molecule explained

The_uncorrected area_is_(A^2) 33.413748775776020 .

The area of the molecule in $Å^2$ without the reaction field correction factor (rfcf)

Parameters:

No._of_Data Points, Division_Factor, Choice

400 0.40000E-03 1

Combo, SiZe

1 0.1396480E-04

All of the parameters from the input file

Pie_1, Pie_2, Pie_3, Pie_4

12. 12. 12. 12.

Quad: 1 Point: 1 Distance: 0.000000 Max_A: 2.951267 Max_B: 0.000000
Quad: 1 Point: 2 Distance: 2.974596 Max_A: 2.951267 Max_B: 0.371811
Quad: 1 Point: 3 Distance: 3.329870 Max A: 3.240201 Max_B: 0.767550

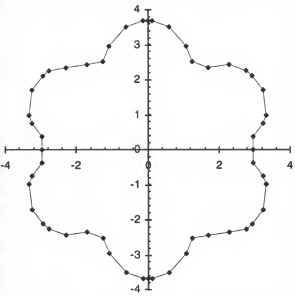

A plot of Max A vs Max B is the outside points of the benzene molecule that describes the excluded area

Quad Max_B: 0.994510
Quad Max_B: 1.722764
Quad Max_B: 2.128322
Quad Max_B: 2.268590
Quad Max_B: 2.423499
Quad Max_B: 2.342776
Quad Max_B: 2.508581
Quad Max_B: 2.967722
Quad Max_B: 3.513548
Quad Max_B: 3.668457
Quad Max_B: 3.668457
Quad Max_B: 0.000000
Quad Max_B: 0.371814
Quad Max_B: 0.767554
Quad Max_B: 0.994513
Quad Max_B: 1.722768
Quad Max_B: 2.128325
Quad Max_B: 2.268594
Quad Max_B: 2.423502
Quad Max_B: 2.342777
Quad Max_B: 2.508583
Quad Max_B: 2.967723
Quad Max_B: 3.513549
Quad Max_B: 3.668457

Quad: 2 Point: 14 Distance: 0.000000 Max_A: 0.000000 Max_B: 3.668457
Quad: 3 Point: 1 Distance: 0.000000 Max_A: -2.951267 Max_B: 0.000000
Quad: 3 Point: 2 Distance: 2.974596 Max_A: -2.951267 Max_B: -0.371810
Quad: 3 Point: 3 Distance: 3.329870 Max_A: -3.240201 Max_B: -0.767549
Quad: 3 Point: 4 Distance: 3.459953 Max_A: -3.313944 Max_B: -0.994509
Quad: 3 Point: 5 Distance: 3.669717 Max_A: -3.240202 Max_B: -1.722763
Quad: 3 Point: 6 Distance: 3.634006 Max_A: -2.945547 Max_B: -2.128321
Quad: 3 Point: 7 Distance: 3.566885 Max_A: -2.752485 Max_B: -2.268589
Quad: 3 Point: 8 Distance: 3.324494 Max_A: -2.275724 Max_B: -2.423498
Quad: 3 Point: 9 Distance: 2.897098 Max_A: -1.704283 Max_B: -2.342775
Quad: 3 Point: 10 Distance: 2.800682 Max_A: -1.245329 Max_B: -2.508580
Quad: 3 Point: 11 Distance: 3.159427 Max_A: -1.083800 Max_B: -2.967719
Quad: 3 Point: 12 Distance: 3.563750 Max_A: -0.596083 Max_B: -3.513545
Quad: 3 Point: 13 Distance: 3.670395 Max_A: -0.119322 Max_B: -3.668455
Quad: 3 Point: 14 Distance: 0.000000 Max_A: 0.000000 Max_B: -3.668455
Quad: 4 Point: 1 Distance: 0.000000 Max_A: 2.951264 Max_B: 0.000000
Quad: 4 Point: 2 Distance: 2.974593 Max_A: 2.951264 Max_B: -0.371814
Quad: 4 Point: 3 Distance: 3.329867 Max_A: 3.240197 Max_B: -0.767553
Quad: 4 Point: 4 Distance: 3.459950 Max_A: 3.313940 Max_B: -0.994512
Quad: 4 Point: 5 Distance: 3.669713 Max_A: 3.240196 Max_B: -1.722767
Quad: 4 Point: 6 Distance: 3.634003 Max_A: 2.945541 Max_B: -2.128324
Quad: 4 Point: 7 Distance: 3.566882 Max_A: 2.752478 Max_B: -2.268592
Quad: 4 Point: 8 Distance: 3.324492 Max_A: 2.275718 Max_B: -2.423501
Quad: 4 Point: 9 Distance: 2.897095 Max_A: 1.704276 Max_B: -2.342777
Quad: 4 Point: 10 Distance: 2.800683 Max_A: 1.245327 Max_B: -2.508582
Quad: 4 Point: 11 Distance: 3.159427 Max_A: 1.083795 Max_B: -2.967721
Quad: 4 Point: 12 Distance: 3.563750 Max_A: 0.596078 Max_B: -3.513546
Quad: 4 Point: 13 Distance: 3.670394 Max_A: 0.119316 Max_B: -3.668454
Quad: 4 Point: 14 Distance: 0.000000 Max_A: 0.000000 Max_B: -3.668454

References

(1) Adamson, A. W. *Physical Chemistry of Surfaces*, 5th ed.; John Wiley and Sons: New York, 1990.

(2) Young, D. M.; Crowell, A. D. *Physical Adsorption of Gases*; Butterworths: London, 1962, pp 230-231.
Gregg, S. J.; Sing, K. S. W. *Adsorption, Surface Area, and Porosity*; Academic Press: London, 1967; pp 68-69.

(3) Young, D. M.; Crowell, A. D. *Physical Adsorption of Gases*; Butterworths: London, 1962; p 230.

(4) Gregg, S. J.; Jacobs, J. *Trans. Faraday Soc.* **1948**, *44*, 574-588.

(5) Gregg, S. J. *Surface Chemistry of Solids*; Reinhold: London, 1951, p 104.

(6) Drago, R. S.; Webster, C. E; McGilvray, J. M. *J. Am. Chem. Soc.* **1998**, *120*, 538-547.

(7) (a) Drago, R. S.; Kassel, W. S.; Burns, D. S.; McGilvray, J. M.; Lafrenz, T. J.; Showalter, S. K. *J. Phys. Chem. B* **1997**, *101*, 7548-7555.
(b) Kassel, W. S.; Drago, R. S. *Microporous Mat.* **1997**, *12*, 189-195.

(8) Reid, R. C.; Prausnitz, J. M.; Sherwood, T. K. *The Properties of Gases and Liquids*; McGraw-Hill: New York, 1977; pp 57-68.
Partington, J. R. *An Advanced Treatise on Physical Chemistry: Vol. II, The Properties Liquids*; Longmans, Green and Co.: London, 1951; pp 17-36.

(9) McClellan, A. L.; Harnsberger, H. F. *J. Colloid. Sci.* **1967**, *23*, 577-599.

(10) Hill, T. L. *J. Chem. Phys.* **1948**, *16*, 181-189.

(11) Livingston, H. K. *J. Colloid. Sci.* **1949**, *4*, 447-458.
Livingston, H. K. *J. Am. Chem. Soc.* **1944**, *66*, 569-573.

(12) ZINDO; Zerner, M. C. and co-workers, Department of Chemistry, University of Florida, Gainesville, FL 32611
Zerner, M. C. *Reviews of Computational Chemistry*; VCH Publishing: New York, 1991; Vol. 2, pp 313-366.

(13) GEPOL93; Pascual-Ahuir, J. C.; Silla, E.; Tunon, I.
Silla, E.; Tunon, I.; Pascual-Ahuir, J. C.; *J. Comput. Chem.* **1991**, *12*, 1077-1088.

(14) Webster, C. E.; Cottone, A. C.; Drago, R. S. Accepted for publication in *J. Am. Chem. Soc.*, 1999

(15) June, R. L.; Bell, A. T.; Theodorou, D. N. *J. Phys. Chem.* **1990**, *94*, 1508-1516.
June, R. L.; Bell, A. T.; Theodorou, D. N. *J. Phys. Chem.* **1992**, *96*, 1051-1060.
Bates, S. P.; van Well, W. J. M.; van Santen, R. A.; Smit, B. *J. Phys. Chem.* **1996**, *100*, 17573-17581.

(16) Csicsery, S. M. *Zeolites* **1984**, *4*, 202-213.
Csicsery, S. M. *Pure and Appl. Chem.* **1986**, *58*, 841-856.

(17) Anderson, M. W.; Klinowski, J. *J. Am. Chem. Soc.* **1990**, *112*, 10-16.
Anderson, M. W.; Klinowski, J. *Nature* **1989**, *339*, 200-203.

(18) Webster, C. E.; Drago, R. S.; Zerner, M. C. *J. Phys. Chem. B* **1999**, *103*, 1242-1249.

(19) Drago, R. S.; Diaz, S.; Torrealba, M.; de Lima, L. *J. Am. Chem. Soc.* **1997**, *119*, 4444-4452.

(20) Hill, T. L. *An Introduction to Statistical Thermodynamics*; Addison-Wesley: Reading, Massachusetts; 1960; p 484.

(21) Breck, D. W. *Zeolite Molecular Sieves*; John Wiley and Sons: New York, 1974; p 636

(22) Reid, R. C.; Prausnitz, J. M.; Sherwood, T. K. *The Properties of Gases and Liquids*; McGraw-Hill: New York, 1977; pp 678-679.

(23) (a) Hayhurst, D. T.; Paravar, A. *Zeolites* **1988**, *8*, 27-29.
(b) Chen, N. Y.; Degnan, T. F., Jr.; Smith, C. M. *Molecular Transport and Reaction in Zeolites*; VCH Publishers: New York, 1994; pp 81-86.

(24) Yang, Y. C.; Baker, J. A.; Ward, J. R. *Chem. Rev.* **1992**, *92*, 1729.

(25) Gregg, S. J.; Sing, K. S. W. *Adsorption, Surface Area, and Porosity*, Academic Press: London, 1967

(26) Drago, R. S.; Burns, D. S.; Lafrenz, T. J. *J. Phys. Chem.* **1996**, *100*, 1718-1724.

(27) Everett, D.H; Powl, J. C. *J. Chem. Soc. Faraday Trans. 1* **1976**, *72*, 619-636.

(28) Breck, D. W. *Zeolite Molecular Sieves*; John Wiley and Sons: New York, 1974.

(29) Chen, N. Y.; Degnan, T. F.; Smith, C. M. *Molecular Transport and Reaction in Zeolites*; VCH Publishers: New York, 1994.

(30) Dyer, A. *An Introduction to Zeolite Molecular Sieves*; John Wiley and Sons: New York, 1988.

(31) Jansen, J. C.; Stocker, M.; Karge, H. G.; Weitkamp, J. Eds. *Advanced Zeolite Science and Applications*; Vol 85; Elsevier: Amsterdam, 1994.

(32) Olson, D. H.; Kokotailo, G. T.; Lawton, S. L.; Meier, W. M. *J. Phys. Chem.* **1981**, *85*, 2238-2243.

(33) June, R. L.; Bell, A. T.; Theodoro, D. N. *J. Phys. Chem.*, **1990**, *94*, 1508-1516.

(34) Bhatia, S. *Zeolite Catalysis: Principles and Applications*; CRC Press: Boca Raton, Florida, 1990.

(35) Iler, R. K. *The Chemistry of Silica*; John Wiley and Sons: New York, 1979.

(36) Saito, A.; Foley, H. C. *Microporous Materials*, **1995**, *3*, 543-556.

(37) Brunauer, S.; Emmett, P. H.; Teller, E. *J. Am. Chem. Soc.*, **1938**, *60*, 309-319.

(38) Harkins, W. D.; Jura, G. *J. Am. Chem. Soc.*, **1944**, *66*, 1366-1373.

(39) Barrett, E. P.; Joyner, L. G.; Halenda, P. P. *J. Am. Chem Soc.*, **1951**, *73*, 373-380.

(40) Gordon, A. J.; Ford, R. A. *The Chemist's Companion*; John Wiley and Sons: New York, 1972, p 451.

(41) White, M. *Heterogeneous Catalysis*; Prentice Hall: New Jersey, 1990.

(42) Person, W. B. *J. Am. Chem. Soc.* **1962**, *84*, 536-540.

(43) Webster, C. E.; Drago, R. S.; Zerner, M.C. *J. Am. Chem. Soc.* **1998**, *120*, 5509-5516.

(44) Gregg, S. J.; Sing, K. S. W. *Adsorption, Surface Area, and Porosity*, 2nd ed.; Academic Press: London, 1982.

(45) Langmuir, I. *J. Am. Chem. Soc.* **1918**, *40*, 1361-1403.

(46) Drago, R.S.; Dias, S. C.; McGilvray, J. M.; Mateus, A. *J. Phys. Chem. B.* **1998**, *102*, 1508-1514.

(47) Dias, S. C.; Webster, C. E.; Cottone, A.; Drago, R.S. To be submitted.

(48) van Koningsveld, H.; van Bekkum, H.; Jansen, J.C. *Acta. Crystallogr.* **1987**, *B43*, 127-132.

(49) (a) Meier, W. M. *Z. Kristallogr.* **1961**, *115*, 439-450.
(b) Barrer, R. M.; White, E. A. D. *J. Chem. Soc.* **1952**, 1561.

(50) Csicsery, S. M. *J. Catal.* **1971**, *23*, 124-130.

(51) (a) Karge, H. G.; Dondur, V. *J. Phys. Chem.* **1990**, *94*, 765.
(b) Karge, H. G.; Dondur, V.; Weitkamp, J. *J. Phys. Chem.* **1991**, *95*, 283.
(c) Katada, N.; Igi, H.; Kim, J.; Niwa, M. *J. Phys. Chem. B* **1997**, *101*, 5969-5977.

(52) (a) Thomas, J. M.; Klinowski, *J. Adv. Catal.* **1985**, *33*, 199.
(b) Klinowski, J. *Chem. Rev.* **1991**, *91*, 1459-1479.
(c) Pfiefer, H. *Colloids Surf.* **1989**, *36*, 169.
(d) Xu, Q.; Eguchi, T.; Nakayam, H.; Makamura, N. *J. Chem. Soc., Faraday Trans.*, **1996**, *92*, 4601-4603.

(53) (a) Wakabayashi, F. Kondo, J. N., Wada, A.; Domen, K.; Hirose, C. *J. Phys. Chem.* **1993**, *97*, 10761-10768.
(b) Wakabayashi, F.; Kondo, J. N.; Wada, A.; Domen, K.; Hirose, C. *J. Phys. Chem.* **1996**, *100*, 18882.
(c) Wakabayashi, F. Kondo, J. N.; Wada, A.; Domen, K.; Hirose, C. *Microporous Materials* **1997**, *8*, 29-37.
(d) Bordiga, S.; Lamberti, C.; Geobaldo, F.; Zecchina, A.; Palomino, G. T.; Areán, C. O. *Langmuir* **1995**, *11*, 527-533.
(e) Geobaldo, F.; Lamberti, C.; Ricchiardi, G.; Bordiga, S.; Zecchina, A.;
Palomino, G. T.; Areán, C. O. *J. Phys. Chem.* **1995**, *99*, 11167-11177.
(f) Areán, C. O.; Palomino, G. T.; Geobaldo, F.; Zecchina, A. *J. Phys. Chem.* **1996**, *100*, 6678-6690.
(g) Zecchina, A.; Geobaldo, F.; Lamberti, C.; Ricchiardi, G.; Bordiga, S. *J. Phys. Chem.* **1996**, *100*, 18883.
(h) Gruver, V.; Fripiat, J. J. *J. Phys. Chem.* **1994**, *98*, 8549-8554.
(i) Auroux, A.; Datka, J. *Applied Catalysis A: General* **1997**, *165*, 473-479.

(54) Kassel, W. S. Ph.D. Thesis. University of Florida, 1998.

(55) Barclay, l. M.; Butler, J. A. V. *Trans. Faraday Soc.* **1938**, *34*, 1445-1454.

(56) Nivarthi, S. S.; Van Tassel, P. R.; Davis, H. T.; McCormick, A. V. *J. Chem. Phys.* **1995**, *103*, 3029-3037.

(57) Joesten, M. D.; Drago, R. S. *J. Am. Chem. Soc.* **1962**, *84*, 3817-3821.

(58) Ohgushi, T.; Yokoyama, H. *J. Chem. Soc Faraday Trans. 1* **1992**, *88*, 3095-3099.

(59) Chang, C. D. *Hydrocarbons from Methanol*; Marcel Dekker, Inc: New York, 1983.
Chen, N. Y.; Degnan, T. F., Jr.; Smith, C. M. *Molecular Transport and Reaction in Zeolites*; VCH Publishers: New York, 1994.
Chen, N. Y.; Garwood, W. E., Jr.; Dwyer, F. G. *Shape Selective Catalysis in Industrial Applications*, 2nd ed.; Marcel Dekker, Inc.: New York, 1996.

(60) Barrer, R. M. *Zeolites and Clay Minerals as Sorbents and Molecular Sieves*; Academic Press: London, 1978.
Breck, D. W. *Zeolite Molecular Sieves*; John Wiley and Sons: New York, 1974.
Dyer, A. *An Introduction to Zeolite Molecular Sieves*; John Wiley and Sons: New York, 1988.
Rabo, J. A. *Zeolite Chemistry and Catalysis, ACS Monograph 171*; American Chemical Society: Washington, D.C., 1976.

(61) Davis, M. E.; Suib, S. L. *Selectivity in Catalysis*, ACS Symposium Series 517; American Chemical Society: Washington, D.C., 1993.

(62) Dyer, A. *An Introduction to Zeolite Molecular Sieves*; John Wiley and Sons: New York, 1988; p 117.

(63) Chen, N. Y.; Degnan, T. F., Jr.; Smith, C. M. *Molecular Transport and Reaction in Zeolites*; VCH Publishers: New York, 1994; p 174.

(64) Davis, M. E.; Suib, S. L. *Selectivity in Catalysis*, ACS Symposium Series 517; American Chemical Society: Washington, D.C., 1993; p 209.

(65) Csicery, S.M. *Chem. Br.* **1985**, *May*, 473.

(66) Davis, M. E.; Suib, S. L. *Selectivity in Catalysis*, ACS Symposium Series 517; American Chemical Society: Washington, D.C., 1993; pp 210-211.

(67) Chen, N. Y.; Degnan, T. F., Jr.; Smith, C. M. *Molecular Transport and Reaction in Zeolites*; VCH Publishers: New York, 1994; p 182.

(68) Derouane, E. G., Nagy, J. B., Dejaifve, P., van Hoof, J. H. C.; Spekman, B. P.; Vedrine, J. C.; Naccache, C. *J. Catal.* **1978**, *53*, 40-55.

(69) Dyer, A. *An Introduction to Zeolite Molecular Sieves*; John Wiley and Sons: New York; 1988; pp 97-98.

(70) Chen, N. Y.; Degnan, T. F., Jr.; Smith, C. M. *Molecular Transport and Reaction in Zeolites*; VCH Publishers: New York, 1994; p 132.

(71) Bendoraitis, J. G.; Chester, A. W.; Dwyer, F. G.; Garwood, W. E. *New Developments in Zeolite Science and Technology*; Elsevier: New York, 1986; pp 669-675.

(72) Young, D. M.; Crowell, A. D. *Physical Adsorption of Gases*; Butterworths: London, 1962; p 19.

(73) Derouane, E. G. *J. Catal.* **1986**, *100*, 541-544.
Derouane, E. G.; Andre,J. M.; Lucas, A. A. *J. Catal.* **1988**, *110*, 58-73.

(74) Chen, N. Y.; Degnan, T. F., Jr.; Smith, C. M. *Molecular Transport and Reaction in Zeolites*; VCH Publishers: New York, 1994; p 189.

(75) Chen, N. Y.; Degnan, T. F., Jr.; Smith, C. M. *Molecular Transport and Reaction in Zeolites*; VCH Publishers: New York, 1994; p 133.

(76) Dean, J. A. *Lange's Handbook of Chemistry*, 14th ed.; McGraw-Hill, Inc: New York, 1992; p 4·18.
Emsley, J. *The Elements*; Oxford University Press, Inc.: New York, 1991; p 136.

(77) (a) Fraenkel, D.; Levy, M. *J. Catal.* **1989**, *118*, 487-493.
(b) Fraenkel, D.; Levy, M. *J. Catal.* **1989**, *118*, 10-21.

(78) Chang, C. D.; Silvestri, A. J. *J. Catal.* 1977, *47*, 249-259.

(79) Weisz, P. B. *Ind. Eng. Chem. Res.* **1995**, 34, 2692-2699.

(80) Anderson, J. R.; Dong, Q. N.; Chang, Y. F.; Western, R. J. *J. Catal.* **1991**, *127*, 113-127.
Anderson, J. R.; Chang, Y. F.; Western, R. J. *J. Catal.* **1989**, *118*, 466.

(81) Chen, N. Y.; Kaeding, W. W.; Dwyer, F. G. *J. Am. Chem. Soc.* **1979**, *101*, 6783-4.

(82) Hastings, S. H.; Nicholson, D. E. *J. Chem. Eng. Data* **1961**, *6*, 1-4.

(83) (a) Masel, R. I. *Principles of Adsorption and Reaction on Solid Surfaces*; John Wiley and Sons, Inc.: New York, 1996.
(b) Tien, C. *Adsorption Calculations and Modeling*; Butterworth-Heinemann: Boston, 1994.
(c) Chen, N. Y.; Degnan, T. F.; Smith, C. M. *Molecular Transport and Reaction in Zeolites*; VCH Publishers: New York, 1994.
(d) Gregg, S.J.; Sing, K.S.W. *Adsorption, Surface Area, and Porosity*; Academic Press: London, 1982.

(84) Patrick J. W. *Porosity in Carbons: Characterization and Application*; Halsted Press: New York, 1995.

(85) Jenkins, G. M.; Kawamura, K. *Polymeric Carbons–Carbon Fibre, Glass, and Char*; Cambridge University Press: New York, 1976.

(86) Faust, S. D.; Aly, O. M.; *Adsorption Processes For Water Treatment*; Butterworths: Boston, 1987.

(87) Dyer, A. *An Introduction to Zeolite Molecular Sieves*; John Wiley and Sons: New York, 1988; pp 2-3.

(88) Wampler, T. P. *Applied Pyrolysis Handbook*; Marcel Dekker: New York, 1995.

(89) Neely, J. W.; Isacoff, E. G. *Carbonaceous Adsorbents for the Treatment of Ground and Surface Waters*; Marcel Dekker: New York, 1982.
Faust, S. D.; Aly, O. M.; *Chemistry of Water Treatment*; Butterworths: Boston, 1983.

(90) Perrich, J. R. *Activated Carbon Adsorption for Wastewater Treatment*; CRC Press, Inc.: Boca Raton, FL, 1981.

(91) Suzuki, M. *Adsorption Engineering*; Elsevier: New York, 1990.
Modeling and Simulation:
Cracknell, R. F.; Gordon, P. Gubbins, K. E. *J. Phys. Chem.* **1993**, *97*, 494-499

(92) Slejko, F. L. *Adsorption Technology*; Marcel Dekker: New York, 1985.
Modeling and Simulation:
Sowers, S. L.; Gubbins, K. E. *Fundamentals of Adsorption*; Kluwer Academic: Boston, MA, 1996, pp 855-863.
Keffer, D.; Davis, H. T.; McCormick, A. V. *J. Phys. Chem.* **1996**, *100*, 638-645.
Jiang, S.; Gubbins, K. E.; Balbuena, P. B. *J. Phys. Chem.* **1994**, *98*, 2403-2411.
Tan, Z.; Gubbins, K. E. *J. Phys. Chem.* **1992**, *96*, 845-854.

(93) Carbons:
(a) Gusev, V. Y.; O'Brien, J. A. *Langmuir* **1997**, *13*, 2822-2824.
(b) Gusev, V. Y.; O'Brien, J. A.; Seaton, N. A. *Langmuir* **1997**, *13*, 2815-2821.
(c) Vega, L. F.; Müller, E. A.; Rull, L. F.; Gubbins, K. E. *Fundamentals of Adsorption*; Kluwer Academic: Boston, MA, 1996, pp 993-1000.
(d) Tan, Z.; Gubbins, K. E. *J. Phys. Chem.* **1990**, *94*, 6061-6069.

(93) (e) Avgul, N. N.; Bezus, A. G.; Dobrova, E. S.; Kiselev, A. V. *J. Colloid Interface Sci.* **1973**, *38*, 486-495.
(f) Poshkus, D. P.; Afreimovitch, A. Y. *J. Chromatogr.* **1971**, *58*, 55-59.
(g) Kiselev, A. V.; Poshkus, D. P.; Afreimovitch, A. Y. *Zh. Fiz. Khim.* **1970**, *44*, 981-986.
(h) Kiselev, A. V.; Poshkus, D. P.; Afreimovitch, A. Y. *Zh. Fiz. Khim.* **1968**, *42*, 2546-2552.
(i) Kiselev, A. V.; Poshkus, D. P.; Afreimovitch, A. Y. *Zh. Fiz. Khim.* **1968**, *42*, 2553-2555.
(j) Kiselev, A. V.; Poshkus, D. P.; Afreimovitch, A. Y. *Zh. Fiz. Khim.* **1964**. *38*, 1514-1522.

(94) Zeolites:
Vlugt, T. J. H.; Zhu, W.; Kapteijen, F.; Moulijn, J. A.; Smit, B.; Krishna, R. *J. Am. Chem. Soc.* **1998**, *120*, 5599-5600.
Gladden, L. F.; Sousa-Goncalves, J. A.; Alexander, P. *J. Phys. Chem. B* **1997**, *101*, 10121-10127.
Bates, S. P.; van Well, W. J. M.; van Santen, R. A.; Smit, B. *J. Phys. Chem.* **1996**, *100*, 17573-17581.
Nivarthi, S. S.; van Tassel, P. R.; McCormick, A. V.; Davis, H. T. *J. Chem. Phys.* **1995**, *103*, 3029-3037.
Mitchell, M. C.; McCormick, A. V.; Davis, H. T. *Mol. Phys.* **1995**, *103*, 3029-3037.
Karavias, F.; Myers, A. L. *Mol. Sim.* **1991**, *8*, 23-50.
Razmus, D. M.; Hall, C. K. *AIChE J.* **1991**, *37*, 769-779.
June, R. L.; Bell, A. T.; Theodorou, D. N. *J. Phys. Chem.* **1990**, *94*, 8232-8240.
June, R. L.; Bell, A. T.; Theodorou, D. N. *J. Phys. Chem.* **1990**, *94*, 1508-1516.
Ruthven, D. M.; Wong, F. *Ind. Eng. Chem. Fundam.* **1985**, *24*, 27-32.
Kiselev, A. V.; Lopatkin, A. A.; Shulga, A. A. *Zeolites* **1985**, *5*, 261-267.
Bezus, A. G.; Kiselev, A. V.; Lopatkin, A. A.; Du, P. Q. *J. Colloid Interface Sci.* **1973**, *45*, 386-395.
Breuer, P.; Kiselev, A. V.; Lesnik, E. A.; Lopatkin, A. A. *Zh. Fiz. Khim.* **1969**, *43*, 1519-1524.
Kiselev, A. V.; Poshkus, D. P.; Afreimovitch, A. Y. *Zh. Fiz. Khim.* **1968**, *42*, 2556-2562.

(95) Gubbins, K. E.; Sliwinski-Bartkowiak, M.; Suh, S. *Mol. Sim.* **1996**, *17*, 333-367.

(96) Nouacer, M.; Shing, K.S. *Mol. Sim.* **1989**, *2*, 55-68.

(97) Coutinho, K.; Canuto, S.; Zerner, M. C. *Int. K. Quant. Chem.* **1997**, *65*, 885-891.
Gubbins, K. E. *Mol. Sim.* **1989**, 2, 223-252.

(98) López-Ramón, M. V.; Jagiello, J; Bandosz, T. J.; Seaton, N. A. *Langmuir* **1997**, *13*, 4435-4445.

(99) Dubinin, M. M. *Carbon* **1989**, *27*, 457-467.
Bering, B. P.; Dubinin, M. M.; Serpinsky, V. V. *J. Colloid Interface Sci.* **1966**, *21*, 378-393.
Dubinin, M. M. *Zh. Fiz. Khim.* **1965**, *39*, 1305.
Dubinin, M. M. *Chem. Rev.* **1960**, *60*, 235-241.
Nikolaev, K. M.; Dubinin, M. M. *Izest. Akad. Nauk SSSR, Otdel. Khim. Nauk* **1958**, 1165-1174.
Dubinin, M. M.; Zhukovskaia, E. G. *Izest. Akad. Nauk SSSR, Otdel. Khim. Nauk* **1958**, 535-544.
Dubinin, M. M.; Zaverina, E. D.; Timofeev, D. P. *Izest. Akad. Nauk SSSR, Otdel. Khim. Nauk* **1957**, 670-677.

(100) Polanyi, M. *Verh. deut. Physik. Ges.* **1914**, *16*, 1012.

(101) Avgul, N. N.; Bezus, A. G.; Dobrova, E. S.; Kiselev, A. V. *J. Colloid Interface Sci.* **1973**, *38*, 486-495.

(102) (a) Lewis, W. K.; Gilliland, E. R.; Chertow, B.; Cadogan, W. P. *Ind. Eng. Chem.* **1950**, *42*, 1326-1332.
(b) Reucroft, P. J.; Simpson, W. H.; Jonas, L. A. *J. Phys. Chem.* **1971**, *75*, 3526-3531.
(c) Ginoux, J. L.; Lang, J. C.; Bonnetain, L. *Molecular Sieves*, Advances in Chemistry Series 121; American Chemical Society: Washington, D.C. 1973, pp382-391.
(d) Abe, I.; Hayashi, K.; Kitagawa, M. *Bull. Chem. Soc. Jpn.* **1981**, *54*, 2819-2820.
(e) Noll, K. E.; Wang, D.; Shen, T. *Carbon*, **1989**, *27*, 236-45.

(103) (a) Maslan, F. D.; Altman, M.; Aberth, E. R. *J. Phys. Chem.* **1953**, *57*, 106-109.
(b) Potter, C.; Sussman, M. V. *Ind. Eng. Chem.* **1957**, *49*, 1763-1768.
(c) Reich, R.; Ziegler, W. T.; Rogers, K. A. *Ind. Eng. Chem. Process Des. Dev.* **1980**, *19*, 336-344.
(d) Crittendon, J. C.; Rigg, T. J. Perram, D. L.; Tang, S. R.; Hand, D. W. *J. Env. Eng.* **1989**, *115*, 560-573.

(104) Grant, R. J.; Manes, M. *Ind. Eng. Chem. Fundam.* **1966**, *5*, 490-498.
Lewis, W. K.; Gilliland, E. R.; Chertow, B.; Cadogan, W. P. *Ind. Eng. Chem.* **1950**, *42*, 1319-1326.

(105) John, P. T.; Suri, D. K.; Nagpal, K. C. *Carbon* **1979**, *17*, 491-493.

(106) Chen, S. G.; Yang, R. T. *Langmuir* **1994**, *10*, 4244-4249.

(107) Chen, W. N.; Guthrie, J. T.; Lin, L. *Dyes Pigm* **1992**, *19*, 129-147.

(108) (a) Tien, C. *Adsorption Calculations and Modeling*; Butterworth-Heinemann: Boston, 1994, pp 49-56.
(b) Crittendon, J. C.; Rigg, T. J. Perram, D. L.; Tang, S. R.; Hand, D. W. *J. Env. Eng.* **1989**, *115*, 560-573.
(c) Crittendon, J. C.; Luft, P.; Hand, D. W.; Oravitz, J. L.; Loper, S. W.; Ari, M. *Environ. Sci. Technol.* **1985**, *19*, 1037-1043.
(d) Wilson, R. J.; Danner, R. P. *J. Chem. Eng. Data* **1983**, *28*, 14-18.
(e) Okazaki, M.; Tamon, H. Toei, R. *J. Chem. Eng. Jpn.* **1978**, *11*, 209-215.

(109) Huggahalli, M.; Fair, J. R. *Ind. Eng. Chem. Res.* **1996**, *35*, 2071-2074.

(110) Marczewski, A. W.; Derylo-Marczewski, A. Jaroniec, M. *Chemica Scripta* **1988**, *28*, 173-184.
Quiñones, I.; Guiochon, G. *J. Chromatogr. A* **1996**, *734*, 83-96.

(111) Choudary, N. V.; Jasra, R. V.; Bhat, S. G. T. *Sep. Sci. Tech.* **1995**, *30*, 2337-2348.
Zhu, J.; Guiochon, G. *J. Chromatogr.* **1991**, *552*, 71-89.
Wood, G. O.; Moyer, E. S. *Am. Ind. Hyg. Assoc. J.* **1991**, *52*, 235-242.
McKay, G.; Al-Duri, B. *Chem. Eng. Sci.* **1988**, *43*, 1133-1142.
Kaul, B. K. *Ind. Eng. Chem. Process Des. Dev.* **1984**, *23*, 711-716.
Fernbacher, J. M.; Wenzel, L.A. *Ind. Eng. Chem. Fundam.* **1972**, *11*, 457-465.

BIOGRAPHICAL SKETCH

Charles Edwin Webster was born April 30, 1973, in Pensacola, Florida, to William Charles Webster and Eileen H. Webster. He has one older brother, William Alexander. Edwin attended and graduated from Tate High School in Gonzalez, Florida. After graduation from high school, Edwin intended to receive a pharmacy degree but became fascinated by chemistry and graduated from the University of West Florida with a B. S. in Chemistry and Biochemistry. He then went on to the University of Florida to receive his Ph.D. in Chemistry while studying physical inorganic chemistry with Graduate Research Professor Russell S. Drago and, after the death of Dr. Drago, finished his studies with Distinguished Professor Michael C. Zerner and Assistant Professor Michael J. Scott.

I certify that I have read this study and that in my opinion it conforms to acceptable standards of scholarly presentation and is fully adequate, in scope and quality, as a dissertation for the degree of Doctor of Philosophy.

Michael J. Scott, Chair
Assistant Professor of Chemistry

I certify that I have read this study and that in my opinion it conforms to acceptable standards of scholarly presentation and is fully adequate, in scope and quality, as a dissertation for the degree of Doctor of Philosophy.

Michael C. Zerner, Cochair
Distinguished Professor of Chemistry

I certify that I have read this study and that in my opinion it conforms to acceptable standards of scholarly presentation and is fully adequate, in scope and quality, as a dissertation for the degree of Doctor of Philosophy.

David E. Richardson
Professor of Chemistry

I certify that I have read this study and that in my opinion it conforms to acceptable standards of scholarly presentation and is fully adequate, in scope and quality, as a dissertation for the degree of Doctor of Philosophy.

R. Carl Stoufer
Associate Professor Emeritus of Chemistry

I certify that I have read this study and that in my opinion it conforms to acceptable standards of scholarly presentation and is fully adequate, in scope and quality, as a dissertation for the degree of Doctor of Philosophy.

Willis B. Person
Professor of Chemistry

I certify that I have read this study and that in my opinion it conforms to acceptable standards of scholarly presentation and is fully adequate, in scope and quality, as a dissertation for the degree of Doctor of Philosophy.

David A. Denslow
Distinguished Service Professor of Economics

This dissertation was submitted to the Graduate Faculty of the Department of Chemistry in the College of Liberal Arts and Sciences and to the Graduate School and was accepted as partial fulfillment of the requirements for the degree of Doctor of Philosophy.

May 1999

Dean, Graduate School